

Stephanie Maia Acuña

microRNAs e imunometabolismo em macrófagos e células dendríticas em resposta à
infecção com *Leishmania* spp.

microRNAs and immunometabolism of macrophages and dendritic cells during the
response against *Leishmania* spp. genus parasites.

São Paulo

2023

Stephanie Maia Acuña

microRNAs e imunometabolismo em macrófagos e células dendríticas em resposta à
infecção com *Leishmania* spp.

microRNAs and immunometabolism of macrophages and dendritic cells during the
response against *Leishmania* spp. genus parasites.

	<p>Tese apresentada ao Instituto de Biociências da Universidade de São Paulo, para a obtenção de Título de Doutor em Ciências, na Área de Fisiologia Geral.</p> <p>Orientador(a): Dra. Sandra Marcia Muxel</p>
--	--

São Paulo

2023

Ficha catalográfica elaborada pelo Serviço de Biblioteca do Instituto de Biociências da USP,
com os dados fornecidos pelo (a) autor (a) no formulário:
'<https://biblioteca.ib.usp.br/ficha-catalografica/src/ficha.php>'

Maia Acuña, Stephanie

MicroRNAs e imunometabolismo em macrófagos e células dendríticas em resposta à infecção com *Leishmania* spp. / Maia Acuña Stephanie ; orientadora Márcia Muxel Sandra -- São Paulo, 2023.
208 p. + anexo

Tese (Doutorado) -- Instituto de Biociências da Universidade de São Paulo. Ciências Biológicas (Fisiologia).

1. Parasitologia. 2. Imunometabolismo. 3. Relação Parasita-Hospedeiro. 4. Regulação da Expressão Gênica. I. Márcia Muxel, Sandra, orient. Título.

Bibliotecária responsável pela catalogação:
Elisabete da Cruz Neves - CRB - 8/6228

Dedico esta tese a todos os adultos que cresceram até
tornarem-se crianças.
Em especial à Safira, que sonhava em ser astronauta e
morar na Lua. Ela descobriu que existem outros
Universos visíveis ao olhar pelo microscópio.

A chave da felicidade é ficar longe de idiotas, certo? Os adultos levam o tempo demasiado a sério. E é por isso que o perdem de uma forma infantil. Inventam complicações, pensam que não conseguem o que tanto querem e de tanto pensarem que não conseguem não conseguem mesmo, ficam parados diante dos obstáculos. Eu e o Zé Pedro ontem conseguimos passar um obstáculo de quatro metros. Trepámos a uma árvore, depois pusemo-nos às cavalitas um do outro e não demorou mais de dois ou três minutos para um de nós estar do lado de lá. O segredo da vida é tantas vezes trepar a uma árvore e depois usarmo-nos uns aos outros às cavalitas para ultrapassarmos os obstáculos. Só os adultos não sabem disso. Eu já fui adulto, sabem? Mas depois cresci.

Pedro Chagas Santos
A raridade das coisas banais, pág 15
2022

Agradecimentos

A gratidão é um dos sentimentos mais nobres que um ser humano pode nutrir, pois dá o devido reconhecimento às pessoas que nos foram importantes, cujo papel foi e é essencial para o cumprimento de nossas metas.

Assim sendo, devo agradecimentos especiais à minha orientadora: Dra. Sandra Márcia Muxel, quem acreditou em mim desde o primeiro momento, quando iniciamos a nossa história em 2014, ano em que começamos a nossa parceria com meu estágio de iniciação científica. Desde então criamos muitos projetos juntas, passamos por momentos de muito sucesso, e, também, de muita dificuldade. Hoje a profissional que eu sou deve-se muito ao fato de termos tido tamanha confiança uma na outra, em especial a confiança de eu ser a primeira aluna de pós-graduação a ser orientada por ela. Sandrinha, agradeço imensamente por todo aprendizado e tenho certeza de que seguiremos crescendo fortes.

Além de minha orientadora, não posso deixar de agradecer à Prof^ª. Dra. Lucile Maria Floeter-Winter, que nos acolheu em seu laboratório por tantos anos, e que, embora tenhamos tido nossas diferenças, tenho total respeito e admiração pela profissional que ela é. Também agradeço a todos os alunos e técnicos que foram minhas companhias ao longo de tantos anos de jornada.

Agradeço com muito carinho à Dra. Paola Minóprio e toda a equipe que trabalhou na Força-Tarefa SARS-CoV-2 na Região Metropolitana de São Paulo, onde pude passar o período de pandemia em um trabalho voluntário que me trouxe muita experiência, vivência e expandiu a minha capacidade de pensar a ciência e em como devolver nosso trabalho à sociedade.

Também coloco aqui meus agradecimentos ao Doutor Ricardo Silvestre, pesquisador do Instituto de Investigação de Ciências da Vida e Saúde, na Universidade do Minho, Braga, Portugal; que me acolheu em seu laboratório do período de estágio de pesquisa no exterior, onde aprendi muito sobre a prática da imunologia e como a ciência é feita em outro país, com suas glórias e dificuldades.

Além da estrutura física e dos responsáveis de cada laboratório, eu não teria chegado aonde cheguei se não fossem meus colegas, muitos dos quais tornaram-se grandes amigos e irmãos. Não há espaço para todos, mas quero deixar o registro nominal de alguns. Em primeiro lugar às minhas irmãs de profissão que se tornaram irmãs de vida: Rúbia Heloísa Vanderlinde, Ana Paula Pessoa Vilela e Sónia Maria Barros de Carvalho. Aos meus irmãos de orientação: Jonathan Miguel Zanatta, Juliane Cristina Ribeiro Fernandes, Camilla Bento

de Almeida e Samantha Maia. Agradeço a todos os estagiários que pude acompanhar e passar treinamento e meu conhecimento adquirido ao longo dos anos. Agradeço aos meus professores por terem me passado seus conhecimentos.

Agradeço à Universidade de São Paulo por ter sido minha segunda casa por tantos anos, desde à graduação até este momento. Agradeço em especial à Fundação de Amparo à Pesquisa do Estado de São Paulo e ao Conselho Nacional de Pesquisa e Desenvolvimento pelo financiamento dos projetos em que participei. À FAPESP pela bolsa de Doutorado Direto (Processo nº 2017/23519-2) e BEPE (Processo nº 2021/07144-4).

Ademais aos agradecimentos acadêmicos, agradeço aos meus familiares por me apoiarem e participarem comigo desta caminhada – meus pais, minha amada irmã Milena, minhas avós Joana e Marta. E um agradecimento especial ao meu avô José Roberto, que infelizmente não está mais entre nós para ver os meus logros e méritos acadêmicos, dos quais ele tinha muito orgulho de falar. Aos meus amigos brasileiros e portugueses que acreditaram em mim, que eu poderia chegar cada vez mais longe, e dando-me forças quando eu já não tinha mais. À minha querida psicóloga Caroline Rocha, quem me ouviu chorar por tantos momentos e que pode se relacionar à minha vivência por também ser uspiana. E um agradecimento muitíssimo especial ao meu filhinho de quatro patas, pelo negro e os miados mais fofos do mundo, por ter sido meu animal de suporte emocional e um companheiro sempre presente.

Também quero prestar uma homenagem a uma pessoa que se tornou muito mais do que uma companhia em Portugal, e que também teve um papel crucial na reta final desta minha trajetória: Nuno Xavier. Faltam-me palavras para agradecer tudo o que fizeste e ainda fazes por mim; por veres o melhor de mim o tempo todo; por amar-me e aceitar-me exatamente como eu sou. Obrigada por ter sido o melhor guia turístico que eu poderia ter. E mais ainda: obrigada por ter-me dado uma família para chamar de minha, uma sogra para chamar de mãe e um novo país para chamar de casa. Obrigada por ser meu lar, em qualquer país em que estejamos no mundo, onde estivermos juntos, ali será nosso lar. Amo-te imenso!

Ao fim, porém com a maior importância, agradeço a mim mesma por ter conseguido chegar até aqui. Passei por inúmeras transformações pessoais e profissionais ao longo dos anos de doutoramento. Tive imensas dores, muitas das quais tiveram força o suficiente para me convencerem de que não existir era a opção mais viável. Mas de força pessoal eu sou especialista, e pude ver a mim mesma renascer, crescer e ter uma vitalidade ímpar, ao qual eu jamais havia alcançado. Agradeço à minha eu do passado por ter resistido e perseguido

seus sonhos, ainda que feita em muitos pedaços. Agradeço a mim mesma pela minha capacidade de me adaptar, sonhar, criar, planejar e principalmente: saber mudar de direção.

Sumário

Introdução Geral	15
1. As leishmanioses e seu agente etiológico: <i>Leishmania</i> spp.	15
3. Metabolismo da célula hospedeira em resposta à infecção	23
4. Regulação da expressão gênica na célula hospedeira mediados por miRNAs	28
Hipótese	33
Objetivos	33
Objetivo Geral	33
Objetivos específicos	33
Capítulo 1 Melatonina altera a infectividade de <i>Leishmania amazonensis</i> por meio de miR-294, miR-30e e miR-302d, impactando na expressão de <i>Tnf</i>, <i>Mcp-1</i> e <i>Nos2</i>.	34
Resumo	34
Introduction	36
Materials and methods.....	38
Results	42
Discussion.....	49
Supplementary information	52
References	54
Capítulo 2 Receptores do tipo Toll e o miRNA let-7e possuem como alvo a resposta inflamatória em macrófagos infectados com <i>Leishmania amazonensis</i>	61
Resumo	61
Abstract.....	62
Introduction	63
Materials and Methods	65
Results	70
Discussion.....	79
Supplementary material.....	84
References	88
Capítulo 3. Resposta inflamatória aguda contra <i>Leishmania amazonensis</i> leva à expressão de miRNAs reguladores da expressão de <i>Tnfa</i>	94
Resumo	94
Abstract.....	95
Introduction	96
Materials and Methods	98
In silico miRNA binding site prediction	98
Parasite Culture	98
BMDM harvesting and culture	98
Macrophage infection	98

Infection assessment.....	98
RNA extraction and cDNA preparation	98
Transcript quantification.....	99
miRNA inhibition.....	100
Ethics Statement.....	100
Results	101
Discussion.....	108
References	111
Capítulo 4 Imunometabolismo da resposta de macrófagos infectados com <i>Leishmania amazonensis</i>	115
Resumo	115
Abstract.....	116
Introduction	117
Materials and Methods	119
Results	123
Discussion.....	133
Supplementary Material	138
References	144
Capítulo 5 A ausência de NNT mitocondrial piora a capacidade de camundongos resolverem a infecção com <i>Leishmania amazonensis</i>	151
Resumo	151
Abstract.....	152
Introduction	153
Materials and Methods	153
Results	154
Discussion.....	157
References	159
Capítulo 6 Imunometabolismo de Células Dendríticas iCD103⁺ infectadas com <i>Leishmania infantum</i>	162
Resumo	162
Abstract.....	163
Introduction	164
Materials and methods.....	165
Results and Discussion	168
Discussão Geral e Conclusões	183
Resumo Geral	187
General abstract	188
Referências Bibliográficas	189

Anexos e Apêndices	204
Biografia Stephanie Maia Acuña	205
Títulos.....	205
Trajetória científica.....	205
Participação em Congressos e Simpósios:	205
Apresentação de Trabalhos:	206
Publicações	206
Trajetória acadêmica.....	207

Lista de Figuras

Figura 1. Painel demonstrativo das leishmanioses tegumentares.	17
Figura 2. Painel demonstrativo da leishmanioses visceral.....	19
Figura 3. Representação esquemática de macrófagos infectados com <i>Leishmania</i> spp. e seus possíveis fenótipos.....	25
Figura 4. Representação esquemática da biogênese de miRNAs.....	29
Figure 5. Melatonin inhibition of <i>L. amazonensis</i> infectivity in a dose dependent manner.	42
Figure 6. Quantification of mRNA involved in L-arginine transport and metabolism and NO production.	43
Figure 7 Cytokine and chemokines production after melatonin treatment and <i>L. amazonensis</i> infection.	44
Figure 8. Volcano plot showing melatonin modulation of miRNA profile in macrophages infected with <i>L. amazonensis</i> in a time dependent manner.....	46
Figure 9. Functional analysis of miR-181c, miR-294-5p, miR-30e and miR302d inhibition.	48
Figure 10. Infectivity of <i>L. amazonensis</i> in macrophages from WT, MyD88 ^{-/-} , TLR2 ^{-/-} or TLR4 ^{-/-} mice.	70
Figure 11. Lack of TLR signaling leads to differential expression of genes involved in the polyamine and NO production pathways.....	71
Figure 12. Volcano plot of the miRNA profiles of macrophages WT or MyD88, TLR2 and TLR4 null mice infected with <i>L. amazonensis</i>	73
Figure 13 Venn diagram representing unique and common miRNAs significantly expressed in macrophages from WT or MyD88, TLR2 and TLR4 null mice infected with <i>L. amazonensis</i>	74
Figure 14. Inhibition of let-7 functions increased gene modulation and reduced <i>L. amazonensis</i> infectivity.	76
Figure 15. Venn diagram representing unique and common mRNA of TLR pathway molecules and cytokines significantly expressed during let-7e inhibition in <i>L. amazonensis</i> infected macrophages.	78
Figure 16 Schematic representation of TLR pathway and let-7e-targets mRNAs.	83
Figure 17. MicroRNAs can regulate the inflammatory branch of L-arginine uptake and consumption of infected macrophages with <i>Leishmania amazonensis</i>	101
Figure 18. <i>In silico</i> microRNA binding prediction in the 3'UTR region of genes involved in L-arginine metabolism.....	102

Figure 19. Quantification of L-arginine metabolism-related gene transcripts and miRNA levels on macrophages infected with <i>L. amazonensis</i>.	104
Figure 20. miRNA functional inhibition.	106
Figure 21. <i>Tnfa</i> is an miR-294 and miR-301b target.	107
Figure 22. Infection index and NO production in C57BL/6 macrophages infected with <i>L. amazonensis</i> La-WT or La-arg⁻.	124
Figure 23. Partial least squares discriminant analysis (PLS-DA) and Orthogonal partial least-squares-discriminant analysis (OPLS-DA) analysis of variation between the two groups of <i>L. amazonensis</i> infected C57BL/6-macrophages.	125
Figure 24. Metabolic profile of infected macrophages with <i>L. amazonensis</i>.	128
Figure 25. Antioxidant systems glutathione and trypanothione.	129
Figure 26. Heatmap of 58 metabolites differentially modulated in the metabolomic analysis of macrophages infected with La-WT or La-arg⁻ versus uninfected macrophages.	130
Figure 27. Metabolic pathways associated with metabolite enrichment in <i>L. amazonensis</i> infected macrophages.	131
Figure 28. Modulation of metabolite content in the L-arginine metabolic pathways in macrophages infected with La-arg⁻ compared to La-WT.	132
Figure 29. Schematic representation of L-arginine metabolism in Leishmania-infected macrophages.	137
Figure 30. <i>In vitro</i>, and <i>in vivo</i>, infection with <i>L. amazonensis</i>.	155
Figure 31. Expression of <i>Nnt</i> transcripts during BMDM <i>L. amazonensis</i> infection.	156
Figure 32. <i>Tnfa</i> transcripts behavior in <i>L. amazonensis</i> BMDM infection.	156
Figure 33. Schematic view of the iCD103⁺-DC differentiation protocol.	169
Figure 34. iCD103⁺-DCs number and morphology along the differentiation protocol.	170
Figure 35. Infectivity of <i>L. infantum</i> into iCD103⁺-DCs.	171
Figure 36. <i>L. infantum</i> infected iCD103⁺-DCs maturity.	172
Figure 37. PCA samples group.	173
Figure 38. Top 20 enriched KEGG pathways.	174
Figure 39. Top 20 enriched GO terms.	175
Figure 40. Modulated genes FPKM comparison.	176

Figure 41. Modulated genes on the glycolytic pathway.	176
Figure 42. Glucose/Lactate Kinetics behavior during the early infection.....	178
Figure 43. Glycolysis pathway inhibition.....	178

Introdução Geral

1. As leishmanioses e seu agente etiológico: *Leishmania* spp.

Dentre os mais diversos tipos de classificação de doenças, há aquelas que são complexas, tanto em suas manifestações quanto ao diagnóstico, tratamento e, principalmente, prevenção. A Organização Mundial da Saúde (OMS / WHO – *World Health Organization*) define algumas dessas doenças complexas como Doenças Tropicais Negligenciadas (DNTs), que são um conjunto de vinte condições diferentes, que são prevalentes principalmente na faixa tropical do globo e são impactadas pelo clima, conservação ambiental, pobreza e desnutrição. Juntas, elas causam um enorme impacto na sociedade seja em saúde, ou mesmo a economia de países em desenvolvimento (“WHO | World Health Organization”, 2023). O grupo de doenças possui algumas parasitoses transmitidas por artrópodes, como a malária, doença de chagas, filariose linfática, entre outras das quais destacamos a leishmaniose. O Brasil, um imenso país tropical e com mais da metade da população vivendo em pobreza, é área endêmica para a leishmaniose.

As doenças conhecidas por leishmaniose são um conjunto de diferentes manifestações clínicas causadas por, ao menos, 20 espécies de protozoários parasitas pertencentes ao gênero *Leishmania* spp. Tais manifestações podem ser classificadas em três tipos principais: leishmaniose visceral (LV), cutânea (LC) e mucocutânea (LMC).

As leishmanioses tegumentares (LTs) são o conjunto formado por doenças que acometem o sistema tegumentar, podendo ser cutâneas ou mucocutâneas. A figura 1-A apresenta algumas das manifestações mais comuns das LTs: lesão clássica ulcerativa com bordas em vulcão (fig. 1-A1); lesões nodulares da leishmaniose cutânea difusa (fig. 1-A2) e lesões ulcerativas em regiões de mucosa como as fossas nasais (fig. 1-A3). Juntas, as LTs causam grande impacto social na vida dos pacientes acometidos, pois são doenças debilitantes e desfigurantes, gerando um grande estigma social. No Brasil, as espécies causadoras das LTs mais comuns são a *L. amazonensis* e *L. guyanensis* causadoras da forma cutânea e a *L. braziliensis*, causadora da mucocutânea (ALVAR *et al.*, 2012; PAN AMERICAN HEALTH ORGANIZATION, 2020).

Em todo o globo, países que ocupam a faixa tropical apresentam registros da doença. No ano de 2021, um total de 78 231 casos de LT foram notificados à OMS, sendo o Brasil e países do Oriente Médio os que tiveram os maiores números de casos (fig.1-B1). No Brasil, o número de casos reportados à Secretaria de Vigilância Sanitária do Ministério da Saúde (SVS/MS), no mesmo ano, foi de 15 023 casos (“Situação Epidemiológica da LT — Ministério da Saúde”, 2023). É possível observar que todo o território nacional apresenta casos, sendo o maior número concentrado na Região Norte do país (fig.1-B2). No entanto, estados do sudeste como o Estado de São Paulo também apresentam casos. Em 2021, o Estado de São Paulo registrou 202 casos de LT. Esses casos estão distribuídos de maneira irregular ao longo do território do estado (fig.1-B3). A vigilância epidemiológica é feita por municípios. Cada município reporta a existência ou ausência de casos a um Grupo de Vigilância Epidemiológica (GVE). O estado é dividido em 28 GVEs (fig.1-B3). No ano de 2021, o GVE responsável pela região da cidade de Registro, no sul do estado, registrou um total de 60 casos, sendo o GVE com o maior número de notificações. Já os GVEs da Capital e de Santo André foram os grupos

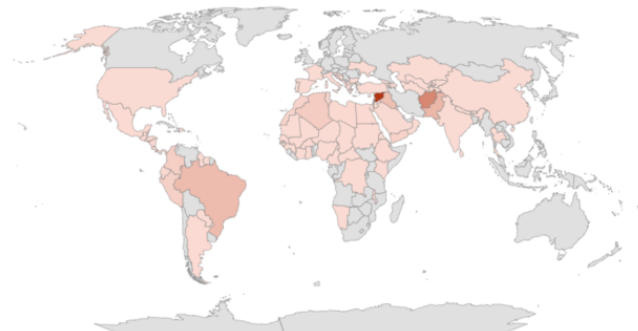
que não apresentaram nenhuma ocorrência de LT. No entanto, apesar de a cidade de São Paulo não ter registrado nenhum caso, cidades do entorno da Capital, registradas nos GVE de Osasco e Franco da Rocha, registraram juntas um total de 17 casos. É interessante apontar que cidades pertencentes a esses dois GVEs são consideradas cidades dormitório da Capital Paulista, podendo levar à cidade de São Paulo uma população flutuante portadora das enfermidades. Deve-se sempre lembrar que as leishmanioses possuem um forte componente socioeconômico que deixa as populações periféricas mais vulneráveis a contraírem a doença.

A. Manifestações Clínicas Mais Comuns

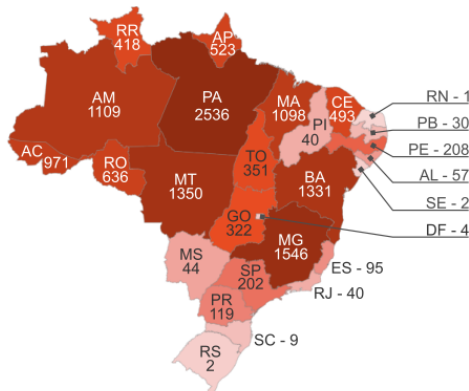


B. Epidemiologias - Mundial, no Brasil e no Estado de São Paulo. 2021.

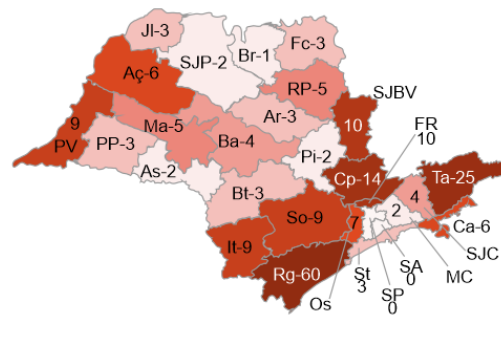
Casos Reportados 0 78231 Sem Dados



B1. Distribuição mundial da leishmaniose tegumentar. Dados OMS.



B2. Distribuição no Brasil. Dados SVS/MS.



B3. Distribuição Estado de São Paulo. Dados CVE/SP.

Figura 1. Painel demonstrativo das leishmanioses tegumentares. (A) Manifestações clínicas mais comuns das leishmanioses tegumentares, sendo: (A1) lesão clássica ulcerativa de leishmaniose cutânea com borda em vulcão. (A2) lesões nodulares da leishmaniose cutânea difusa; e (A3) lesão muco-cutânea ulcerativa. (B) Epidemias das leishmanioses tegumentares no mundo, no Brasil e no Estado de São Paulo em 2021. (B1) Distribuição global das leishmanioses tegumentares segundo notificação à OMS em 2021. Os países com coloração alaranjada apresentaram notificações, ainda que sem a detecção da doença em seu território. Os países de coloração acinzentada não apresentaram nenhuma notificação no ano de 2021. (B2) Número de casos notificados por Unidade Federativa à Secretaria de Vigilância Sanitária do Ministério da Saúde (SVS/MS) do Brasil. (B3) Número de casos notificados ao Centro de Vigilância Epidemiológica “Prof. Alexandre Vranjac”. Cada região representa um Grupo de Vigilância Epidemiológica (GVE). Em ordem alfabética, as abreviações são os nomes de cada GVE: Aç – Araçatuba. Ar – Araraquara. As – Assis. Ba – Bauru. Br – Barretos. Bt – Botucatu. Ca – Caraguatatuba. Cp – Campinas. Fc – Franca. FR – Franco da Rocha. It – Itapeva. Jl – Jales. Ma – Marília. MC – Mogi das Cruzes. Os – Osasco. Pi – Piracicaba. PP – Presidente Prudente. PV – Presidente Venceslau. Rg – Registro. RP – Ribeirão Preto. SA – Santo André. SJBV – São João da Boa Vista. SJC – São José dos Campos. SJP – São José do Rio Preto. So – Sorocaba. SP – São Paulo Capital. St – Santos. Ta – Taubaté. As imagens A2 e A3 foram extraídas do Atlas Interativo das Leishmanioses nas Américas, publicado pela Organização Pan Americana para a Saúde (OPAS/PAHO). Os mapas B1 e B2 foram produzidos pela ferramenta de mapas da Microsoft Bing. O mapa B3 é uma adaptação do mapa do CVE/SP de leishmanioses tegumentares de 2007 a 2019.

De igual maneira, a LV também possui um forte fator socioeconômico. A LV também conhecida como *Kala-Azar* (febre negra em hindi), é causada pelas espécies *Leishmania infantum* e *Leishmania donovani*, sendo a forma mais letal da doença, pois afeta órgãos internos como o fígado, baço e medula óssea. Os principais sintomas são: febre, anemia, hepatoesplenomegalia (crescimento anormal de fígado e baço), perda acentuada de peso, entre outros (fig.2-A). Sem o tratamento adequado leva cerca de 95% dos pacientes infectados à morte (PAN AMERICAN HEALTH ORGANIZATION, 2020). A subnotificação é um problema sério de saúde pública, pois estima-se que o número de novos casos da doença são de aproximadamente 50.000 a 90.000 por ano em todo o globo, porém apenas de 20 a 40% dos casos são reportados à OMS (“WHO | World Health Organization”, 2023). Ainda assim, no ano de 2021, 3 323 casos foram reportados à OMS (fig.2-B).

O Brasil está entre os países mais afetados do mundo, com uma média de 3.000 novos casos registrados por ano, segundo dados da SVS/MS (“Situação epidemiológica da Leishmaniose Visceral — Ministério da Saúde”, 2023). O último relatório da SVS/MS revelou que o número de casos registrados de LV (causados por *L. infantum*) no Brasil no ano de 2021 foram de 1.683 casos, sendo a Região Nordeste a mais afetada pela doença (fig.2-C1). Em todo o país, os homens de idades entre 20 e 49 anos foram os mais infectados, possivelmente por ser o grupo mais ativo em atividades florestais e peridomiciliares, onde podem ser infectados (fig.2-C2). A letalidade geral da doença foi de 10,5%, porém tem maiores taxas em crianças e idosos, chegando a cerca de 50% no último grupo (fig.2-C3). Apesar disso, houve um comportamento de redução no número de casos ao longo dos últimos 5 anos de registro (2017-2021), em que o ano de 2017 foi o de maior número de registro no período. O comportamento pode ser explicado pelo fato de que as políticas de controle da doença, combinados com o período pandêmico de COVID-19, favoreceram a diminuição dos números de casos no país. No entanto, a taxa de letalidade em 2021 foi a maior do período (fig.2-C3).

O Estado de São Paulo apresentou, em 2021, um total de 61 casos, porém não foi possível recuperar a informação sobre a localidade desses casos. Ainda assim, pôde-se acompanhar a evolução epidemiológica da doença ao longo do período que compreende os anos de 2017 a 2021 (fig.2-C4 e tabela 1), nos quais os casos registrados foram em apenas 12 GVEs ao longo dos 5 anos analisados.

A. Manifestações Clínicas B. Epidemiologia mundial em 2021.

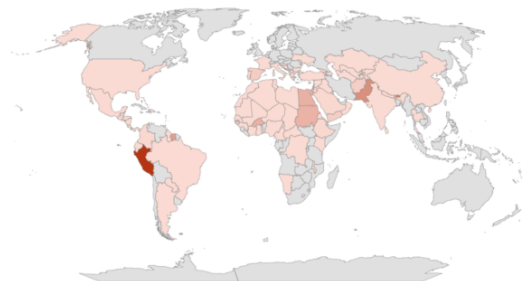


A1 - Adulto apresentando desnutrição e importante esplenomegalia.



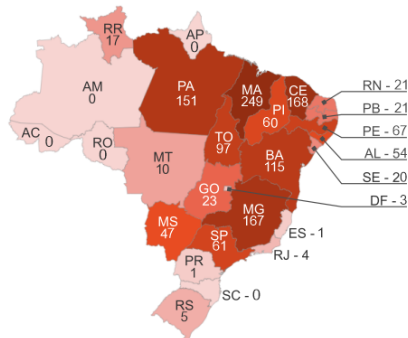
A2 - Criança apresentando icterícia, sinalizando lesão hepática

Casos Reportados 0 3323 Sem Dados

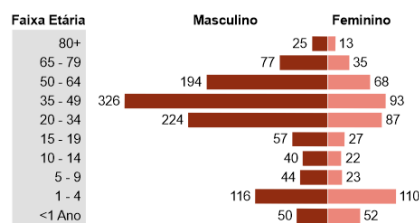


Distribuição mundial da leishmaniose visceral. Dados OMS.

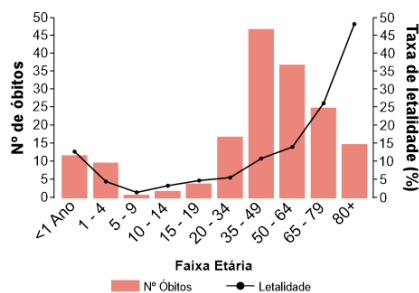
C. Dados epidemiológicos da Leishmaniose Visceral no Brasil em 2021.



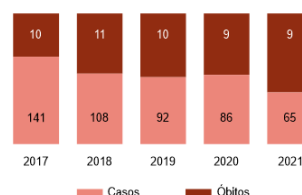
C1. Distribuição no Brasil. Dados SVS/MS.



C2. Distribuição de casos em faixa etária e gênero. Dados SVS/MS.



C3. Número de óbitos e taxa letalidade. Dados SVS/MS..



C4. Número de casos e óbitos no Estado de São Paulo. Dados CVE/SP.

Figura 2. Painel demonstrativo da leishmaniose visceral. (A) Manifestações clínicas mais comuns da leishmaniose visceral, sendo: (A1) Indivíduo adulto apresentando desnutrição severa com aumento importante do baço - esplenomegalia. (A2) olhos amarelados (icterícia) de uma criança infectada, indicando lesões hepáticas. (B) Epidemiologia mundial da leishmaniose visceral. Distribuição global segundo notificação à OMS em 2021. Os países com coloração alaranjada apresentaram notificações, ainda que sem a detecção da doença em seu território. Os países de coloração acinzentada não apresentaram nenhuma notificação no ano de 2021. (C) Dados epidemiológicos no Brasil no ano de 2021. (C1) Número de casos notificados por Unidade Federativa à Secretaria de Vigilância Sanitária do Ministério da Saúde (SVS/MS) do Brasil. (C2) Distribuição de casos por faixa etária e gênero, em todo o país. (C3) Distribuição de número de óbitos e taxa de letalidade por faixa etária, em todo o país. (C4) Número de casos confirmados e óbitos no Estado de São Paulo no período de 2017 a 2021. As imagens A1 e A2 foram extraídas do Atlas Interativo das Leishmanioses nas Américas, publicado pela Organização Pan Americana para a Saúde (OPAS/PAHO). Os mapas B e C1 foram produzidos pela ferramenta de mapas da Microsoft Bing. Os gráficos C2 e C3 são reproduções de material divulgado pela Secretaria de Vigilância Sanitária do Ministério da Saúde do Brasil. O gráfico C4 foi gerado a partir de dados disponibilizados pelo Centro de Vigilância Epidemiológica “Prof. Alexandre Vranjac” da Secretaria de Saúde do Estado de São Paulo.

Tabela 1. Número de casos de LV registrados por GVE no Estado de São Paulo, no período de 2017 a 2021.

GVE	2017		2018		2019		2020		2021	
	Casos	Obitos	Casos	Obitos	Casos	Obitos	Casos	Obitos	Casos	Obitos
Osasco	0	0	1	0	0	0	0	0	0	0
Araçatuba	31	4	33	3	22	4	20	2	29	4
Araraquara	0	0	0	0	1	0	0	0	0	0
Bauru	29	1	13	3	11	2	10	1	7	1
Botucatu	0	0	0	0	0	0	1	1	0	0
Marília	35	0	20	3	25	2	16	1	9	1
Pres. Prudente	5	1	2	0	6	0	8	0	5	0
Pre. Venceslau	31	2	22	0	16	0	24	4	10	2
Santos	1	0	0	0	0	0	0	0	0	0
S J Rio Preto	5	2	8	0	3	2	3	0	2	0
Jales	3	0	8	1	8	0	4	0	3	1
Sorocaba	1	0	1	1	0	0	0	0	0	0
Estado de São Paulo	141	10	108	11	92	10	86	9	65	9

Embora sejam ao menos 20 espécies causadoras das leishmanioses, o ciclo de vida do parasita é comum a todas às espécies, sendo todas elas uma importante zoonose, uma vez que o ser humano é um hospedeiro acidental para o parasita. O protozoário apresenta ciclo de vida dimórfico, isto é, apresenta duas formas morfológicamente distintas ao longo de seu ciclo: promastigotas e amastigotas. As formas promastigotas apresentam o corpo celular alongado e fusiforme, com flagelo aparente. São encontradas nos hospedeiros invertebrados, os flebotomíneos, insetos hematófagos pertencentes aos gêneros *Lutzomya* e *Phlebotomus*, presentes nas Américas e Eurásia, respectivamente. Esses insetos, que são popularmente chamados de mosquito-palha no Brasil, transmitem os parasitas ao hospedeiro vertebrado durante o repasto sanguíneo. Quando os parasitas entram no hospedeiro vertebrado, são rapidamente fagocitados por células do sistema imune, onde sofrem um processo de diferenciação para a forma amastigota. Tal forma apresenta formato arredondado, com encolhimento do flagelo e habitam em um ambiente ácido e hostil.

2. Resposta imune de hospedeiros vertebrados à *Leishmania*

Tão logo os parasitas são injetados, na pele dos vertebrados, são reconhecidos por células fagocíticas como macrófagos residentes, neutrófilos e células dendríticas (BOGDAN, CHRISTIAN, 2008). Apesar de cada tipo celular desempenhar um papel importante na resposta contra a *Leishmania*, elas são capazes de reconhecer os parasitas de forma similar: por meio do reconhecimento de padrões. Essas células são recobertas de receptores reconhecedores de padrão (PRRs – *Pattern recognition receptors*), que são capazes de reconhecer padrões moleculares associados a patógenos (PAMPs – *Pathogen associated molecular pattern*) ou a danos celulares e teciduais (DAMPs – *Damage associated molecular pattern*). Tal evento leva ao início de uma cascata de sinalização, ativando uma resposta imunológica. Os PRRs mais conhecidos por serem ativados por *Leishmania* são os Receptores Semelhantes a Toll (TLR – *Toll-like receptors*) e os Receptores Semelhantes a NOD (NLRs – *Nucleotide-binding and oligomerization domain NOD-like receptors*)(LIMA-JUNIOR *et al.*, 2013a). Neste trabalho daremos destaque aos TLRs.

Os TLRs pertencem a uma família altamente conservada de proteínas de membrana, a qual os mamíferos possuem 12 genes codificantes. Todos os representantes são glicoproteínas, com domínios transmembrana, de reconhecimento e transdução de sinal, fazendo a ponte entre o ambiente externo à célula com o citoplasma. Essa transdução de sinal é feita por meio de uma cascata de sinalização, em que há a participação de diversas outras moléculas. Isso ocorre porque a porção citosólica dos TLRs, chamada de domínio TIR (*Toll-Interleukin-1 receptor (TIR) homology domain*), é capaz de interagir com proteínas adaptadoras que também apresentam o domínio TIR. Elas são: MyD88 (*Myeloid differentiation primary response 88*), TIRAP (*TIR-domain-containing adapter protein*), TRIF (*TIR-domain-containing adapter-inducing interferon- β*) e TRAM (*TRIF-related adapter molecule*) (AKIRA; SATO, 2003; TAKEDA; KAISHO; AKIRA, 2003; UEMATSU; AKIRA, 2006). Diferentes combinações dessas moléculas, em conjunto com os TLRs, são capazes de definir o tipo de resposta que será executada. De modo geral, todas as respostas ativam a translocação de fatores de transcrição – moléculas iniciadoras da transcrição da informação em DNA para RNA – para o núcleo, expressão de moléculas efetoras e recrutamento de outras células (TAKEDA; KAISHO; AKIRA, 2003). Os fatores de transcrição ativados pelas vias de TLR que geralmente são associados a atividades pró-inflamatórias, são NF- κ B (*Nuclear factor kappa-light-chain-enhancer of activated B cells*), AP-1 (*Activator Protein-1*), IRF3 e IRF7 (*Interferon Response Factors*)(TAKEDA; KAISHO; AKIRA, 2003).

A *Leishmania* possui PAMPs que são reconhecidos pelos PRRs (FARIA; REIS; LIMA, 2012a; TUON *et al.*, 2008). Por exemplo, o receptor TLR2 é ativado diretamente por lipofosfoglicano (LPG) de *L. major* (BECKER *et al.*, 2003). Também foi verificado que o LPG de outras espécies pode ativar ao TLR2: *L. mexicana*, *L. aethiopica* e *L. tropica* (DE VEER *et al.*, 2003). Além disso, o TLR4 também foi demonstrado como sendo um receptor importante na resolução de lesões causadas por *L. major* (KROPF *et al.*, 2004). O TLR9 reconhece padrões de ácidos nucleicos estrangeiros, sendo ativado, também por *L. donovani*, *L. major* e *L. brasiliensis* (Liese *et al.*, 2007; Schleicher *et al.*, 2007; Weinkopff *et al.*, 2013).

A ativação desses receptores também leva à produção e secreção de citocinas, moléculas sinalizadoras do tipo de respostas iniciada no interior dos fagócitos. Perfis pró-inflamatórios

possuem como citocinas clássicas: TNF α , IL-1, IL-6 e IL-12. sendo a última de extrema importância para a sinalização de respostas do tipo 1 em linfócitos T CD4⁺ (T_h1 – T auxiliar – *helper* 1) (ACUÑA *et al.*, 2022; BACELLAR *et al.*, 2000; DONNELLY *et al.*, 1995; LIMA-JUNIOR *et al.*, 2013a; STÄGER *et al.*, 2006; TANNAHILL *et al.*, 2013a; “The Induction of IL-1 β Secretion Through the NLRP3 Inflammasome During Ebola Virus Infection.”, [S.d.]; WILHELM *et al.*, 2001). Ainda, há a secreção de quimiocinas, moléculas que promovem o recrutamento de outros leucócitos ao sítio da lesão, dentre as quais destacam-se: MCP-1 e RANTES(FERNANDES *et al.*, 2019b). Para além das respostas do tipo 1, há a resposta alternativa ou anti-inflamatória, ao qual a citocina IL-10 é a mais relevante e promove a polarização de células T CD4⁺ para o tipo 2 (T_h2) (BACELLAR *et al.*, 2000; DONNELLY *et al.*, 1995; DOWLING *et al.*, 2021b; FILARDY *et al.*, 2010a; KANE; MOSSER, 2001; O’FARRELL *et al.*, 1998; STÄGER *et al.*, 2006; VERRECK *et al.*, 2004). A imunidade adquirida possui maior especificidade nas respostas frente aos patógenos ou danos quaisquer, sendo os linfócitos os principais atores de tal resposta. Neste contexto, macrófagos e dendríticas possuem papel fundamental, pois fazem a apresentação dos antígenos aos linfócitos (APCs – células apresentadoras de antígeno profissionais – *professional antigen presenter cells*), ativando-os e polarizando-os nos auxiliares 1 ou 2 (DIEFENBACH, 1999; FILARDY *et al.*, 2010a; GHALIB *et al.*, 1995; HSIEH *et al.*, 1993; SHWEASH *et al.*, 2011; STÄGER *et al.*, 2006).

No contexto de infecção com *Leishmania*, as respostas do tipo 1 são eficientes na eliminação dos parasitas, uma vez que a produção de interferon gamma (IFN γ) por parte de células T_h1 ativa aos macrófagos e promove a produção de óxido nítrico (NO) e espécies reativas de oxigênio no interior dos fagolisossomos (WALKER *et al.*, 1999). Caso as respostas do tipo 2 sejam ativadas, o parasita é capaz de sobreviver, já que a produção de IL-4 por parte dos T_h2 promove a produção de moléculas importantes para a restauração do tecido lesionado, às quais *Leishmania* pode consumir em seu benefício próprio, estimulando, além de sua sobrevivência, a proliferação dos parasitas nas células infectadas(SÉGUIN; DESCOTEAUX, 2016).

3. Metabolismo da célula hospedeira em resposta à infecção

O imunometabolismo estuda como cada célula imune é capaz de usar a energia ou as substâncias que produz e/ou capta do ambiente externo a elas, e usam na manutenção de suas atividades. Resumindo, é compreender quais substratos são necessários para cada tipo de resposta em determinado grupo de células imunes. Assim, da mesma maneira que os estudos clássicos de metabolismo são divididos, o imunometabolismo também pode ser classificado em metabolismo energético, redox e o metabolismo de classes de moléculas, como os açúcares, aminoácidos e os lipídios.

3.1. Metabolismo energético

A maneira como cada célula produz suas moléculas de ATP diz muito sobre suas atividades. De modo geral, as células usam a glicose como molécula de primeira escolha na produção de ATP. Para tanto, o açúcar é quebrado e oxidado a piruvato por meio da via glicolítica (fig. 3). O piruvato, no entanto, pode ser reduzido a lactato, formando ATP ao que se chama respiração anaeróbica, que geralmente ocorre na ausência de oxigênio (BARTRONS; CARO, 2007). Além disso, o piruvato pode doar dois carbonos à coenzima CoA, formando o Acetil-CoA, que alimenta o ciclo do ácido tricarboxílico (TCA ou Krebs), que por sua vez alimenta a cadeia de transporte de elétrons, que culmina na produção de ATP por meio da fosforilação oxidativa (OXPHOS) (fig. 3). Embora a OXPHOS produza uma maior quantidade de moléculas de ATP, o processo é demorado e geralmente está associado a atividades quiescentes ou em que o tempo de produção não seja uma variável a ser considerada. Por isso, quando há a necessidade de produção rápida de ATP, a fermentação a lactato pode ser a via de escolha, ainda que haja oxigênio no meio. A isto denomina-se Efeito Warburg (BARTRONS; CARO, 2007)

Tomemos o exemplo dos macrófagos. A ativação clássica do perfil pró-inflamatório (M1) desativa a OXPHOS e favorece a produção de ATP pela via glicolítica, mesmo na presença de oxigênio (O'NEILL; KISHTON; RATHMELL, 2016a; RYAN; O'NEILL, 2020b). Este efeito ocorre nos macrófagos por causa da ativação, via TLRs, da via de sinalização da AMPK (*AMP-activated protein kinase*) (STEIN *et al.*, 2000). A via é ativada pela queda dos níveis de ATP (adenosina tri-fosfato) na célula e aumento de ADP e AMP (adenosina di- e mono-fosfato), indicando um déficit energético, que sinaliza a mudança da produção de ATP de OXPHOS para glicólise (STEIN *et al.*, 2000). O fim desta via é o fator de transcrição HIF1 α (*hypoxia induced fator 1 alpha*), que mobiliza a maquinaria celular para a glicólise, permitindo o uso do oxigênio na produção de espécies reativas de oxigênio e/ou nitrogênio (DENGLER, 2020; WINTERBOURN, 2008), produzido nos fagolisossomos. As enzimas envolvidas no processo são a NADPH oxidase 1 e 2 (NOX2) e a Óxido Nítrico Sintase 2 (NOS2) (NATHAN; XIE, 1994). Ambas usam o oxigênio como acceptor de elétrons. Além disso, a molécula de óxido nítrico (NO), por si só é um inibidor potente da função mitocondrial, contribuindo para a inibição da OXPHOS (NISOLI *et al.*, 2004). No entanto, se os macrófagos assumirem um perfil de ativação classicamente conhecido como anti-inflamatório (M2), a produção de ATP é feita preferencialmente por meio da OXPHOS (BLAGIH; JONES, 2012b; LOCATI; CURTALE; MANTOVANI, 2020b; RYAN; O'NEILL, 2020b; VIOLA *et al.*, 2019b; WANG, YAFANG *et al.*, 2021). É importante ressaltar que a ativação clássica dos macrófagos no espectro em M1-pró-inflamatório e M2-anti-inflamatório; deixa de lado a existência de outros perfis de ativação,

com padrões de respiração, secreção de citocinas e quimiocinas diversos (NAKAI *et al.*, 2017; SHEN *et al.*, 2018). Neste trabalho, abordamos aspectos concernentes aos macrófagos M1 e M2 clássicos.

No contexto da leishmaniose, os fenótipos de ativação são diversos e influenciam no prognóstico da doença. Nosso grupo identificou anteriormente que macrófagos murinos infectados com *L. amazonensis* apresentaram um perfil transcriptômico misto entre M1 e M2 (AOKI, J I *et al.*, 2019; AOKI, J.I.; MUXEL; ZAMPIERI; LARANJEIRA-SILVA; *et al.*, 2017a). Corroborando com nossos achados anteriores, SCORZA (e CARVALHO; WILSON, 2017), apresentaram uma revisão sobre a severidade do grau de lesão de pacientes correlacionada com o fenótipo do macrófago encontrado no local. É possível notar que a maneira como os macrófagos sinalizam e usam os nutrientes provoca uma resposta dos linfócitos T CD4+, provocando a diferenciação em Th1 e Th2 (MOREIRA *et al.*, 2015).

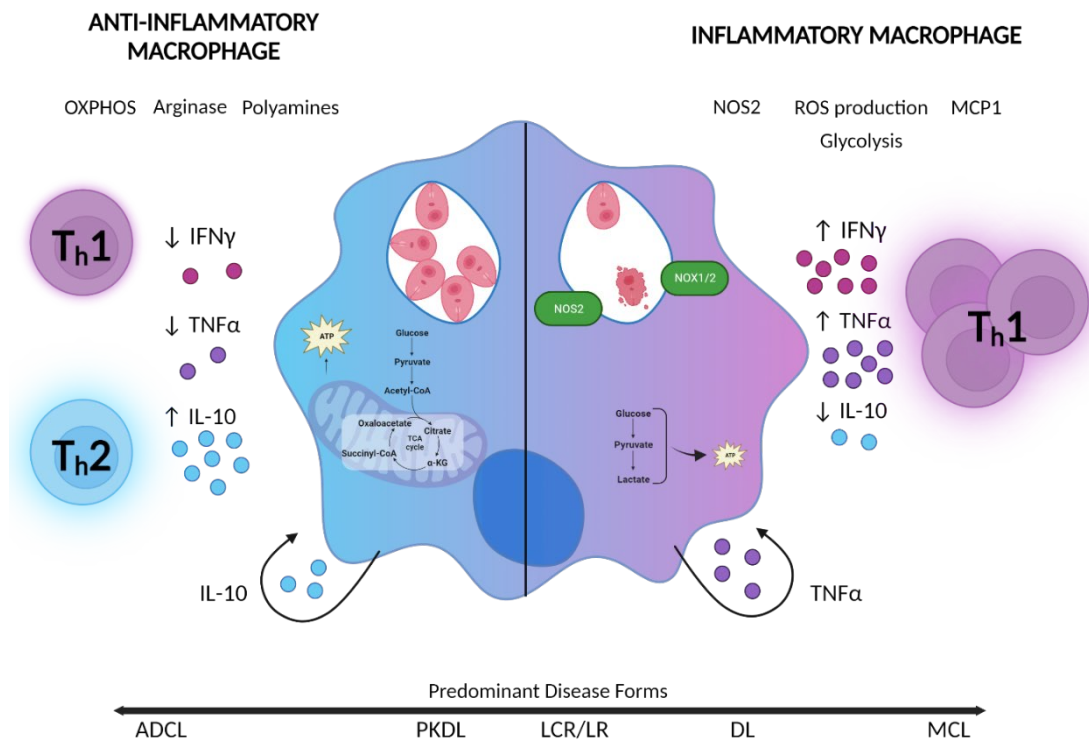
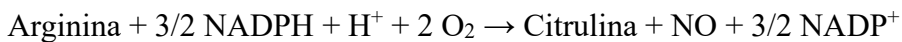


Figura 3. Representação esquemática de macrófagos infectados com *Leishmania* spp. e seus possíveis fenótipos. Quando macrófagos são infectados com *Leishmania*, apresentam fenótipos dentro de um espectro de ativação. Tais fenótipos favorecem a proliferação parasitária ou controle de infecção. À esquerda do quadro, estão representadas as características predominantes de macrófagos com fenótipo mais anti-inflamatório: produção de energia por meio de OXPHOS, aumento da atividade de arginase e produção de poliaminas. Além disso, apresentam sinalização por meio de IL-10, que ativa a linfócitos Th2, que produzem mais IL-10. Tais sinalizações e fluxos metabólicos favorecem a proliferação do parasita. À direita do quadro, estão representadas as características de fenótipos mais inflamatórios, em que há a geração de ATP por meio da via glicolítica, produção de espécies reativas de oxigênio/nitrogênio pelas enzimas NOX1/2 e NOS2, respectivamente. Quanto à sinalização, há secreção de TNF α por parte dos macrófagos, que sinaliza a ativação de linfócitos Th1. Estes passam a secretar mais TNF α , além da produção de IFN γ , ativando ainda mais aos macrófagos. Na parte inferior do quadro é possível ver uma régua com o posicionamento das formas de lesão predominantes em leishmaniose tegumentar, de acordo com o fenótipo apresentado pelos macrófagos, respeitando a existência de perfis mistos. As siglas representam, da esquerda para a direita: ADCL – anergic diffuse cutaneous leishmaniasis; PKDL – Post kala-azar dermal leishmaniasis; LCR/LR – Localized Cutaneous Leishmaniasis; DL – Disseminated Leishmaniasis; MCL – Mucocutaneous leishmaniasis. Adaptado de Scorza (et al, 2017). Feito com BioRender App.

3.2. Metabolismo de arginina e outros aminoácidos

O espectro de ativação dos macrófagos também altera a forma como a célula metaboliza alguns aminoácidos como a L-arginina. Respostas com perfil M1 utilizam L-arginina para a produção de NO, enquanto respostas M2 usam a L-arginina para a produção de poliaminas e outras moléculas reparadoras de danos (BRONTE; ZANOVELLO, 2005)

Ambas as respostas são dependentes da concentração intracelular de L-arginina e estimulam a expressão dos transportadores CAT1 e CAT2B (*Cationic Aminoacid Transporter 1 e 2B*, respetivamente) do macrófago, aumentando a tomada de L-arginina (WANASEN, NANCHAYA *et al.*, 2007a; WANASEN, NANCHAYA; SOONG, 2008a; YERAMIAN, ANDREE; MARTIN-JAULAR; SOLER, 2006). Para as respostas do tipo Th1, após a tomada de arginina pelos transportadores, a NOS2 se liga ao substrato e inicia a reação de oxidação do nitrogênio do grupo guanidino da arginina, por meio de uma cadeia de transporte de elétrons, dependente de FAD, FMN, o grupo heme e tetrahydrobiopterina (HB4), obedecendo à equação:



Durante a reação, se não houver oxigênio suficiente, ocorre a doação de elétrons para o oxigênio, gerando espécies reativas de oxigênio (ROS) além das espécies reativas de nitrogênio (RNS) dos quais o NO se destaca (NATHAN; CUNNINGHAM-BUSSEL, 2013). NO é um radical livre abundante em sistemas biológicos, pois além de seu papel microbicida, existe o papel de sinalização celular que é a ele atribuído (PACHER; BECKMAN; LIAUDET, 2007). Sua curta meia vida dificulta os métodos de identificação e quantificação, sendo a maioria dos métodos realizados por via indireta, pela quantificação de nitritos no sobrenadante das culturas celulares que possuem NOS ativas (BRYAN; GRISHAM, 2007). No contexto da infecção por *Leishmania*, essa é uma das respostas imune que leva à morte dos parasitas (BOGDAN, C., 2001; BOGDAN, C, 2001; SCHINDLER; BOGDAN, 2001).

As respostas do tipo Th2 induzem a atividade enzimática da arginase 1 (ARG1) nos macrófagos. Essa é uma resposta reparadora do tecido lesado pela infecção é importante no controle de patógenos extracelulares (MURRAY, P. J.; WYNN, 2011; MURRAY, PETER J.; WYNN, 2011). A ARG1 cliva a L-arginina gerando ureia e ornitina e esta será utilizada para a produção de poliaminas via Ornitina Descarboxilase (ODC) (DUQUE-CORREA *et al.*, 2014). As poliaminas são responsáveis em promover a proliferação celular (BRONTE; ZANOVELLO, 2005). A infecção por *Leishmania* possui uma alteração especial na resposta, uma vez que a subverte de modo a privilegiar respostas do tipo Th2, resultando na proliferação dos parasitas (INIESTA, VIRGINIA *et al.*, 2002). Quando a ARG1 é bloqueada, há controle do crescimento do parasita (GOLDMAN-PINKOVICH *et al.*, 2016; MUXEL, S.M.; AOKI; *et al.*, 2018b). Para respostas a patógenos extracelulares, como helmintos, as poliaminas bloqueiam a motilidade do parasita (ESSER-VON BIEREN *et al.*, 2013; WANASEN, NANCHAYA; SOONG, 2008a). Efeito oposto ao observado para infecções por *Leishmania* (BOGDAN, CHRISTIAN, 2008; GREEN *et al.*, 1990).

3.3. Metabolismo redox

Além da respiração celular, a resposta inflamatória produz e ROS e RNS de modo a controlar a infecção parasitária. A produção destas moléculas pode ser danosa ao próprio sistema, uma vez que essas espécies reativas também promovem a degradação de moléculas do hospedeiro e gerar dano tecidual. Essas espécies podem ser o ânion superóxido, ($O_2^{\cdot-}$), NO, peróxido de hidrogênio (H_2O_2), peroxinitritos, radical hidroxila e o ácido hipocloroso/hipoclorito (HALLIWELL, 2006). Essas moléculas realizam a degradação de outras moléculas por meio de diversas reações, em que ocorre um intenso fluxo de elétrons, por isso são denominadas de reações de redução e oxidação, ou simplesmente redox. No contexto inflamatório, o desbalanço redox pode exacerbar a inflamação por gerar DAMPs (HALLIWELL, 2006).

O equilíbrio do balanço redox é alcançado por diversos mecanismos, alguns intracelulares e outros de ação sistêmica. A maioria desses sistemas está baseado na oxidação e redução de moléculas de sacrifício, como no caso da glutathione (DEMIRKOL; ERCAL, 2014; MARÍ *et al.*, 2009; RIBAS; GARCÍA-RUIZ; FERNÁNDEZ-CHECA, 2014b). Esta molécula está em abundância no organismo, auxiliando na prevenção de danos. Devido à sua alta concentração, ela é oxidada quando os níveis de espécies reativas aumentam, resultando na desativação destas. A glutathione oxidada precisa ser reduzida, para estar novamente disponível para a oxidação. Essa reciclagem é mediada por enzimas dependentes de NADPH como co-fator (KUSAKABE; KUNINAKA; YOSHINO, 1982).

O NADPH está compartimentalizado nas células, estando presente tanto no citosol como no interior mitocondrial. No entanto a produção do co-fator é independente em ambos os compartimentos. No citosol, a via metabólica das pentoses-fosfato produz o *pool* do compartimento; enquanto na mitocôndria a produção é feita por três vias redundantes: enzimas málicas (isoformas da Malato Desidrogenase), Isocitrato Desidrogenase (IDH2) e a enzima Trans-hidrogenase de Nucleotídeos de Nicotinamida (NNT – Nicotinamide Nucleotide Transhydrogenase), que sozinha é responsável por cerca de 50% da produção de NADPH mitocondrial (RONCHI, JULIANA APARECIDA *et al.*, 2016).

A NNT produz o NADPH aproveitando a força iônica gerada pelo potencial da membrana interna da mitocôndria, gerado pela cadeia de transporte de elétrons. Ou seja, quanto maior a atividade de respiração mitocondrial, maior a eficiência do sistema de antioxidação. Este processo foi bem descrito em ratos (*Rattus norvegicus*) e humanos, porém permaneceu desconhecido em camundongos (*Mus musculus*) até 2006, quando foi descrita uma mutação espontânea no locus de *Nnt* de indivíduos da linhagem C57BL/6J (HUANG *et al.*, 2006), gerando nocautes naturais para a enzima. As demais linhagens apresentam o locus selvagem.

Embora a deleção da NNT em camundongos C57BL/6J não seja letal, traz prejuízos ao balanço redox mitocondrial, pois, em situações de estresse, a quantidade de NADPH disponível para detoxificar a célula do excesso de H_2O_2 produzida não é suficiente, gerando um dano que aparenta ser permanente. Assim, esses animais são mais susceptíveis aos efeitos do envelhecimento, quando ocorre um acúmulo de espécies reativas nas células; mais propensos a terem distúrbios metabólicos (FONTAINE; DAVIS, 2016). Há poucos estudos do efeito da diminuição do NADPH mitocondrial em contextos infecciosos e/ou inflamatórios, sendo um campo aberto à exploração.

4. Regulação da expressão gênica na célula hospedeira mediados por miRNAs

4.1. Função e biogênese de microRNAs

Descrevemos, até este ponto, como células do sistema imune são capazes de reconhecerem sinais de *Leishmania* e suas reações, seja na produção de moléculas sinalizadoras ou respostas efetoras contra o parasita. Tais respostas possuem diversos graus de complexidade, o que torna o sistema passível de regulação. Tal regulação pode ser dividida em níveis, fases e localizações. Quanto à localidade, podem ser respostas sistêmicas ou locais, e ainda serem subdivididas em extra ou intracelulares. Quanto às fases podemos descrevê-las quanto à duração da resposta, sendo aguda ou crônica. Já em relação aos níveis, podem ser descritos de acordo com o processo celular que está regulando, seja antes ou depois da transcrição; migração da mensagem do núcleo para o citoplasma; tradução da mensagem em proteína e a disponibilidade da proteína em exercer sua atividade. Neste trabalho, nós exploramos a regulação intracelular no nível pós-transcricional, mediada por microRNAs (miRNAs), durante a fase aguda de macrófagos infectados com *Leishmania amazonensis*.

Os miRNAs são pequenas moléculas de RNA de aproximadamente 20 nucleotídeos, não codificadores de proteínas, que promovem regulações pós-transcricionais dos genes-alvo. São transcritos a partir de lócus gênicos específicos de um ou mais miRNAs (mono ou policistrônicos) e são codificados a partir de regiões intragênicas, exônicas, intrônicas ou na fita anti-senso. Sua biogênese ocorre a partir da transcrição em fitas de miRNAs primários (pri-miRNA) que possuem conformação em dupla-fita em forma de grampo. Ainda no núcleo, pri-miRNAs são clivados pelo complexo formado pelas proteínas Drosha (também conhecida por RN3 – antirribonuclease 3) e a proteína DGCR8 (DiGeorge Critical Region 8). Essa clivagem gera uma estrutura de fita-dupla em grampo denominada pre-miRNA. Este é exportado para o citosol através da exportina 5. Ao chegar ao citosol o pre-miRNA é acoplado às enzimas Dicer e TRBP (transactivation response element RNA-binding protein – molécula adaptadora) que clivam o grampo de RNA dupla fita deixando as duas fitas livres. Uma das fitas utilizada na formação do miRISC (miRNA induced silencing complex) é complementar às sequências-alvo do mRNA e em conjunto com uma proteína argonauta (AGO 1-4) promove o silenciamento de sua expressão (BARTEL, 2004; DAVIS-DUSENBERY; HATA, 2010; KIM; HAN; SIOMI, 2009). O silenciamento pode ocorrer das seguintes formas: deadenilação e decapeamento, com subsequente direcionamento desses mRNAs silenciados para o P body onde podem ser armazenados ou degradados; bloqueio de início de tradução, pela repressão do cap ou impossibilitando a junção da subunidade 60S do complexo ribossomal, nessa abordagem também há o direcionamento para o P body; proteólise da proteína nascente; e, finalmente bloqueio da elongação pela retardação da reação ou inibição do ribossomo. A figura 3 apresenta um modelo de biogênese dos miRNAs (ACUÑA; FLOETER-WINTER; MUXEL, 2020b; BARTEL, 2004; DAVIS-DUSENBERY; HATA, 2010; KIM; HAN; SIOMI, 2009).

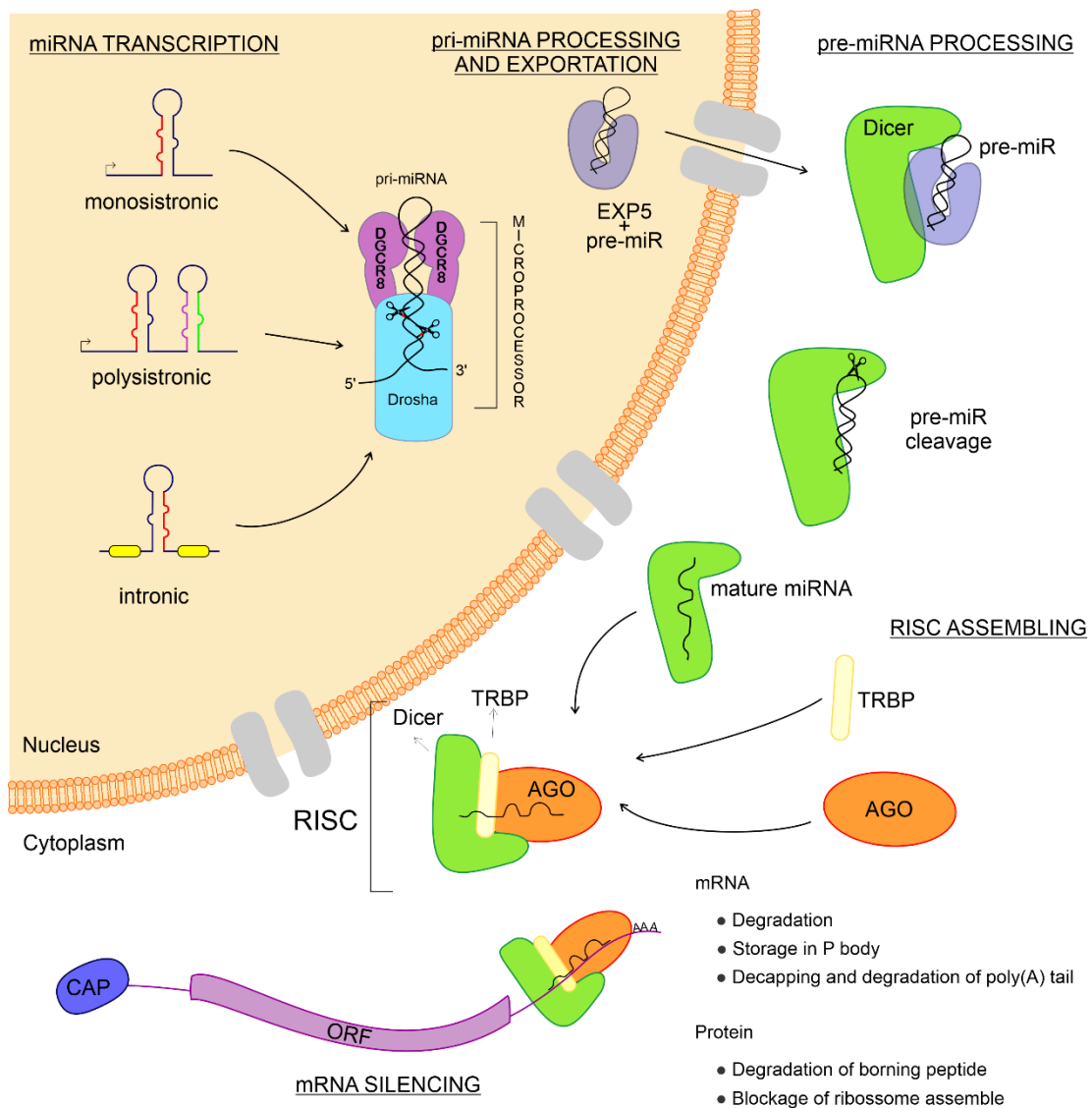


Figura 4. Representação esquemática da biogênese de miRNAs. Os miRNAs são pequenas moléculas de RNA não codificante que são transcritos a partir de seqüências de DNA que podem ser monossistêmicas ou polissistêmicas; presentes no interior de éxons, introns ou um gene único para eles. Após a transcrição, esse novo RNA é denominado miRNA primário (pri-miRNA). Este está arranjado em uma estrutura de grampo, que é complexado com o microprocessador: um complexo formado pelas enzimas DGCR8 e a RNase Drosha, que juntas clivam o pri-miRNA, formando o miRNA precursor (pre-miRNA). O pre-miRNA é então exportado para o citosol por meio da Exportina 5. No citosol, o pre-miRNA é complexado com a enzima Dicer, que cliva o pre-miRNA, formando o miRNA maduro. Quando maduro, o complexo miRNA-Dicer liga-se com as proteínas Argonata e TRBP, formando o complexo de silenciamento induzido por RNA (RISC). O RISC formado é capaz de se ligar a mRNAs-alvo, que serão silenciados, regulando a expressão gênica em nível pós-transcricional. Extraído de.(ACUÑA; FLOETER-WINTER; MUXEL, 2020b).

4.2. Regulação do perfil de miRNA em contexto da infecção com *Leishmania*

Embora os miRNAs sejam muitos e tenham funções variadas, eles auxiliam na regulação das respostas, seja no contexto inflamatório ou anti-inflamatório. Por exemplo, alguns miRNAs foram identificados regulando o processo de polarização dos macrófagos no espectro M1/M2, sendo os miR-146 e miR-210 mais relacionados ao polo M1; e os miR-130a, miR-130b, miR-155, miR-21, miR-19a, miR-23a, miR-125a, miR-125b, miR-26a, miR-26b e miR-720, relacionados com o polo M2 (ACUÑA; FLOETER-WINTER; MUXEL, 2020b; LI, H. *et al.*, 2018b). Isso indica que durante processos infecciosos, como no caso da infecção com *Leishmania*, o enquadramento do macrófago infectado no espectro M1/M2 também pode apresentar alteração no perfil de miRNAs.

Estudos anteriores descreveram a modulação da expressão de miRNAs em macrófagos infectados com *L. amazonensis*, *L. infantum*, *L. major* e *L. donovani*, conforme revisamos anteriormente (ACUÑA; FLOETER-WINTER; MUXEL, 2020b). Os estudos demonstram que a infecção com *Leishmania* pode ser um fator perturbador do perfil de miRNAs e que o parasita o faz de diversas maneiras. Em 2013, (GHOSH *et al.*, 2013a) apresentaram dados que indicam que a glicoproteína GP63 de *L. donovani* inibe a atividade da Dicer1 no fígado de camundongos BALB/C, de modo a diminuir a maturação de miR-122, responsável pela regulação dos níveis séricos de lipídios, conferindo maior sobrevivência ao parasita. Posteriormente, LEMAIRE (MKANNEZ; GUERFALI; GUSTIN; ATTIA; RENARD; *et al.*, 2013) apresentaram dados sobre a modulação do perfil de miRNAs de macrófagos humanos derivados de PBMC (células mononucleares de sangue periférico) infectados com *L. major*. Alguns dos miRNAs identificados haviam sido descritos, anteriormente, como importantes na regulação da atividade apoptótica como miR-210, miR-22, miR-155 e miR-133b. O miR-210 apresentou a expressão alterada ao longo do curso da infecção e tem a transcrição parcialmente controlada pelo fator de transcrição HIF1 α , mas seu silenciamento neste contexto não interfere na apoptose durante a infecção com *L. major*. Anos mais tarde, (KUMAR *et al.*, 2018b) demonstraram que *L. donovani* ativa o HIF-1 α em conjunto com miR-210, diminuindo a expressão e ativação de NF- κ B, modulando a resposta inflamatória. Em outro estudo, a autofagia em macrófagos infectados com *L. major* é relacionada com a expressão de miR-101c, miR-129 e miR-210 (FRANK *et al.*, 2015).

Outros estudos apresentam a expressão de outros miRNAs durante a infecção com *Leishmania*. Assim como no caso de PBMCs murinas infectadas com *L. donovani*, apresentarem um aumento na expressão de miR-21. O bloqueio de miR-21 aumenta a expressão de IL-12 mRNA em DCs murinas infectadas com *L. donovani*, levando a proliferação de células T CD4⁺ (VARIKUTI *et al.*, 2021).

No caso de pacientes que apresentaram leishmaniose cutânea localizada (LCL), causada por *L. brasiliensis*, foi observado um aumento da expressão de miR-361-3p no local da lesão, comparado à pele saudável do mesmo paciente. miR-361-3p já foi demonstrado como regulador de TNF, além de ser um bom biomarcador para o prognóstico da evolução da doença (LAGO *et al.*, 2018). Pacientes de LCL causada por *L. brasiliensis* também apresentam expressão de miR-193b e miR-671, correlacionando-os com a expressão de seus genes-alvo: CD40 e TNFR.

A espécie *L. infantum* conhecida por causar LV em humanos, também é responsável por causar a leishmaniose canina. Foi observado que a infecção com a espécie causou um aumento

na expressão de miR-346 em macrófagos humanos derivados de U937 e THP-1 (DIOTALLEVI, A. *et al.*, 2018). Também em macrófagos canino derivados de DH82 e no plasma de cães naturalmente infectados (BUFFI *et al.*, 2022). miR-364 está associado à redução de transcritos de genes relacionados à apresentação de antígeno via MHC classe I e II, como TAP1, RFX1 e BCAP31. Além disso, a leishmaniose visceral canina em cães sintomáticos naturalmente infectados com *L. infantum* mostrou a modulação diferencial de miR-150, miR-451, miR-192, miR-194 e miR-371 em PBMCs, que podem atingir genes para regular a resposta imune e patogênese, como NF- κ B, TNF- α , CD80 e IFN- γ , que são moléculas relacionadas à resistência contra a doença (SOARES *et al.*, 2021). Além disso, cães naturalmente infectados apresentam uma redução significativa de miR-122-5p em exossomas circulantes no plasma (DI LORIA *et al.*, 2020). Também houve a observação do aumento da expressão de miR-21 em leucócitos de baço de cães infectados. A inibição funcional de miR-21 levou a à diminuição da produção de IL-10. Além disso, miR-21 também regula a expressão de CD69 das células B (BRAGATO *et al.*, 2022).

Nosso grupo mostrou que a *L. amazonensis* modula a expressão de miRNA em macrófagos de camundongos BALB/c e C57BL/6 (MUXEL, SANDRA MARCIA; LARANJEIRA-SILVA; ZAMPIERI; FLOETER-WINTER, 2017a; MUXEL, S.M.; LARANJEIRA-SILVA; ZAMPIERI; FLOETER-WINTER, 2017b). Mostramos também a modulação de miRNAs como miR-372, miR-373, miR-340, miR-302 e miR-548 em macrófagos derivados de THP-1 infectados com *L. amazonensis* (FERNANDES *et al.*, *in prep*), *L. braziliensis* (SOUZA *et al.*, 2021) e *L. infantum* (RAMOS-SANCHEZ *et al.*, *in prep*).

Nós observamos que dentre os miRNAs modulados na infecção por *L. amazonensis* destacamos o aumento dos miR-294-3p e miR-721 em macrófagos de BALB/c (MUXEL, S.M.; LARANJEIRA-SILVA; ZAMPIERI; FLOETER-WINTER, 2017b), que interagem a região 3'UTR de transcritos de *Nos2*. Essa interação miRNA/mRNA foi validada em ensaios de inibição funcional do miRNA, levou ao aumento na expressão de *Nos2* e produção de NO, além de redução na infecção por *L. amazonensis* (MUXEL, SANDRA MARCIA; FERNANDA; SILVA; ZAMPIERI; *et al.*, 2017a; MUXEL, S.M.; LARANJEIRA-SILVA; ZAMPIERI; FLOETER-WINTER, 2017b).

Os miRNAs let-7a, let-7b e miR-103 são regulados positivamente em DCs e macrófagos derivados de PBMC infectados com *L. donovani* (GERACI; TAN; MCDOWELL, 2015), mas regulados negativamente em infecções por *L. major* (HASHEMI *et al.*, 2016). Nós apresentamos previamente a regulação de let-7e relacionada com a via de sinalização de TLR2/4 e MyD88, durante a infecção de macrófagos murinos com *L. amazonensis* (MUXEL, SANDRA MARCIA; ACUÑA; *et al.*, 2018b).

A maioria dos miRNAs modulados durante a infecção com *Leishmania* apresentam como alvo genes relacionados com a inflamação e sua resolução. Alguns são espécie-específicos enquanto outros são comuns a todos os representantes do gênero. E há ainda miRNAs que são específicos de determinados hospedeiros enquanto há aqueles que são comuns em todos os modelos de estudo. Por esta razão é importante conhecer profundamente o modelo de infecção utilizado, bem como a espécie de *Leishmania*, para se conhecer quais são os miRNAs expressos e quais as vias eles regulam. Ainda assim, o estudo dos miRNAs tem se demonstrado como uma área promissora no que diz respeito a novos alvos terapêuticos,

biomarcadores de prognóstico, além de elucidarem pontos-chaves de regulação de vias inflamatórias ou anti-inflamatórias que também podem ser extrapoladas para outros modelos de doença.

Hipótese

Esta tese baseia-se na hipótese de que a infecção com parasitas do gênero *Leishmania* spp. promove alterações na resposta imunológica de seus hospedeiros. Dentre as alterações possíveis destacam-se:

- i. o metabolismo de L-arginina para a produção de poliaminas, favorecendo a proliferação do parasita em detrimento da produção de NO, reduzindo atividade microbicida;
- ii. alteração de mecanismos regulatórios das respostas por meio da modificação do perfil de miRNAs, levando a uma subversão da resposta inflamatória;
- iii. modificação do metabolismo energético das células hospedeiras aumentando a susceptibilidade à infecção.

O conjunto de atividades listadas acima podem decidir o resultado da infecção e sua consequente eliminação ou a susceptibilidade do hospedeiro frente ao parasita.

Objetivos

Com base nas observações apresentadas e a hipótese formulada, fomos capazes de estabelecer os seguintes objetivos para o projeto de tese:

Objetivo Geral

Avaliar como a infecção com *Leishmania* regula a resposta imune de células murinas infectadas por meio da expressão de microRNAs em macrófagos de camundongos BALB/c e C57BL/6 ou por meio de manipulações do metabolismo de macrófagos ou células dendríticas.

Objetivos específicos

- i. Avaliar o perfil de miRNAs em macrófagos de camundongos BALB/c infectados com *L. amazonensis* e sua relação com a susceptibilidade à infecção
- ii. Avaliar o perfil de miRNAs em macrófagos de camundongos C57BL/6 infectados com *L. amazonensis* e a função na regulação da via de TLRs, contribuindo com a resistência
- iii. Analisar a função dos miRNAs na produção de citocinas e mediadores da resposta inflamatória em macrófagos de camundongos resistentes infectados com *L. amazonensis*
- iv. Avaliar a reprogramação metabólica de macrófagos de C57BL/6 infectados com *L. amazonensis* que possuam ou não a arginase
- v. Examinar se a mutação de gene mitocondrial NNT altera a capacidade do hospedeiro eliminar o parasita
- vi. Rastrear o estado metabólico de células dendríticas infectadas com *L. infantum*

Capítulo 1

Melatonina altera a infectividade de *Leishmania amazonensis* por meio de miR-294, miR-30e e miR-302d, impactando na expressão de *Tnf*, *Mcp-1* e *Nos2*.

O texto apresentado a seguir foi publicado no periódico *Frontiers in Cellular and Infection Microbiology*, em 20 de março de 2019, como parte da edição especial *Immunobiology of leishmaniasis*.

O artigo está no volume 9, artigo 60 e contém 15 páginas.

O material está disponível *online* por meio do DOI [10.3389/fcimb.2019.00060](https://doi.org/10.3389/fcimb.2019.00060)

Autores: Juliane Cristina Ribeiro Fernandes, Juliana Ide Aoki, Stephanie Maia Acuña, Ricardo Andrade Zampieri, Regina Pekelman Markus, Lucile Maria Floeter-Winter e Sandra Márcia Muxel.

Título original:

Melatonin alters *Leishmania amazonensis* infectivity through miR-294, miR-30e and miR-302d impacting on *Tnf*, *Mcp-1* and *Nos2* expression

Resumo

As leishmanioses são doenças negligenciadas que causam diferentes manifestações clínicas, variando entre as lesões cutâneas ou viscerais. A resposta inflamatória acontece durante a fagocitose da *Leishmania* e seu estabelecimento no interior do fagolisossomo, dentro dos macrófagos. A melatonina, hormônio sinalizador da escuridão, está envolvido na ativação de macrófagos em processos infecciosos, controlando a resposta inflamatória aos parasitas. Neste trabalho, nós mostramos que o tratamento com melatonina exógena reduziu a infectividade de *Leishmania amazonensis* em macrófagos oriundos de camundongos BALB/c. Além disso, o tratamento com melatonina alterou o perfil de microRNAs (miRNAs), modulando a expressão de miR-181c, miR-30e e miR-302d; também modulou a produção de citocinas e quimiocinas como IL-6, MCP-1, MIP-2, KC, RANTES e IL-10. O papel de miR-294 na infecção de macrófagos oriundos de BALB/c com *L. amazonensis* foi confirmado com o ensaio de inibição de miRNAs, o que levou a um aumento dos transcritos de *Tnf* e *Mcp-1*, além de modular a infectividade. Ademais, tanto o tratamento com melatonina como a inibição de miR-30e ou miR-302d aumentaram os transcritos de *Nos2* e a produção de óxido nítrico (NO), alterando o estado de ativação dos macrófagos e diminuindo a infecção. Este conjunto de dados demonstra o impacto do tratamento com melatonina no perfil de miRNAs de macrófagos oriundos de BALB/c infectados com *Leishmania amazonensis*.

Abstract

Leishmaniasis are neglected diseases that cause a large spectrum of clinical manifestations, from cutaneous to visceral lesions. The initial steps of the inflammatory response occur during phagocytosis of *Leishmania* and its establishment inside the macrophage phagolysosome. Melatonin, the darkness-signaling hormone, is involved in modulation of macrophage activation during infectious diseases, controlling the inflammatory response to parasites. In this work, we show that exogenous melatonin treatment reduced *L. amazonensis* infection BALB/c macrophages. Melatonin treatment also changed the macrophage microRNA (miRNA) profile by modulating miR-181c, miR-30e and miR-302d expression and cytokine production such as IL-6, MCP-1, MIP-2, KC, RANTES and IL-10. The role of miR-294 in *L. amazonensis* BALB/c infection was confirmed with miRNA inhibition assays, which led to increases in *Tnf* and *Mcp-1* expression and modulated infectivity. Additionally, melatonin treatment or miR-30e and miR-302d inhibition increased *Nos2* expression and NO production, altering the macrophage activation state and diminished the infection. Altogether, these data demonstrate that the impact of melatonin treatment on the miRNA profile of BALB/c macrophage infection by *L. amazonensis* defines the outcome of infection.

Introduction

Leishmaniasis are neglected tropical diseases characterized by cutaneous, mucocutaneous or visceral lesions (Alvar et al., 2012; Scott and Novais, 2016), and they are endemic in 98 countries worldwide (Alvar et al., 2012). According to the World Health Organization (WHO), approximately 12 million people are currently infected, and approximately 20,000 to 30,000 deaths occur annually (Alvar et al., 2012; WHO, 2017). The causative agents of leishmaniasis are protozoan parasites of the Trypanosomatidae family belonging to the genus *Leishmania* (Marsden, 1986; Ashford, 2000).

Leishmania survives and replicates inside macrophage phagolysosomes, and it is able to modulate the immune response by reducing the efficiency of inflammation and the development of an adaptive immune response (Nathan and Shiloh, 2000; Gregory and Olivier, 2005; Mosser and Edwards, 2008; Scott and Novais, 2016). Modulation of type 1 (Th1) or type 2 (Th2) polarization of T CD4⁺ lymphocytes is essential to define the fate of infection, inducing either death or proliferation of *Leishmania* amastigotes in macrophages (Corraliza et al., 1995; Munder et al., 1998; Wanasen and Soong, 2008). Some enzymes, such as nitric oxide synthase 2 (NOS2) and arginase 1 (ARG1), are competitively regulated by Th1 or Th2 cytokines, and both enzymes use L-arginine as a substrate. Stimulation with Th1-associated cytokines and chemokines, such as interferon gamma (IFN- γ), tumor necrosis factor alpha (TNF- α) and granulocyte macrophage colony-stimulating factor (GM-CSF), polarizes macrophages to the M1 phenotype by increasing NOS2 and decreasing ARG1 levels, leading to parasite control (Hrabak et al., 1996; Boucher et al., 1999; Mantovani et al., 2004; Wang et al., 2014). Conversely, Th2-associated cytokines and chemokines, such as interleukin 4 (IL-4), IL-13, tumor growth factor beta (TGF- β), IL-10, and macrophage colony-stimulating factor (M-CSF) (Verreck et al., 2004), induce M2 polarization by decreasing NOS2 and increasing ARG1 levels (Martinez et al., 2009), leading to parasite replication and survival (Hrabak et al., 1996; Boucher et al., 1999; Mantovani et al., 2004; Wang et al., 2014).

Melatonin, the darkness hormone, is synthesized at night by the pineal gland under the control of the central clock, the suprachiasmatic nuclei of the hypothalamus; melatonin is also synthesized by immune-competent cells and plays a role in surveillance against infection and in the recovery phase of acute defense responses (Markus et al., 2007; Carrillo-Vico et al., 2013; Markus et al., 2017). The interplay between timing and defense is a fine-tuned regulated process that involves melatonin-mediated restriction of leukocyte migration from the circulation to the tissues under normal conditions (Lotufo et al., 2001; Ren et al., 2015), but suppression of pineal melatonin synthesis can occur in response to pathogen (bacteria and fungi)- and danger-associated molecular patterns (da Silveira Cruz-Machado et al., 2010; Carvalho-Sousa et al., 2011) to allow migration of leukocytes to the lesion site at night as well as during the day; in addition, melatonin can be synthesized “on demand” by macrophages (Pontes et al., 2006; Muxel et al., 2012), dendritic cells (Pires-Lapa et al., 2018) and lymphocytes (Carrillo-Vico et al., 2004) during the recovery phase or under low-grade and chronic inflammatory conditions (Markus et al., 2017). This fine-tuned regulation of melatonin synthesis reduces susceptibility to bacterial infection (Rojas et al., 2002), lethal endotoxemia (Maestroni, 1996; Prendergast et al., 2003) and several parasites such as *Schistosoma mansoni*

(El-Sokkary et al., 2002), *Plasmodium* (Hotta et al., 2000), *Trypanosoma cruzi* (Santello et al., 2007), *Leishmania infantum* (Elmahallawy et al., 2014) and *Leishmania amazonensis* (Laranjeira-Silva et al., 2015). Melatonin promotes the expression of the immunoregulatory phenotype in immune-competent cells (Rojas et al., 2002; Kinsey et al., 2003), acting as a cytoprotector (Luchetti et al., 2010), an antioxidant (Reiter et al., 2013; Zhang and Zhang, 2014) and an immunomodulator (Reiter et al., 2000; Carrillo-Vico et al., 2005; Carrillo-Vico et al., 2013). Unlike bacteria and fungi, *Leishmania amazonensis* does not suppress the nocturnal melatonin surge (Laranjeira-Silva et al., 2015), resulting in lower infectivity in the dark than in the light phase of the day.

The immune response can also be modulated by microRNAs (miRNAs) (Baltimore et al., 2008; O'Neill et al., 2011; Muxel et al., 2017b; Muxel et al., 2018b). miRNAs are small noncoding RNAs that act as posttranscriptional regulators by targeting messenger RNAs (mRNAs) via 3' untranslated region (UTR) sequence complementarity, leading to translational repression or mRNA degradation, among other mechanisms (Bagga et al., 2005; Lim et al., 2005). miRNAs are involved in macrophage activation and polarization (Baltimore et al., 2008; Graff et al., 2012; Banerjee et al., 2013; Wang et al., 2014). In recent years, some studies have described macrophage miRNA modulation during *Leishmania* infections (Ghosh et al., 2013; Lemaire et al., 2013; Frank et al., 2015; Geraci et al., 2015; Mukherjee et al., 2015; Muxel et al., 2017b). In this study, we demonstrated that the miRNA profile of *Leishmania*-infected macrophages was modified by melatonin treatment. Also, melatonin reduced the levels of cytokines and chemokines such as IL-6, MCP-1, MIP-2, KC, CCL5/RANTES and IL-10. However, melatonin increased *Nos2* mRNA and NO production during infection. Melatonin treatment, as well as functional inhibition of miRNAs in macrophages, impaired the infectivity of *L. amazonensis*.

Materials and methods

Ethics Statement

Experimental protocols using animals were approved by the Animal Care and Use Committee of the Institute of Bioscience of the University of São Paulo (CEUA 169/2012 and 233/2014). This study was carried out in strict accordance with the recommendations in the guide and policies for the care and use of laboratory animals of the state of São Paulo (Lei Estadual 11.977. de 25/08/2005) and the Brazilian government (Lei Federal 11.794. de 08/10/2008).

Parasite culture

Leishmania amazonensis (MHOM/BR/1973/M2269) promastigotes were maintained in culture at 25°C in M199 medium (Invitrogen, Grand Island, NY, USA) supplemented with 10% heat-inactivated fetal bovine serum (FBS, Invitrogen), 5 ppm hemine, 100 µM adenine, 10 U/mL penicillin (Invitrogen), 10 µg/mL streptomycin (Life Technologies, Carlsbad, CA, USA), 40 mM HEPES-NaOH and 12 mM NaHCO₃ buffer (pH 6.85). Each culture was maintained for 7 days, and only early passages (P1-P5) were used for infection assays.

In vitro macrophage infection

All experiments were performed with 6-8-week-old female BALB/c mice obtained from the Animal Center of the Institute of Bioscience of the University of São Paulo. Bone marrow-derived macrophages (BMDMs) were obtained from femurs and tibias by flushing with 2 mL of PBS, and the collected cells were washed with PBS at 500 x g for 10 min at 4°C and resuspended in RPMI 1640 medium (LGC Biotecnologia, São Paulo, Brazil) supplemented with penicillin (100 U/ml) (Invitrogen, São Paulo, Brazil), streptomycin (100 µg/ml) (Life Technologies, Carlsbad, CA, USA), 10% heat-inactivated FBS (Invitrogen) and 20% L929 cell supernatant. The cells were submitted to differentiation for 7-8 days at 34°C in an atmosphere of 5% CO₂. BMDMs were used after phenotypic analysis by flow cytometry showed at least 95% F4/80- and CD11b-positive cells. Fluorescence detection was performed using an Amnis FlowSight (Merck-Millipore, Darmstadt, Germany) and analyzed using Ideas® Software (Amnis Corporation, Seattle, WA, USA).

For melatonin treatment assays, macrophages (2×10^5) were plated into 8-wells glass chamber slide (Lab-Teck Chamber Slide; Nunc, Naperville, IL, USA) and incubated at 34°C in an atmosphere of 5% CO₂. After, macrophages were treated with 30 or 100 nM melatonin (Tocris, Bristol, United Kingdom), vehicle (0.0005% ethanol in medium, Sigma-Aldrich, St. Louis, MO, USA) or medium only (untreated control) for 1, 2 or 4 h. Then, the macrophages were infected with promastigotes in the stationary growth phase (MOI 5:1), as previously described (Laranjeira-Silva et al., 2015). After 4 h of infection, the cells were washed to remove nonphagocytosed promastigotes, the wells received fresh RPMI medium with 10% FBS. The infectivity was microscopically analyzed after 4 and 24 h of infection, cell-fixation with acetone/methanol (1:1, v:v, Merck, Darmstadt, Germany) for 20 min at -20°C, followed by PBS washing and Panoptic-stained (Laborclin, Parana, Brazil). Infectivity was analyzed in phase-contrast microscopy (Nikon Eclipse E200, NJ, USA) counting the number of infected macrophages and amastigotes per macrophage in at least 1,000 macrophages/treatment were

counted in 3 independent experiments). The infection index was calculated by multiplying the mean number of amastigotes per macrophage by the rate of macrophage infection. The values were normalized based on the average values for the untreated infected macrophages.

RNA extraction, reverse transcription and RT-qPCR for miRNA

Total RNA was extracted using a miRNeasy Mini Kit (Qiagen, Hilden, Germany) following the manufacturer's instructions. cDNA was produced from mature miRNA templates using a miScript II RT Kit (Qiagen). Briefly, 250 ng of total RNA was added to 2 μ L of 5X miScript HiSpec Buffer, 1 μ L of 10X Nucleic Mix and 1 μ L of miScript Reverse Transcriptase Mix. RNase-free water was added to a final volume of 10 μ L. The RNA was incubated for 60 min at 37°C to insert a poly-A tail downstream of the miRNA sequence and anneal a T-tail tag for the elongation of the cDNA. The enzyme was inactivated at 95°C for 5 min. The reaction was performed in a Mastercycler Gradient thermocycler (Eppendorf, Hamburg, Germany), and the product was stored at -20°C until use.

An array of 84 miRNAs was measured using a Mouse Inflammatory Response & Autoimmunity miRNA PCR Array kit (MIMM-105Z, Qiagen) and a miScript SYBR PCR Kit (Qiagen). The reaction was performed with 2X QuantiTect SYBR Green PCR Master Mix, 10X miScript Universal Primer and 105 μ L of cDNA (triplicate samples of the 10-fold diluted cDNA). RNase-free water was added to a final volume of 2,625 μ L (25 μ L/well).

For specific amplification of miR-181c, miR-294-3p, miR-30e, miR-302d and SNORD95A (used as a normalizer), reactions were prepared with 2X QuantiTect SYBR Green PCR Master Mix, 10X miScript Universal Primer, 10X specific primer, 5 μ L of cDNA (3-4 samples 10-fold diluted) and RNase-free water to a final volume of 25 μ L/well. qPCR started with activation of the HotStart DNA Polymerase for 15 sec at 95°C and 40 cycles of 15 sec at 94°C for denaturation, 30 sec at 55°C for primer annealing and 30 sec at 70°C for elongation. The reaction was performed in a Thermocycler ABI Prism 7300 (Applied Biosystems, Carlsbad, CA, USA), and the relative Ct was analyzed using online tools provided with the kit (miScript miRNA PCR Array Data Analysis software). The geometric average Ct of the miRNAs was normalized based on the SNORD95A values, and then the fold changes were calculated to compare untreated, vehicle-treated or melatonin-treated and infected macrophages in relation to untreated and uninfected macrophages at the same time of culture. The RT-qPCR efficiencies were determined, and a negative control reaction without reverse transcriptase enzyme was included to verify the absence of any DNA contamination in the RNA samples. The fold regulation (FR) was considered to be the negative inverse of the fold change (function = $-1 \times (1/\text{fold change value})$). FR values greater than or equal to 1.5 were considered to indicate upregulation, and levels less than or equal to -1.5 were considered to indicate downregulation, as previously described (Muxel et al., 2017a).

Reverse transcription and RT-qPCR for mRNA

Reverse transcription was performed using 2 μ g of RNA and 20 nmol of random primer (Applied Biosystems) to a final volume of 13 μ L. The mixture was incubated at 70°C for 5 min and then at 15°C for addition of the mix including 4 μ L of 5X buffer, 2 μ L of 10 mM dNTPs and 1 μ L (2U) of RevertAid™ Reverse Transcriptase (Fermentas Life Sciences, Burlington, Ontario, Canada). The reaction was incubated at 37°C for 5 min and at 42°C for

60 min. The enzyme activity was blocked by heat inactivation at 75°C for 15 min, and the cDNA was stored at -20°C until use. A negative control reaction without reverse transcriptase enzyme was included to verify the absence of any DNA contamination in the RNA samples in the RT-qPCR assays. Reactions were performed with 2X SYBR Green PCR Master Mix (Applied Biosystems), 200 nM of each primer pair, 5 µL of cDNA (100-fold diluted) and RNase-free water to a final volume of 25 µL. The reactions were performed in an Exicycler™ 96 Real-Time Quantitative Thermal Block (Bioneer, Daejeon, Korea). The mixture was incubated at 94°C for 5 min followed by 40 cycles of 94°C for 30 sec and 60°C for 30 sec. Quantification of target gene expression was performed based on a standard curve prepared from a ten-fold serial dilution of a quantified and linearized plasmid containing the target DNA. The following primer pairs were used for mouse mRNA analysis: *Nos2*: 5'-agagccacagctcctctttgc-3' and 5'-gctcctctccaaggtgctt-3'; *Arg1*: 5'-agcactgaggaaagctggtc-3' and 5'-cagaccgtgggtctctcaca-3'; *Cat-2b*: 5'-tatgtgtctcggcaggctc-3' and 5'-gaaaagcaaccctcctccg-3'; *Cat1*: 5'-cgtaatgccactgtgacct-3' and 5'-ggctggtaccgtaagaccaa-3'; *Mcp-1/Ccl2*: 5'-tgateccaatgagtaggctgg-3' and 5'-gcacagacctctctcttgagc-3', *Rantes/Ccl5*: 5'-ggagtattctacaccagcagca-3' and 5'-cccacttctctctgggttg-3', *Tnf*: 5'-ccaccagctctctgtcta-3' and 5'-agggtctgggcatagaact-3' and *Gapdh*: 5'-ggcaaattcaacggcacagt-3' and 5'-cctttgctccaccctca-3'.

Transfection of miRNA inhibitors

For miRNA expression analysis, 5×10^5 cells/well were plated into 24-well plates (SPL Life Sciences, Pocheon, Korea). For infectivity analysis, 2×10^5 cells/well were plated into 8-well glass Lab-Teck chamber slides (Thermo Scientific, NY, USA) and incubated at 34°C in an atmosphere of 5% CO₂ for 18 h. Then, the cells were incubated with 30 or 100 nM of the inhibitors miR-181c-5p, miR-294-3p, miR-30e-5p, or miR-302d-3p or the negative control (Ambion, Carlsbad, CA, USA) or only medium (untreated), which were previously incubated for 20 min at room temperature with 3 µL of the FuGENE HD transfection reagent (Roche, Madison, WI, USA) in 250 µL of 10% FBS RPMI 1640 medium (LGC Biotechnologia, São Paulo, Brazil). After 36h since transfection, the cells were infected as previously described.

Cytokine quantification

The cytokines IL-1 α , IL-1 β , IL-4, IL-6, TNF- α , IL-13, IL-10 and IL-12 and the chemokines RANTES/CCL5, KC/CXCL1, MIP-2/CXCL2 and MCP-1/CCL2 were quantified using 25 µL of the supernatant of 1×10^6 cells of uninfected or infected macrophages that were untreated, vehicle-treated or melatonin-treated using a MILLIPLEX MAP Mouse Cytokine/Chemokine Panel I kit (Merck Millipore, MA, USA), according to the manufacturer's instructions.

Nitric oxide (NO) quantification

Nitric oxide (NO) quantification was performed with DAF-FM (4-amino-5-methylamino-2',7'-difluorofluorescein diacetate; Life Technologies, Eugene, OR, USA) labeling and analyzed by flow cytometry (FlowSight, Merck Millipore, Germany), as previously described (Muxel et al., 2017a; Muxel et al., 2017b).

In silico analysis

To analyze miRNA-mRNA interactions, we used the miRecords platform (<http://cl accurascience.com/miRecords/>), which provides information on predicted mRNA

targets by integrating data from various tools: DIANA-microT, MicroInspector, miRanda, MirTarget2, miTarget, NBmiRTar, PicTar, PITA, RNA22, RNAhybrid, and TargetScan/TargetScanS.

Statistical analysis

Statistical analyses were performed using GraphPad Prism Software (GraphPad Software Inc, La Jolla, CA, USA). Significance was determined based on Student's t-test, and $p < 0.05$ was considered significant.

Results

Melatonin reduces macrophage-*L. amazonensis* infectivity in a dose- and time-dependent manner.

Melatonin modulation was evaluated in BMDMs infected with *L. amazonensis* for 4 and 24 h. Melatonin treatment (3 or 30 nM) for 1 and 2 h did not modify the macrophage infection rate (as showed in the normalized data in Fig. 1A-B and original data in S1 Fig.), mean number of amastigotes per infected macrophage (3-5 amastigotes. Fig. D-E) or infection index (Fig. 1G-H) compared to vehicle treatment.

Otherwise, melatonin treatment for 4 h reduced the number of infected macrophages by 30%, while melatonin treatment with 3 nM melatonin had no effect (Fig. 1C; S1 Fig.). The number of amastigotes per infected cell was reduced by the same percentage (20-25%) with 3 or 30 nM (Fig. 1F), and the infection index was reduced at both concentrations (20-30% 3 nM, 60% 30 nM; Fig. 1I). Subsequent analyses were performed based on treatment with 30 nM melatonin for 4 h.

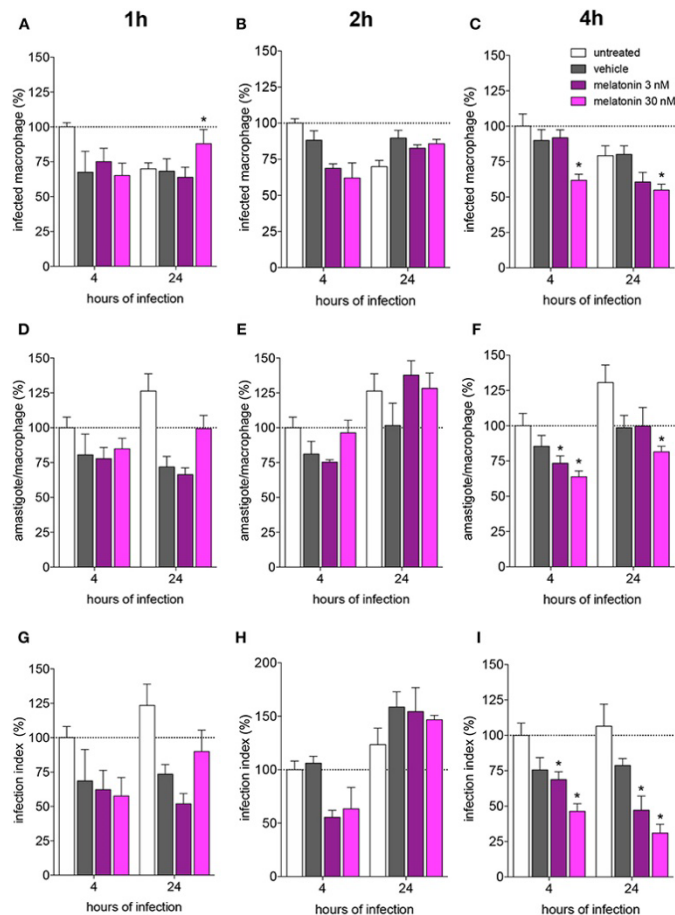


Figure 5. Melatonin inhibition of *L. amazonensis* infectivity in a dose dependent manner. BALB/c macrophages (2×10^5 cells) were pre-incubated for 1, 2 or 4 h with medium (untreated, white bar), vehicle (ethanol 0.0005%, gray bar), or 3 (purple bar) or 30 (magenta bar) nM of melatonin. After, macrophages were infected with *L. amazonensis* (MOI 5:1) and analyzed after 4 and 24 h. A, B and C – Percentage of infected macrophages; D, E and F – number of amastigotes per infected macrophage; G, H and I – Infection index (rate of infected macrophages multiplied by the number of amastigotes per infected macrophage). Each bar represents the mean \pm SEM of values normalized by untreated macrophages at 4h of infection. The data were representative of 3 independent experiments (n=5-8). * $p < 0.05$, comparing the melatonin treatment with the vehicle-treated macrophage at the same concentration and time.

Melatonin modulates the expression of genes related to L-arginine transport and metabolism in *L. amazonensis*-infected macrophages.

Considering that parasite survival in macrophages is affected by deviation of L-arginine metabolism to the production of polyamines (Muxel et al., 2018c), we evaluated the gene expression in melatonin-treated macrophages in comparison with vehicle-treated macrophages, quantifying mRNAs of *Cat2B* and *Cat1*, which are involved in L-arginine uptake and the mRNAs of the enzymes *Arg1*, which contributes for polyamine production and *Nos2* that produces NO, (Fig. 2).

Based on the mRNA expression levels, we observed that at both times during infection, early (4 h) and established (24 h), *L. amazonensis* induced sustained expression of *Cat2B* and *Cat1* mRNA (Fig. 2A and B). *Arg1* and *Nos2* were transiently expressed in early (4 h) infection in infected macrophages compared to uninfected macrophages. Exposure to vehicle and melatonin modulated mRNA levels in uninfected macrophages, increasing the basal levels of *Cat2B* and *Arg1* (Fig. 2A, B and C). However, in infected macrophages, melatonin treatment did not alter the *Cat2B*, *Cat1* or *Arg1* mRNA levels (Fig. 2A-C) compared to vehicle treatment. However, melatonin sustained the levels of *Nos2* mRNA (Fig. 2D) and increased the frequency of NO-producing cells (Fig. 2E) and the amount of NO per cell (Fig. 2F) at 24 h of infection. Our data revealed that melatonin treatment of macrophages promoted modulation of the expression of mRNA involved in L-arginine metabolism during infection, inducing *Nos2* to the detriment of *Arg1* and thus altering infectivity.

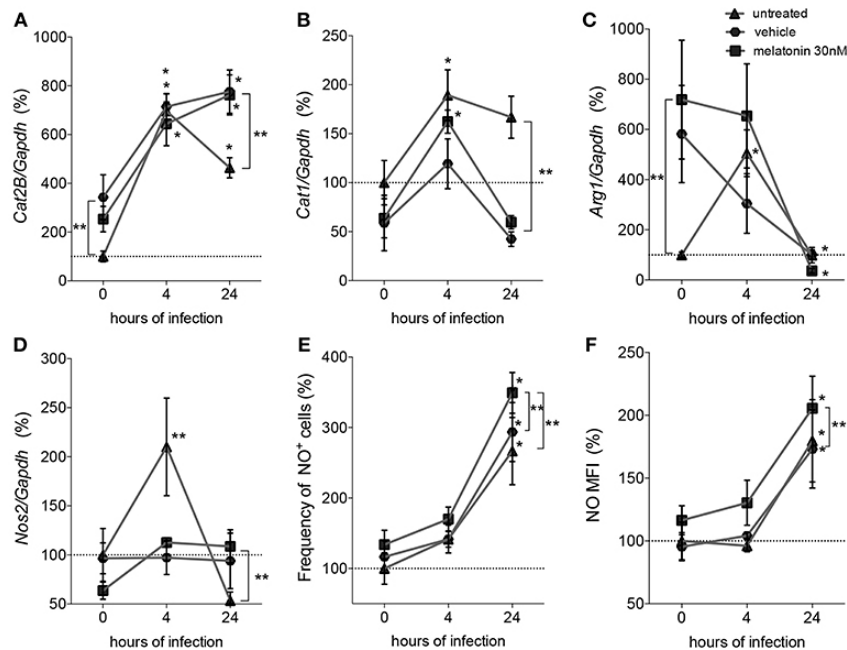


Figure 6. Quantification of mRNA involved in L-arginine transport and metabolism and NO production. Macrophages (5×10^6) were treated with 30nM of melatonin (squared dots), vehicle (5×10^{-6} % ethanol, hexagonal dots) or untreated (triangular dots) for 4 hours, infected with *L. amazonensis* (MOI 5:1) and collected after 4 and 24 h of infection. RT-qPCR of *Cat2B* (A), *Cat1* (B), *Arg1* (C) and *Nos2* (D) were normalized by *Gapdh* quantification and the values were normalized by untreated-uninfected condition (0 hours); (E) Frequency of NO producing cells and (F) mean of fluorescence intensity (MFI) of NO were quantified by DAF-FM label using flow cytometry. Each bar represents the average \pm SEM of the values obtained in 3 independent experiments (n=6-8). Statistical significance was determined based on two-tailed Student's t test. *p<0.05, infected macrophages (4h or 24h) compared to non-infected (0h) ** p<0.05, melatonin-treated compared to untreated or vehicle.

Melatonin modifies cytokine and chemokine production in *L. amazonensis*-infected macrophages.

Furthermore, we analyzed cytokine and chemokine production in response to melatonin treatment and *L. amazonensis* infection. The basal levels of the cytokines IL-4, IL-1 β , IL-13, IL-6, TNF- α and IL-12 and the chemokine RANTES were not changed after 4 and 24 h of infection, whereas IL-1 α (2-fold), IL-10 (5-fold), MIP-2/CXCL2 (8-fold) and KC/CXCL1 (4-fold) levels were decreased after 24 h of infection on untreated macrophages compared to those in uninfected macrophages (Fig. 3). In contrast, MCP-1/CCL2 (2-fold) showed increased levels in infected macrophages (untreated) compared to uninfected macrophages (24 h)(Fig. 3).

Melatonin treatment reduced the levels of IL-6 (2-fold), MCP-1 (5-fold) and RANTES (6-fold) compared to vehicle treatment during 4 or 24 h of infection (Fig. 3). Our data demonstrated that melatonin modulates *L. amazonensis*-induced synthesis of the cytokines IL-6 and IL-10 and the chemokines MIP-2/CXCL2, MCP-1/CCL2 and KC/CXCL1.

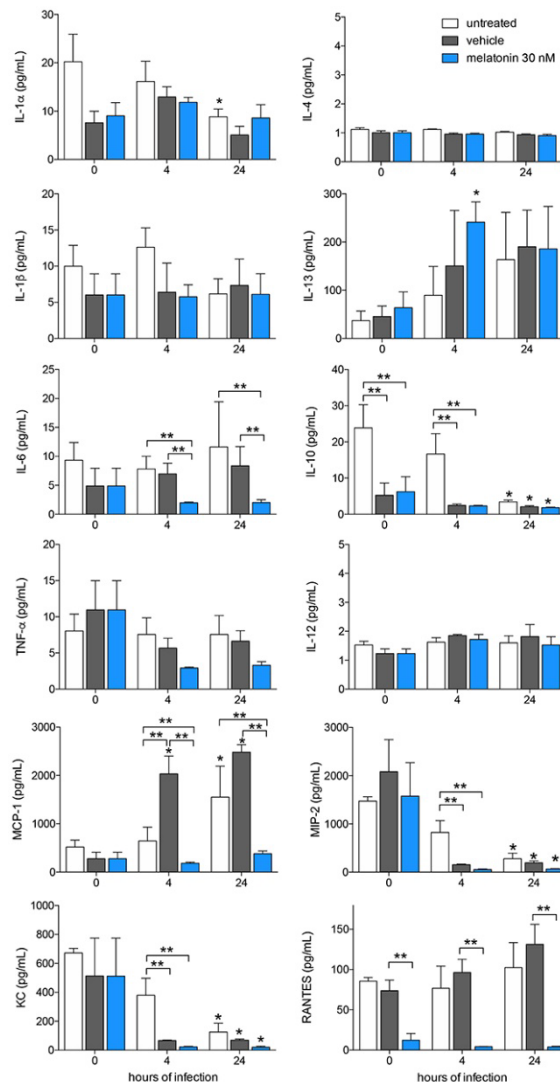


Figure 7 Cytokine and chemokines production after melatonin treatment and *L. amazonensis* infection. Cytokine and chemokine quantifications were performed with macrophage supernatants ($1 \times 10^6/500 \mu\text{L}$) treated with melatonin (30 nM, blue bar), vehicle (5×10^{-6} % ethanol, gray bar) or untreated (white bar) for 4 h, infected with *L. amazonensis* (MOI 5:1) and collected after 4 and 24 h of infection. The time 0 corresponds to non-infected macrophages. Each bar represents medium \pm SEM of values obtained in 3 independent experiments (n=4-5). *p < 0.05, infected compared to uninfected macrophages (0h) ** p < 0.05, melatonin-treated compared to untreated or vehicle

Melatonin antagonizes changes in the miRNA profile in *L. amazonensis*-infected macrophages.

The effect of melatonin on the miRNA expression profile was also evaluated after 4 and 24 h of infection. In vehicle-treated macrophages at 4 h of infection, miR-294-3p, miR-410-3p, miR-669h-3p and miR-721 appeared upregulated, while miR-26a-5p, miR-130b-3p and miR-181c-5p appeared downregulated (Fig. 4). In addition, at 24 h of infection, the expression of miR-302d-3p, miR-30e-5p and miR-669h-3p appeared upregulated, while miR-181c-5p and miR-26a-5p appeared downregulated. In untreated and 24 h-infected macrophages, only miR-410-3p, miR-495-3p and miR-294-3p appeared upregulated.

Melatonin treatment induced the expression of miR-294-3p, miR-410-3p, miR-669h-3p but only miR-694 was exclusively affected by melatonin since it was not observed in vehicle treatment at early infection (4 h). However, at 4 or 24 h, only miR-26a-5p was downregulated, suggesting that melatonin blocks the downregulation of miR-130b-3p and miR-181c-5p observed after vehicle treatment at 4h of infection. Melatonin treatment modulated only the expression of miR-26a-5p at 24 h of infection, suggesting that melatonin blocks the downregulation of miR-181c-5p as well as the upregulation of miR-30e-5p, miR-302d-3p and miR-669h-3p at 24h (Fig. 4). Our data demonstrated that melatonin treatment can modify the miRNA profile of *L. amazonensis*-infected macrophages (Table S1).

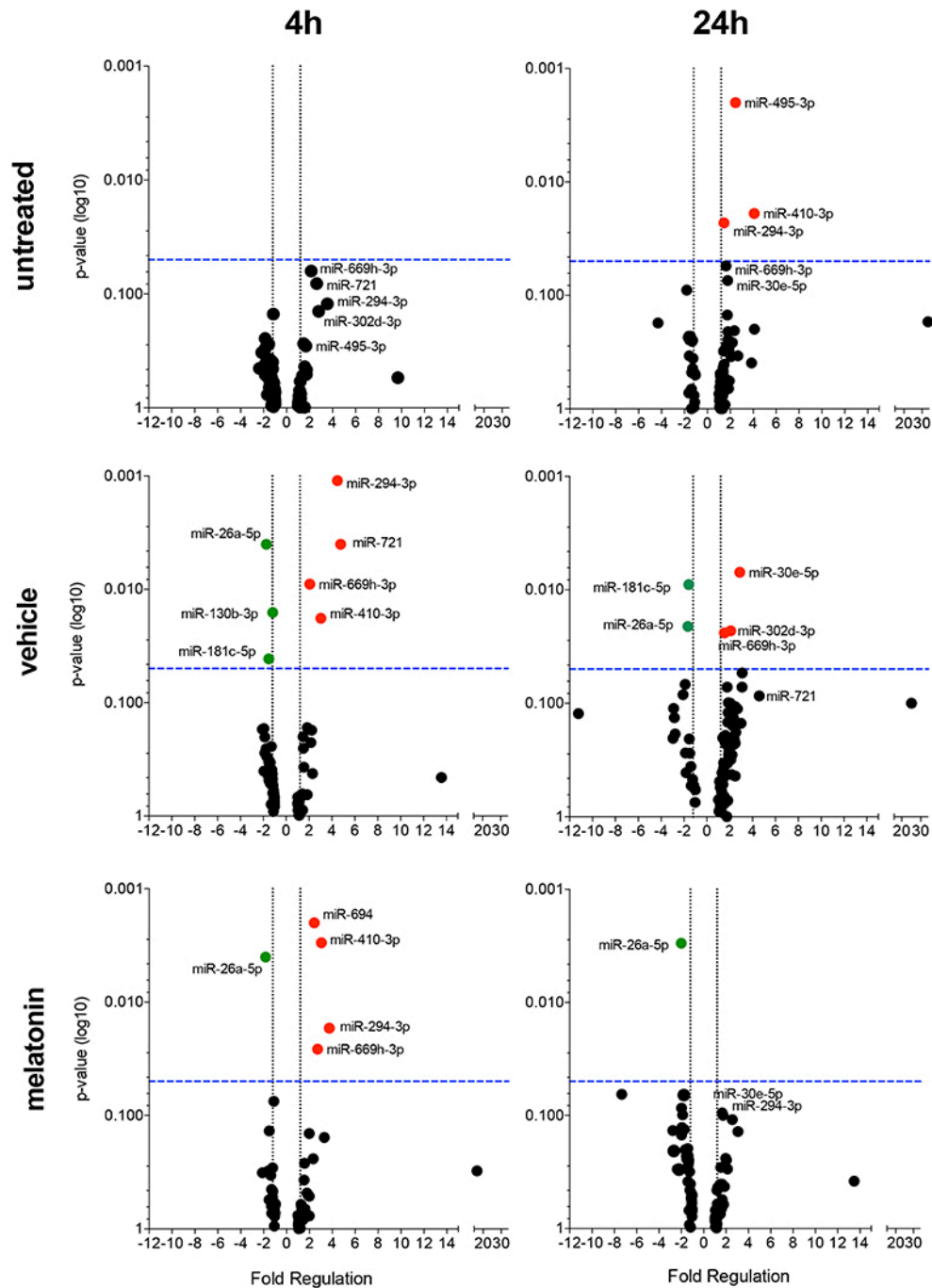


Figure 8. Volcano plot showing melatonin modulation of miRNA profile in macrophages infected with *L. amazonensis* in a time dependent manner. Each dot represents one miRNA in untreated, vehicle or melatonin (30nM) treated in macrophages infected for 4 or 24 h with *L. amazonensis*. The red dots indicate up-regulated miRNA and green dots indicate down-regulated miRNAs. Blue dotted line corresponds to $p = 0.05$, \log_{10} . The relative up- and down-regulation of miRNAs, expressed as boundaries of 1.5 or -1.5 of Fold Regulation, respectively. p-value was determined based on unpaired two-tailed Student's t test. The data are representative of three independent experiments ($n=3-4$).

Inhibition of miR-181c, miR-294, miR-30e and miR-302d reduces the infectivity of *L. amazonensis* by modulating mRNA expression.

To determine the impact of those miRNAs modulated in melatonin-treated infected macrophages on mRNA expression during infection, we performed *in silico* analysis, and based on a miRecord search, we found that miR-181c, miR-294, miR-30e and miR-302d can interact with thousands of target mRNAs (Table S2-5).

As *in silico* analysis indicated interactions of miR-181c, miR-294, miR-30e and miR-302d with *Nos2*, *Tnf*, *Mcp-1* and *Rantes* mRNA, we performed *in vitro* validation by miRNA inhibition of infection-induced expression at 4 and 24 h. miRNA inhibition was confirmed by reductions in the levels of these miRNAs at 4 h, but not at 24 h, of infection compared to the levels in untreated or negative control -transfected macrophages (Fig. 5A).

Nos2 mRNA levels appeared to be increased after inhibition of miR-30e and miR-302d compared to the levels in the negative control group (Fig 5B), indicating the role of the interaction of these miRNAs with *Nos2*. The levels of *Tnf* mRNA increased after inhibition of miR-294 and miR-302d compared to those in the negative control group (Fig. 5C-D), indicating the role of the interaction of these miRNAs with *Tnf*. *Mcp-1* mRNA levels appeared to be increased after inhibition of miR-294 (Fig. 5D), indicating the role of the interaction of this miRNA and *Mcp-1*. Interestingly, *Mcp-1* mRNA levels appeared to be decreased after inhibition of miR-181c (Fig. 5D). Since we observed no miRNA inhibition at 24 h of infection (Fig. 5A), we did not infer a role for an interaction between miR-294 and *Rantes* mRNA (Fig. 5E).

Inhibition of miR-181c, miR-294, miR-30e and miR-302d at 30 or 100nM reduced the infection index at 4 h of infection, but only 30nM of miR-294, miR-30e and miR-302d inhibitors presented this effect at 24 h (Fig. 5F). *Nos2* was a predicted target of miR-302d, while other cytokines/chemokines modulated in melatonin-treated infected macrophages, such as *Tnf*, *Mcp-1* and *Rantes*, could be indirect targets of pointed miRNAs. The present data indicate that modulation of macrophage infection by melatonin is dependent on miRNA expression and therefore on changes in the cell defense program, rather than on only isolated effects at one enzyme or receptor.

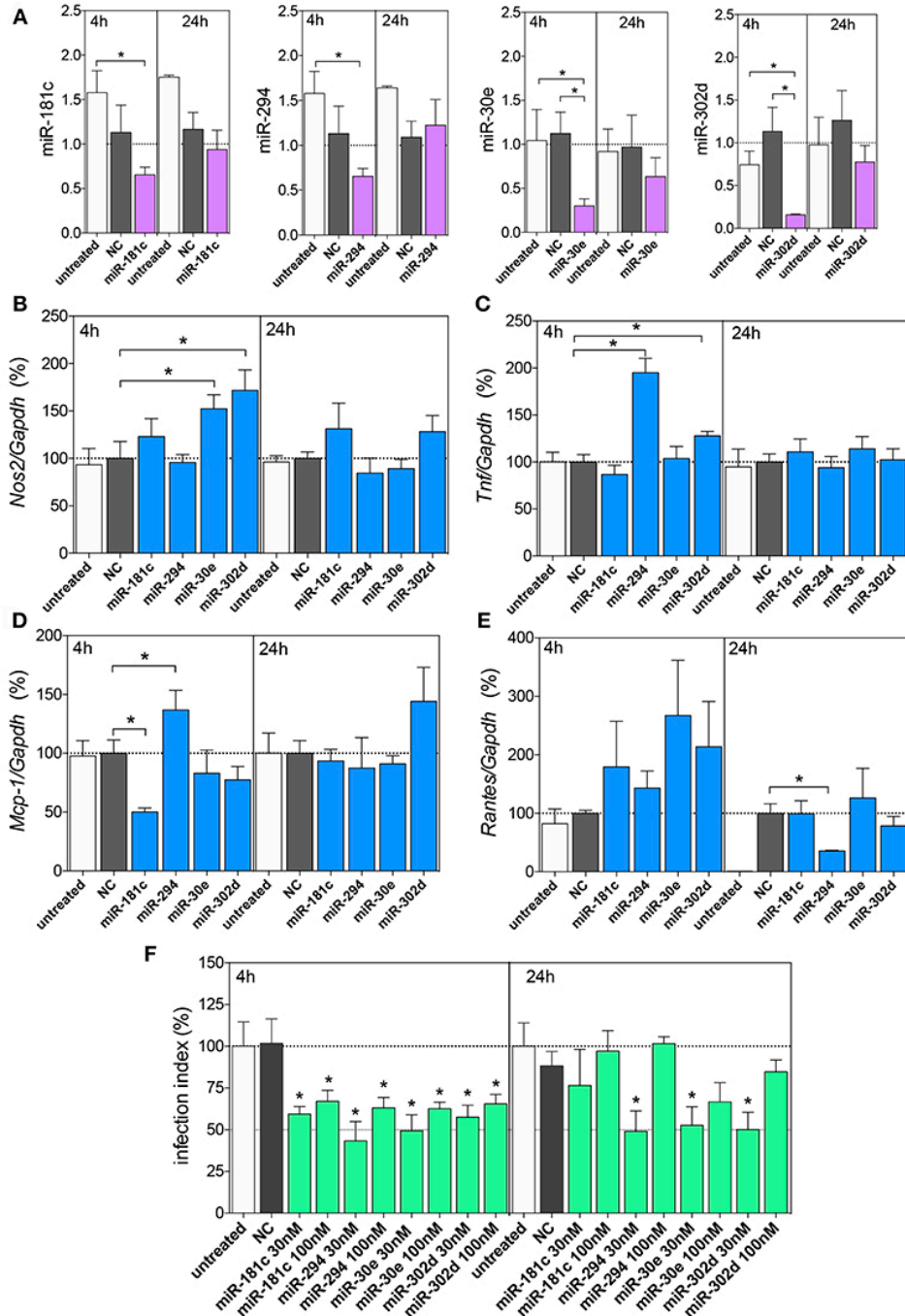


Figure 9. Functional analysis of miR-181c, miR-294-5p, miR-30e and miR302d inhibition. Macrophages (5×10^5) were transiently transfected with the negative control (NC, gray bars), 30 or 100 nM of miR-181c, miR-294-5p, miR-30e or miR-302d inhibitors (purple bars), or left non-transfected (untreated, white bars). After 36 h of incubation, the cells were infected with *L. amazonensis* (MOI 5:1) for 4 and 24 h. The inhibition with 100nM of NC or miRNAs were performed to evaluated miR-181c, miR-294-5p, miR-30e or miR-302d expression (A) and for *Nos2* (B), *Tnf*, (C) *Mcp-1* (D) and *Rantes* (E) mRNA expression, by qPCR; the inhibition with 30 or 100 nM of NC or miRNAs were also performed for infectivity evaluation (F) by microscopy analysis, counting the numbers of infected macrophages and amastigotes per macrophage (n=1,000 macrophages/treatment). The values of miRNAs were represented by Fold change using SNORD95, as a normalizing endogenous control. The values of mRNAs were normalized (100%) based on the average values of the negative control (NC) at 4h of infection. Each bar represents the average \pm SEM of the values obtained in 3 independent experiments (n=4-6). Statistical significance was determined based on unpaired two-tailed Student's t test. In infectivity analysis (F), * represent $p < 0.05$, compared to negative control (NC) infected macrophages.

Discussion

Macrophages are essential components of innate immunity and are capable of differentiating into cells with a wide range of functions. These cells are able to respond to different stimuli, such as microbial molecules, damaged cell components, costimulatory molecules, cytokines and chemokines, by changing their phenotypes (Mosser and Edwards, 2008; Zhang and Mosser, 2008). In addition, melatonin can act as a pro- or anti-inflammatory agent depending on cell activation state and/or cell type. Melatonin primes macrophages to a phenotype that reduces *L. amazonensis* infectivity (Laranjeira-Silva et al., 2015).

Melatonin can also act in the modulation of gene expression through transcriptional and posttranscriptional mechanisms, and these intricate regulatory mechanisms interfere with melatonin production. Several studies have shown the role of melatonin in inhibiting arginine uptake via CAT2B (Laranjeira-Silva et al., 2015), CAT1 (Gilad et al., 1998; Deng et al., 2006; Nair et al., 2011), and NOS2 activity (Xia et al., 2012). In contrast, our work with BALB/c BMDMs treated with melatonin showed increased *Nos2* mRNA expression and NO production in infected macrophages, leading to a decreased infection index. *Nos2* expression leads to reduced infectivity in C57BL/6 murine macrophages (Muxel et al., 2018b). Moreover, *Nos2* expression and NO production kill parasites and result in resistance to infection (Ghalib et al., 1995; Wei et al., 1995; Vieira et al., 1996; Wilhelm et al., 2001; Yang et al., 2007; Ben-Othman et al., 2009; Srivastava et al., 2012; Muxel et al., 2017b; Muxel et al., 2018c).

Melatonin reduced IL-6, RANTES, MCP-1 and MIP-2 protein levels in infected macrophages, which could correlate with macrophage activation and cell recruitment to the inflammation site. In contrast, melatonin also reduced IL-10 levels, which could help in immune response modulation induced by infection and pathogenesis. Melatonin in the μM -mM range inhibits IL-1 β , TNF- α , IL-6, IL-8, IL-13 and IL-10 and attenuates NOS2 activation induced by LPS (Zhou et al., 2010; Xia et al., 2012). However, melatonin in the pM-nM range promotes increased phagocytosis of fungus-derived particles (zymosan) by macrophages (Muxel et al., 2012) and can also reduce the entrance and replication of *L. amazonensis* in peritoneal macrophages (Laranjeira-Silva et al., 2015) and in BMDMs. IL-1 β plays a role in macrophage activation, increasing NO production and leading to host resistance to *Leishmania* infection (Lima-Junior et al., 2013). However, melatonin treatment increases TNF- α , IFN- γ and IL-12 production but reduces NO levels during *Trypanosoma cruzi* infection (Santello et al., 2008a; Santello et al., 2008b). It was recently demonstrated that melatonin also inhibits the production of proinflammatory cytokines, such as TNF- α , IL-6 and IL-12, by TLR-9-stimulated peritoneal macrophages through ERK1/2 and AKT pathways (Xu et al., 2018).

In this work, we showed that another effect of melatonin is related to modulation of miRNA profile changes imposed by *L. amazonensis* infection. Both miR-294 and miR-721 appeared upregulated in vehicle-treated macrophages after 4 h of infection, but miR-721 was downregulated in melatonin-treated infected macrophages. Our previous studies showed that these miRNAs reduce *Nos2* expression and NO production, enabling the establishment of infection (Muxel et al., 2017b). Here, *Nos2* mRNA expression and NO production were higher in melatonin-treated infected macrophages than in vehicle-treated or untreated infected macrophages. Additionally, melatonin blocked the downregulation of miR-130b-3p and miR-

181c-5p compared to vehicle. Functional inhibition of miR-181c, miR-30e and miR-302d increased *Nos2* mRNA expression, impairing infectiveness.

Here, we show that *L. amazonensis* infection of BALB/c untreated-macrophages promoted a reduction in IL-1 α production and did not alter IL-1 β , IL-6, TNF- α or IL-12 protein levels. However, in C57BL/6-macrophages, the levels of *Il1b*, *Tnf*, *Il10* and *Il6* receptor transcripts increase during infection (Muxel et al., 2018b). IL-1 receptor signaling induces NF- κ B activation (Ikeda and Dikic, 2008; David et al., 2010; Roh et al., 2014; Fletcher et al., 2015), suggesting a negative regulation of inflammatory cytokine production in infected macrophages. This is in contrast to the upregulation of proinflammatory cytokine gene expression in human macrophages after infection with *L. amazonensis* and *L. major*, such as that of *Il-1b*, *Tnf* and *Il-6* (Fernandes et al., 2016), and in murine macrophages after *L. major* infection, in which *Tnf*, *Il-1* and *Il-6* are upregulated (Dillon et al., 2015). However, melatonin treatment reduced IL-6 levels in infected macrophages compared to untreated infected macrophages. Indeed, melatonin inhibits IL-1 β , IL-6 and TNF production mediated via LPS-TLR4 signaling (Xia et al., 2012).

In this way, inhibition of miR-294 and miR-302d increased *Tnf* levels, which reduced infectivity. In *L. amazonensis* infection of BALB/c-macrophages, miR-294 targets *Nos2* mRNA reducing NOS2 expression and NO production impacting in infectivity (Muxel et al., 2017b). The signaling via TLR4 by LPS injection on mice downregulates miR-294 levels in blood and lung samples (Hsieh et al., 2012), whereas the miR-294 is overexpressed in C57BL/6-macrophages infected with *L. amazonensis* independently of TLR2, TLR4 and MyD88 (Muxel et al., 2018a), suggesting an alternative induction of this miRNA.

Additionally, miR-302d encompasses a miR-302/367 cluster that is highly conserved in vertebrates (Gao et al., 2015). miR-302d is expressed at the early time and downregulated in late time of exudate during acute inflammation in murine peritonitis induced via TLR2/Zymosan stimuli. (Recchiuti et al., 2011). In contrast, miR-302d appears at lower levels in plasma of experimental autoimmune encephalomyelitis mouse model and systemic lupus erythematosus and regulates IFN type I gene expression targeting interferon regulator factor-9 (IRF-9) in murine model (Smith et al., 2017). Interestingly, the IRF9, STAT1, STA3 and NF- κ B bind to promoter region of *Nos2* gene and induce its transcription during *Listeria monocytogenes* infection (Farlik et al., 2010), suggesting both direct and indirect routes for miR-302d regulation of *Nos2* expression.

Moreover, miR-30e alters cell proliferation, colony formation and invasiveness in cancer cells, interfering with NF- κ B/I κ B α negative feedback and apoptosis (Jiang et al., 2012; Hershkovitz-Rokah et al., 2015; Zhuang et al., 2017). miR-30e leads to hyperactivation of NF- κ B by targeting I κ B α 3'UTR, which induces IFN- β and suppresses dengue virus replication (Zhu et al., 2014). miR-30e is overexpressed in *Mycobacterium tuberculosis*-infected THP-1-macrophages (Wu et al., 2017), and in neutrophils of traumatic injured patients correlating to systemic inflammation (Yang et al., 2013).

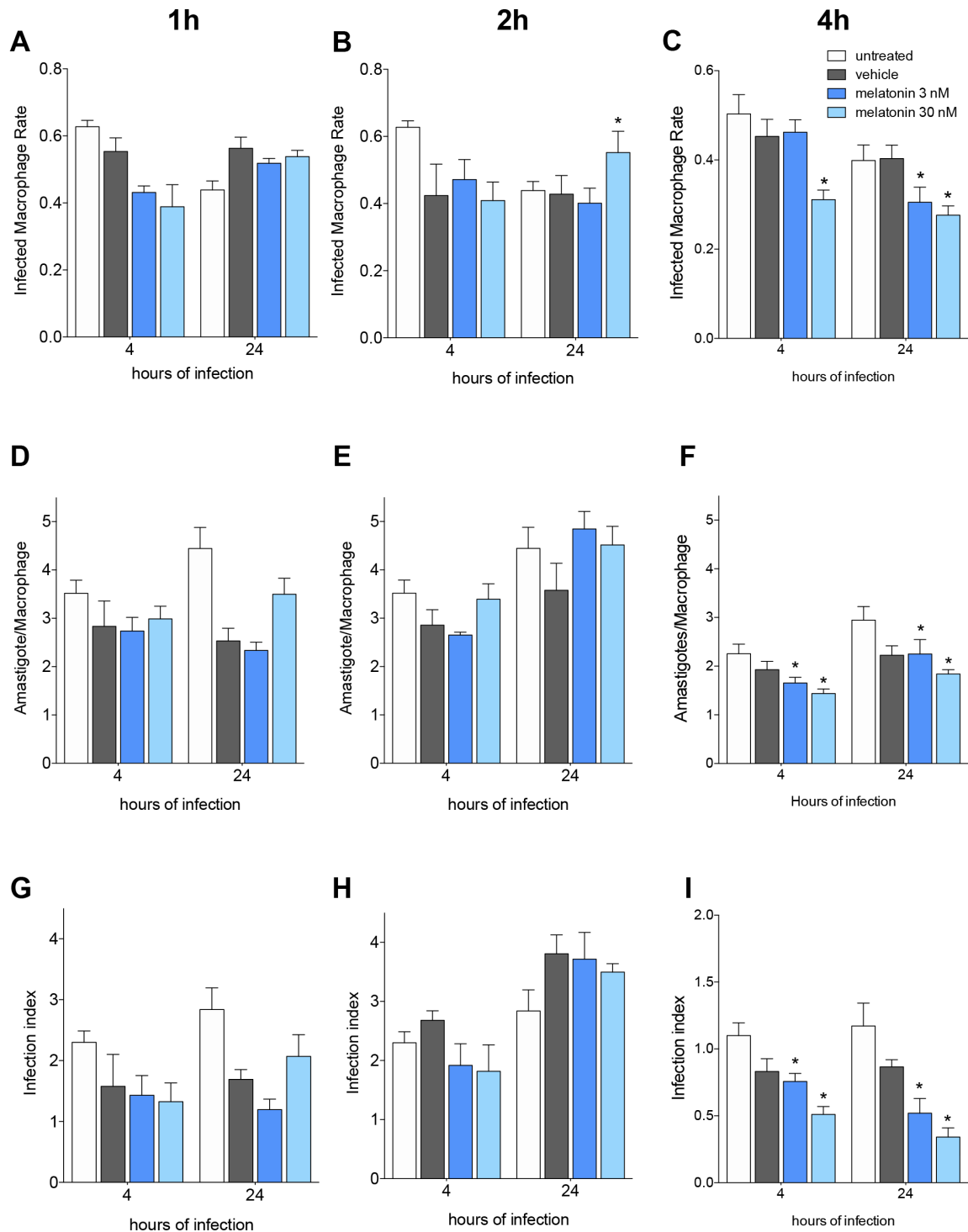
Additionally, infection and melatonin treatment reduced the levels of KC/CXCL1 and MIP-2 produced by macrophages. These chemokines recruit neutrophils to sites of *Leishmania* infection (Muller et al., 2001). RANTES/CCL5 levels produced by *L. amazonensis*-infected and noninfected macrophages were reduced in melatonin-treated macrophages compared with untreated macrophages. *Rantes* mRNA levels tended to increase after functional inhibition of

miR-30e and miR-302d. The cytokines KC/CXCL1, MIP-2 and RANTES/CCL5 are associated with neutrophil, monocyte and lymphocyte recruitment to the inflammatory focus (Schall et al., 1993; Ohmori and Hamilton, 1994; Hornung et al., 1997; Hornung et al., 2001; Lebovic et al., 2001), and nocturnal levels of melatonin reduce neutrophil and monocyte migration to inflammatory sites *in vivo* (Lotufo et al., 2001; Lotufo et al., 2006; Tamura et al., 2010; Marçola et al., 2013).

Interestingly, MCP-1/CCL2 levels were enhanced after infection with *L. amazonensis*, but melatonin treatment reduced this chemokine production in infected macrophages. Melatonin (pretreatment with 100 μ M for 4 h) also reduces MCP-1/CCL2 levels and the levels of RANTES/CCL5 produced by PBMCs stimulated with LPS (Park et al., 2007). Corroborating the role of melatonin in miRNA modulation in infected macrophages, inhibition of miR-294 increased *Mcp-1* mRNA levels, impacting *Leishmania* infectivity. The downregulation of miR-181c occurred in the absence of TLR4 signaling in C57BL/6-macrophages infection with *L. amazonensis* (Muxel et al., 2018a), whereas inhibition of miR-181c reduced *Mcp-1* mRNA levels and reduced infectivity in BALB/c-macrophages.

Our data corroborate the idea that *Leishmania* infection may regulate cytokine, chemokine and NO production to prevent or delay macrophage activation, allowing parasite entrance and replication. These data reinforce the importance of studying miRNA expression during infection and its role in macrophage activation. Additionally, we demonstrate that melatonin can modulate the miRNA profile and consequently alter the activation phenotype of infected macrophages.

Supplementary information



Supplementary Figure 1 *Leishmania* infectivity in melatonin-treated macrophages. BALB/c macrophages (2×10^5 cells) were pre-incubated for 1, 2 or 4 h with medium (untreated, white bar), vehicle (ethanol 0.0005%, gray bar), or 3 (blue bar) or 30 (light blue bar) nM of melatonin. After, macrophages were infected with *L. amazonensis* (MOI 5:1) and analyzed after 4 and 24 h. A-C – percentage of infected macrophages; D-F – number of amastigotes per infected macrophage; G-I – infection index (rate of infected macrophages multiplied by the number of amastigotes per infected macrophage). Each bar represents the mean \pm SEM of 3 independent experiments ($n=5-8$). * represent $p < 0.05$, comparing the melatonin treatment with the vehicle-treated macrophage at the same concentration and time.

Supplementary Table 1: miRNAs Up-Down Regulation in melatonin and infected *L. amazonensis* infected macrophages compared to uninfected. The relative up- and down-regulation of miRNAs, expressed as boundaries of 1.5 and -1.5 of Fold Regulation, respectively. $p < 0.05$ was considered statistically significant. p-value was determined based on two-tailed Student's t test. The data are representative of three independent experiments. Untreated: only 10% FBS RPMI 1640 medium; Vehicle: ethanol 0.0005% in 10% FBS RPMI 1640 medium; Melatonin 30nM diluted 10% FBS RPMI 1640 medium.

Supplementary Table 2: Predicted mRNA-targets for miR-30e. The miRNA-mRNA interaction was predicted using miRecord tools (<http://c1.accurascience.com/miRecords/>) based in the integration of various prediction tools: DIANA-microT, MicroInspector, miRanda, MirTarget2, miTarget, NBmiRTar, PicTar, PITA, RNA22, RNAhybrid, and TargetScan/TargetScanS.

Supplementary Table 3: Predicted mRNA-targets for miR-181c.

The miRNA-mRNA interaction was predicted using miRecord tools (<http://c1.accurascience.com/miRecords/>) based in the integration of various prediction tools: DIANA-microT, MicroInspector, miRanda, MirTarget2, miTarget, NBmiRTar, PicTar, PITA, RNA22, RNAhybrid, and TargetScan/TargetScanS.

Supplementary Table 4: Predicted mRNA-targets for miR-294.

The miRNA-mRNA interaction was predicted using miRecord tools (<http://c1.accurascience.com/miRecords/>) based in the integration of various prediction tools: DIANA-microT, MicroInspector, miRanda, MirTarget2, miTarget, NBmiRTar, PicTar, PITA, RNA22, RNAhybrid, and TargetScan/TargetScanS.

Supplementary Table 5: Predicted mRNA-targets for miR-302d.

The miRNA-mRNA interaction was predicted using miRecord tools (<http://c1.accurascience.com/miRecords/>) based in the integration of various prediction tools: DIANA-microT, MicroInspector, miRanda, MirTarget2, miTarget, NBmiRTar, PicTar, PITA, RNA22, RNAhybrid, and TargetScan/TargetScanS.

References

- Alvar, J., Velez, I.D., Bern, C., Herrero, M., Desjeux, P., Cano, J., et al. (2012). Leishmaniasis worldwide and global estimates of its incidence. *PLoS One* 7, e35671.
- Ashford, R.W. (2000). The leishmaniasis as emerging and reemerging zoonoses. *Int J Parasitol* 30, 1269-1281.
- Bagga, S., Bracht, J., Hunter, S., Massirer, K., Holtz, J., Eachus, R., et al. (2005). Regulation by let-7 and lin-4 miRNAs results in target mRNA degradation. *Cell* 122, 553-563.
- Baltimore, D., Boldin, M.P., O'connell, R.M., Rao, D.S., and Taganov, K.D. (2008). MicroRNAs: new regulators of immune cell development and function. *Nat Immunol* 9, 839-845.
- Banerjee, S., Xie, N., Cui, H., Tan, Z., Yang, S., Icyuz, M., et al. (2013). MicroRNA let-7c regulates macrophage polarization. *J Immunol* 190, 6542-6549.
- Ben-Othman, R., Dellagi, K., and Guizani-Tabbane, L. (2009). Leishmania major parasites induced macrophage tolerance: implication of MAPK and NF-kappaB pathways. *Mol Immunol* 46, 3438-3444.
- Boucher, J.L., Moali, C., and Tenu, J.P. (1999). Nitric oxide biosynthesis, nitric oxide synthase inhibitors and arginase competition for L-arginine utilization. *Cell Mol Life Sci* 55, 1015-1028.
- Carrillo-Vico, A., Calvo, J.R., Abreu, P., Lardone, P.J., Garcia-Maurino, S., Reiter, R.J., et al. (2004). Evidence of melatonin synthesis by human lymphocytes and its physiological significance: possible role as intracrine, autocrine, and/or paracrine substance. *FASEB J* 18, 537-539.
- Carrillo-Vico, A., Guerrero, J.M., Lardone, P.J., and Reiter, R.J. (2005). A review of the multiple actions of melatonin on the immune system. *Endocrine* 27, 189-200.
- Carrillo-Vico, A., Lardone, P.J., Alvarez-Sanchez, N., Rodriguez-Rodriguez, A., and Guerrero, J.M. (2013). Melatonin: buffering the immune system. *Int J Mol Sci* 14, 8638-8683.
- Carvalho-Sousa, C.E., Da Silveira Cruz-Machado, S., Tamura, E.K., Fernandes, P.A., Pinato, L., Muxel, S.M., et al. (2011). Molecular basis for defining the pineal gland and pinealocytes as targets for tumor necrosis factor. *Front Endocrinol (Lausanne)* 2, 10.
- Corraliza, I.M., Soler, G., Eichmann, K., and Modolell, M. (1995). Arginase induction by suppressors of nitric oxide synthesis (IL-4, IL-10 and PGE2) in murine bone-marrow-derived macrophages. *Biochem Biophys Res Commun* 206, 667-673.
- Da Silveira Cruz-Machado, S., Carvalho-Sousa, C.E., Tamura, E.K., Pinato, L., Cecon, E., Fernandes, P.A., et al. (2010). TLR4 and CD14 receptors expressed in rat pineal gland trigger NFkB pathway. *J Pineal Res* 49, 183-192.
- David, Y., Ziv, T., Admon, A., and Navon, A. (2010). The E2 ubiquitin-conjugating enzymes direct polyubiquitination to preferred lysines. *J Biol Chem* 285, 8595-8604.
- Deng, W.G., Tang, S.T., Tseng, H.P., and Wu, K.K. (2006). Melatonin suppresses macrophage cyclooxygenase-2 and inducible nitric oxide synthase expression by inhibiting p52 acetylation and binding. *Blood* 108, 518-524.
- Dillon, L.A., Suresh, R., Okrah, K., Corrada Bravo, H., Mosser, D.M., and El-Sayed, N.M. (2015). Simultaneous transcriptional profiling of *Leishmania major* and its murine macrophage host cell reveals insights into host-pathogen interactions. *BMC Genomics* 16, 1108.
- Dixit, V., and Mak, T.W. (2002). NF-kappaB signaling. Many roads lead to madrid. *Cell* 111, 615-619.

- El-Sokkary, G.H., Omar, H.M., Hassanein, A.F., Cuzzocrea, S., and Reiter, R.J. (2002). Melatonin reduces oxidative damage and increases survival of mice infected with *Schistosoma mansoni*. *Free Radic Biol Med* 32, 319-332.
- Elmahallawy, E.K., Jimenez-Aranda, A., Martinez, A.S., Rodriguez-Granger, J., Navarro-Alarcon, M., Gutierrez-Fernandez, J., et al. (2014). Activity of melatonin against *Leishmania infantum* promastigotes by mitochondrial dependent pathway. *Chem Biol Interact* 220, 84-93.
- Farlik, M., Reutterer, B., Schindler, C., Greten, F., Vogl, C., Muller, M., et al. (2010). Nonconventional initiation complex assembly by STAT and NF-kappaB transcription factors regulates nitric oxide synthase expression. *Immunity* 33, 25-34.
- Fernandes, M.C., Dillon, L.A., Belew, A.T., Bravo, H.C., Mosser, D.M., and El-Sayed, N.M. (2016). Dual Transcriptome Profiling of *Leishmania*-Infected Human Macrophages Reveals Distinct Reprogramming Signatures. *MBio* 7.
- Fletcher, A.J., Mallery, D.L., Watkinson, R.E., Dickson, C.F., and James, L.C. (2015). Sequential ubiquitination and deubiquitination enzymes synchronize the dual sensor and effector functions of TRIM21. *Proc Natl Acad Sci U S A* 112, 10014-10019.
- Frank, B., Marcu, A., De Oliveira Almeida Petersen, A.L., Weber, H., Stigloher, C., Mottram, J.C., et al. (2015). Autophagic digestion of *Leishmania major* by host macrophages is associated with differential expression of BNIP3, CTSE, and the miRNAs miR-101c, miR-129, and miR-210. *Parasit Vectors* 8, 404.
- Gao, Z., Zhu, X., and Dou, Y. (2015). The miR-302/367 cluster: a comprehensive update on its evolution and functions. *Open Biol* 5, 150138.
- Geraci, N.S., Tan, J.C., and McDowell, M.A. (2015). Characterization of microRNA expression profiles in *Leishmania*-infected human phagocytes. *Parasite Immunol* 37, 43-51.
- Ghalib, H.W., Whittle, J.A., Kubin, M., Hashim, F.A., El-Hassan, A.M., Grabstein, K.H., et al. (1995). IL-12 enhances Th1-type responses in human *Leishmania donovani* infections. *J Immunol* 154, 4623-4629.
- Ghosh, J., Bose, M., Roy, S., and Bhattacharyya, S.N. (2013). *Leishmania donovani* targets Dicer1 to downregulate miR-122, lower serum cholesterol, and facilitate murine liver infection. *Cell Host Microbe* 13, 277-288.
- Gilad, E., Wong, H.R., Zingarelli, B., Virag, L., O'connor, M., Salzman, A.L., et al. (1998). Melatonin inhibits expression of the inducible isoform of nitric oxide synthase in murine macrophages: role of inhibition of NFkappaB activation. *FASEB J* 12, 685-693.
- Graff, J.W., Dickson, A.M., Clay, G., McCaffrey, A.P., and Wilson, M.E. (2012). Identifying functional microRNAs in macrophages with polarized phenotypes. *J Biol Chem* 287, 21816-21825.
- Gregory, D.J., and Olivier, M. (2005). Subversion of host cell signalling by the protozoan parasite *Leishmania*. *Parasitology* 130 Suppl, S27-35.
- Hershkovitz-Rokah, O., Modai, S., Pasmanik-Chor, M., Toren, A., Shomron, N., Raanani, P., et al. (2015). MiR-30e induces apoptosis and sensitizes K562 cells to imatinib treatment via regulation of the BCR-ABL protein. *Cancer Lett* 356, 597-605.
- Hornung, D., Bentzien, F., Wallwiener, D., Kiesel, L., and Taylor, R.N. (2001). Chemokine bioactivity of RANTES in endometriotic and normal endometrial stromal cells and peritoneal fluid. *Mol Hum Reprod* 7, 163-168.
- Hornung, D., Ryan, I.P., Chao, V.A., Vigne, J.L., Schriock, E.D., and Taylor, R.N. (1997). Immunolocalization and regulation of the chemokine RANTES in human endometrial and endometriosis tissues and cells. *J Clin Endocrinol Metab* 82, 1621-1628.
- Hotta, C.T., Gazarini, M.L., Beraldo, F.H., Varotti, F.P., Lopes, C., Markus, R.P., et al. (2000). Calcium-dependent modulation by melatonin of the circadian rhythm in malarial parasites. *Nat Cell Biol* 2, 466-468.

Houbaviy, H.B., Murray, M.F., and Sharp, P.A. (2003). Embryonic stem cell-specific MicroRNAs. *Dev Cell* 5, 351-358.

Hrabak, A., Bajor, T., Temesi, A., and Meszaros, G. (1996). The inhibitory effect of nitrite, a stable product of nitric oxide (NO) formation, on arginase. *FEBS Lett* 390, 203-206.

Hsieh, C.H., Rau, C.S., Jeng, J.C., Chen, Y.C., Lu, T.H., Wu, C.J., et al. (2012). Whole blood-derived microRNA signatures in mice exposed to lipopolysaccharides. *J Biomed Sci* 19, 69.

Ikeda, F., and Dikic, I. (2008). Atypical ubiquitin chains: new molecular signals. 'Protein Modifications: Beyond the Usual Suspects' review series. *EMBO Rep* 9, 536-542.

Jiang, L., Lin, C., Song, L., Wu, J., Chen, B., Ying, Z., et al. (2012). MicroRNA-30e* promotes human glioma cell invasiveness in an orthotopic xenotransplantation model by disrupting the NF-kappaB/IkappaBalpha negative feedback loop. *J Clin Invest* 122, 33-47.

Kinsey, S.G., Prendergast, B.J., and Nelson, R.J. (2003). Photoperiod and stress affect wound healing in Siberian hamsters. *Physiol Behav* 78, 205-211.

Laranjeira-Silva, M.F., Zampieri, R.A., Muxel, S.M., Floeter-Winter, L.M., and Markus, R.P. (2015). Melatonin attenuates *Leishmania (L.) amazonensis* infection by modulating arginine metabolism. *J Pineal Res*.

Lebovic, D.I., Chao, V.A., Martini, J.F., and Taylor, R.N. (2001). IL-1beta induction of RANTES (regulated upon activation, normal T cell expressed and secreted) chemokine gene expression in endometriotic stromal cells depends on a nuclear factor-kappaB site in the proximal promoter. *J Clin Endocrinol Metab* 86, 4759-4764.

Lemaire, J., Mkannez, G., Guerfali, F.Z., Gustin, C., Attia, H., Sghaier, R.M., et al. (2013). MicroRNA expression profile in human macrophages in response to *Leishmania major* infection. *PLoS Negl Trop Dis* 7, e2478.

Lim, L.P., Lau, N.C., Garrett-Engle, P., Grimson, A., Schelter, J.M., Castle, J., et al. (2005). Microarray analysis shows that some microRNAs downregulate large numbers of target mRNAs. *Nature* 433, 769-773.

Lima-Junior, D.S., Costa, D.L., Carregaro, V., Cunha, L.D., Silva, A.L., Mineo, T.W., et al. (2013). Inflammasome-derived IL-1beta production induces nitric oxide-mediated resistance to *Leishmania*. *Nat Med* 19, 909-915.

Lotufo, C.M., Lopes, C., Dubocovich, M.L., Farsky, S.H., and Markus, R.P. (2001). Melatonin and N-acetylserotonin inhibit leukocyte rolling and adhesion to rat microcirculation. *Eur J Pharmacol* 430, 351-357.

Lotufo, C.M., Yamashita, C.E., Farsky, S.H., and Markus, R.P. (2006). Melatonin effect on endothelial cells reduces vascular permeability increase induced by leukotriene B4. *Eur J Pharmacol* 534, 258-263.

Luchetti, F., Canonico, B., Betti, M., Arcangeletti, M., Pilolli, F., Piroddi, M., et al. (2010). Melatonin signaling and cell protection function. *FASEB J* 24, 3603-3624.

Maestroni, G.J. (1996). Melatonin as a therapeutic agent in experimental endotoxic shock. *J Pineal Res* 20, 84-89.

Mantovani, A., Sica, A., Sozzani, S., Allavena, P., Vecchi, A., and Locati, M. (2004). The chemokine system in diverse forms of macrophage activation and polarization. *Trends Immunol* 25, 677-686.

Marçola, M., Da Silveira Cruz-Machado, S., Fernandes, P.A., Monteiro, A.W., Markus, R.P., and Tamura, E.K. (2013). Endothelial cell adhesiveness is a function of environmental lighting and melatonin level. *J Pineal Res* 54, 162-169.

Markus, R.P., Fernandes, P.A., Kinker, G.S., Da Silveira Cruz-Machado, S., and Marçola, M. (2017). Immune-Pineal Axis - Acute inflammatory responses coordinate melatonin synthesis by pinealocytes and phagocytes. *Br J Pharmacol*.

- Markus, R.P., Ferreira, Z.S., Fernandes, P.a.C.M., and Cecon, E. (2007). The immune-pineal axis: a shuttle between endocrine and paracrine melatonin sources. *Neuroimmunomodulation* 14, 126-133.
- Marsden, P.D. (1986). Mucosal leishmaniasis ("espundia" Escomel, 1911). *Trans R Soc Trop Med Hyg* 80, 859-876.
- Martinez, F.O., Helming, L., and Gordon, S. (2009). Alternative activation of macrophages: an immunologic functional perspective. *Annu Rev Immunol* 27, 451-483.
- Mosser, D.M., and Edwards, J.P. (2008). Exploring the full spectrum of macrophage activation. *Nat Rev Immunol* 8, 958-969.
- Mukherjee, B., Paul, J., Mukherjee, S., Mukhopadhyay, R., Das, S., Naskar, K., et al. (2015). Antimony-Resistant *Leishmania donovani* Exploits miR-466i To Deactivate Host MyD88 for Regulating IL-10/IL-12 Levels during Early Hours of Infection. *J Immunol* 195, 2731-2742.
- Muller, K., Van Zandbergen, G., Hansen, B., Laufs, H., Jahnke, N., Solbach, W., et al. (2001). Chemokines, natural killer cells and granulocytes in the early course of *Leishmania major* infection in mice. *Med Microbiol Immunol* 190, 73-76.
- Munder, M., Eichmann, K., and Modolell, M. (1998). Alternative metabolic states in murine macrophages reflected by the nitric oxide synthase/arginase balance: competitive regulation by CD4+ T cells correlates with Th1/Th2 phenotype. *J Immunol* 160, 5347-5354.
- Muxel, S.M., Acuna, S.M., Aoki, J.I., Zampieri, R.A., and Floeter-Winter, L.M. (2018a). Toll-Like Receptor and miRNA-let-7e Expression Alter the Inflammatory Response in *Leishmania amazonensis*-Infected Macrophages. *Front Immunol* 9, 2792.
- Muxel, S.M., Acuña, S.M., Aoki, J.I., Zampieri, R.A., and Floeter-Winter, L.M. (2018b). Toll-like receptor and miRNA-let-7e expression alter the inflammatory response in *Leishmania amazonensis*-infected macrophages *Frontiers in Immunology*.
- Muxel, S.M., Aoki, J.I., Fernandes, J.C.R., Laranjeira-Silva, M.F., Zampieri, R.A., Acuna, S.M., et al. (2018c). Arginine and Polyamines Fate in *Leishmania* Infection. *Front Microbiol* 8, 2682.
- Muxel, S.M., Laranjeira-Silva, M.F., Zampieri, R.A., Aoki, J.I., Acuña, S.M., and Floeter-Winter, L.M. (2017a). Functional validation of miRNA-mRNA interactions in macrophages by inhibition/competition assays based in transient transfection. *Protocol Exchange*.
- Muxel, S.M., Laranjeira-Silva, M.F., Zampieri, R.A., and Floeter-Winter, L.M. (2017b). *Leishmania (Leishmania) amazonensis* induces macrophage miR-294 and miR-721 expression and modulates infection by targeting NOS2 and L-arginine metabolism. *Sci Rep* 7, 44141.
- Muxel, S.M., Pires-Lapa, M.A., Monteiro, A.W., Cecon, E., Tamura, E.K., Floeter-Winter, L.M., et al. (2012). NF-kappaB drives the synthesis of melatonin in RAW 264.7 macrophages by inducing the transcription of the arylalkylamine-N-acetyltransferase (AA-NAT) gene. *PLoS One* 7, e52010.
- Nair, S.M., Rahman, R.M., Clarkson, A.N., Sutherland, B.A., Taurin, S., Sammut, I.A., et al. (2011). Melatonin treatment following stroke induction modulates L-arginine metabolism. *J Pineal Res* 51, 313-323.
- Nathan, C., and Shiloh, M.U. (2000). Reactive oxygen and nitrogen intermediates in the relationship between mammalian hosts and microbial pathogens. *Proc Natl Acad Sci U S A* 97, 8841-8848.
- O'Neill, L.A., Sheedy, F.J., and McCoy, C.E. (2011). MicroRNAs: the fine-tuners of Toll-like receptor signalling. *Nat Rev Immunol* 11, 163-175.
- Ohmori, Y., and Hamilton, T.A. (1994). IFN-gamma selectively inhibits lipopolysaccharide-inducible JE/monocyte chemoattractant protein-1 and KC/GRO/melanoma

growth-stimulating activity gene expression in mouse peritoneal macrophages. *J Immunol* 153, 2204-2212.

Park, H.J., Kim, H.J., Ra, J., Hong, S.J., Baik, H.H., Park, H.K., et al. (2007). Melatonin inhibits lipopolysaccharide-induced CC chemokine subfamily gene expression in human peripheral blood mononuclear cells in a microarray analysis. *J Pineal Res* 43, 121-129.

Pires-Lapa, M.A., Carvalho-Sousa, C.E., Cecon, E., Fernandes, P.A., and Markus, R.P. (2018). beta-Adrenoceptors Trigger Melatonin Synthesis in Phagocytes. *Int J Mol Sci* 19.

Pontes, G.N., Cardoso, E.C., Carneiro-Sampaio, M.M., and Markus, R.P. (2006). Injury switches melatonin production source from endocrine (pineal) to paracrine (phagocytes) - melatonin in human colostrum and colostrum phagocytes. *J Pineal Res* 41, 136-141.

Prendergast, B.J., Hotchkiss, A.K., Bilbo, S.D., Kinsey, S.G., and Nelson, R.J. (2003). Photoperiodic adjustments in immune function protect Siberian hamsters from lethal endotoxemia. *J Biol Rhythms* 18, 51-62.

Recchiuti, A., Krishnamoorthy, S., Fredman, G., Chiang, N., and Serhan, C.N. (2011). MicroRNAs in resolution of acute inflammation: identification of novel resolvin D1-miRNA circuits. *FASEB J* 25, 544-560.

Reiter, R.J., Calvo, J.R., Karbownik, M., Qi, W., and Tan, D.X. (2000). Melatonin and its relation to the immune system and inflammation. *Ann N Y Acad Sci* 917, 376-386.

Reiter, R.J., Tan, D.X., Rosales-Corral, S., and Manchester, L.C. (2013). The universal nature, unequal distribution and antioxidant functions of melatonin and its derivatives. *Mini Rev Med Chem* 13, 373-384.

Ren, D.L., Li, Y.J., Hu, B.B., Wang, H., and Hu, B. (2015). Melatonin regulates the rhythmic migration of neutrophils in live zebrafish. *J Pineal Res* 58, 452-460.

Roh, Y.S., Song, J., and Seki, E. (2014). TAK1 regulates hepatic cell survival and carcinogenesis. *J Gastroenterol* 49, 185-194.

Rojas, I.G., Padgett, D.A., Sheridan, J.F., and Marucha, P.T. (2002). Stress-induced susceptibility to bacterial infection during cutaneous wound healing. *Brain Behav Immun* 16, 74-84.

Santello, F.H., Frare, E.O., Caetano, L.C., Alonsotoldo, M.P., and Do Prado, J.C., Jr. (2008a). Melatonin enhances pro-inflammatory cytokine levels and protects against Chagas disease. *J Pineal Res* 45, 79-85.

Santello, F.H., Frare, E.O., Dos Santos, C.D., Caetano, L.C., Alonso Toldo, M.P., and Do Prado, J.C., Jr. (2008b). Suppressive action of melatonin on the TH-2 immune response in rats infected with *Trypanosoma cruzi*. *J Pineal Res* 45, 291-296.

Santello, F.H., Frare, E.O., Dos Santos, C.D., Toldo, M.P., Kawasse, L.M., Zucoloto, S., et al. (2007). Melatonin treatment reduces the severity of experimental *Trypanosoma cruzi* infection. *J Pineal Res* 42, 359-363.

Schall, T.J., Bacon, K., Camp, R.D., Kaspari, J.W., and Goeddel, D.V. (1993). Human macrophage inflammatory protein alpha (MIP-1 alpha) and MIP-1 beta chemokines attract distinct populations of lymphocytes. *J Exp Med* 177, 1821-1826.

Scott, P., and Novais, F.O. (2016). Cutaneous leishmaniasis: immune responses in protection and pathogenesis. *Nat Rev Immunol* 16, 581-592.

Smith, S., Fernando, T., Wu, P.W., Seo, J., Ni Gabhann, J., Piskareva, O., et al. (2017). MicroRNA-302d targets IRF9 to regulate the IFN-induced gene expression in SLE. *J Autoimmun* 79, 105-111.

Srivastava, A., Singh, N., Mishra, M., Kumar, V., Gour, J.K., Bajpai, S., et al. (2012). Identification of TLR inducing Th1-responsive *Leishmania donovani* amastigote-specific antigens. *Mol Cell Biochem* 359, 359-368.

- Tamura, E.K., Fernandes, P.A., Marçola, M., Da Silveira Cruz-Machado, S., and Markus, R.P. (2010). Long-lasting priming of endothelial cells by plasma melatonin levels. *PLoS One* 5, e13958.
- Verreck, F.A., De Boer, T., Langenberg, D.M., Hoeve, M.A., Kramer, M., Vaisberg, E., et al. (2004). Human IL-23-producing type 1 macrophages promote but IL-10-producing type 2 macrophages subvert immunity to (myco)bacteria. *Proc Natl Acad Sci U S A* 101, 4560-4565.
- Vieira, L.Q., Goldschmidt, M., Nashleanas, M., Pfeffer, K., Mak, T., and Scott, P. (1996). Mice lacking the TNF receptor p55 fail to resolve lesions caused by infection with *Leishmania major*, but control parasite replication. *J Immunol* 157, 827-835.
- Wanasen, N., and Soong, L. (2008). L-arginine metabolism and its impact on host immunity against *Leishmania* infection. *Immunol Res* 41, 15-25.
- Wang, N., Liang, H., and Zen, K. (2014). Molecular mechanisms that influence the macrophage m1-m2 polarization balance. *Front Immunol* 5, 614.
- Wang, Y., Liang, Y., and Lu, Q. (2008). MicroRNA epigenetic alterations: predicting biomarkers and therapeutic targets in human diseases. *Clin Genet* 74, 307-315.
- Wei, X.Q., Charles, I.G., Smith, A., Ure, J., Feng, G.J., Huang, F.P., et al. (1995). Altered immune responses in mice lacking inducible nitric oxide synthase. *Nature* 375, 408-411.
- Who, W.H.O. (2017). "Leishmaniasis".
- Wilhelm, P., Ritter, U., Labbow, S., Donhauser, N., Rollinghoff, M., Bogdan, C., et al. (2001). Rapidly fatal leishmaniasis in resistant C57BL/6 mice lacking TNF. *J Immunol* 166, 4012-4019.
- Wu, Y., Sun, Q., and Dai, L. (2017). Immune regulation of miR-30 on the *Mycobacterium tuberculosis*-induced TLR/MyD88 signaling pathway in THP-1 cells. *Exp Ther Med* 14, 3299-3303.
- Xia, M.Z., Liang, Y.L., Wang, H., Chen, X., Huang, Y.Y., Zhang, Z.H., et al. (2012). Melatonin modulates TLR4-mediated inflammatory genes through MyD88- and TRIF-dependent signaling pathways in lipopolysaccharide-stimulated RAW264.7 cells. *J Pineal Res* 53, 325-334.
- Xu, X., Wang, G., Ai, L., Shi, J., Zhang, J., and Chen, Y.X. (2018). Melatonin suppresses TLR9-triggered proinflammatory cytokine production in macrophages by inhibiting ERK1/2 and AKT activation. *Sci Rep* 8, 15579.
- Yang, J., Liang, Y., Han, H., and Qin, H. (2013). Identification of a miRNA signature in neutrophils after traumatic injury. *Acta Biochim Biophys Sin (Shanghai)* 45, 938-945.
- Yang, Z., Mosser, D.M., and Zhang, X. (2007). Activation of the MAPK, ERK, following *Leishmania amazonensis* infection of macrophages. *J Immunol* 178, 1077-1085.
- Zhang, H.M., and Zhang, Y. (2014). Melatonin: a well-documented antioxidant with conditional pro-oxidant actions. *J Pineal Res* 57, 131-146.
- Zhang, X., and Mosser, D.M. (2008). Macrophage activation by endogenous danger signals. *J Pathol* 214, 161-178.
- Zheng, G.X., Ravi, A., Calabrese, J.M., Medeiros, L.A., Kirak, O., Dennis, L.M., et al. (2011). A latent pro-survival function for the mir-290-295 cluster in mouse embryonic stem cells. *PLoS Genet* 7, e1002054.
- Zhou, L.L., Wei, W., Si, J.F., and Yuan, D.P. (2010). Regulatory effect of melatonin on cytokine disturbances in the pristane-induced lupus mice. *Mediators Inflamm* 2010.
- Zhu, X., He, Z., Hu, Y., Wen, W., Lin, C., Yu, J., et al. (2014). MicroRNA-30e* suppresses dengue virus replication by promoting NF-kappaB-dependent IFN production. *PLoS Negl Trop Dis* 8, e3088.

Zhuang, L., Shou, T., Li, K., Gao, C.L., Duan, L.C., Fang, L.Z., et al. (2017).
MicroRNA-30e-5p promotes cell growth by targeting PTPN13 and indicates poor survival
and recurrence in lung adenocarcinoma. *J Cell Mol Med* 21, 2852-2862

Capítulo 2

Receptores do tipo Toll e o miRNA let-7e possuem como alvo a resposta inflamatória em macrófagos infectados com *Leishmania amazonensis*

O texto apresentado a seguir foi publicado no periódico *Frontiers in Immunology*, em 29 de novembro de 2018, como parte da edição especial *Immune Evasion Mechanisms in the Pathogenesis of Trypanosomatid Infection*.

O artigo está no volume 9, artigo 2792 e contém 17 páginas.

O material está disponível *online* por meio do DOI [10.3389/fimmu.2018.02792](https://doi.org/10.3389/fimmu.2018.02792)

Autores: Sandra Marcia Muxel, Stephanie Maia Acuña, Juliana Ide Aoki, Ricardo Andrade Zampieri, Lucile Maria Floeter-Winter.

Título original:

Toll-like receptors and miRNA-let-7e expression target inflammatory response in *Leishmania amazonensis* infected macrophages

Resumo

O reconhecimento de parasitas por meio dos Receptores Semelhantes a Toll (TLRs); contribui para a ativação de macrófagos a fim de controlar a infecção por *Leishmania*. Tal controle dá-se por meio da produção de citocinas pró-inflamatórias e moléculas microbidas. A infecção pode modular o perfil de microRNAs (miRNAs) do hospedeiro, mediando um controle pós-transcricional de genes envolvidos em atividades leishmanicidas. Neste trabalho, avaliamos a contribuição da sinalização dos TLRs para o perfil de miRNAs no contexto da infecção de macrófagos murinos por *Leishmania amazonensis*. A infectividade de *L. amazonensis* foi maior em macrófagos derivados de medula óssea de camundongos MyD88^{-/-}, TLR2^{-/-} ou TLR4^{-/-}, em contraste com macrófagos selvagens (WT - C57BL/6). A infecção promoveu nos macrófagos selvagens uma modulação de 32% dos miRNAs analisados, sendo 50% tiveram expressão aumentada. A ausência de MyD88, TLR2 ou TLR4 altera a expressão de miRNAs durante a infecção, como a diminuição da expressão de let-7e. Além disso, a ausência dos sinais mediados pelas moléculas nocauteadas reduziu o número de transcritos de *Nos2*, durante a infecção. No entanto, a inibição de let-7e, em macrófagos infectados (4-24h), aumentou a expressão de *Nos2* em níveis de transcritos, proteicos, e, também, a produção de NO. A combinação da ausência de TLR2 e a inibição de let-7e promoveu um aumento nos transcritos de *Arg1*, mas não observamos aumento nos níveis proteicos, durante a infecção. Apesar disso, os transportadores de L-arginina, *Cat1* e *Cat2B*, tiveram níveis maiores na ausência da sinalização por MyD88, mas não houve alteração quando let-7e foi inibido. Tal inibição de let-7e promoveu um impacto global na transcrição de genes envolvidos com a sinalização de TLRs, aumentando a expressão de receptores e moléculas adaptadoras como *Tlr6*, *Tlr9*, *Ly96*, *Tirap*, *traf6*, *Ticam*, *Tollip*, *Casp8*, *Map3k1*, *Nfkbib*, *Nfkb1l*, *Ppara*, *Mapk8ip3*, *Hspd1* e *Ube2n*; além de imuno-moduladores como *Ptgs2/Cox*, *Csf2*, *Csf3*, *Infbl*, *Il6ra* e *Ilr1*, impactando na expressão de NOS2, produção de NO e na infectividade dos

parasitas. Concluimos que *L. amazonensis* altera a via de sinalização de TLRs por meio de miRNAs em macrófagos como forma de subversão da resposta imunológica do hospedeiro.

Abstract

The parasite recognition via Toll-like receptors (TLRs) contribute in macrophage activation to control *Leishmania* infection, through the coordinated production of pro-inflammatory and microbicide effector molecules. The modulation of microRNAs (miRNAs) expression by *Leishmania* infection, could mediate the post-transcriptional regulation of genes involved in leishmanicidal activity. Here, the contribution of TLR signaling on the miRNA profile and gene expression was evaluated in *Leishmania amazonensis* infected murine macrophages. The infectivity of *L. amazonensis* was higher in murine Bone Marrow-Derived macrophages derived from MyD88^{-/-}, TLR2^{-/-} or TLR4^{-/-} mice than wild type C57BL/6 (WT). *L. amazonensis* infection of WT-macrophages modulated 32% of miRNA analyzed, while 50% were upregulated. The absence of MyD88, TLR2 and TLR4 alters the percentage of miRNAs modulated during *L. amazonensis* infection, such as downregulating let-7e expression. Moreover, the absence of signals mediated via MyD88, TLR2 or TLR4 reduced nitric oxide synthase 2 (*Nos2*) mRNA expression during infection. Indeed, the inhibition of let-7e increased *Nos2* mRNA and NOS2 (or iNOS) protein levels and nitric oxide (NO) production in *L. amazonensis* infected macrophages (4-24h). The absence of TLR2 and inhibition of let-7e increased the arginase 1 mRNA but did not alter the protein level during infection. However, during infection the levels of L-arginine transporters, *Cat2B* and *Cat1*, were higher in the absence of Myd88 signaling, but were not altered in the let-7e inhibition. The let-7e inhibition impacted globally in TLR pathway gene expression, upregulating the expression of recognition and adaptors molecules, such as *Tlr6*, *Tlr9*, *Ly96*, *Tirap*, *Traf6*, *Ticam1*, *Tollip*, *Casp8*, *Map3k1*, *Mapk8*, *Nfkbib*, *Nfkbil1*, *Ppara*, *Mapk8ip3*, *Hspd1*, and *Ube2n*; and also immunomodulators, such as *Ptgs2/Cox2*, *Csf2*, *Csf3*, *Ifnb1*, *Il6ra* and *Ilr1* expression impacting in NOS2 expression, NO production and parasite infectiveness. In conclusion, *L. amazonensis* infection alters the TLR signaling pathways via miRNA modulation in macrophages to subvert the host immune responses.

Introduction

Protozoan parasites of the genus *Leishmania* are the agent causative of leishmaniasis, diseases that affect more than 12 million people worldwide (Alvar et al., 2012). Cutaneous leishmaniasis is widespread in Brazil, the most affected country in the Americas, with an estimated incidence of 100.000 cases per year (Alvar et al., 2012). *L. amazonensis* is related to induce cutaneous and/or diffuse cutaneous manifestations (Bogdan, 2008; Liese et al., 2008).

Host-parasite interactions during innate immune response to *Leishmania* is mediated by pattern recognition receptors (PRRs), such as Toll-like receptors (TLRs) and recognizing pathogen-associated molecules (PAMPs), mainly expressed in phagocytes and presenting cells, as neutrophils, macrophages and dendritic cells (Liu and Uzonna, 2012; Carlsen et al., 2015). The surface of *Leishmania* spp is covered with molecules that could be recognized by TLRs (Tuon et al., 2008), which play a central role in macrophage activation, signaling to phagocytosis, parasite healing or persistence and in innate to adaptive immunity control of infections (Akira and Sato, 2003; Takeda et al., 2003; Akira et al., 2006; Gazzinelli and Denkers, 2006; Uematsu and Akira, 2006).

The interaction of TLR2 or TLR4 starts the signal transduction through the adaptor molecules such as Myeloid differentiation factor 88 (MyD88) and Toll-like receptor adapter inducing interferon β (TRIF/TICAM1) (Kagan et al., 2008), mediating *Leishmania* recognition and modulation of infectivity into macrophages (Kropf et al., 2004; Flandin et al., 2006; Vargas-Inchaustegui et al., 2009). The activation of TLR2 or TLR4 signaling cascade by LPG stimulation and also *L. donovani*, *L. major* or *L. amazonensis* infections can lead to modulation of the transcription factors, such as nuclear factor kappa β (NF- κ B), interferon regulatory factors (IRFs) and mitogen-activated protein kinase (MAPK), that induce the transcription of pro-inflammatory cytokines, as tumor necrosis factor (TNF), and also NO and superoxide production (Dixit and Mak, 2002; Janeway and Medzhitov, 2002; Becker et al., 2003; Flandin et al., 2006; Medzhitov, 2007; Whitaker et al., 2008; Dillon et al., 2015). However, the regulation of the signal for activation of TLR signaling is not completely understood.

The NO production in initial steps of inflammatory response can lead to leishmanicidal activity (Nathan and Shiloh, 2000; Gregory and Olivier, 2005; Flandin et al., 2006; Lima-Junior et al., 2013). The outcome of *Leishmania* infection depends on the balance between inducing NOS2 expression to produce NO resulting in parasite killing (Ghalib et al., 1995; Vieira et al., 1996; Wilhelm et al., 2001; Yang et al., 2007; Ben-Othman et al., 2009; Srivastava et al., 2012; Muxel et al., 2017c); versus induction of arginase 1 (ARG1) expression to produce polyamines leading to *Leishmania* survival (Nasseri and Modabber, 1979; Bacellar et al., 2000; Bhattacharyya et al., 2001; Kane and Mosser, 2001; Yang et al., 2007). Interestingly, L-arginine is the same substrate of both NOS2 and ARG1. Depending on the environmental conditions and immune response, the prevalence of one activity over the other results in the killing of the parasite or its survival. The cationic amino acid transporters (CAT) expression and its role in L-arginine uptakes into macrophages can help the fate of infectiveness (Liew et al., 1990; Iniesta et al., 2001; Iniesta et al., 2002; Wanasen and Soong, 2008; Laranjeira-Silva et al., 2015b).

The immune response can be subverted by post-transcriptional regulation via microRNAs (miRNAs), leading to survival of *Leishmania* (Geraci et al., 2015; Singh et al.,

2016;Muxel et al., 2017c). The miRNAs are evolutionary conserved small (18-25 nucleotides) non-coding RNAs, which fine-tune gene expression by base-pairing complementary to 3'untranslated region (3'UTR) sequence of a target mRNA, leading to block target-mRNA translation or its degradation (Bernstein et al., 2001;Schwarz et al., 2003;Vaucheret et al., 2004;Bagga et al., 2005;Lim et al., 2005;Wang et al., 2009). The miRNAs are divided in several families and one of them includes *lethal-7* (let-7) family, which was first described in the nematode *Caenorhabditis elegans*, as responsible for the developmental time regulation (Reinhart et al., 2000) and are conserved among various species, including *Drosophila melanogaster* (fruit fly), *Mus musculus* (mouse) and human (*Homo sapiens*) (Pasquinelli et al., 2000;Lagos-Quintana et al., 2002). The let-7e isoform comprises the let-7 family in mice (Pasquinelli et al., 2000;Lagos-Quintana et al., 2002;Landgraf et al., 2007) and can regulate pro- and anti-inflammatory responses during infection or TLR/PAMPs-stimulation, mediating the NF-kB activation, as well as cytokines production (Androulidaki et al., 2009;de la Rica et al., 2015;Dong et al., 2015;Elizabeth et al., 2016;Kalantari et al., 2017).

In this study, we analyzed the activation of TLRs cascade signaling and the miRNAs-mRNAs interactions on trial to understand the outcome of *L. amazonensis* infection in C57BL/6 macrophages. TLR2 and TLR4 mediated *L. amazonensis* recognition and infectivity resistance into macrophages. Other MyD88-dependent receptors may participate in macrophage activation in response to *L. amazonensis*. We observed that *L. amazonensis* infection altered the gene expression of TLRs signaling, transcription factors and pro-inflammatory molecules. MyD88, TLR2 and TLR4 regulated the miRNA expression, such as let-7e, during the course of infection. In addition, the functional inhibition of let-7e lead to the alteration of TLR pathway and *Nos2*/NOS2 expression and NO production, impacting in the infectiveness of parasite.

Materials and Methods

Ethics Statement

Experimental protocol for the animal experiments was approved by the Comissão de Ética no Uso de Animais (CEUA) from Instituto de Biociências of the Universidade de São Paulo (the approval number CEUA-IB: 233/2014). This study was carried out in strict accordance with the recommendations in the guide and policies for the care and use of laboratory animals of the São Paulo State (Lei Estadual 11.977, de 25/08/2005) and Brazil government (Lei Federal 11.794, de 08/10/2008).

Parasite culture

L. amazonensis (MHOM/BR/1973/M2269) promastigotes were maintained in culture at 25°C in M199 medium (Invitrogen, Grand Island, NY, USA) supplemented with 10% heat-inactivated fetal bovine serum (Invitrogen), 5 ppm hemin, 100 µM adenine, 100 U penicillin, 100 µg/mL streptomycin, 40 mM HEPES-NaOH and 12 mM NaHCO₃, pH 7.0 for a week-long culture at a low passage (P1 to P5).

In vitro macrophage infections

All experiments were performed using female mice (6-8-weeks-old) C57BL/6 wild type (WT), or the knockout strains MyD88^{-/-}, TLR2^{-/-} or TLR4^{-/-} from Biotério do Departamento de Imunologia, Instituto de Ciências Biomédicas - Universidade de São Paulo and maintained in the Biotério do Departamento de Fisiologia, Instituto de Biociências - Universidade de São Paulo. The animals were sacrificed in a CO₂ chamber and femurs were collected to obtain bone marrow-derived macrophages (BMDMs). The femurs were washed with 2 mL of cold PBS, collected at 1,500xg for 10 min at 4°C and resuspended in RPMI 1640 medium (LGC Biotecnologia, São Paulo, SP, Brazil), supplemented with penicillin (100 U/ml) (Invitrogen), streptomycin (100 µg/ml) (Invitrogen), 5% heat-inactivated FBS (Invitrogen) and 20% L9-29 supernatant. The cells were cultivated for 7-8 days at 34°C in an atmosphere of 5% CO₂. After differentiation, cellular viability was evaluated by flow cytometry (FlowSight, MerckMillipore), showing the presence of 95% F4/80⁻ and CD11b⁺ cells.

Approximately 2x10⁵ BMDMs were plated into 8-wells glass chamber slide (Lab-Teck Chamber Slide; Nunc, Naperville, IL, USA) and incubated at 34°C in an atmosphere of 5% CO₂ for infectivity analysis. Approximately 3x10⁶ BMDMs were plated into 6-wells plate (SPL, Lifescience, Pocheon, Korea) and incubated at 34°C in an atmosphere of 5% CO₂ for miRNA and mRNA analysis. After 18 h of incubation, non-adherent cells were removed by PBS washing and the infection was performed with promastigotes in the stationary growth phase (MOI 5:1). After 4 h of incubation, non-phagocytosed promastigotes were removed by washing with fresh medium. Thereafter the infection course was followed for 4, 24 and 48 h. Non-infected macrophages maintained in culture at the same conditions were used as control. The infectivity were microscopically analyzed after cell-fixation with acetone/methanol (1:1, v:v, Merck, Darmstadt, Germany) for 20 min at -20°C, followed by PBS washing and DAPI staining (Invitrogen). The infectivity indexes (rate of infected macrophages multiplied by the average number of amastigotes per infected macrophage) were calculated by randomly counting of at

least 600 macrophages per slide. For RNA analysis, the cells were washed with PBS, resuspended in QIAzol (Qiagen, Germantown, MD, USA) and stored at -20°C until use.

RNA extraction, reverse transcription and miRNA PCR array

RNA extraction was performed using miRneasy® Mini kit (Qiagen, Hilden, Germany), according to the manufacturer's instructions. cDNA was produced from mature miRNA using the miScript II RT kit (Qiagen, Hilden, Germany), according to the manufacturer's instructions. Briefly, 250 ng of total RNA were added to 2 µL of 5X miScript HiSpec Buffer, 1 µL of 10X Nucleic Acids Mix, 1 µL of miScript Reverse Transcriptase Mix and RNase-free water to a final volume of 10 µL. The mixture was incubated for 60 min at 37°C for the insertion of poli-A⁺ at the end of the miRNA sequence (downstream) and the annealing of a T-tail-tag for the elongation of the cDNA. The enzyme was inactivated at 95°C for 5 min. The reaction was performed in a Thermocycler Mastercycler gradient (Eppendorf, Hamburg, Germany). The cDNAs were stored at -20°C until use.

miRNA PCR array was performed with ten-fold diluted cDNA as template, using Mouse Inflammatory Response & Autoimmunity miRNA PCR Array: MIMM-105Z (Qiagen, Germantown, MD, USA) and the miScript SYBR PCR Kit (Qiagen, Hilden, Germany), as previously described (Muxel et al., 2017b). Briefly, the pool mixture was performed with 2X QuantiTect SYBR Green PCR Master Mix, 10X miScript Universal Primer, 105 µL of cDNA, and RNase-free water to a final volume of 2,625 µL, then distributed 25 µL/well. The specific amplification of let-7e-5p by RT-qPCR was performed with 2X QuantiTect SYBR Green PCR Master Mix, 10X miScript Universal Primer, 10X Specific Primer, 5 µL of cDNA, and RNase-free water to a final volume of 25 µL. The reactions consisted in the activation of the HotStart Polymerase for 15 sec at 95°C and 40 cycles of 15 sec at 94°C, followed by 30 sec at 55°C and 30 sec at 70°C, performed in the Thermocycler ABI Prism 7300 (Applied Biosystems, Carlsbad, CA, USA). The relative Ct was analyzed using the miScript miRNA PCR Array Data Analysis software (www.qiagen.com). Triplicate samples were analyzed for each condition. The average Ct was calculated to represent the gene expression variation with good accuracy. The geometric average Ct of the miRNAs was normalized based on the average of SNORD95A. The PCR and RT-qPCR kit controls were performed according to the manufacturer's instructions and determined by efficiency reactions. A negative control containing all reaction components, except the reverse transcriptase enzyme was included and subjected to RT-qPCR to check the absence of DNA contamination in RNA samples. The Fold Regulation (FR) consisted in the negative inverse of the fold-change (function = $-1*(1/\text{fold-change value})$). The FR levels ≥ 1.2 were considered to indicate up-regulation, and levels ≤ 1.2 were considered to indicate down-regulation. Venn Diagram was designed based in Venny 2.1 tool (<http://bioinfogp.cnb.csic.es/tools/venny/index.html>) (Oliveros, 2007-2015) and modified to include miRNA or mRNA names inside the areas.

Reverse transcription and RT-qPCR for mRNA

cDNA synthesis for mRNAs analysis was performed using 2 µg of total RNA, 20 nmol random primer (Applied Biosystems, Carlsbad, CA, USA) and water to a final volume of 28 µL. The RNA was incubated at 65°C for 5 min and then cooled to 10°C. Thereafter, the mix 2

containing 8 μ L of 5X buffer, 2 μ L of 10 mM dNTPs and 2 μ L of RevertAid™ Reverse Transcriptase (200U/ μ L) (Fermentas Life Sciences, Burlington, Ontario, Canada), were added to the reaction, followed by incubation at 25°C for 5 min and 42°C for 60 min. The enzyme was inactivated at 70°C for 10 min, and the reaction was stored at -20°C until use. A negative control containing all reaction components except the reverse transcriptase enzyme was included and subjected to RT-qPCR to check the absence of DNA contamination in the RNA samples.

For mRNA quantification, we used 100-fold diluted cDNA as template. The reaction was performed with SYBR Green PCR Master Mix (Applied Biosystems), 0.4 μ M of each corresponding primers pair, 5 μ L of cDNA, and RNase-free water to a final volume of 25 μ L. The PCR reaction consisted of 40 cycles of 30 sec at 94°C followed by 30 sec at 60°C, and performed in the Exicycler™ 96 Real-Time Quantitative Thermal Block (Bioneer, Daejeon, Korea). Triplicate samples were analyzed for each condition. Target gene expression was quantified based on a standard curve prepared from a ten-fold serial dilution of a quantified and linearized plasmid containing the target DNA. The following primers pairs were used for mammalian mRNA analysis: *Nos2*: 5'-agagccacagctctctttg-3' and 5'-gctccttccaaggtgett-3'; *Arg1*: 5-agcactgaggaaagctgg-3' and 5'-cagaccgtgggttcttcaca-3'; *Cat-2b*: 5'-tatgtgtctcggcaggctc-3' and 5'-gaaaagcaaccatctctcg-3'; *Cat1*: 5'-cgtaatcgccactgtgacct-3' and 5'-ggctggtaccgtaagaccaa-3'; and *Gapd*: 5'-ggcaaattcaacggcacagt-3' and 5'-cctttgctccaccctca-3'.

Reverse transcription and TLR PCR Array

cDNA was produced from 1 μ g of total RNA using RT2 First Strand Kit (Qiagen, Hilden, Germany), according to the manufacturer's instructions. The reactions were performed in a Thermocycler Mastercycler gradient (Eppendorf, Hamburg, Germany) and stored at -20°C until use.

TLR PCR array was performed with ten-fold diluted cDNA as template, using RT² Profiler™ PCR Array Mouse Toll-Like Receptor Signaling Pathway (PAMM-018Z) (Qiagen, Germantown, MD, USA) and RT2 SYBR Green qPCR Mastermix (Qiagen, Hilden, Germany). The reactions were performed with 2X RT2 SYBR Green Master Mix and 100 μ L of cDNA and RNase-free water to a final volume of 2,700 μ L (25 μ L/well). The PCR reaction consisted of the activation of the HotStart Polymerase for 10 sec at 95°C and 40 cycles of 15 sec at 95°C, followed by 1 min at 60°C, and performed in Thermocycler ABI Prism 7300 (Applied Biosystems, Carlsbad, CA, USA). The relative Ct was analyzed using the RT PCR Array Data Analysis software (www.qiagen.com). Quadruplicate samples were analyzed for each condition. The average Ct was calculated to represent the gene expression variation with good accuracy. The geometric average Ct of the mRNAs was normalized based on the average of housekeeping gene, *B2 microglobulin*. The PCR and RT-PCR kit controls were performed according to the manufacturer's instructions and determined by efficiency reactions. A negative control containing all reaction components except the reverse transcriptase enzyme was included and subjected to real-time PCR to check the absence of DNA contamination in the RNA samples. The Fold Regulation (FR) is the negative inverse of the fold-change (function = $-1 \cdot (1/\text{fold-change value})$). The FR levels ≥ 1.2 were considered to indicate up-regulation, and

levels ≤ -1.2 were considered to indicate down-regulation.

Transfection of miRNA inhibitors

BMDMs were collected, plated and incubated, as previously described (Muxel et al., 2017b). Thereafter, the macrophages were incubated with 100 nM of the let-7e-5p inhibitor or with the negative control (Ambion, Carlsbad, CA, USA) previously incubated for 20 min at room temperature with 3 μ L of the FugeneHD transfection reagent (Roche, Madison, WI, USA) in 500 μ L of RPMI 1640 medium (LGC Biotecnologia, São Paulo, SP, Brazil), supplemented as previously described. After 24 h of transfection, the cells were infected with *L. amazonensis* promastigote forms, as previously described.

Flow cytometry to detection of NOS2 and Arg1

Infected BMDMs were fixed with 1% paraphormaldehyde (1 h, at 4°C) and permeabilized with 0.05% Tween20 for 30 min at 4°C, followed by blocking with Odyssey blocking buffer (LI-COR, Bad Homburg, Germany) for 1 h at room temperature. Then, the samples were incubated with 1:200 dilutions of rabbit anti-NOS2 (sc651) or mouse anti-ARG1-actin (sc20150) antibodies (Santa Cruz, CA, USA) for 16 h at 4°C. The samples were then incubated with 1:300 dilution of FITC-conjugated goat anti-rabbit IgG (F7512, Sigma-Aldrich) antibody for 1 h at room temperature. The fluorescence signal was measured in channel 2 from single cells using FlowSight Amnis (Merck-Millipore, Darmstadt, Germany) and analyzed using the Ideas® Software (Amnis Corporation, Seattle, WA, USA).

Quantification of NO production

BMDMs were seeded into 24-well plates (SPL) (1×10^6 /well) for 18 h of incubation at 34°C in an atmosphere of 5% CO₂. Then, the macrophages were infected, as described above for 4 and 24 h. The samples were detached with 0.5 M EDTA in PBS for 10 min at 37°C, scraped and washed with PBS. The samples were incubated with 5 μ M DAF-FM (for NO quantification) (Molecular Probes, Life Technologies, Darmstadt, Germany) in PBS for 30 min at 34°C in an atmosphere of 5% CO₂, as described previously (Muxel et al., 2017b; Muxel et al., 2017c). Fluorescence acquisition was measured in channel 2 from single cells using FlowSight Amnis (Merck-Millipore, Darmstadt, Germany) and analyzed using the Ideas® Software (Amnis Corporation, Seattle, WA, USA).

In silico analysis

For miRNA-mRNA target, we used the databases miRecords and Dianna tools. miRecords platform (<http://c1.accurascience.com/miRecords/>) is based on predicted mRNA targets, which integrates the predicted targets from various predicted tools: DIANA-microT, MicroInspector, miRanda, MirTarget2, miTarget, NBmiRTar, PicTar, PITA, RNA22, RNAhybrid, and TargetScan/TargetScanS. Dianna platform (<http://diana.imis.athena-innovation.gr/DianaTools/index.php?r=site/index>) is based on validated mRNA targets.

Statistical analysis

Statistical analyzes was performed based on Student's *t* or ANOVA tests, using the

GraphPad Prism Software 7 (GraphPad Software, Inc., La Jolla, CA, USA). The obtained p-values were indicated throughout the Results section.

Results

Absence of MyD88, TLR2 or TLR4 genes increased *L. amazonensis* infectivity.

The role of MyD88, TLR2 and TLR4 in the recognition of the parasite and defining the fate of *L. amazonensis* infection was evaluated by rate of infected macrophages, amastigotes per infected macrophage and infectivity index in BMDMs from WT, MyD88^{-/-}, TLR2^{-/-} or TLR4^{-/-} mice, after 4, 24 and 48 h of infection (Fig. 1). We observed increased TLR4^{-/-} infected macrophages rate levels during the time course of infection, and increased infected macrophages rate in TLR2^{-/-} only after 48 h of infection (Fig. 1A). The number of amastigotes per infected macrophage appeared increased in all mice strains compared to WT strain during the time course of infection (Figure 1B). Interestingly, the infectivity index appeared increased in all MyD88^{-/-}, TLR2^{-/-} or TLR4^{-/-} mice strains during the time course of infection when compared to WT infected-macrophages (Fig. 1C), confirming the involvement of TLR2, TLR4 and MyD88 in the recognition of the parasite and defining the fate of *L. amazonensis* infection.

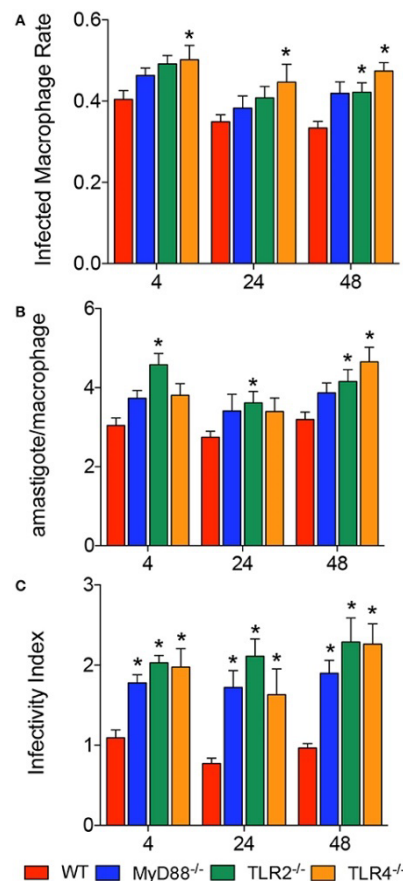


Figure 10. Infectivity of *L. amazonensis* in macrophages from WT, MyD88^{-/-}, TLR2^{-/-} or TLR4^{-/-} mice. The evaluation of infected macrophage rate (A), amastigotes per infected macrophage (B) and infectivity index (C) in BMDMs from WT (red), MyD88^{-/-} (blue), TLR2^{-/-} (green) or TLR4^{-/-} (orange) mice. Each bar represents the mean ± SEM of the values obtained in 3 independent experiments (n=6-9). Statistical significance was determined based on non-parametric two-way ANOVA. (*) p < 0.05, compared to WT

Modulation of NO/polyamines pathway mRNA expression is TLR signaling dependent .

We demonstrated the role of MyD88, TLR2 and TLR4 in the *L. amazonensis* *in vitro* infection. Further, we analyzed how TLR signaling could interfere in L-arginine metabolism to produce polyamines for parasite replication or to produce NO for parasite killing. First, we analyzed the basal mRNA levels of *Cat1*, *Cat2B*, *Arg1* and *Nos2* among mice strains compared to WT strain and we observed that TLR4^{-/-} expressed lower amounts of *Cat1*, *Cat2B*, *Arg1* and *Nos2* transcripts (Fig 2A-2D). MyD88^{-/-} showed lower basal amounts of *Arg1* and *Nos2* transcripts (Fig. 2C and 2D). TLR2^{-/-} did not show different basal amount of any transcripts (Fig. 2A-2D).

Based on *L. amazonensis* infection, we analyzed the amount of those transcripts after 4, 24 and 48 h of infection. The only transcript modulated during the time course of infection was *Nos2*, which was increased at 24 h and decreased at 48 h after infection (Fig 2D). The transcript amount in comparison to WT mice strain revealed increased levels of *Cat2B* after 48 h of infection and increased levels of *Cat1* after 4, 24 and 48 h of infection in MyD88^{-/-} (Fig. 2A and 2B, respectively). In contrast, MyD88^{-/-} showed decreased levels of *Arg1* and *Nos2* transcripts in all infections periods analyzed (Fig 2C and 2D, respectively). The comparison between WT and TLR2^{-/-} showed increased amounts of *Arg1* transcript after 4 h of infection and decreased amount of *Nos2* transcript in all infection period analyzed (Fig 2C and 2D, respectively). The comparison between WT and TLR4^{-/-} presented decreased amounts of *Arg1* and *Nos2* transcripts during all time course of infection (Fig 2C and 2D, respectively). These data demonstrated that the involvement of MyD88, TLR2 and TLR4 signaling altered the expression of genes involved in polyamines/NO production in *L. amazonensis* infected macrophages.

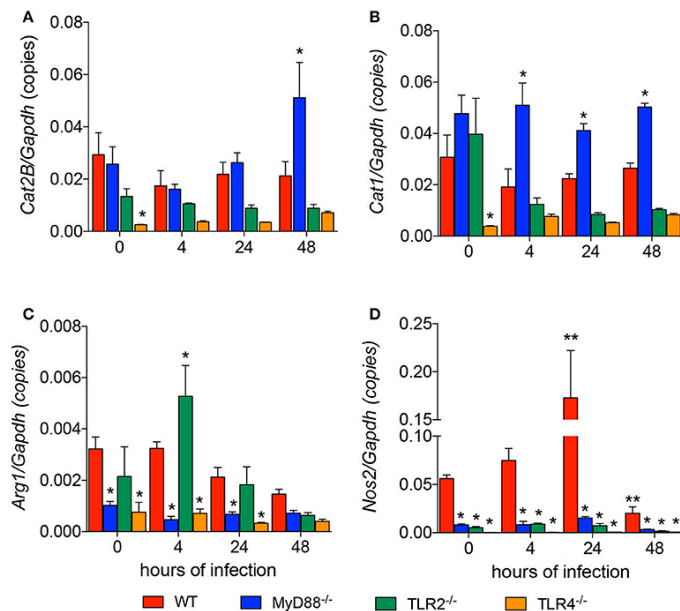


Figure 11. Lack of TLR signaling leads to differential expression of genes involved in the polyamine and NO production pathways. The BMDMs (5×10^6) from WT (red), MyD88^{-/-} (blue), TLR2^{-/-} (green) or TLR4^{-/-} (orange) mice were infected with *L. amazonensis* (MOI 5:1). After 4, 24 and 48 h of infection, the copy numbers of mRNAs of *Cat2B* (A), *Cat1* (B), *Arg1* (C), and *Nos2* (D) from macrophages were quantified by RT-qPCR. Uninfected macrophages (0 hours). Each bar represents the average ± SEM of the values obtained in 3 independent experiments (n=6-8). Statistical significance was determined based on two-tailed Student's t test. *, p<0.05, all knockout macrophages compared to WT **, p<0.05, compared to uninfected macrophages.

TLR modulates miRNA profile in *L. amazonensis* infected macrophage.

To investigate the importance of post-transcriptional regulation of gene expression mediated by miRNAs participation, we evaluated the miRNAs profile during infection and the impact of the absence of TLR signaling to miRNA expression, analyzing the miRNA profile of macrophages from WT, MyD88^{-/-}, TLR2^{-/-} or TLR4^{-/-} mice infected with *L. amazonensis* for 4, 24 and 48 h, compared to uninfected-macrophages (Fig. 3 and 4, S1 Table, S1 Fig).

The miRNA profile of WT infected-macrophages revealed the regulation of 32% (27/84) of the analyzed miRNAs during the time course of infection, compared to WT uninfected-macrophages. Among those miRNAs, 14/27 were up-regulated. The let-7e, miR-182, miR-294, miR-30b, miR-369, miR-429, mir-466d, miR-495, miR-497a, miR-699h and miR-721 were significantly up-regulated after 4 h of infection. The up-regulation of let-7e, mir-294 and miR-721 was maintained after 24-48 h of infection. The miRNAs let-7f and let-7g appeared up-regulated after 24 and 48 h of infection. The miR-369 appeared up-regulated only after 24 h of infection, while miR-712 appeared up-regulated only after 48 h of infection (Fig. 3, S1 Table). Interestingly, we did not detected down-regulation of miRNAs expression after 4h of infection. On the other hand, after 24 and 48 h of infection we observed down-regulation of miR-130a, miR-15a, miR-221, miR-27b, miR-295, miR-30a, miR-340, miR-350 and miR-497a; as well as down-regulation of miR-17, miR-19a, miR-221, miR-27b, miR-29a, miR-30a, miR-340, miR-350 and miR-98, respectively (Fig. 3).

The miRNA profile of MyD88^{-/-} infected-macrophages showed a regulation of 35% (30/84) of analyzed miRNAs, being 50% of them up-regulated and 50% down-regulated (Fig 3). Unexpected, the miRNA profile of TLR2^{-/-} infected-macrophages, revealed low miRNA modulation during the time course of infection. We observed only 12% (10/84) of miRNAs were regulated, being 80% of them were down-regulated. And no miRNA modulation was observed after 48 h of infection. The miRNA profile of TLR4^{-/-} infected-macrophages showed a regulation of 28% (24/84) of analyzed miRNAs, being 92% of them down-regulated (Fig. 3).

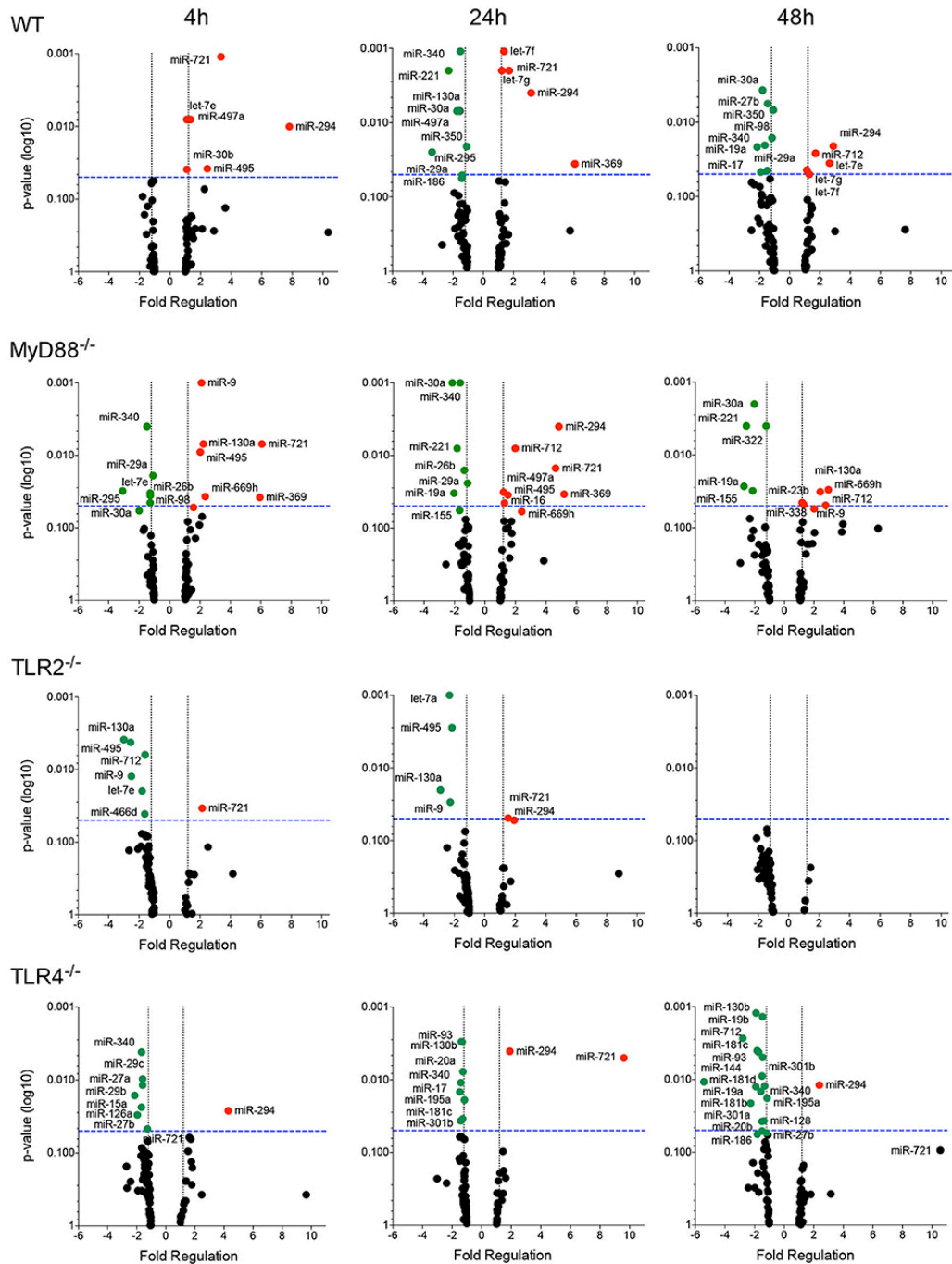


Figure 12. Volcano plot of the miRNA profiles of macrophages WT or MyD88, TLR2 and TLR4 null mice infected with *L. amazonensis*. Each dot represents one miRNA of BMDMs from WT, MyD88^{-/-}, TLR2^{-/-} or TLR4^{-/-} mice infected for 4, 24 and 48 h with *L. amazonensis*. The red dot indicated up-regulated miRNA and green dot indicated down-regulated miRNAs. Blue dotted line corresponds to $p=0.05$, \log_{10} . The relative up- and down-regulation of miRNAs, expressed as boundaries of 1.2 or -1.2 of Fold Regulation, respectively. P-value was determined based on two-tailed Student's t test. The data are representative from three independent experiments

On trial to elucidate the relationship of the miRNA expression among the groups we performed a Venn diagram, which demonstrated those exclusively and commonly miRNA expressed (Fig. 4). miR-294 and miR-721 appeared commonly up-regulated in all the four groups (Fig 4A). In addition, exclusively up-regulated miRNAs let-7e, let-7f and let-7g were observed in WT in comparison to MyD88^{-/-}, TLR2^{-/-} and TLR4^{-/-} (Fig. 4A). Also, let-7e was common down-regulated miRNA between MyD88^{-/-} and TLR2^{-/-} infected-macrophages, which expression was reduced in TLR4^{-/-}, but not significantly (p = 0.055).

The expression of miR-30b, miR-369, miR-429, miR-466d, miR-495, miR-497a, miR-669h and miR-712 were common up-regulated in WT and MyD88^{-/-} infected-macrophages. Also, miR-130a, miR-16, miR-338, and miR-9 were unique expressed in MyD88^{-/-} infected-macrophages.

Moreover, the Venn diagram showed the exclusively down-regulated miRNAs in WT infected-macrophages: miR-182, miR-186 and miR-497a, in MyD88^{-/-}: miR-155, miR-23b, miR-26b and miR-322, in TLR2^{-/-}: let-7a, miR-135a, miR-466d, miR-495 and miR-9, and in TLR4^{-/-}: miR-126a, miR-128, miR-130b, miR-181b, miR-181c, miR-181d, miR-195a, miR-19b, miR-20a, miR-27a, miR-29b, miR-29c and miR-93 (Fig. 4B). The commonly down-regulated in WT and MyD88^{-/-}: miR-221, miR-295, miR-29a, miR-30a, miR-350 and miR-98-5p; WT and TLR2^{-/-}: miR-130a; WT and TLR4^{-/-}: miR-15a, miR-17 and miR-27b; and WT, MyD88^{-/-} and TLR4^{-/-}: miR-144, miR-19a and miR-340. The miR-301a and miR-301b were common down-regulated in MyD88^{-/-} and TLR4^{-/-} infected-macrophages. Also, miR-712 was common down-regulated in TLR2^{-/-} and TLR4^{-/-} infected-macrophages (Fig. 4B).

Altogether, our data demonstrated a regulation of miRNAs profile in *L. amazonensis* infected macrophages in a MyD88, TLR2 and TLR4 signaling dependent manner.

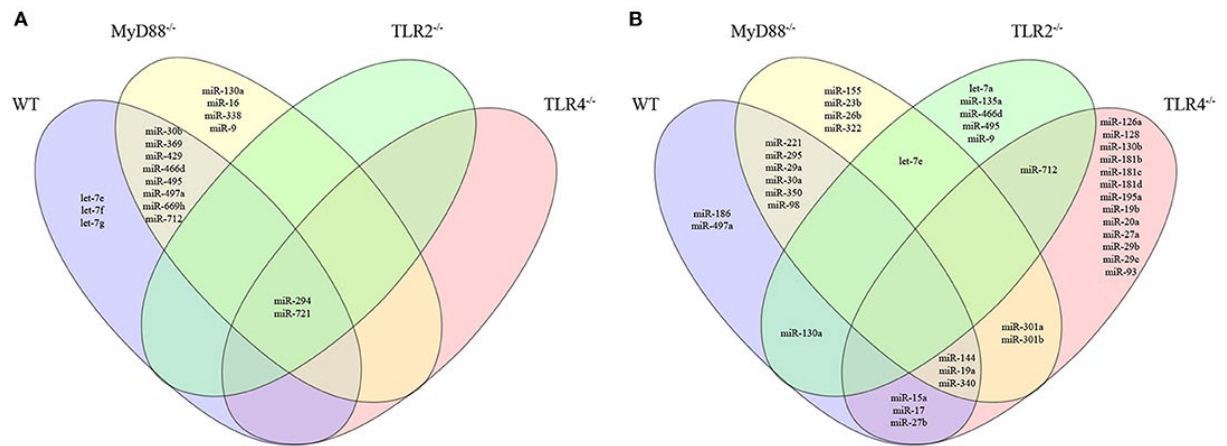


Figure 13 Venn diagram representing unique and common miRNAs significantly expressed in macrophages from WT or MyD88, TLR2 and TLR4 null mice infected with *L. amazonensis*. The miRNAs expression was divided into four groups including WT, (purple), MyD88^{-/-} (yellow), TLR2^{-/-} (green) or TLR4^{-/-} (red) infected-macrophages. The up-regulated (A) and down-regulated (B) miRNAs in each group compared to uninfected macrophages. The relative up- and down-regulation of miRNAs, expressed as boundaries of 1.2 or -1.2 of Fold Regulation, respectively. P-value < 0.05.

let-7e in silico mRNA target.

Since we observed the modulation of let-7e in the MyD88 and TLR2 deficient mice strains infected with *L. amazonensis*, we decided to check the impact of this miRNA in the mRNA-targeting of TLRs. *In silico* analysis based on miRecords search, we identified let-7e presenting 3357 predicted interactions (S2 Table). On the other hand, based on Dianna tool search for experimental validated target we viewed that let-7e can target for *Tlr4*, *Tbk1*, *Map2k4*, *Map3k1*, *Chuk*, *Tnf*, *Tnfrsf1a*, *Tnfrsf1b*, *Tnfrsf1c*, *Tnfrsf1d*, *Tnfrsf1e*, *Tnfrsf1f*, *Tnfrsf1g*, *Tnfrsf1h*, *Tnfrsf1i*, *Tnfrsf1j*, *Tnfrsf1k*, *Tnfrsf1l*, *Tnfrsf1m*, *Tnfrsf1n*, *Tnfrsf1o*, *Tnfrsf1p*, *Tnfrsf1q*, *Tnfrsf1r*, *Tnfrsf1s*, *Tnfrsf1t*, *Tnfrsf1u*, *Tnfrsf1v*, *Tnfrsf1w*, *Tnfrsf1x*, *Tnfrsf1y*, *Tnfrsf1z*, *Tnfrsf1aa*, *Tnfrsf1ab*, *Tnfrsf1ac*, *Tnfrsf1ad*, *Tnfrsf1ae*, *Tnfrsf1af*, *Tnfrsf1ag*, *Tnfrsf1ah*, *Tnfrsf1ai*, *Tnfrsf1aj*, *Tnfrsf1ak*, *Tnfrsf1al*, *Tnfrsf1am*, *Tnfrsf1an*, *Tnfrsf1ao*, *Tnfrsf1ap*, *Tnfrsf1aq*, *Tnfrsf1ar*, *Tnfrsf1as*, *Tnfrsf1at*, *Tnfrsf1au*, *Tnfrsf1av*, *Tnfrsf1aw*, *Tnfrsf1ax*, *Tnfrsf1ay*, *Tnfrsf1az*, *Tnfrsf1ba*, *Tnfrsf1bb*, *Tnfrsf1bc*, *Tnfrsf1bd*, *Tnfrsf1be*, *Tnfrsf1bf*, *Tnfrsf1bg*, *Tnfrsf1bh*, *Tnfrsf1bi*, *Tnfrsf1bj*, *Tnfrsf1bk*, *Tnfrsf1bl*, *Tnfrsf1bm*, *Tnfrsf1bn*, *Tnfrsf1bo*, *Tnfrsf1bp*, *Tnfrsf1bq*, *Tnfrsf1br*, *Tnfrsf1bs*, *Tnfrsf1bt*, *Tnfrsf1bu*, *Tnfrsf1bv*, *Tnfrsf1bw*, *Tnfrsf1bx*, *Tnfrsf1by*, *Tnfrsf1bz*, *Tnfrsf1ca*, *Tnfrsf1cb*, *Tnfrsf1cc*, *Tnfrsf1cd*, *Tnfrsf1ce*, *Tnfrsf1cf*, *Tnfrsf1cg*, *Tnfrsf1ch*, *Tnfrsf1ci*, *Tnfrsf1cj*, *Tnfrsf1ck*, *Tnfrsf1cl*, *Tnfrsf1cm*, *Tnfrsf1cn*, *Tnfrsf1co*, *Tnfrsf1cp*, *Tnfrsf1cq*, *Tnfrsf1cr*, *Tnfrsf1cs*, *Tnfrsf1ct*, *Tnfrsf1cu*, *Tnfrsf1cv*, *Tnfrsf1cw*, *Tnfrsf1cx*, *Tnfrsf1cy*, *Tnfrsf1cz*, *Tnfrsf1da*, *Tnfrsf1db*, *Tnfrsf1dc*, *Tnfrsf1dd*, *Tnfrsf1de*, *Tnfrsf1df*, *Tnfrsf1dg*, *Tnfrsf1dh*, *Tnfrsf1di*, *Tnfrsf1dj*, *Tnfrsf1dk*, *Tnfrsf1dl*, *Tnfrsf1dm*, *Tnfrsf1dn*, *Tnfrsf1do*, *Tnfrsf1dp*, *Tnfrsf1dq*, *Tnfrsf1dr*, *Tnfrsf1ds*, *Tnfrsf1dt*, *Tnfrsf1du*, *Tnfrsf1dv*, *Tnfrsf1dw*, *Tnfrsf1dx*, *Tnfrsf1dy*, *Tnfrsf1dz*, *Tnfrsf1ea*, *Tnfrsf1eb*, *Tnfrsf1ec*, *Tnfrsf1ed*, *Tnfrsf1ee*, *Tnfrsf1ef*, *Tnfrsf1eg*, *Tnfrsf1eh*, *Tnfrsf1ei*, *Tnfrsf1ej*, *Tnfrsf1ek*, *Tnfrsf1el*, *Tnfrsf1em*, *Tnfrsf1en*, *Tnfrsf1eo*, *Tnfrsf1ep*, *Tnfrsf1eq*, *Tnfrsf1er*, *Tnfrsf1es*, *Tnfrsf1et*, *Tnfrsf1eu*, *Tnfrsf1ev*, *Tnfrsf1ew*, *Tnfrsf1ex*, *Tnfrsf1ey*, *Tnfrsf1ez*, *Tnfrsf1fa*, *Tnfrsf1fb*, *Tnfrsf1fc*, *Tnfrsf1fd*, *Tnfrsf1fe*, *Tnfrsf1ff*, *Tnfrsf1fg*, *Tnfrsf1fh*, *Tnfrsf1fi*, *Tnfrsf1fj*, *Tnfrsf1fk*, *Tnfrsf1fl*, *Tnfrsf1fm*, *Tnfrsf1fn*, *Tnfrsf1fo*, *Tnfrsf1fp*, *Tnfrsf1fq*, *Tnfrsf1fr*, *Tnfrsf1fs*, *Tnfrsf1ft*, *Tnfrsf1fu*, *Tnfrsf1fv*, *Tnfrsf1fw*, *Tnfrsf1fx*, *Tnfrsf1fy*, *Tnfrsf1fz*, *Tnfrsf1ga*, *Tnfrsf1gb*, *Tnfrsf1gc*, *Tnfrsf1gd*, *Tnfrsf1ge*, *Tnfrsf1gf*, *Tnfrsf1gg*, *Tnfrsf1gh*, *Tnfrsf1gi*, *Tnfrsf1gj*, *Tnfrsf1gk*, *Tnfrsf1gl*, *Tnfrsf1gm*, *Tnfrsf1gn*, *Tnfrsf1go*, *Tnfrsf1gp*, *Tnfrsf1gq*, *Tnfrsf1gr*, *Tnfrsf1gs*, *Tnfrsf1gt*, *Tnfrsf1gu*, *Tnfrsf1gv*, *Tnfrsf1gw*, *Tnfrsf1gx*, *Tnfrsf1gy*, *Tnfrsf1gz*, *Tnfrsf1ha*, *Tnfrsf1hb*, *Tnfrsf1hc*, *Tnfrsf1hd*, *Tnfrsf1he*, *Tnfrsf1hf*, *Tnfrsf1hg*, *Tnfrsf1hh*, *Tnfrsf1hi*, *Tnfrsf1hj*, *Tnfrsf1hk*, *Tnfrsf1hl*, *Tnfrsf1hm*, *Tnfrsf1hn*, *Tnfrsf1ho*, *Tnfrsf1hp*, *Tnfrsf1hq*, *Tnfrsf1hr*, *Tnfrsf1hs*, *Tnfrsf1ht*, *Tnfrsf1hu*, *Tnfrsf1hv*, *Tnfrsf1hw*, *Tnfrsf1hx*, *Tnfrsf1hy*, *Tnfrsf1hz*, *Tnfrsf1ia*, *Tnfrsf1ib*, *Tnfrsf1ic*, *Tnfrsf1id*, *Tnfrsf1ie*, *Tnfrsf1if*, *Tnfrsf1ig*, *Tnfrsf1ih*, *Tnfrsf1ii*, *Tnfrsf1ij*, *Tnfrsf1ik*, *Tnfrsf1il*, *Tnfrsf1im*, *Tnfrsf1in*, *Tnfrsf1io*, *Tnfrsf1ip*, *Tnfrsf1iq*, *Tnfrsf1ir*, *Tnfrsf1is*, *Tnfrsf1it*, *Tnfrsf1iu*, *Tnfrsf1iv*, *Tnfrsf1iw*, *Tnfrsf1ix*, *Tnfrsf1iy*, *Tnfrsf1iz*, *Tnfrsf1ja*, *Tnfrsf1jb*, *Tnfrsf1jc*, *Tnfrsf1jd*, *Tnfrsf1je*, *Tnfrsf1jf*, *Tnfrsf1jg*, *Tnfrsf1jh*, *Tnfrsf1ji*, *Tnfrsf1jj*, *Tnfrsf1jk*, *Tnfrsf1jl*, *Tnfrsf1jm*, *Tnfrsf1jn*, *Tnfrsf1jo*, *Tnfrsf1jp*, *Tnfrsf1jq*, *Tnfrsf1jr*, *Tnfrsf1js*, *Tnfrsf1jt*, *Tnfrsf1ju*, *Tnfrsf1jv*, *Tnfrsf1jw*, *Tnfrsf1jx*, *Tnfrsf1jy*, *Tnfrsf1jz*, *Tnfrsf1ka*, *Tnfrsf1kb*, *Tnfrsf1kc*, *Tnfrsf1kd*, *Tnfrsf1ke*, *Tnfrsf1kf*, *Tnfrsf1kg*, *Tnfrsf1kh*, *Tnfrsf1ki*, *Tnfrsf1kj*, *Tnfrsf1kk*, *Tnfrsf1kl*, *Tnfrsf1km*, *Tnfrsf1kn*, *Tnfrsf1ko*, *Tnfrsf1kp*, *Tnfrsf1kq*, *Tnfrsf1kr*, *Tnfrsf1ks*, *Tnfrsf1kt*, *Tnfrsf1ku*, *Tnfrsf1kv*, *Tnfrsf1kw*, *Tnfrsf1kx*, *Tnfrsf1ky*, *Tnfrsf1kz*, *Tnfrsf1la*, *Tnfrsf1lb*, *Tnfrsf1lc*, *Tnfrsf1ld*, *Tnfrsf1le*, *Tnfrsf1lf*, *Tnfrsf1lg*, *Tnfrsf1lh*, *Tnfrsf1li*, *Tnfrsf1lj*, *Tnfrsf1lk*, *Tnfrsf1ll*, *Tnfrsf1lm*, *Tnfrsf1ln*, *Tnfrsf1lo*, *Tnfrsf1lp*, *Tnfrsf1lq*, *Tnfrsf1lr*, *Tnfrsf1ls*, *Tnfrsf1lt*, *Tnfrsf1lu*, *Tnfrsf1lv*, *Tnfrsf1lw*, *Tnfrsf1lx*, *Tnfrsf1ly*, *Tnfrsf1lz*, *Tnfrsf1ma*, *Tnfrsf1mb*, *Tnfrsf1mc*, *Tnfrsf1md*, *Tnfrsf1me*, *Tnfrsf1mf*, *Tnfrsf1mg*, *Tnfrsf1mh*, *Tnfrsf1mi*, *Tnfrsf1mj*, *Tnfrsf1mk*, *Tnfrsf1ml*, *Tnfrsf1mm*, *Tnfrsf1mn*, *Tnfrsf1mo*, *Tnfrsf1mp*, *Tnfrsf1mq*, *Tnfrsf1mr*, *Tnfrsf1ms*, *Tnfrsf1mt*, *Tnfrsf1mu*, *Tnfrsf1mv*, *Tnfrsf1mw*, *Tnfrsf1mx*, *Tnfrsf1my*, *Tnfrsf1mz*, *Tnfrsf1na*, *Tnfrsf1nb*, *Tnfrsf1nc*, *Tnfrsf1nd*, *Tnfrsf1ne*, *Tnfrsf1nf*, *Tnfrsf1ng*, *Tnfrsf1nh*, *Tnfrsf1ni*, *Tnfrsf1nj*, *Tnfrsf1nk*, *Tnfrsf1nl*, *Tnfrsf1nm*, *Tnfrsf1nn*, *Tnfrsf1no*, *Tnfrsf1np*, *Tnfrsf1nq*, *Tnfrsf1nr*, *Tnfrsf1ns*, *Tnfrsf1nt*, *Tnfrsf1nu*, *Tnfrsf1nv*, *Tnfrsf1nw*, *Tnfrsf1nx*, *Tnfrsf1ny*, *Tnfrsf1nz*, *Tnfrsf1oa*, *Tnfrsf1ob*, *Tnfrsf1oc*, *Tnfrsf1od*, *Tnfrsf1oe*, *Tnfrsf1of*, *Tnfrsf1og*, *Tnfrsf1oh*, *Tnfrsf1oi*, *Tnfrsf1oj*, *Tnfrsf1ok*, *Tnfrsf1ol*, *Tnfrsf1om*, *Tnfrsf1on*, *Tnfrsf1oo*, *Tnfrsf1op*, *Tnfrsf1oq*, *Tnfrsf1or*, *Tnfrsf1os*, *Tnfrsf1ot*, *Tnfrsf1ou*, *Tnfrsf1ov*, *Tnfrsf1ow*, *Tnfrsf1ox*, *Tnfrsf1oy*, *Tnfrsf1oz*, *Tnfrsf1pa*, *Tnfrsf1pb*, *Tnfrsf1pc*, *Tnfrsf1pd*, *Tnfrsf1pe*, *Tnfrsf1pf*, *Tnfrsf1pg*, *Tnfrsf1ph*, *Tnfrsf1pi*, *Tnfrsf1pj*, *Tnfrsf1pk*, *Tnfrsf1pl*, *Tnfrsf1pm*, *Tnfrsf1pn*, *Tnfrsf1po*, *Tnfrsf1pp*, *Tnfrsf1pq*, *Tnfrsf1pr*, *Tnfrsf1ps*, *Tnfrsf1pt*, *Tnfrsf1pu*, *Tnfrsf1pv*, *Tnfrsf1pw*, *Tnfrsf1px*, *Tnfrsf1py*, *Tnfrsf1pz*, *Tnfrsf1qa*, *Tnfrsf1qb*, *Tnfrsf1qc*, *Tnfrsf1qd*, *Tnfrsf1qe*, *Tnfrsf1qf*, *Tnfrsf1qg*, *Tnfrsf1qh*, *Tnfrsf1qi*, *Tnfrsf1qj*, *Tnfrsf1qk*, *Tnfrsf1ql*, *Tnfrsf1qm*, *Tnfrsf1qn*, *Tnfrsf1qo*, *Tnfrsf1qp*, *Tnfrsf1qq*, *Tnfrsf1qr*, *Tnfrsf1qs*, *Tnfrsf1qt*, *Tnfrsf1qu*, *Tnfrsf1qv*, *Tnfrsf1qw*, *Tnfrsf1qx*, *Tnfrsf1qy*, *Tnfrsf1qz*, *Tnfrsf1ra*, *Tnfrsf1rb*, *Tnfrsf1rc*, *Tnfrsf1rd*, *Tnfrsf1re*, *Tnfrsf1rf*, *Tnfrsf1rg*, *Tnfrsf1rh*, *Tnfrsf1ri*, *Tnfrsf1rj*, *Tnfrsf1rk*, *Tnfrsf1rl*, *Tnfrsf1rm*, *Tnfrsf1rn*, *Tnfrsf1ro*, *Tnfrsf1rp*, *Tnfrsf1rq*, *Tnfrsf1rr*, *Tnfrsf1rs*, *Tnfrsf1rt*, *Tnfrsf1ru*, *Tnfrsf1rv*, *Tnfrsf1rw*, *Tnfrsf1rx*, *Tnfrsf1ry*, *Tnfrsf1rz*, *Tnfrsf1sa*, *Tnfrsf1sb*, *Tnfrsf1sc*, *Tnfrsf1sd*, *Tnfrsf1se*, *Tnfrsf1sf*, *Tnfrsf1sg*, *Tnfrsf1sh*, *Tnfrsf1si*, *Tnfrsf1sj*, *Tnfrsf1sk*, *Tnfrsf1sl*, *Tnfrsf1sm*, *Tnfrsf1sn*, *Tnfrsf1so*, *Tnfrsf1sp*, *Tnfrsf1sq*, *Tnfrsf1sr*, *Tnfrsf1ss*, *Tnfrsf1st*, *Tnfrsf1su*, *Tnfrsf1sv*, *Tnfrsf1sw*, *Tnfrsf1sx*, *Tnfrsf1sy*, *Tnfrsf1sz*, *Tnfrsf1ta*, *Tnfrsf1tb*, *Tnfrsf1tc*, *Tnfrsf1td*, *Tnfrsf1te*, *Tnfrsf1tf*, *Tnfrsf1tg*, *Tnfrsf1th*, *Tnfrsf1ti*, *Tnfrsf1tj*, *Tnfrsf1tk*, *Tnfrsf1tl*, *Tnfrsf1tm*, *Tnfrsf1tn*, *Tnfrsf1to*, *Tnfrsf1tp*, *Tnfrsf1tq*, *Tnfrsf1tr*, *Tnfrsf1ts*, *Tnfrsf1tt*, *Tnfrsf1tu*, *Tnfrsf1tv*, *Tnfrsf1tw*, *Tnfrsf1tx*, *Tnfrsf1ty*, *Tnfrsf1tz*, *Tnfrsf1ua*, *Tnfrsf1ub*, *Tnfrsf1uc*, *Tnfrsf1ud*, *Tnfrsf1ue*, *Tnfrsf1uf*, *Tnfrsf1ug*, *Tnfrsf1uh*, *Tnfrsf1ui*, *Tnfrsf1uj*, *Tnfrsf1uk*, *Tnfrsf1ul*, *Tnfrsf1um*, *Tnfrsf1un*, *Tnfrsf1uo*, *Tnfrsf1up*, *Tnfrsf1uq*, *Tnfrsf1ur*, *Tnfrsf1us*, *Tnfrsf1ut*, *Tnfrsf1uu*, *Tnfrsf1uv*, *Tnfrsf1uw*, *Tnfrsf1ux*, *Tnfrsf1uy*, *Tnfrsf1uz*, *Tnfrsf1va*, *Tnfrsf1vb*, *Tnfrsf1vc*, *Tnfrsf1vd*, *Tnfrsf1ve*, *Tnfrsf1vf*, *Tnfrsf1vg*, *Tnfrsf1vh*, *Tnfrsf1vi*, *Tnfrsf1vj*, *Tnfrsf1vk*, *Tnfrsf1vl*, *Tnfrsf1vm*, *Tnfrsf1vn*, *Tnfrsf1vo*, *Tnfrsf1vp*, *Tnfrsf1vq*, *Tnfrsf1vr*, *Tnfrsf1vs*, *Tnfrsf1vt*, *Tnfrsf1vu*, *Tnfrsf1vv*, *Tnfrsf1vw*, *Tnfrsf1vx*, *Tnfrsf1vy*, *Tnfrsf1vz*, *Tnfrsf1wa*, *Tnfrsf1wb*, *Tnfrsf1wc*, *Tnfrsf1wd*, *Tnfrsf1we*, *Tnfrsf1wf*, *Tnfrsf1wg*, *Tnfrsf1wh*, *Tnfrsf1wi*, *Tnfrsf1wj*, *Tnfrsf1wk*, *Tnfrsf1wl*, *Tnfrsf1wm*, *Tnfrsf1wn*, *Tnfrsf1wo*, *Tnfrsf1wp*, *Tnfrsf1wq*, *Tnfrsf1wr*, *Tnfrsf1ws*, *Tnfrsf1wt*, *Tnfrsf1wu*, *Tnfrsf1wv*, *Tnfrsf1ww*, *Tnfrsf1wx*, *Tnfrsf1wy*, *Tnfrsf1wz*, *Tnfrsf1xa*, *Tnfrsf1xb*, *Tnfrsf1xc*, *Tnfrsf1xd*, *Tnfrsf1xe*, *Tnfrsf1xf*, *Tnfrsf1xg*, *Tnfrsf1xh*, *Tnfrsf1xi*, *Tnfrsf1xj*, *Tnfrsf1xk*, *Tnfrsf1xl*, *Tnfrsf1xm*, *Tnfrsf1xn*, *Tnfrsf1xo*, *Tnfrsf1xp*, *Tnfrsf1xq*, *Tnfrsf1xr*, *Tnfrsf1xs*, *Tnfrsf1xt*, *Tnfrsf1xu*, *Tnfrsf1xv*, *Tnfrsf1xw*, *Tnfrsf1xx*, *Tnfrsf1xy*, *Tnfrsf1xz*, *Tnfrsf1ya*, *Tnfrsf1yb*, *Tnfrsf1yc*, *Tnfrsf1yd*, *Tnfrsf1ye*, *Tnfrsf1yf*, *Tnfrsf1yg*, *Tnfrsf1yh*, *Tnfrsf1yi*, *Tnfrsf1yj*, *Tnfrsf1yk*, *Tnfrsf1yl*, *Tnfrsf1ym*, *Tnfrsf1yn*, *Tnfrsf1yo*, *Tnfrsf1yp*, *Tnfrsf1yq*, *Tnfrsf1yr*, *Tnfrsf1ys*, *Tnfrsf1yt*, *Tnfrsf1yu*, *Tnfrsf1yv*, *Tnfrsf1yw*, *Tnfrsf1yx*, *Tnfrsf1yy*, *Tnfrsf1yz*, *Tnfrsf1za*, *Tnfrsf1zb*, *Tnfrsf1zc*, *Tnfrsf1zd*, *Tnfrsf1ze*, *Tnfrsf1zf*, *Tnfrsf1zg*, *Tnfrsf1zh*, *Tnfrsf1zi*, *Tnfrsf1zj*, *Tnfrsf1zk*, *Tnfrsf1zl*, *Tnfrsf1zm*, *Tnfrsf1zn*, *Tnfrsf1zo*, *Tnfrsf1zp*, *Tnfrsf1zq*, *Tnfrsf1zr*, *Tnfrsf1zs*, *Tnfrsf1zt*, *Tnfrsf1zu*, *Tnfrsf1zv*, *Tnfrsf1zw*, *Tnfrsf1zx*, *Tnfrsf1zy*, *Tnfrsf1zz*.

let-7e affecting *L. amazonensis* infectivity via L-arginine metabolism.

Further, we analyzed the impact of let-7e expression in *L. amazonensis*-infected macrophages. First, macrophages were transfected with 100 nM of let-7e inhibitor or negative-control (NC). Then, macrophages were infected with *L. amazonensis* for 4 and 24 h. The let-7e inhibition was validated in expression quantification assays and we observed that this inhibition abrogated the amount of the miRNA let-7e expression at 4 and 24 h of infection when compared to negative-control infected macrophages (S2 Fig). The impact of let-7e inhibition was also evaluated in the *L. amazonensis* infectivity. According to Fig 5A-C, the infected macrophage rate, amastigotes number per infected macrophage and infectivity index at 4h of infection were reduced approximately 10%, 30% and 35%, respectively, when compared to NC (Fig. 5A, B and C).

To check if the let-7e inhibition and reduced infectivity could be through the L-arginine metabolism, we measured the amount of *Cat2B*, *Cat1*, *Arg1* and *Nos2* transcripts (Fig. 5E and H and S2 Fig). We observed no modulation of *Cat2* and *Cat1* transcripts among the samples (S2 Fig). *Arg1* transcript was increased in let-7e inhibition after 24 h of infection (35%, Fig. 5D), but the frequency of cells expressing ARG1 (Fig. 6E) and mean of intensity of ARG1 (Fig. 5F) appeared not modified. *Nos2* transcript presented a reduced level in let-7e inhibition after 4 h of infection, but *Nos2* were increased at 24 h of infection (Fig. 5G). Moreover, the frequency of cells expressing NOS2 (Fig. 5H), mean of intensity of NOS2 (Fig 5I) and producing NO were increased in let-7e inhibition infected macrophages compared to NC, as observed by DAF-FM+ cells (Fig. 5K) and mean of DAF-FM intensity signal (Fig. 5L). Altogether, these results indicated that let-7e inhibition could indirectly impacted in gene expression of L-arginine metabolism favoring NO production and consequently in infectiveness.

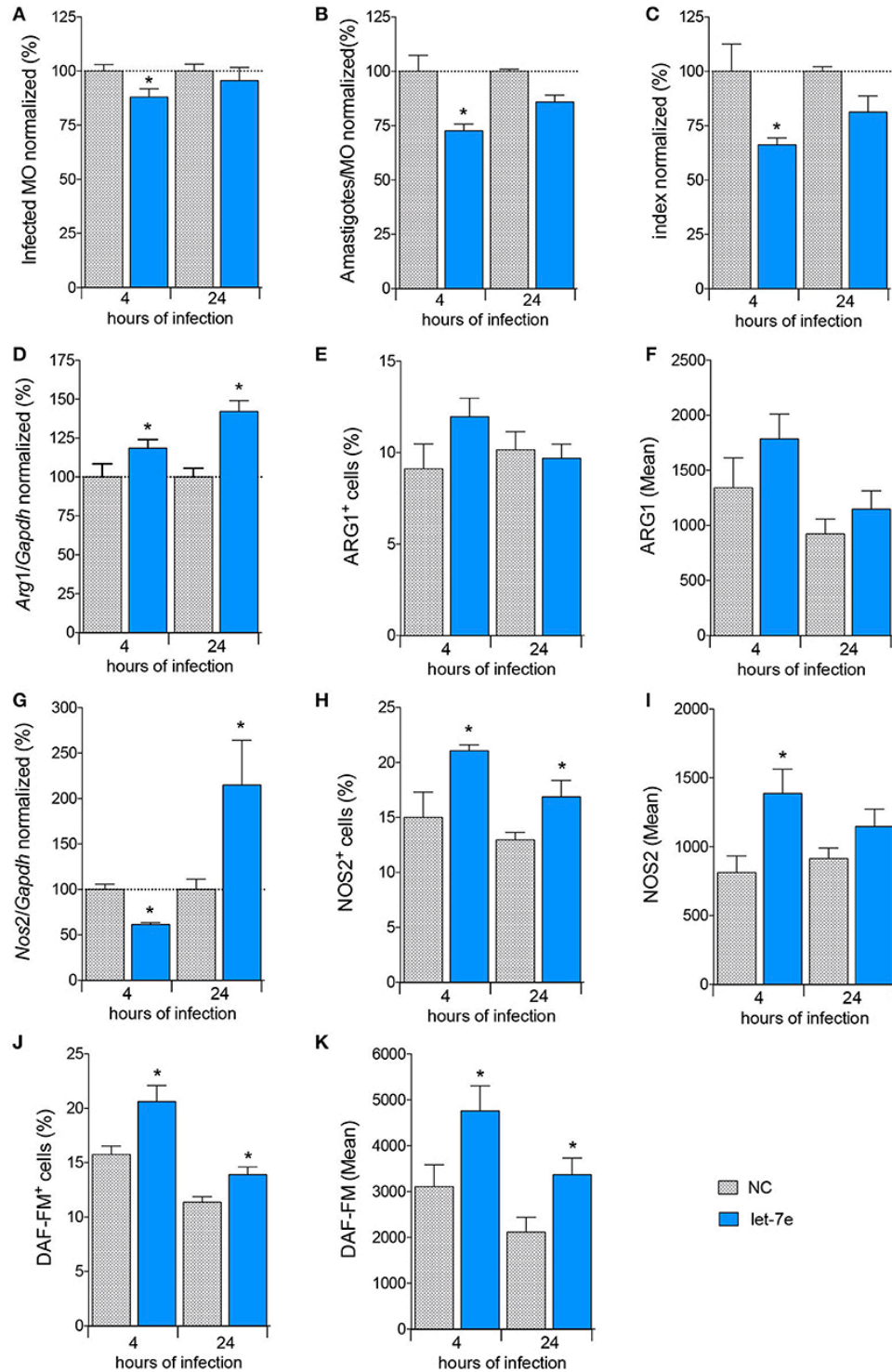


Figure 14. Inhibition of let-7 functions increased gene modulation and reduced *L. amazonensis* infectivity. BMDMs were transiently transfected with the negative control (NC - filed pattern bar) or 100 nM of let-7e-5p inhibitor (miR-inhib - blue bar). After 24 h of incubation, the cells were co-cultivated with *L. amazonensis* (MOI 5:1) for 4 h, and the cultures were then washed. After 4 and 24 h of infection, the samples were analyzed for infectivity via microscopy analysis, counting of the numbers of infected macrophages (A), amastigotes per infected macrophage (B) and infectivity index (C) (n=1,000 macrophages/treatment); mRNA levels via RT-qPCR of total RNA, for *Arg1* (D) and *Nos2* (G); frequency of cell expressing ARG1 (E) or NOS2 (H) and fluorescence intensity of ARG1 (F) or NOS2 (I) by flow cytometry; and frequency of NO-producing cells (DAF-FM⁺ cells - K) and fluorescence intensity of NO production per cells (DAF-FM mean - L) by flow cytometry. The values were normalized based on the average values of NC infected macrophages (100%). Each bar represents the average \pm SEM of the values obtained in 3 independent experiments (n=4-8). Statistical significance was determined based on two-tailed Student's t test. *, p<0.05, compared to negative control infected macrophages.

let-7e impacts in global variation of TLR pathway gene expression in *L. amazonensis* infected macrophages.

To study the role of let-7e in the regulation of TLR pathway molecules during recognition and establishment of infection, we evaluated and compared the transcript levels of molecules involved in recognition/binding, downstream signaling, adapters, transcription factors, cytokines/chemokines production and cytokines receptors in WT infected-macrophages or negative-control (NC) and let-7e-inhibited after 4 and 24 h of *L. amazonensis* infection compared to uninfected macrophages (Fig. 6, S3 Fig and S3 Table).

First, we compared the gene expression of TLR signaling cascade in infected macrophages after 4 h and 24 h (Fig. 6A and 6B; and S3 Fig). After 4 h of infection revealed a large amount of genes up-regulated: *Tlr1*, *Tlr2*, C-type lectin domain family 4-member e (*Clec4e/Mincle*), Heat shock protein 1A (*Hspa1a/HSP70*), Interferon regulatory factor 1 (*Irf1*), Receptor interacting protein kinase 2 (*Ripk2*), Nuclear factor kappa B subunit 1 (*Nfkb1*), NFkB inhibitor alpha (*Nfkb1a/Ikbalpha*), CD86 antigen (*Cd86*), Interleukin 1 alpha (*Il1a*), prostaglandin-endoperoxide synthase 2 (*Ptgs2/Cox-2*), Tumor necrosis factor (*Tnf*) and TNF alpha induced protein 3 (*Tnfaip3*). From these, only *Hspa1a* and *Il1a* were maintained after 24h of infection, and heat shock protein 1 (*Hspd1*) gene was up-regulated (Fig. 6A).

And few genes appeared down-regulated after 4 h of infection: Caspase 8 (*Casp8*), Nuclear receptor subfamily 2, group C, member 2 (*Nr2c2/TAK1*), Mitogen-activated protein kinase 9 (*Mapk9/JNK2*) and Interleukin 6 receptor-alpha (*Il6ra*). Also, the following genes were down-regulated after 24 h: *Tlr2*, *Tlr5*, *Nfkb1* (p105/p50), *Nfkb2* (p100/p52), *Nfkb1a/Ikbalpha*, Chemokine CXC-motif ligand 10 (*Cxcl10*), Interleukin 1 beta (*Il1b*) and Interleukin 10 (*Il10*) (Fig. 6B, S3 Fig and S3 Table).

The let-7e inhibition compared to NC infected macrophages after 4 h of infection, we detected the following genes up-regulated: *Tlr6*, *Tlr9*, Toll-interleukin 1 receptor (TIR) domain-containing adaptor protein (*Tirap*), Tnf receptor-associated factor 6 (*Traf6*), Toll-like receptor adaptor molecule 1 (*Ticam1*), *Tollip*, *Nfkbib/TRIP9*, *Nfkbil1*, Peroxisome proliferator activated receptor alpha (*Ppara*), *Mapk8ip3/Jip3*, *Ptgs2/Cox2*, Colony stimulating factor 2 (*Csf2/GMCSF*), *Hspd1*, *Csf3*, Interferon beta 1 (*Infb1*), *Il6ra* and *Ilr1* (Fig 6C). And few genes down-regulated: *Tlr1*, CD14 antigen (*Cd14*), Lymphocyte antigen 86 (*Ly86/MD-1*), conserved helix-loop-helix ubiquitous kinase (*Chuk/IKBKA*) and *Il10* (Fig 6D). The let-7e inhibition compared to NC infected macrophages after 24 h of infection showed genes up-regulated: *Tlr7*, *Ly96/MD-2*, *Casp8*, *Map3k1*, *Mapk8*, *Ptgs2/Cox2*, *Csf3/GCSF* and Ubiquitin-conjugating enzyme E2N (*Ube2n*). Indeed, the let-7e-inhibition did not alter the down-regulated genes when compared to NC infected macrophages.

Also, let-7e inhibition increased the levels of predicted mRNA-targets, as *Traf6*, *Ppara*, *Mapk8ip3/Jip3*, *Map3k1* and *Ube2n* in infected macrophages (S2-3 table). These data suggest a modulation of TLR pathways gene expression during *L. amazonensis* infection. Indeed, let-7e inhibition during *L. amazonensis* infection impacts in global variation of TLR pathways gene expression (Fig. 6) and infectiveness (Fig. 5A-C).

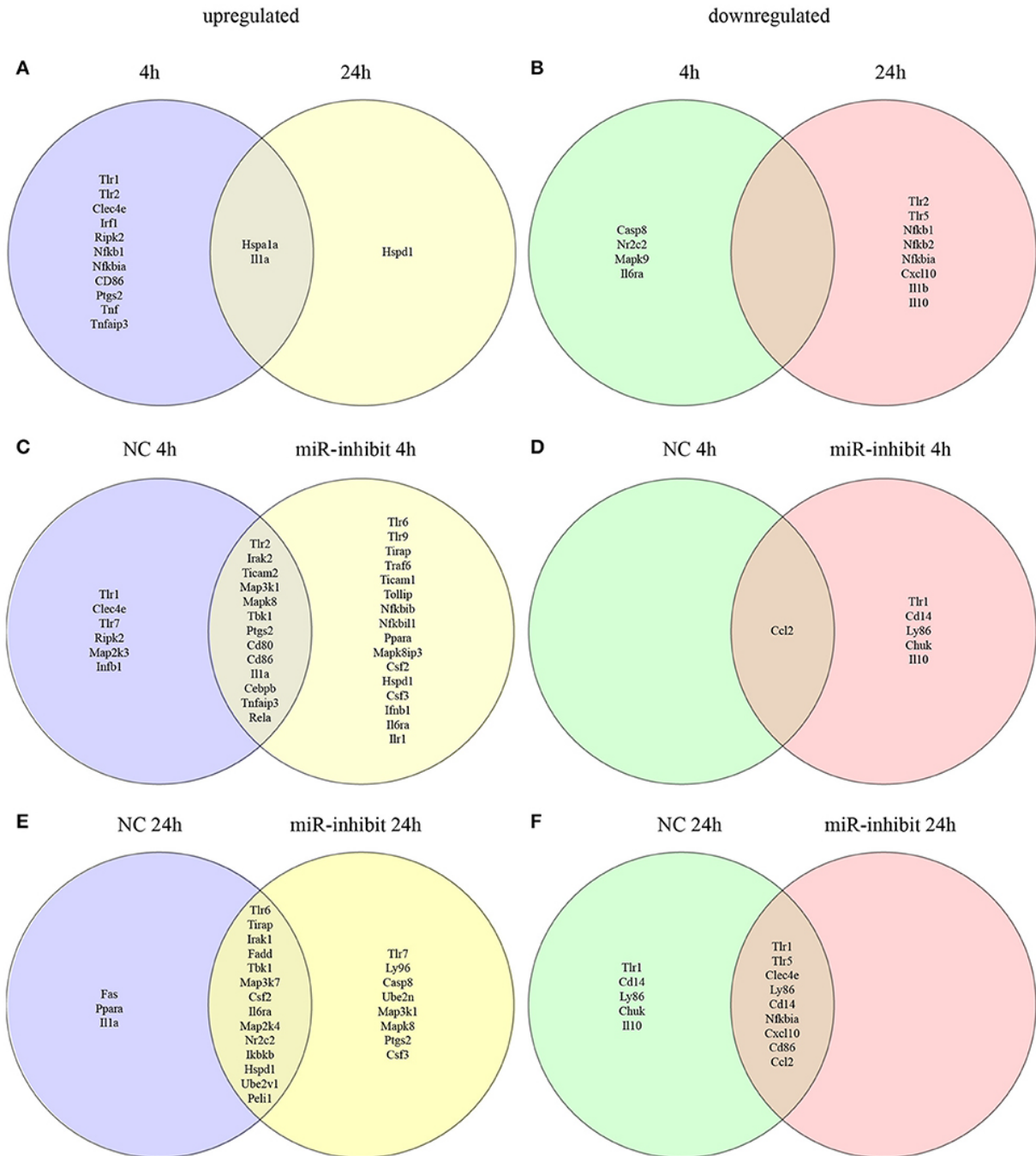


Figure 15. Venn diagram representing unique and common mRNA of TLR pathway molecules and cytokines significantly expressed during let-7e inhibition in *L. amazonensis* infected macrophages. BMDMs were transiently transfected with the negative control (NC) or 100 nM of let-7e-5p inhibitor (miR-inhib). After 24 h of incubation, the cells were co-cultivated with *L. amazonensis* (MOI 5:1) for 4 h, and the cultures were then washed. After 4 and 24 h of infection, the samples were analyzed for mRNAs of TLRs signaling cascade molecules via RT-qPCR of total RNA. The up-regulated (A) and down-regulated (B) mRNAs comparing 4h versus 24 h of infection; Comparison of mRNA in NC and let-7e inhibition (miR-inhib): up-regulated at 4h (C) or 24h (D) and down-regulated at 4h (E) or 24h (F). The relative up- and down-regulation of miRNAs, expressed as boundaries of 1.2 or -1.2 of Fold Regulation, respectively. P-value < 0.05

Discussion

The importance of *Leishmania*-TLRs interaction enabling the activation of macrophage in healing and protection in leishmaniasis has been extensively studied, however, the findings are very controversial. Some studies showed the macrophages ability to recognize the parasite, inducing a pro-inflammatory response and microbicidal mechanisms. TLR4 induces TIRAP-MyD88 signaling and then endocytosis, whereas TRIF-TRAM is activated in early endosomes (Kagan et al., 2008). The trafficking of TLRs 3, 7, 8, and 9 from the endoplasmic reticulum to the endolysosomal compartment collaborates in the recognition of PAMPs and DAMPs (Kagan et al., 2008). Here, we showed the role of TLR2, TLR4 and the adaptor molecule MyD88 in mediating the phagocytosis of *L. amazonensis* and conferring resistance to infection, contrasting with higher infectivity index in the absence of those molecules.

The recognition of virulence factors, as LPG and aGalb1,4Mana-PO(4)-containing phosphoglycans from *L. major*, via TLR2, requires the adaptor MyD88 (de Veer et al., 2003;Flandin et al., 2006). The TLR2-stimulation induces the production of pro-inflammatory cytokines, such as TNF and IL-6, as well as reactive oxygen species (ROS) (de Veer et al., 2003;Kavoosi et al., 2009), and also own suppressors of cytokine signaling family SOCS-1 and SOCS-3 (de Veer et al., 2003;Kavoosi et al., 2009;Vargas-Inchaustegui et al., 2009). P8 proteoglycolipid complex (P8 PGLC) from *L. pifanoi*, via TLR4/MD2-CD14, induces production of TNF and IL-12 in macrophages. Also, TNF production and parasite burden is dependent of TLR2 and MyD88 molecules (Whitaker et al., 2008). Furthermore, MyD88 helps in recognition of *L. donovani* and maturation of dendritic cells during infection (De Trez et al., 2004). Indeed, TLR2, TLR3, MyD88 and IRAK-1 are involved in phagocytosis of *L. donovani* and production of TNF- α and NO, despite only IFN- γ -primed macrophages presents leishmanicidal activity (Flandin et al., 2006).

Several studies have been described the participation of factors, such as transcription factors and miRNAs acting in transcriptional and post-transcriptional regulation of gene expression, respectively (Lin et al., 2015). The miRNA modulation was described in *L. major* (Lemaire et al., 2013), and *L. donovani* (Geraci et al., 2015;Singh et al., 2016) in human-derived infected macrophages. In BALB/c-infected macrophages with *L. amazonensis*, the miRNA profile appeared modulated and the involvement of miR-294, miR-497a and miR-721 (Muxel et al., 2017c). The results presented in this work corroborated these data, showing that *L. amazonensis* infection regulated miRNA profile of C57BL/6 WT, MyD88^{-/-}, TLR2^{-/-} or TLR4^{-/-} infected-macrophages, as well as let-7e expression among the mice strains. The miRNAs let-7e, let-7f, let-7g miR-30b, miR-369, miR-495 and miR-712 appeared upregulated only in C57BL/6 WT-infected macrophages, while TLR2, TLR4 or MyD88 deficient mice modulated other miRNA expression during *L. amazonensis* infection. These evidences indicated that the expression of let-7e, let-7f and let-7g are dependent of MyD88, TLR2 and TLR4 signaling during *L. amazonensis* infection and reveals the role of TLR pathway in the transcriptional and post-transcriptional regulation of gene expression during *Leishmania* infection.

The miRNA let-7 family is highly conserved, from bacteria to mammal, and can modulates some anti-inflammatory effector molecules, as IL-10 (Swaminathan et al., 2012), and also pro-inflammatory effector molecules, as IL-6 (let-7a) (Meng et al., 2007) and IL-13 (let-7d) (Kumar et al., 2011). Bacterial infection, as *Mycobacterium* and *Neisseria* induces let-

7e in macrophages (Elizabeth et al., 2016; Kalantari et al., 2017). The let-7e expression acting in p65 NF- κ B activation (de la Rica et al., 2015) and phosphoinositide-3 kinase/serine-threonine protein kinase (Pi3k/Akt) (Androulidaki et al., 2009; Kalantari et al., 2017) was previously described. Indeed, let-7e appeared downregulating TLR4 and reducing pro-inflammatory signals, such as TNF, IFN- α , IL-6, IL-17, MCP-1, MIP-1 and IP-10 (Androulidaki et al., 2009; Dong et al., 2015; Kalantari et al., 2017). Also, let-7e targeted the suppressor of cytokine signaling 4 (SOCS4) and regulated IL-13 in allergic process (Li et al., 2018).

Here, we showed that *L. amazonensis* infection in C57BL/6 WT-macrophages increased the levels of recognizing molecules, as *Tlr1*, *Tlr2*, *Tlr5* and *Clec4e/Mincle*, supporting the involvement of TLRs to identify and phagocyte the parasite. Moreover, the augment in adaptors and effectors molecules, such as *Hspa1a*, *Hspd1*, *Irf1*, *Ripk2*, *Nfkb1*, *Nfkb2*, *Nfkbia/Ikbalpha*; and immunomodulators, such as *Cxcl10*, *Cd86*, *Il1a*, *Il1b*, *Tnf*, *Il10* and *Tnfaip3*, and a decrease of *Casp8*, *Nr2c2/TAK1*, *Mapk9/JNK2* and *Il6ra* during infection indicates that *L. amazonensis* modulated the macrophage activation.

Interestingly, functional inhibition of let-e during *L. amazonensis* infection reduced the infectivity and impacted globally in mRNA from TLR signaling cascade, as showed in figure 7, increasing the amount of predicted targets, such *Traf6*, *Ppara*, *Mapk8ip3/Jip3*, *Map3k1* and *Ube2n* (represented in red), and also indirect targets (represented in orange): recognizing molecules, such *Tlr9* and *Ly96/MD-2*; adaptors and effectors molecules, such *Tirap*, *Ticam1*, *Tollip*, *Casp8*, *Map3k1*, *Peli1*, *Nfkbib/TRIP9*, *Nfkbil1* and *Hspd1*; and immunomodulators, such as *Ptgs2/Cox2*, *Csf2/GMCSF*, *Csf3/GCSF*, and *Ilr1*. Despite, let-7e validated targets previously described, *Tnfaip3*, *Map2k4*, *Tbk1* and *Tnf*, appeared up-regulated during *L. amazonensis* infection, whereas, the negative modulation of *Chuk/IKBKA* and *Il10* during infection was not reverted by let-7e inhibition.

The TLR/IL-1R signaling pathways have been extensively studied in the ubiquitin-dependent NF- κ B activation, as well as the subcellular trafficking. The ubiquitination system is based in ubiquitin-activation E1, ubiquitin-conjugating E2 enzymes, and ubiquitin ligases E3. The E2 UBE2n dimerizes with UBE2v, forming K63-linked ubiquitin chain to polyubiquitinate adaptors molecules, as TRAF6 to recruit of complex TAB2/TAK1 and active NF- κ B, as showed in figure 6 (Ikeda and Dikic, 2008; David et al., 2010; Roh et al., 2014; Fletcher et al., 2015). Despite, the role of ubiquitination in immune response to *Leishmania* is not studied. Other molecule, PPAR α was not previously described in *Leishmania* infection. However, TLR4 transcription and signaling is negatively regulated via PPAR α , which inhibits NF- κ B signaling pathway (Shen et al., 2014). Also, PPAR α regulates genes involved in free fatty acids metabolism, which could bind to TLR4 and interfere in the inflammatory response. In addition, Tollip is a negative regulator of TLRs signaling pathway and regulating inflammatory cytokines production, as IL-6 and TNF (Liew et al., 2005) and could influence the response to cutaneous *L. guyanensis* infection (de Araujo et al., 2015). Mapk8ip3/JIP3 helps TLR4 signaling cascade increasing the JNK activation and MEK1/2 pathway (Ito et al., 1999; Matsuguchi et al., 2003).

Indeed, early step of infection of human-macrophages with *L. amazonensis* and *L. major* upregulated pro-inflammatory cytokines genes, such as *Il1b*, *Tnf* and *Il6*, and also others

molecules involved in tissue growth and repair, such as *Csf2* and *Ptgs2/Cox2* (Fernandes et al., 2016). In the same way, *L. major* infection of murine-macrophage increased the levels of *Tnf*, *Il1*, *Il6*, *Nos2*, *Ilrap* and *Csf3*, as well as molecules of NF- κ B and MAPK signaling (Dillon et al., 2015).

Here we showed that TLR2 and TLR4 induced the *Cat2B* and *Cat1* mRNA expression in *L. amazonensis* infected macrophages, while MyD88 absence allowed their expression, helping the control of L-arginine uptake. The L-arginine uptake mediation through *Cat2B* helps to control *L. amazonensis* infectiveness (Laranjeira-Silva et al., 2015b). The regulation of polyamines production via *Arg1* mRNA expression was dependent of TLR4 and MyD88. Thus, the *Nos2* expression depends of TLR2, TLR4 and MyD88 molecules during infection and its activation in C57BL/6 mice-macrophages could help in the resistance to infection, as previously shown in the absence of *Nos2* in murine macrophages (Wei et al., 1995). The let-7e inhibition modulations reflect in regulation of *Arg1* and *Nos2* expression during infection, corroborating to the importance of TLR signaling cascade to regulate *Arg1* and *Nos2* expression at transcriptional level. NF- κ B pathway regulates the *Nos2* expression at the transcriptional level (Beck and Sterzel, 1996), as observed for *L. major* and *L. amazonensis* infections, increasing the nuclear translocation of the NF- κ B p50/p50 dimer, which correlate with the decrease of *Nos2* and *Cat2B* transcripts amount (Dixit and Mak, 2002). In *L. amazonensis* infection, miR-294-3p and miR-721 acted in a post-transcriptional level by degrading *Nos2* mRNA in BALB/c macrophage (Muxel et al., 2017c). *Leishmania* also had a L-arginine uptake mediated by amino acid permease 3 (Castilho-Martins et al., 2011;Castilho-Martins et al., 2015;Aoki et al., 2017a) and amino acid metabolism via arginase (Laranjeira-Silva et al., 2012;Aoki et al., 2017b) and *NOS-like* (Acuna et al., 2017). L-arginine is essential to parasite survival and interferes in macrophage activation during infection (Muxel et al., 2017a). Indeed, parasite arginase competes by L-arginine and also reduced the host *Nos2* expression and NO production in *L. amazonensis* infection (Muxel et al., 2017c).

NOS2 activity to NO production trigger macrophage inflammatory response and kill the parasites (Green et al., 1990a;Green et al., 1990b;Liew et al., 1991;Wanasen and Soong, 2008). The balance between polyamines production, via ARG1, and NO production, via NOS2, can influence the fate of infectivity in different mice models. The IL-12 production and NOS2 expression reduce the infectivity in C57BL/6 mice. In contrast, the IL-4 production and *Arg1* expression increased the infectivity in BALB/c (Iniesta et al., 2001;Iniesta et al., 2002;Muxel et al., 2017a). Both cytokines, IL-12 or IL-4 induces CAT2B expression and L-arginine uptake enabling the outcome of infection, a substrate to ARG1 and NOS2, while a negative modulation of CAT2B can also reduce the infectivity of *L. amazonensis* (Laranjeira-Silva et al., 2015a).

Interestingly, TLR4 contributes to the control of parasite growth in initial and later steps of *L. major* infection (Kropf et al., 2004). In addition, *L. major* infection induced NOS2 expression via TLR4 activation, even that the ARG1 expression is independent of TLR4 during infection *in vivo* and *in vitro* (Kropf et al., 2004). The TLR9 induced NOS2 expression, IL-12 and IFN- γ and helped in control parasite burden in *L. major* infection of BALB/c and C57BL/6 mice (Liese et al., 2007). Despite, MyD88 signaling increased the ratio of IL-12/IL-10 in *L. amazonensis* and *L. braziliensis* infected dendritic cells (Vargas-Inchaustegui et al., 2009). MyD88 helps in resistance to *L. braziliensis* infection in C57BL/6 mice, regardless

TLR2 enhanced regulation of immune response, reducing the ratio of IL-12/IL-10 (Vargas-Inchaustegui et al., 2009).

Some works have shown that *L. amazonensis* infection regulates the activation of MAPK in BALB/c macrophages, regulating IL-10 production (Yang et al., 2007). Despite, p38-MAPK activation reduced the infectivity of *L. donovani* (Junghae and Raynes, 2002). On the other hand, *L. mexicana* Glycosylphosphatidylinositol-anchored lipophosphoglycan (LPG)/TLR stimulation regulated MAPK and NF- κ B pathways to alters IL-12 production (Cameron et al., 2004;Argueta-Donohue et al., 2008). The chaperone Hsp60 serves as danger signaling of stressed or damaged cells and could due an anti-apoptotic activity via HSP60/pC3 complex formation (Chandra et al., 2007). The TNF or TLR signaling lead to Fas-associated protein with death domain (FADD)/pro-caspase 8 complex formation and activation of caspase 8, which can induces apoptosis via direct cleavage of downstream caspases, caspase-3/7 (Feltham et al., 2017). In *L. major* infection, the inhibition of caspase 8 increases Th1 and Th2 cytokines and also NO production (Pereira-Manfro et al., 2014), contrasting with antiapoptotic signaling mediated by caspase 8 during *L. infantum* infection (Cianciulli et al., 2018). The modulation of the amount of mRNAs in TLR pathway impacted in the infectivity of *L. amazonensis*.

Our data corroborated the idea that *Leishmania* infection may regulate TLR pathway and consequently the cytokines and chemokines production, as well as NO/polyamines production, to control macrophage activation and infectiveness. Emphasizing the importance of TLR signals and miRNA expression during infection and the integration of these molecules for regulation of gene expression to fate *Leishmania* infection, as well as potential new target to control infectivity and pathogenesis.

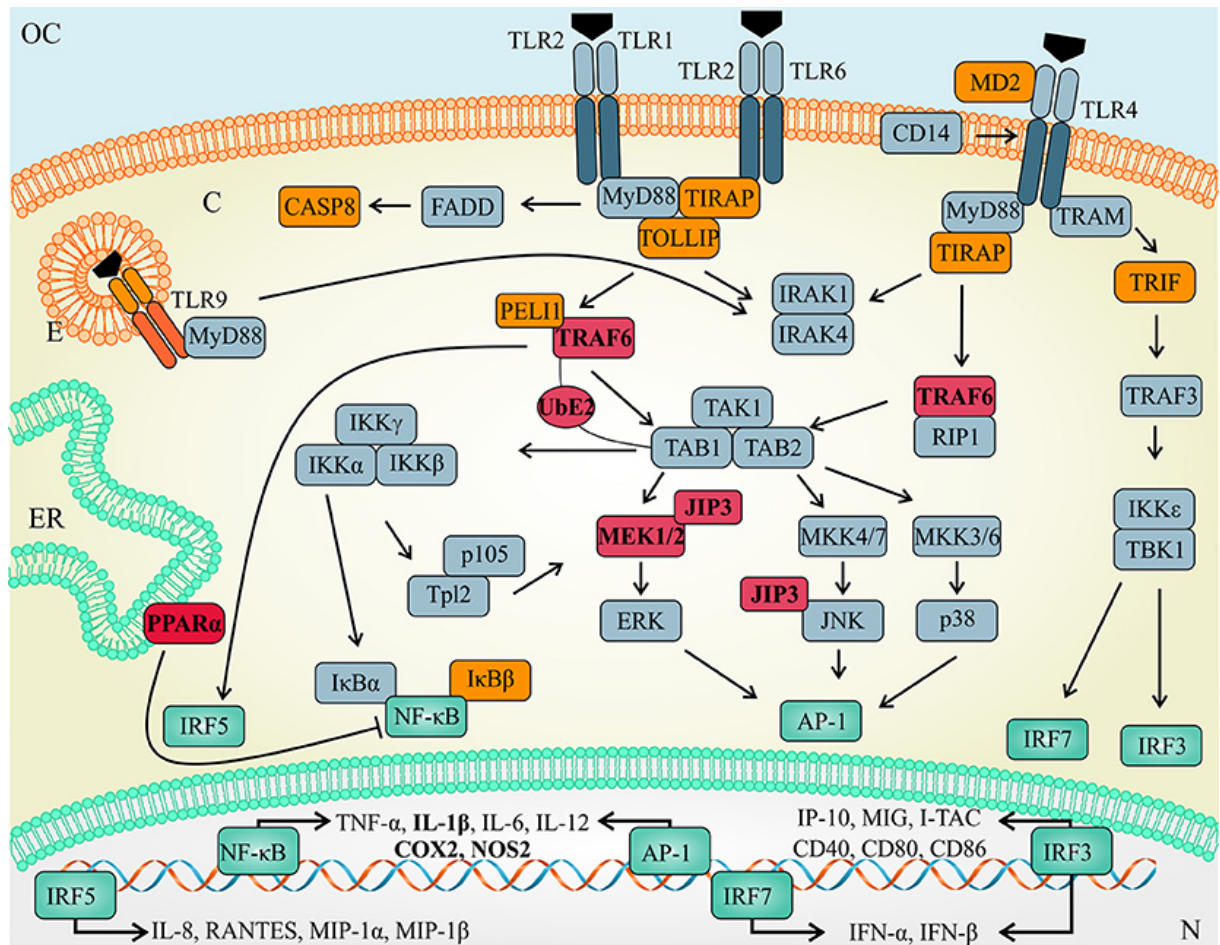
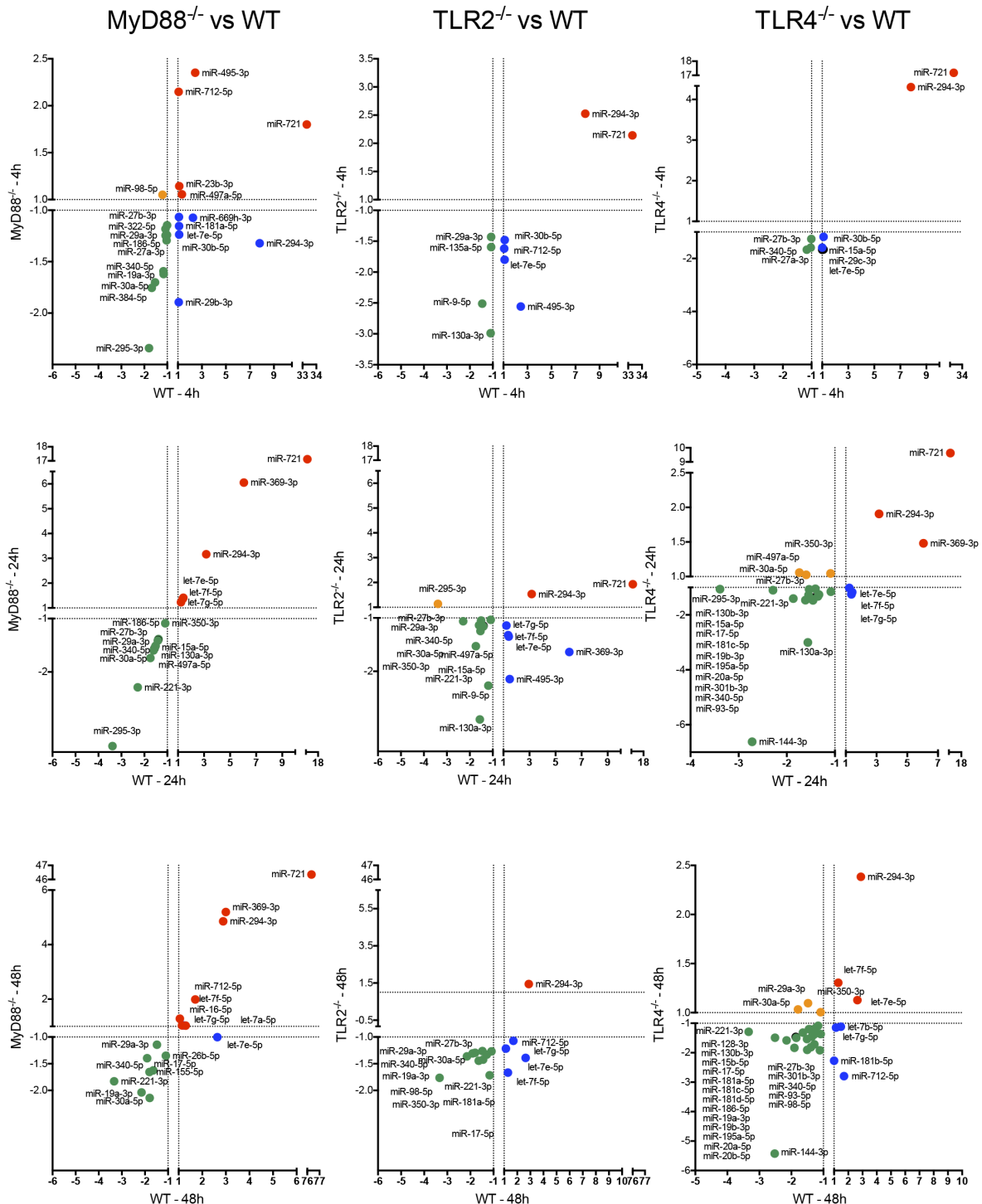
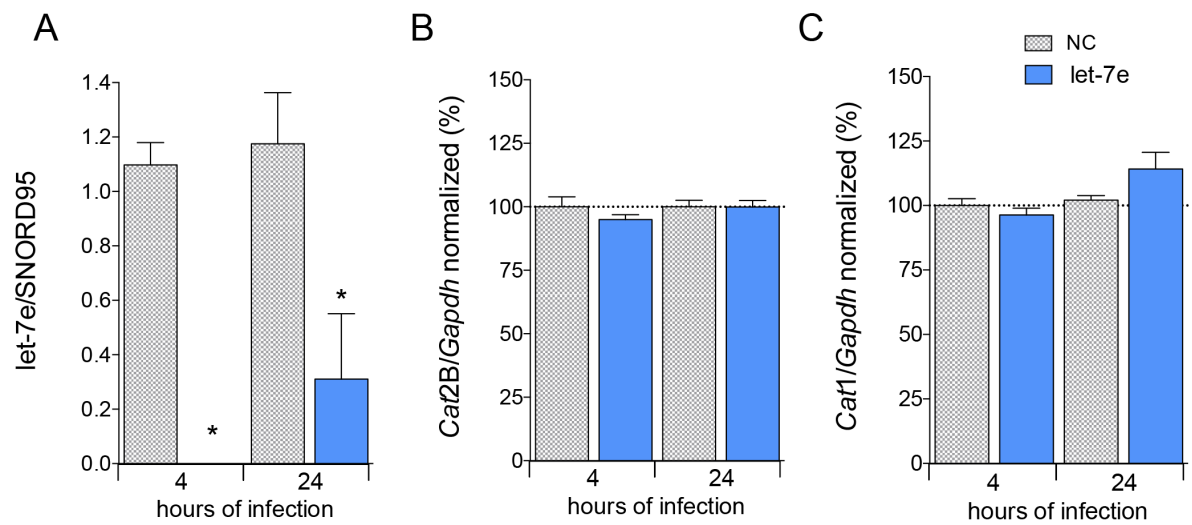


Figure 16 Schematic representation of TLR pathway and let-7e-targets mRNAs. TLR activation could be regulated via let-7e post-transcriptional mechanisms, acting directly (predicted targets in red) or indirectly (molecules in orange) in mRNA/protein expression, modulating the molecules involved in recognizing, adaptors and effector molecules, as well as transcription factors (green), which modulates the expression of cytokines, chemokines and others immunomodulators.

Supplementary material



Supplementary Figure 2. Scatter plot of the miRNA profiles of C57BL/6 (WT), MyD88^{-/-}, TLR2^{-/-} and TLR4^{-/-} murine BMDMs infected with *L. amazonensis*. Each dot represents one miRNA of BMDMs infected for 4, 24 and 48 h with *L. amazonensis*. The red dot indicates up-regulated miRNAs and green dot indicate down-regulated miRNAs in both comparisons; blue dot indicates up-regulated miRNAs in WT compared to knockouts and orange dot indicates down-regulated miRNAs in WT compared to knockouts. The relative up- and down-regulation of miRNAs, expressed as boundaries of 1.2 or -1.2 of Fold Regulation, respectively. An only significant ($p < 0.05$) Fold Regulation value was represented.



Supplementary Figure 3. Inhibition of let-7 functions. BMDMs were transiently transfected with the negative control or 100 nM of let-7e-5p inhibitor. After 24 h of incubation, the cells were co-cultivated with *L. amazonensis* (MOI 5:1) for 4 h, and the cultures were then washed. After 4 and 24 h of infection, the samples were analyzed for let-7e levels normalized by SNORD95 via RT-qPCR (A), and mRNA levels via RT-qPCR of total RNA, for *Cat2B* (B) and *Cat1* (C). The values were normalized based on the average values of NC infected macrophages (100%). Each bar represents the average \pm SEM of the values obtained in 3 independent experiments (n=3-6). Statistical significance was determined based on two-tailed Student's t test. *, p<0.05, compared to negative control infected macrophages

S1 Table: C57BL/6 (WT), MyD88^{-/-}, TLR2^{-/-} and TLR4^{-/-} murine macrophage microRNA regulation during *L. amazonensis* infection. FR (Fold Regulation) represents the Fold Change results at a biological magnitude. Values >1.2 indicate positive regulation and values <-1.2 indicate negative regulation.

S2 Table: Predicted targets-mRNA for let-7e miRNA. The miRNA-mRNA interaction prediction in miRecord tools (<http://c1.accurascience.com/miRecords/>) based in the integration of the predicted targets from various predicted tools: DIANA-microT, MicroInspector, miRanda, MirTarget2, miTarget, NBmiRTar, PicTar, PITA, RNA22, RNAhybrid, and TargetScan/TargertScanS, such as at least 3 tools.

S3 Table: Let-7e inhibition impacts in the amount of mRNAs of impact in WT-Macrophage TLR pathway regulation during *L. amazonensis* infection. FR (Fold Regulation) represents the Fold Change results at a biological magnitude. Values >1.2 indicates positive regulation and values <-1.2 indicate negative regulation.

References

- Acuna, S.M., Aoki, J.I., Laranjeira Da Silva, M.F., Zampieri, R.A., Fernandes, J.C., Muxel, S.M., et al. (2017). Arginase expression modulates Nitric Oxide production in *Leishmania (Leishmania) amazonensis*. *PLoS One*.
- Akira, S., and Sato, S. (2003). Toll-like receptors and their signaling mechanisms. *Scand J Infect Dis* 35, 555-562.
- Akira, S., Uematsu, S., and Takeuchi, O. (2006). Pathogen recognition and innate immunity. *Cell* 124, 783-801.
- Alvar, J., Vélez, I.D., Bern, C., Herrero, M., Desjeux, P., Cano, J., et al. (2012). Leishmaniasis worldwide and global estimates of its incidence. *PLoS One* 7, e35671.
- Androulidaki, A., Iliopoulos, D., Arranz, A., Doxaki, C., Schworer, S., Zacharioudaki, V., et al. (2009). The kinase Akt1 controls macrophage response to lipopolysaccharide by regulating microRNAs. *Immunity* 31, 220-231.
- Aoki, J.I., Muxel, S.M., Zampieri, R.A., Acuna, S.M., Fernandes, J.C.R., Vanderlinde, R.H., et al. (2017a). L-arginine availability and arginase activity: Characterization of amino acid permease 3 in *Leishmania amazonensis*. *PLoS Negl Trop Dis* 11, e0006025.
- Aoki, J.I., Muxel, S.M., Zampieri, R.A., Laranjeira-Silva, M.F., Muller, K.E., Nerland, A.H., et al. (2017b). RNA-seq transcriptional profiling of *Leishmania amazonensis* reveals an arginase-dependent gene expression regulation. *PLoS Negl Trop Dis* 11, e0006026.
- Argueta-Donohue, J., Carrillo, N., Valdes-Reyes, L., Zentella, A., Aguirre-Garcia, M., Becker, I., et al. (2008). *Leishmania mexicana*: participation of NF-kappaB in the differential production of IL-12 in dendritic cells and monocytes induced by lipophosphoglycan (LPG). *Exp Parasitol* 120, 1-9.
- Bacellar, O., D'oliveira, A., Jr., Jeronimo, S., and Carvalho, E.M. (2000). IL-10 and IL-12 are the main regulatory cytokines in visceral leishmaniasis. *Cytokine* 12, 1228-1231.
- Bagga, S., Bracht, J., Hunter, S., Massirer, K., Holtz, J., Eachus, R., et al. (2005). Regulation by let-7 and lin-4 miRNAs results in target mRNA degradation. *Cell* 122, 553-563.
- Beck, K.F., and Sterzel, R.B. (1996). Cloning and sequencing of the proximal promoter of the rat iNOS gene: activation of NFkappaB is not sufficient for transcription of the iNOS gene in rat mesangial cells. *FEBS Lett* 394, 263-267.
- Becker, I., Salaiza, N., Aguirre, M., Delgado, J., Carrillo-Carrasco, N., Kobeh, L.G., et al. (2003). *Leishmania* lipophosphoglycan (LPG) activates NK cells through toll-like receptor-2. *Mol Biochem Parasitol* 130, 65-74.
- Ben-Othman, R., Dellagi, K., and Guizani-Tabbane, L. (2009). *Leishmania major* parasites induced macrophage tolerance: implication of MAPK and NF-kappaB pathways. *Mol Immunol* 46, 3438-3444.
- Bernstein, E., Caudy, A.A., Hammond, S.M., and Hannon, G.J. (2001). Role for a bidentate ribonuclease in the initiation step of RNA interference. *Nature* 409, 363-366.
- Bhattacharyya, S., Ghosh, S., Jhonson, P.L., Bhattacharya, S.K., and Majumdar, S. (2001). Immunomodulatory role of interleukin-10 in visceral leishmaniasis: defective activation of protein kinase C-mediated signal transduction events. *Infect Immun* 69, 1499-1507.
- Bogdan, C. (2008). Mechanisms and consequences of persistence of intracellular pathogens: leishmaniasis as an example. *Cell Microbiol* 10, 1221-1234.
- Cameron, P., McGachy, A., Anderson, M., Paul, A., Coombs, G.H., Mottram, J.C., et al. (2004). Inhibition of lipopolysaccharide-induced macrophage IL-12 production by *Leishmania mexicana* amastigotes: the role of cysteine peptidases and the NF-kappaB signaling pathway. *J Immunol* 173, 3297-3304.

- Carlsen, E.D., Liang, Y., Shelite, T.R., Walker, D.H., Melby, P.C., and Soong, L. (2015). Permissive and protective roles for neutrophils in leishmaniasis. *Clin Exp Immunol* 182, 109-118.
- Castilho-Martins, E.A., Canuto, G.A., Muxel, S.M., Da Silva, M.F., Floeter-Winter, L.M., Del Aguila, C., et al. (2015). Capillary electrophoresis reveals polyamine metabolism modulation in *Leishmania (Leishmania) amazonensis* wild type and arginase knockout mutants under arginine starvation. *Electrophoresis*.
- Castilho-Martins, E.A., Laranjeira Da Silva, M.F., Dos Santos, M.G., Muxel, S.M., and Floeter-Winter, L.M. (2011). Axenic *Leishmania amazonensis* promastigotes sense both the external and internal arginine pool distinctly regulating the two transporter-coding genes. *PLoS One* 6, e27818.
- Chandra, D., Choy, G., and Tang, D.G. (2007). Cytosolic accumulation of HSP60 during apoptosis with or without apparent mitochondrial release: evidence that its pro-apoptotic or pro-survival functions involve differential interactions with caspase-3. *J Biol Chem* 282, 31289-31301.
- Cianciulli, A., Porro, C., Calvello, R., Trotta, T., and Panaro, M.A. (2018). Resistance to apoptosis in *Leishmania infantum*-infected human macrophages: a critical role for anti-apoptotic Bcl-2 protein and cellular IAP1/2. *Clin Exp Med* 18, 251-261.
- David, Y., Ziv, T., Admon, A., and Navon, A. (2010). The E2 ubiquitin-conjugating enzymes direct polyubiquitination to preferred lysines. *J Biol Chem* 285, 8595-8604.
- De Araujo, F.J., Da Silva, L.D., Mesquita, T.G., Pinheiro, S.K., Vital Wde, S., Chrusciak-Talhari, A., et al. (2015). Polymorphisms in the TOLLIP Gene Influence Susceptibility to Cutaneous Leishmaniasis Caused by *Leishmania guyanensis* in the Amazonas State of Brazil. *PLoS Negl Trop Dis* 9, e0003875.
- De La Rica, L., Garcia-Gomez, A., Comet, N.R., Rodriguez-Ubreva, J., Ciudad, L., Vento-Tormo, R., et al. (2015). NF-kappaB-direct activation of microRNAs with repressive effects on monocyte-specific genes is critical for osteoclast differentiation. *Genome Biol* 16, 2.
- De Trez, C., Brait, M., Leo, O., Aebischer, T., Torrentera, F.A., Carlier, Y., et al. (2004). Myd88-dependent in vivo maturation of splenic dendritic cells induced by *Leishmania donovani* and other *Leishmania* species. *Infect Immun* 72, 824-832.
- De Veer, M.J., Curtis, J.M., Baldwin, T.M., Didonato, J.A., Sexton, A., Mcconville, M.J., et al. (2003). MyD88 is essential for clearance of *Leishmania major*: possible role for lipophosphoglycan and Toll-like receptor 2 signaling. *Eur J Immunol* 33, 2822-2831.
- Dillon, L.A., Suresh, R., Okrah, K., Corrada Bravo, H., Mosser, D.M., and El-Sayed, N.M. (2015). Simultaneous transcriptional profiling of *Leishmania major* and its murine macrophage host cell reveals insights into host-pathogen interactions. *BMC Genomics* 16, 1108.
- Dixit, V., and Mak, T.W. (2002). NF-kappaB signaling. Many roads lead to madrid. *Cell* 111, 615-619.
- Dong, G., Fan, H., Yang, Y., Zhao, G., You, M., Wang, T., et al. (2015). 17beta-Estradiol enhances the activation of IFN-alpha signaling in B cells by down-regulating the expression of let-7e-5p, miR-98-5p and miR-145a-5p that target IKKepsilon. *Biochim Biophys Acta* 1852, 1585-1598.
- Elizabeth, M.C., Hernandez De La Cruz, O.N., and Mauricio, C.A. (2016). Infection of J774A.1 with different Mycobacterium species induces differential immune and miRNA-related responses. *Microbiol Immunol* 60, 356-363.
- Feltham, R., Vince, J.E., and Lawlor, K.E. (2017). Caspase-8: not so silently deadly. *Clin Transl Immunology* 6, e124.
- Fernandes, M.C., Dillon, L.A., Belew, A.T., Bravo, H.C., Mosser, D.M., and El-Sayed, N.M. (2016). Dual Transcriptome Profiling of *Leishmania*-Infected Human Macrophages Reveals Distinct Reprogramming Signatures. *MBio* 7.

- Flandin, J.F., Chano, F., and Descoteaux, A. (2006). RNA interference reveals a role for TLR2 and TLR3 in the recognition of *Leishmania donovani* promastigotes by interferon-gamma-primed macrophages. *Eur J Immunol* 36, 411-420.
- Fletcher, A.J., Mallery, D.L., Watkinson, R.E., Dickson, C.F., and James, L.C. (2015). Sequential ubiquitination and deubiquitination enzymes synchronize the dual sensor and effector functions of TRIM21. *Proc Natl Acad Sci U S A* 112, 10014-10019.
- Gazzinelli, R.T., and Denkers, E.Y. (2006). Protozoan encounters with Toll-like receptor signalling pathways: implications for host parasitism. *Nat Rev Immunol* 6, 895-906.
- Geraci, N.S., Tan, J.C., and Mcdowell, M.A. (2015). Characterization of microRNA expression profiles in *Leishmania*-infected human phagocytes. *Parasite Immunol* 37, 43-51.
- Ghalib, H.W., Whittle, J.A., Kubin, M., Hashim, F.A., El-Hassan, A.M., Grabstein, K.H., et al. (1995). IL-12 enhances Th1-type responses in human *Leishmania donovani* infections. *J Immunol* 154, 4623-4629.
- Green, S.J., Crawford, R.M., Hockmeyer, J.T., Meltzer, M.S., and Nacy, C.A. (1990a). *Leishmania major* amastigotes initiate the L-arginine-dependent killing mechanism in IFN-gamma-stimulated macrophages by induction of tumor necrosis factor-alpha. *J Immunol* 145, 4290-4297.
- Green, S.J., Meltzer, M.S., Hibbs, J.B., Jr., and Nacy, C.A. (1990b). Activated macrophages destroy intracellular *Leishmania major* amastigotes by an L-arginine-dependent killing mechanism. *J Immunol* 144, 278-283.
- Gregory, D.J., and Olivier, M. (2005). Subversion of host cell signalling by the protozoan parasite *Leishmania*. *Parasitology* 130 Suppl, S27-35.
- Ikeda, F., and Dikic, I. (2008). Atypical ubiquitin chains: new molecular signals. 'Protein Modifications: Beyond the Usual Suspects' review series. *EMBO Rep* 9, 536-542.
- Iniesta, V., Gomez-Nieto, L.C., and Corraliza, I. (2001). The inhibition of arginase by N(omega)-hydroxy-L-arginine controls the growth of *Leishmania* inside macrophages. *J Exp Med* 193, 777-784.
- Iniesta, V., Gomez-Nieto, L.C., Molano, I., Mohedano, A., Carcelen, J., Miron, C., et al. (2002). Arginase I induction in macrophages, triggered by Th2-type cytokines, supports the growth of intracellular *Leishmania* parasites. *Parasite Immunol* 24, 113-118.
- Ito, M., Yoshioka, K., Akechi, M., Yamashita, S., Takamatsu, N., Sugiyama, K., et al. (1999). JSAP1, a novel jun N-terminal protein kinase (JNK)-binding protein that functions as a Scaffold factor in the JNK signaling pathway. *Mol Cell Biol* 19, 7539-7548.
- Janeway, C.A., Jr., and Medzhitov, R. (2002). Innate immune recognition. *Annu Rev Immunol* 20, 197-216.
- Junghae, M., and Raynes, J.G. (2002). Activation of p38 mitogen-activated protein kinase attenuates *Leishmania donovani* infection in macrophages. *Infect Immun* 70, 5026-5035.
- Kagan, J.C., Su, T., Horng, T., Chow, A., Akira, S., and Medzhitov, R. (2008). TRAM couples endocytosis of Toll-like receptor 4 to the induction of interferon-beta. *Nat Immunol* 9, 361-368.
- Kalantari, P., Harandi, O.F., Agarwal, S., Rus, F., Kurt-Jones, E.A., Fitzgerald, K.A., et al. (2017). miR-718 represses proinflammatory cytokine production through targeting phosphatase and tensin homolog (PTEN). *J Biol Chem* 292, 5634-5644.
- Kane, M.M., and Mosser, D.M. (2001). The role of IL-10 in promoting disease progression in leishmaniasis. *J Immunol* 166, 1141-1147.
- Karagkouni, D., Paraskevopoulou, M.D., Chatzopoulos, S., Vlachos, I.S., Tastsoglou, S., Kanellos, I., et al. (2018). DIANA-TarBase v8: a decade-long collection of experimentally supported miRNA-gene interactions. *Nucleic Acids Res* 46, D239-D245.

Kavoosi, G., Ardestani, S.K., and Kariminia, A. (2009). The involvement of TLR2 in cytokine and reactive oxygen species (ROS) production by PBMCs in response to *Leishmania major* phosphoglycans (PGs). *Parasitology* 136, 1193-1199.

Kropf, P., Freudenberg, M.A., Modolell, M., Price, H.P., Herath, S., Antoniazzi, S., et al. (2004). Toll-like receptor 4 contributes to efficient control of infection with the protozoan parasite *Leishmania major*. *Infect Immun* 72, 1920-1928.

Kumar, M., Ahmad, T., Sharma, A., Mabalirajan, U., Kulshreshtha, A., Agrawal, A., et al. (2011). Let-7 microRNA-mediated regulation of IL-13 and allergic airway inflammation. *J Allergy Clin Immunol* 128, 1077-1085 e1071-1010.

Lagos-Quintana, M., Rauhut, R., Yalcin, A., Meyer, J., Lendeckel, W., and Tuschl, T. (2002). Identification of tissue-specific microRNAs from mouse. *Curr Biol* 12, 735-739.

Landgraf, P., Rusu, M., Sheridan, R., Sewer, A., Iovino, N., Aravin, A., et al. (2007). A mammalian microRNA expression atlas based on small RNA library sequencing. *Cell* 129, 1401-1414.

Laranjeira-Silva, M.F., Zampieri, R.A., Muxel, S.M., Beverley, S.M., and Floeter-Winter, L.M. (2012). *Leishmania amazonensis* arginase compartmentalization in the glycosome is important for parasite infectivity. *PLoS One* 7, e34022.

Laranjeira-Silva, M.F., Zampieri, R.A., Muxel, S.M., Floeter-Winter, L.M., and Markus, R.P. (2015a). Melatonin attenuates *Leishmania (L.) amazonensis* infection by modulating arginine metabolism. *J Pineal Res* 59, 478-487.

Laranjeira-Silva, M.F., Zampieri, R.A., Muxel, S.M., Floeter-Winter, L.M., and Markus, R.P. (2015b). Melatonin attenuates *Leishmania (L.) amazonensis* infection by modulating arginine metabolism. *J Pineal Res*.

Lemaire, J., Mkannez, G., Guerfali, F.Z., Gustin, C., Attia, H., Sghaier, R.M., et al. (2013). MicroRNA expression profile in human macrophages in response to *Leishmania major* infection. *PLoS Negl Trop Dis* 7, e2478.

Li, L., Zhang, S., Jiang, X., Liu, Y., Liu, K., and Yang, C. (2018). MicroRNA-let-7e regulates the progression and development of allergic rhinitis by targeting suppressor of cytokine signaling 4 and activating Janus kinase 1/signal transducer and activator of transcription 3 pathway. *Exp Ther Med* 15, 3523-3529.

Liese, J., Schleicher, U., and Bogdan, C. (2007). TLR9 signaling is essential for the innate NK cell response in murine cutaneous leishmaniasis. *Eur J Immunol* 37, 3424-3434.

Liese, J., Schleicher, U., and Bogdan, C. (2008). The innate immune response against *Leishmania* parasites. *Immunobiology* 213, 377-387.

Liew, F.Y., Li, Y., Moss, D., Parkinson, C., Rogers, M.V., and Moncada, S. (1991). Resistance to *Leishmania major* infection correlates with the induction of nitric oxide synthase in murine macrophages. *Eur J Immunol* 21, 3009-3014.

Liew, F.Y., Millott, S., Parkinson, C., Palmer, R.M., and Moncada, S. (1990). Macrophage killing of *Leishmania* parasite in vivo is mediated by nitric oxide from L-arginine. *J Immunol* 144, 4794-4797.

Liew, F.Y., Xu, D., Brint, E.K., and O'Neill, L.A. (2005). Negative regulation of toll-like receptor-mediated immune responses. *Nat Rev Immunol* 5, 446-458.

Lim, L.P., Lau, N.C., Garrett-Engele, P., Grimson, A., Schelter, J.M., Castle, J., et al. (2005). Microarray analysis shows that some microRNAs downregulate large numbers of target mRNAs. *Nature* 433, 769-773.

Lima-Junior, D.S., Costa, D.L., Carregaro, V., Cunha, L.D., Silva, A.L., Mineo, T.W., et al. (2013). Inflammasome-derived IL-1 β production induces nitric oxide-mediated resistance to *Leishmania*. *Nat Med* 19, 909-915.

Lin, Y., Sibanda, V.L., Zhang, H.M., Hu, H., Liu, H., and Guo, A.Y. (2015). MiRNA and TF co-regulatory network analysis for the pathology and recurrence of myocardial infarction. *Sci Rep* 5, 9653.

Liu, D., and Uzonna, J.E. (2012). The early interaction of *Leishmania* with macrophages and dendritic cells and its influence on the host immune response. *Front Cell Infect Microbiol* 2, 83.

Matsuguchi, T., Masuda, A., Sugimoto, K., Nagai, Y., and Yoshikai, Y. (2003). JNK-interacting protein 3 associates with Toll-like receptor 4 and is involved in LPS-mediated JNK activation. *EMBO J* 22, 4455-4464.

Medzhitov, R. (2007). Recognition of microorganisms and activation of the immune response. *Nature* 449, 819-826.

Meng, F., Henson, R., Wehbe-Janek, H., Smith, H., Ueno, Y., and Patel, T. (2007). The MicroRNA let-7a modulates interleukin-6-dependent STAT-3 survival signaling in malignant human cholangiocytes. *J Biol Chem* 282, 8256-8264.

Muxel, S.M., Aoki, J.I., Fernandes, J.C.R., Laranjeira-Silva, M.F., Zampieri, R.A., Acuna, S.M., et al. (2017a). Arginine and Polyamines Fate in *Leishmania* Infection. *Front Microbiol* 8, 2682.

Muxel, S.M., Laranjeira-Silva, M.F., Zampieri, R.A., Aoki, J.I., Acuña, S.M., and Floeter-Winter, L.M. (2017b). Functional validation of miRNA-mRNA interactions in macrophages by inhibition/competition assays based in transient transfection. *Protocol Exchange*.

Muxel, S.M., Laranjeira-Silva, M.F., Zampieri, R.A., and Floeter-Winter, L.M. (2017c). *Leishmania* (*Leishmania*) *amazonensis* induces macrophage miR-294 and miR-721 expression and modulates infection by targeting NOS2 and L-arginine metabolism. *Sci Rep* 7, 44141.

Nasseri, M., and Modabber, F.Z. (1979). Generalized infection and lack of delayed hypersensitivity in BALB/c mice infected with *Leishmania tropica major*. *Infect Immun* 26, 611-614.

Nathan, C., and Shiloh, M.U. (2000). Reactive oxygen and nitrogen intermediates in the relationship between mammalian hosts and microbial pathogens. *Proc Natl Acad Sci U S A* 97, 8841-8848.

Oliveros, J.C. (2007-2015). Venny. An interactive tool for comparing lists with Venn's diagrams. [Online]. Available: <http://bioinfogp.cnb.csic.es/tools/venny/index.html> [Accessed].

Pasquinelli, A.E., Reinhart, B.J., Slack, F., Martindale, M.Q., Kuroda, M.I., Maller, B., et al. (2000). Conservation of the sequence and temporal expression of let-7 heterochronic regulatory RNA. *Nature* 408, 86-89.

Pereira-Manfro, W.F., Ribeiro-Gomes, F.L., Filardy, A.A., Vellozo, N.S., Guillermo, L.V., Silva, E.M., et al. (2014). Inhibition of caspase-8 activity promotes protective Th1- and Th2-mediated immunity to *Leishmania major* infection. *J Leukoc Biol* 95, 347-355.

Reinhart, B.J., Slack, F.J., Basson, M., Pasquinelli, A.E., Bettinger, J.C., Rougvie, A.E., et al. (2000). The 21-nucleotide let-7 RNA regulates developmental timing in *Caenorhabditis elegans*. *Nature* 403, 901-906.

Roh, Y.S., Song, J., and Seki, E. (2014). TAK1 regulates hepatic cell survival and carcinogenesis. *J Gastroenterol* 49, 185-194.

Schwarz, D.S., Hutvagner, G., Du, T., Xu, Z., Aronin, N., and Zamore, P.D. (2003). Asymmetry in the assembly of the RNAi enzyme complex. *Cell* 115, 199-208.

Shen, W., Gao, Y., Lu, B., Zhang, Q., Hu, Y., and Chen, Y. (2014). Negatively regulating TLR4/NF-kappaB signaling via PPARalpha in endotoxin-induced uveitis. *Biochim Biophys Acta* 1842, 1109-1120.

Singh, A.K., Pandey, R.K., Shaha, C., and Madhubala, R. (2016). MicroRNA expression profiling of *Leishmania donovani*-infected host cells uncovers the regulatory role of MIR30A-3p in host autophagy. *Autophagy* 12, 1817-1831.

- Srivastava, A., Singh, N., Mishra, M., Kumar, V., Gour, J.K., Bajpai, S., et al. (2012). Identification of TLR inducing Th1-responsive *Leishmania donovani* amastigote-specific antigens. *Mol Cell Biochem* 359, 359-368.
- Swaminathan, S., Suzuki, K., Seddiki, N., Kaplan, W., Cowley, M.J., Hood, C.L., et al. (2012). Differential regulation of the Let-7 family of microRNAs in CD4⁺ T cells alters IL-10 expression. *J Immunol* 188, 6238-6246.
- Takeda, K., Kaisho, T., and Akira, S. (2003). Toll-like receptors. *Annu Rev Immunol* 21, 335-376.
- Tuon, F.F., Amato, V.S., Bacha, H.A., Almusawi, T., Duarte, M.I., and Amato Neto, V. (2008). Toll-like receptors and leishmaniasis. *Infect Immun* 76, 866-872.
- Uematsu, S., and Akira, S. (2006). Toll-like receptors and innate immunity. *J Mol Med (Berl)* 84, 712-725.
- Vargas-Inchaustegui, D.A., Tai, W., Xin, L., Hogg, A.E., Corry, D.B., and Soong, L. (2009). Distinct roles for MyD88 and Toll-like receptor 2 during *Leishmania braziliensis* infection in mice. *Infect Immun* 77, 2948-2956.
- Vaucheret, H., Vazquez, F., Crete, P., and Bartel, D.P. (2004). The action of ARGONAUTE1 in the miRNA pathway and its regulation by the miRNA pathway are crucial for plant development. *Genes Dev* 18, 1187-1197.
- Vieira, L.Q., Goldschmidt, M., Nashleanas, M., Pfeffer, K., Mak, T., and Scott, P. (1996). Mice lacking the TNF receptor p55 fail to resolve lesions caused by infection with *Leishmania major*, but control parasite replication. *J Immunol* 157, 827-835.
- Wanasen, N., and Soong, L. (2008). L-arginine metabolism and its impact on host immunity against *Leishmania* infection. *Immunol Res* 41, 15-25.
- Wang, B., Li, S., Qi, H.H., Chowdhury, D., Shi, Y., and Novina, C.D. (2009). Distinct passenger strand and mRNA cleavage activities of human Argonaute proteins. *Nat Struct Mol Biol* 16, 1259-1266.
- Wei, X.Q., Charles, I.G., Smith, A., Ure, J., Feng, G.J., Huang, F.P., et al. (1995). Altered immune responses in mice lacking inducible nitric oxide synthase. *Nature* 375, 408-411.
- Whitaker, S.M., Colmenares, M., Pestana, K.G., and McMahon-Pratt, D. (2008). *Leishmania pifanoi* proteoglycolipid complex P8 induces macrophage cytokine production through Toll-like receptor 4. *Infect Immun* 76, 2149-2156.
- Wilhelm, P., Ritter, U., Labbow, S., Donhauser, N., Rollinghoff, M., Bogdan, C., et al. (2001). Rapidly fatal leishmaniasis in resistant C57BL/6 mice lacking TNF. *J Immunol* 166, 4012-4019.
- Yang, Z., Mosser, D.M., and Zhang, X. (2007). Activation of the MAPK, ERK, following *Leishmania amazonensis* infection of macrophages. *J Immunol* 178, 1077-1085.

Capítulo 3.

Resposta inflamatória aguda contra *Leishmania amazonensis* leva à expressão de miRNAs reguladores da expressão de *Tnfa*

O texto apresentado a seguir foi publicado no periódico *Frontiers in Immunology*, em 29 de novembro de 2018, como parte da edição especial *Immune Evasion Mechanisms in the Pathogenesis of Trypanosomatid Infection*.

O artigo está no volume 9, artigo 2792 e contém 17 páginas.

O material está disponível *online* por meio do DOI [10.3389/fimmu.2018.02792](https://doi.org/10.3389/fimmu.2018.02792)

Autores: Stephanie Maia Acuña, Jonathan Miguel Zanatta, Camilla de Almeida Bento, Lucile Maria Floeter-Winter and Sandra Marcia Muxel

Título original:

miR-294 and miR-410 negatively regulate *Tnf*, arginine transporter *Cat1/2*, and *Nos2* mRNAs in murine macrophages infected with *Leishmania amazonensis*

Resumo

MicroRNAs são pequenas moléculas de RNA não codificante que modulam processos celulares por meio da regulação pós-transcricional de genes, incluindo genes envolvidos com a resposta imune. A mudança do perfil de miRNAs de macrófagos murinos infectados com *Leishmania amazonensis* podem alterar a resposta inflamatória e o metabolismo, como o metabolismo de L-arginina, sua disponibilidade e conversão em outros produtos, como o óxido nítrico pela Óxido Nítrico Sintase 2 (*Nos2*) ou ornitina (um precursor de poliaminas) pela Arginase 1 ou 2 (*Arg1/2*). O balanço entre as duas vias é parte da regulação de respostas microbicidas dos macrófagos. Este trabalho tem como objetivo avaliar a função de miR-294, miR-301b e miR-410 durante a infecção aguda de macrófagos derivados de medula óssea oriundos de camundongos C57BL/6 com *Leishmania amazonensis*. Observamos um aumento na expressão de miR-294 e miR-410, mas não de miR-301b. O mesmo comportamento não foi observado em macrófagos estimulados com LPS, um indutor de inflamação. Também observamos uma diminuição dos transcritos de genes-alvo desses miRNAs durante a infecção, como os transportadores de arginina *Cat1/Slc7a1*, *Cat2/Slc7a2* e *Nos2*, aumentados na estimulação com LPS. A inibição funcional de miR-294 levou a um aumento dos transcritos de *Cat2* e *Tnfa*, e uma desregulação nos níveis de *Nos2*; enquanto a inibição de miR-410 levou ao aumento de *Cat1*. A inibição de miR-294 reduziu a infectividade. Essas interações entre miRNA-mRNA dificultaram a infectividade. Esses dados sugerem que *L. amazonensis* induz mudanças no perfil inflamatório de macrófagos, regulando miRNAs e contribuindo para o resultado da infecção.

Abstract

MicroRNAs are small non-coding RNAs that regulate cellular processes by post-transcriptional regulation of gene expression, including immune responses. The shift in miRNA profiling of murine macrophages infected with *Leishmania amazonensis* can change the inflammatory response and metabolism. L-arginine availability and its conversion into nitric oxide by nitric oxide synthase 2 (*Nos2*) or ornithine (a polyamine precursor) by arginase 1/2 regulate macrophage microbicidal activity. This work aimed to evaluate the function of miR-294, miR-301b, and miR-410 during C57BL/6 bone marrow-derived macrophage early infection with *L. amazonensis*. We observed an upregulation of miR-294 and miR-410 at 4 h of infection, but the levels of miR-301b was not modified. This profile was not observed in LPS-stimulated macrophages. We also observed a decreased levels of those miRNAs target genes during infection, as Cationic amino acid transporters 1 (*Cat1/Slc7a1*), *Cat2/Slc7a2* and *Nos2*; genes upregulated in LPS stimuli. The functional inhibition of miR-294 led to upregulation of *Cat2* and *Tnfa* and dysregulation of *Nos2*, while miR-410 increased *Cat1* levels. miR-294 inhibition reduced infectivity. These miRNA–mRNA interactions hindered infectivity. These data suggest that *L. amazonensis* induces changes in macrophages' inflammatory profiles, regulating miRNAs and contributing to infection outcomes.

Introduction

MicroRNAs (miRNAs) are small non-coding RNAs with 18–25 nucleotides that mediate the post-transcriptional regulation of genes involved in physiological and pathological conditions, including the inflammatory response (BALTIMORE *et al.*, 2008; NEILL; SHEEDY; MCCOY, 2011). miRNAs are transcribed from intergenic, exonic, or intronic regions by the RNA polymerase II and processed into primary miRNA transcripts (pri-miRNA), and they subsequently enter the precursor (pre-miRNA) and mature form across a series of steps involving class 2 RNase III DROSHA and Dicer (LEUNG, 2015; MATHEW *et al.*, 2019). miRNAs recognize the complementary sequences in the 3' untranslated regions (3'UTR) of given transcripts, which cause their degradation or translational repression (LEUNG, 2015; MATHEW *et al.*, 2019). miRNA dysregulation occurs through various mechanisms, encompassing perturbations of miRNA transcription, epigenetic mechanisms, and disruption of the miRNA synthesis machinery (ACUÑA; FLOETER-WINTER; MUXEL, 2020a).

Different miRNA expressions display macrophage polarization during infection, affecting the macrophage activation and the polarization to classically characterized M1-pro-inflammatory or M2-anti-inflammatory/pro-resolution phenotype (LI, H. *et al.*, 2018a). The regulation of cytokine/chemokine production, such as by interferon-gamma (IFN- γ), tumor necrosis factor-alpha (TNF- α), and granulocyte-macrophage colony-stimulating factor (GM-CSF), as well as activation of Toll-like receptor (TLR), leads to macrophage differentiation into the M1 phenotype, which increases nitric oxide synthase 2 (NOS2) expression and NO production with microbicidal activity. Moreover, interleukin 4 (IL-4), IL-13, transforming growth factor-beta (TGF- β), IL-10, and macrophage colony-stimulating factor (M-CSF) differentiate macrophages into the M2 phenotype, expressing higher levels of arginase 1 (ARG1) and polyamine production (MARTINEZ, FERNANDO O.; HELMING; GORDON, 2009).

Leishmaniasis is a neglected tropical disease caused by the *Leishmania* parasite, which manifests through a broad range of clinical outcomes, from cutaneous to visceral disease, depending on the species that is infecting the host. *Leishmania amazonensis* causes a cutaneous disease (AKHOUNDI *et al.*, 2016; ASHFORD, 2000; BURZA; CROFT; BOELAERT, 2018a). The parasite switches between an invertebrate host (sand fly *Phlebotomus* or *Lutzomyia*) and vertebrate hosts, such as mammals, rodents, and humans. The infected sand fly regurgitates the promastigotes form of *Leishmania* during the bite, which are recognized and phagocytosed by resident macrophages and differentiate into the amastigotes form (GREGORY; OLIVIER, 2005; NATHAN; SHILOH, 2000; ROSSI; FASEL, 2018). *Leishmania* is dependent on the host's L-arginine metabolism for polyamines to proliferate and establish a successful infection (DA SILVA, MARIA FERNANDA LARANJEIRA *et al.*, 2012; MUXEL, SANDRA M; AOKI; *et al.*, 2018a; ROBERTS, SIGRID C *et al.*, 2004). However, the host's immune response also uses this amino acids to produce NO, leading to parasite clearance (WANASEN, NANCHAYA; SOONG, 2008b; YERAMIAN, ANDRÉE *et al.*, 2006). In this case, the amino acid used can indicate how macrophages polarize on the M1/M2 dichotomy (MUXEL, SANDRA M; AOKI; *et al.*, 2018a; SANS-FONS *et al.*, 2013). In this scenario, miRNAs can act as regulators of how the cells decide to use the amino acid.

Over the past two decades, the regulation of physiological and pathophysiological processes mediated by miRNAs has been widely studied, including in cancer studies and inflammatory and infectious diseases (ACUÑA; FLOETER-WINTER; MUXEL, 2020a; FU *et al.*, 2011; MANZANO-ROMÁN; SILES-LUCAS, 2012; PETRINI *et al.*, 2015; REYNOSO *et al.*, 2014). Our previous data revealed that the entrance of the parasite into the macrophages initiated the expression of miRNAs. The miR-294 was upregulated after 4 and 24 h of infection of BMDM from BALB/c mice (MUXEL, SANDRA MARCIA; LARANJEIRA-SILVA; ZAMPIERI; FLOETER-WINTER, 2017b). Additionally, the expression of that miRNA was inversely proportional to the expression of *Nos2*/NOS2, suggesting that they could be interacting with the *Nos2* 3' UTR. We demonstrated that these miRNAs can bind to the 3' UTR portion of the mRNA, and functional inhibition led to an overexpression of *Nos2*/NOS2 (MUXEL, SANDRA MARCIA; LARANJEIRA-SILVA;

ZAMPIERI; FLOETER-WINTER, 2017b), which plays a key role in the macrophage polarization and leading to susceptibility to the infection. Later, we demonstrated that the treatment of these macrophages with melatonin not only regulated the miR-294 expression but also *Nos2* and *Tnf* transcripts (MATHEW *et al.*, 2019). After that, we traced how the depletion of TLR-2, TLR-4, or MyD88 can affect the miRNA profile when C57BL/6J BMDM are infected with *L. amazonensis*, demonstrating that miR-294 expression is independent of these molecules (MUXEL, SANDRA MARCIA; ACUÑA; *et al.*, 2018a), suggesting a role in regulating pro-inflammatory signal and macrophage polarization, but its function was not explored in C57BL/6J, a resistant model for *L. amazonensis* infection *in vitro* and *in vivo* (REF).

In this study, we analyze how miR-294, and two other miRNAs: miR-301b and miR-410 can target *Nos2*, *Arg1*, *Odc1*, *Slc7a1*, *Slc7a2*, and *Tnf* mRNAs and regulate L-arginine metabolism related genes during *L. amazonensis* infection of C57BL/6 macrophage infection. Our findings revealed that *L. amazonensis* upregulated miR-294 and miR-410, but not miR-301b after 4h of infection. In other hand, the *Slc7a1* L-arginine transporter downregulated during the infection and *Nos2*, *Arg1*, *Odc1*, and *Slc7a2* was expressed at similar levels of uninfected macrophages. In addition, miR-294 inhibition upregulated *Slc7a2* and *Tnfa*, and dysregulation of *Nos2*, while miR-410 upregulated *Slc7a1*, reducing infectivity, open a new perspective to study the impact of miR-294 in the modulation of M1/M2 balance. Once LPS stimulation presented a distinct profile, with reduced levels of miRNAs and increased levels of *Nos2*, *Arg1*, *Slc7a1*, *Odc1*, *Arg2*, *Slc7a2*, and *Tnf*.

Materials and Methods

In silico miRNA binding site prediction

The interaction between miRNAs and mRNAs was assessed using the miRMap search tool (). All searches were made setting *Mus musculus* as the specie parameter, using a combination of open $\Delta G > 9$ (mRNA opening free energy), exact probability > 60 (exact distribution of site over-representation probability) and miRmap score > 60 , using Vienna-RNA algorithm (REF).

Parasite Culture

Leishmania amazonensis (MHOM/BR/1973/M2269) promastigotes were cultivated at 25 °C in M199 culture media (Invitrogen, Grand Island, NY, USA), supplemented with 10% heat-inactivated FBS (Invitrogen), 5 ppm hemin, 100 μM adenine, 50 U penicillin, 50 $\mu\text{g}/\text{mL}$ streptomycin (Invitrogen), 40 nM Hepes-NaOH buffer, and 12 mM NaHCO_3 , pH 6.85. The culture was split every 7 days with preset inoculum 1×10^6 cells per 10 mL, and maintained for up to five passages. Neubauer's chamber determined the number of cells, diluting 20 x the cell suspension in phosphate-buffered saline (PBS 1x) plus 1% formaldehyde.

BMDM harvesting and culture

C57BL/6. Tac animals were purchased from the Medicine School of the University of São Paulo at 6 to 8 weeks old. They were euthanized inside a CO_2 chamber. Afterward, bone marrow was extracted from the femurs, tibias, and humeri by flushing with ice-cold PBS 1 x with a 24 G x 3/4 needle. The cell suspension was separated with a 21 G x 1/2 needle, followed by centrifugation at 4 °C, 500 x g, for 10 minutes. The cells were resuspended in complete RPMI 1640 (LGC Biotechnologies, São Paulo, Brazil) supplemented with 10% heat-inactivated FBS (Gibco, South America), 0.5% Pen/Strep (1 U/mL), 2-mercaptoethanol (50 μM), L-glutamine (2 mM), sodium pyruvate (1 mM), and 10% L9-29 supernatant as a source of Macrophage Colony-Stimulating Factor (M-CSF). The cells were cultivated for 7 days at 34 °C, in 5% CO_2 .

Macrophage infection

After the macrophage differentiation, cells were seeded into 24-well plates (1×10^6 cells/well; SPL, Lifescience, Pocheon, Korea) or 8-well chamber slides (5×10^4 cells/well; Millipore, Merck, Darmstadt, Germany). Then, stationary phase promastigotes were added into the wells at MOI 5:1. After 4 h, the cells were washed two times with PBS 1x at room temperature to clean the unphagocytosed parasites. The culture was maintained for 4 and 24 h. The cells were stimulated with LPS (100 ng/mL; Escherichia coli LPS serotype 0127:B8, Sigma-Aldrich, St Louis, MO) to induce M1-inflammatory macrophages.

Infection assessment

After 4 and 24 h of infection, the chamber slides were washed two times with PBS 1x and then fixed with acetone/methanol (1:1 v/v; Sigma-Aldrich, St Louis, MO) and incubated at -20 °C for 24 h, followed by Giemsa staining (Fast Panoptic Kit, Laborclin, São Paulo). At least 600 macrophages were counted per well to achieve the parameters of Macrophage Infection Rate [(infected macrophage/total macrophage)*100], amastigotes per infected macrophage, and the infection index, calculated by multiplying the rate of infected macrophages by the average number of amastigotes per macrophage.

RNA extraction and cDNA preparation

For RNA extraction, macrophages (3×10^6) were mixed with 750 μL of Trizol (Ambion, Thermo Scientific) and 250 μL PBS 1x. Then, chloroform was added to separate the aqueous and organic phases. Following the manufacturer's instructions, the aqueous phase was added into miRNeasy (Qiagen, Hilden, Germany) columns. The extracted RNA was measured using Nanodrop (ND-100, Thermo Scientific) to reach a 200 ng/ μL RNA solution. The total RNA

was used to produce complementary DNA (cDNA) of mature mRNA and miRNA. For miRNA, we used the miScript II RT kit (Qiagen, Hilden, Germany), following the manufacturer's recommendations, starting from 250 ng of RNA. To mature the mRNA, starting from 2 µg of RNA, we used random hexamer primer (1.5 µg/mL; Thermo Scientific), dNTP (10 µM; Fermentas, Thermo Scientific), RevertAid Reverse Transcriptase (200U; Thermo Scientific), and RiboLock (Thermo Scientific), to a final volume of 40 µL. The cycling protocol was used following the manufacturer's recommendations. All cycles were undertaken using Mastercycler Nexus Gradient (Eppendorf, Hamburg, Germany).

Transcript quantification

A quantitative PCR was used to assess the amount of mRNA, using LuminoCt SYBR Green qPCR Ready Mix (Sigma-Aldrich), specific primers (0.1 µM), and a cDNA sample (5 µL, 100-times diluted), to a final volume of 10 µL. The reaction was performed in the QuantStudio Thermocycler (Thermo Scientific), following the following protocol: 94 °C to the initial denaturation, 40 cycles of denaturation (94 °C, 30 s), annealing and extension (60 °C, 30s), and fluorescence capture at the end of every cycle. After 40 cycles, a melting curve was found between 60 °C and 95 °C, with fluorescence registers at every 0.5 °C. The used primers are listed in the table below. The fold-change was calculated using the Delta–Delta Ct ($\Delta\Delta Ct$) method, based on β -2-microglobulin and normalized with the uninfected group or negative control. The fold-change was presented in log₂.

Target gene		Primer (5'-3')
Nitric Oxide Synthase (<i>Nos2</i>)	Forward	5'-agagccacagtctctctttgc-3'
	Reverse	5'-gctctcttccaaggtgctt-3'
Arginase 1 (<i>Arg1</i>)	Forward	5'-agcactgaggaagctggtc-3'
	Reverse	5'-cagaccgtgggttctcaca-3'
Arginase 2 (<i>Arg2</i>)	Forward	5'-tctctccacggcaaattc-3'
	Reverse	5'-cactctagcttcttctgccc-3'
Cationic amino acid transporter 1 (<i>Cat1/Slc7A1</i>)	Forward	5'-cgtaatgccactgtgacct-3'
	Reverse	5'-ggctgtaccgtaagaccaa-3'
Cationic amino acid transporter 2 (<i>Cat2/Slc7A2</i>)	Forward	5'-tccaaaacgaagacaccagt-3'
	Reverse	5'-gccatgaggggtccaataga-3'
Tumor Necrosis Factor alpha (<i>Tnf-α</i>)	Forward	5'-ccaccacgtcttctgtcta-3'
	Reverse	5'-agggtctgggcatagaact-3'
Ornithine decarboxylase (<i>Odc1</i>)	Forward	5'-ctgccagtaacggagtccag-3'
	Reverse	5'-tcagtggcaatccgtagaac-3'
β-2-microglobulin (<i>B2m</i>)	Forward	5'-cactgaattcaccctcactga-3'
	Reverse	5'-acagatggagcgtccagaaag-3'
Glyceraldehyde-3-Phosphate Dehydrogenase (<i>Gapdh</i>)	Forward	5'-ggcaattcaacggcacagt-3'
	Reverse	5'-ccttttggtccaccctca-3'

To assess the amount of miRNA, specific amplification of miR-294-3p, miR-301b-3p, miR-410-3p, and SNORD95A (used in normalization) was carried out by qPCR, performed with miScript SYBR Green (Qiagen), 10x miScript Universal Primer, 10x Specific Primer, and 2 μL of cDNA (diluted 10-fold). RNase-free water was added to a final volume of 10 μL. The reaction was performed in the QuantStudio Thermocycler (Thermo Scientific), with the following protocol: activation of the HotStart DNA Polymerase for 15 s at 95 °C and 40 cycles of 15 s at 94 °C, followed by 30 s at 55 °C and 30 s at 70 °C. The fold-change was calculated using the Delta–Delta Ct ($\Delta\Delta Ct$) method, based on SNORD95 and normalized with the uninfected group or negative control. The fold-change was presented in log₂.

miRNA inhibition

The miR-inhibition was performed by the addition of 50 nM of miR-294-3p, miR-301b-3p, miR-410-3p specific inhibitors (cat 4464084) or the negative control (cat 4464076) (miRVana, Ambion, Thermo Scientific), mixed with 6 μL FuGene Reagent Transfection (Roche, Promega, Madison, WI, USA) that was incubated for 20 min at room temperature, following our previously described protocol (MUXEL, SANDRA MARCIA; LARANJEIRA-SILVA; ZAMPIERI; AOKI; *et al.*, 2017) in 500 μL of serum-free RPMI 1640 medium (LGC Biotecnologia, São Paulo, SP, Brazil) (MUXEL, SANDRA MARCIA; LARANJEIRA-SILVA; ZAMPIERI; FLOETER-WINTER, 2017b). After 24 h of transfection, the cells were infected as described above.

Ethics Statement

The experimental protocol for the animal experiments was approved by the Comissão de Ética no Uso de Animais (CEUA) from the Instituto de Biociências of the Universidade de São Paulo (approval number CEUA-IB: IB-USP 233/2015). This study was carried out in strict accordance with the recommendations in the guide and policies for the care and use of laboratory animals of São Paulo State (Lei Estadual 11.977, de 25/08/2005) and the Brazilian government (Lei Federal 11.794, de 08/10/2008).

Results

MiR-294-3p, miR-301b-3p, and miR-410-3p target the L-arginine metabolic pathway

It is well-known that L-arginine metabolism contributes to macrophage polarization to the M1 or M2 phenotype. We have already demonstrated that infection with *L. amazonensis* promotes alterations to this scenario, leading to an M2-like phenotype of macrophages in the early step of infection (AOKI, JULIANA IDE *et al.*, 2020a). To understand the impact of miRNAs on L-arginine metabolism in C57BL/6 macrophages, we focused on the analysis of transcript levels of two arginine transporters (*Slc7a1* and *Slc7a2* – Cationic Amino Acids 1 and 2, respectively), Arginases 1 and 2 (*Arg1* and *Arg2*), Nitric Oxide Synthase 2 (*Nos2*), and Ornithine Decarboxylase 1 (*Odc1*). Together, these genes are involved in the uptake and first step of arginine metabolism, to produce NO or polyamine biosynthesis (Figure 1).

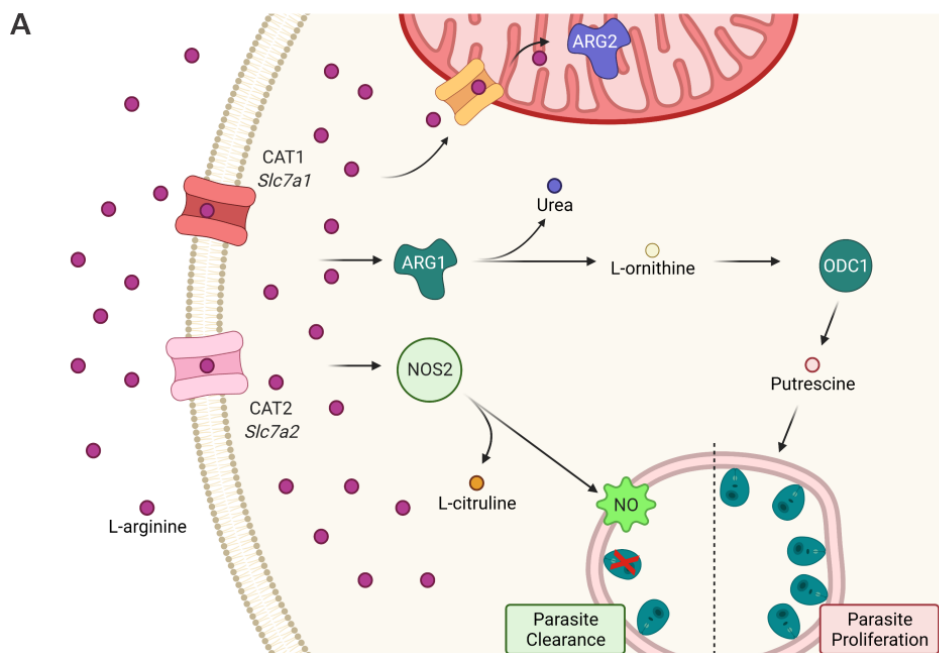


Figure 17. MicroRNAs can regulate the inflammatory branch of L-arginine uptake and consumption of infected macrophages with *Leishmania amazonensis*. (A) The way that cells use L-arginine is one of the markers of macrophage polarization into the M1 or M2 phenotypes. During infection with *L. amazonensis*, macrophages obtain L-arginine via Cationic Amino Acid Transporters 1 and 2 (CAT1 and CAT2, encoded by the Solute Carrier Transporter family members *Slc7a1* and *Slc7a2*). Once inside, the amino acid can be used by Nitric Oxide Synthase 2 (NOS2) to produce the NO free radical, which kills the parasite when at high levels. L-citrulline is a side product of this reaction. Another use of L-arginine is its metabolism into urea and L-ornithine via Arginase 1 (ARG1). Once converted into L-ornithine, it starts the polyamine synthesis pathway, whose Ornithine Decarboxylase 1 (ODC1) is the first branch enzyme. It is accepted that polyamines promote *Leishmania* survival and proliferation. L-arginine can also be transported to the mitochondrion, where it is also converted to urea and L-ornithine. However, the effects of this mitochondrial L-ornithine production are still poorly understood in the inflammatory context. This panel was created using the BioRender App.

Using *in silico* analysis, we found miRNAs, such as miR-294-3p, miR-301b-3p, and miR-410-3p, binding onto the 3'UTR of those gene transcripts, indicating an intricate network of post-transcriptional gene regulation in L-arginine uptake by transporters and their metabolism, beyond just NO production, as we observed previously for miR-294-3p (MUXEL, SANDRA MARCIA; LARANJEIRA-SILVA; ZAMPIERI; FLOETER-WINTER, 2017b). Focusing on the inflammatory branch of this pathway, we showed in Figure 2A-C the predicted binding sites of miR-294-3p, miR-301b-3p, and miR-410-3p.

Despite the binding capacity at the *Nos2* 3'UTR, miR-294-3p can also bind to both the *Slc7a1* and *Slc7a2* transporter 3'UTRs, as shown in Figure 2A. On the other hand, miR-301b can bind to the *Nos2* and *Arg2* 3'UTR (Fig 2B). miR-410-3p can bind to the 3'UTR of *Slc7a1* and *Nos2* (Fig 1C). Based on experimentally validated and predictive evidence found through *in silico* analysis, we hypothesized that miR-294, miR-301b, and miR-410 could modulate gene expression and infection control in the early phase of *in vitro* infection. Furthermore, miR-294 can be a pivotal element in the regulation of this balance by binding in the *Nos2* mRNA-3'UTR and regulates NOS2 protein expression and NO production. Predictive analysis of mRNA-3'UTR of *Nos-2*, *Arg2*, *Slc7a1* and *Slc7a2* showed a putative binding of miR-301b and also miR-410 can bind to *Nos2*.

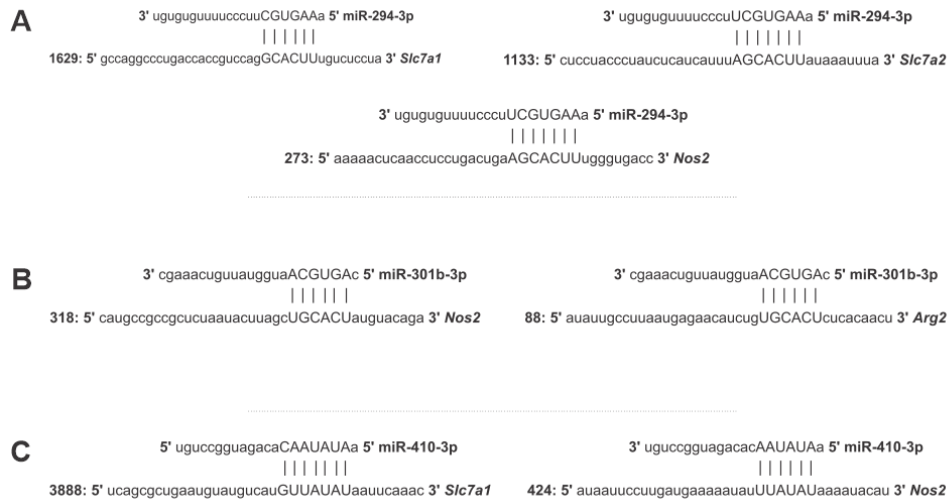


Figure 18. *In silico* microRNA binding prediction in the 3'UTR region of genes involved in L-arginine metabolism. The search for prediction of miRNA target repression of genes *Nos2*, *Slc7a1*, *Slc7a2* and *Arg2* using miRmap (<https://mirmap.ezlab.org/>) (REF), selecting the *Mus musculus* specie, mRNAs and setting the combination of DG open > 9 (mRNA opening free energy), probability exact > 60 (exact distribution of site over-representation probability) and miRmap score > 60 and identified the binding of (A) miR-294-3p. (B) miR-301b-3p and (C) miR-410-3p.

Expression of L-arginine metabolic pathway and miR-294-3p, miR-301b-3p, and miR-410-3p

To understand whether genes involved in L-arginine metabolism and miRNAs miR-294, miR-301b and miR-410 are expressed during the infection, we quantified the mRNA levels of genes involved in L-arginine metabolism and miRNAs in BMDM from B6 mice infected with *L. amazonensis*, compared to LPS, a well-known M1 inducer (Fig 3).

The *L. amazonensis* infection of macrophages decreased the number of *Slc7a1* transcripts after 4 h of infection, and the decreased values were sustained at 24 h, although they were slightly higher than at 4 h compared to uninfected macrophages (Fig 3A). In addition, the LPS stimulation also decreased the transcript amount after 4 h, but it was augmented after 24 h compared to uninfected and infected macrophages. We analyzed whether the *Slc7a2* transporter was regulated, but we observed that it was not modulated during infection, remaining the same as in the uninfected control. However, LPS stimulation revealed that these macrophages respond to inflammatory stimuli, leading to increase in the transcript levels after 4 and 24 h of LPS stimulation (Fig 3B). The LPS promoted a similar increase of *Nos2* at both 4 h, but it was not modified during infection (Fig 3C).

It was expected that *Arg1* would decrease in order to support *Nos2* L-arginine consumption when receiving an inflammatory stimulus. We observed that LPS stimulation increased *Arg1* expression, not observed during infection (Fig 3D). However, the infection did not increase or decrease, showing a similar behavior to the arginine transporter (*Slc7a2*). The mitochondrial isoform of Arginase (*Arg2*) is also slightly regulated by infection with *L. amazonensis* at 4 h, and LPS stimulation at 4 and 24 h. Although even the inflammatory stimulus is a signal to

increase Arg2 transcription, the parasite signalization was not as high as the LPS in both tested periods (Fig 3E). Ornithine decarboxylase is the first enzyme committed to polyamine production from L-arginine metabolism. It was expected that if the inflammatory branch of the L-arginine metabolism pathway was not working, the anti-inflammatory one would be, increasing the polyamine production. However, we did not observe an increase in the *Odc1* transcription during infection (Fig 3F). Even in the LPS stimulation, it was increased after 4 h.

Regarding miRNA expression, we observed that the infection promoted an increase in the level of miR-294 after 4 h of infection, sustaining the same expression level at 24 h. Although LPS stimulation did not promote a modulation at 4-24 h (Fig 3G). The infection and LPS stimulation did not modulate the miR-301b levels (Fig 3H) significantly.

The infected macrophages showed an increase in the levels of miR-410, while LPS-stimulated ones showed a significant reduction at 4 h compared to infected individuals (Fig 3I). After 24 h, the infection led to sustained miR-410 expression. Infection led to a faster response in increasing miR-294, and miR-410, effect not observed in LPS stimulation, as a classical M1 activator that did not interfere with these miRNAs in the studied periods.

The microscopical quantification of infection showed similar levels of infected macrophages, number of amastigotes per infected macrophage, and infection index (Fig 3C), as previously shown by Muxel (MUXEL, SANDRA MARCIA; ACUÑA; *et al.*, 2018a).

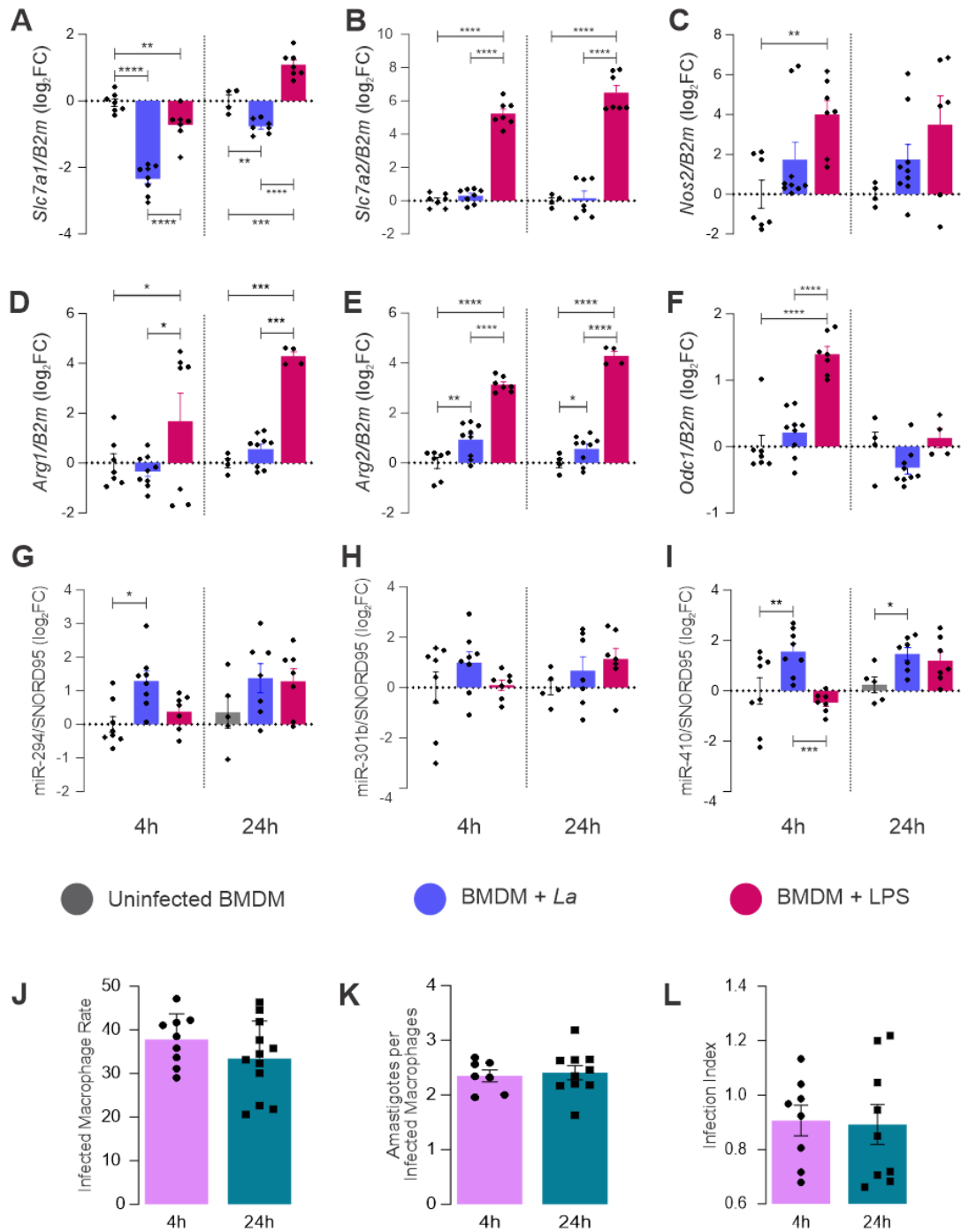


Figure 19. Quantification of L-arginine metabolism-related gene transcripts and miRNA levels on macrophages infected with *L. amazonensis*. Bone Marrow Derived-Macrophages were infected with stationary phase *L. amazonensis* promastigotes (MOI 1:5) or treated with LPS for 4 and 24 h. The total RNA was extracted and converted into cDNA to quantify transcripts of genes related to L-arginine metabolism through RT-qPCR: (a) *Slc7a1*. (b) *Slc7a2*. (c) *Nos2*. (d) *Arg1*. (e) *Arg2*. (f) *Odc1*. The miRNAs levels were assessed through RT-qPCR: (g) miR-294, (h) miR-301b (i), and miR-410. The infected BMDM were fixed and Giemsa stained to assess the number of total macrophages (n=600), infected macrophages and amastigotes. (j) infected macrophage rate [(infected macrophage/total macrophage) *100], (k) amastigotes per infected macrophage, and the product of infected macrophages rate with amastigotes per infected macrophage: (l) infection index (rate of infected macrophages multiplied by number of amastigotes per infected macrophage). Statistics: Each bar represents a total of n = 12 from three independent experiments. Mixed-effects analysis, post-hoc test: Sidak's multiple comparisons. *p*-values: *, *p*≤0.05. **, *p*≤0.001, ***, *p*≤0.0005. ****, *p*≤0.0001.

MiRNAs targeting mRNA from arginine metabolism shift the macrophage response to Leishmania

Based on miRNA binding site prediction and miRNA modulation during *L. amazonensis* infection, we performed a miRNA inhibition assay for the miR-294, miR-301b, and miR-410 sequences, in order to understand their functions in the infection context (Fig 4). The transfection with negative control was used as the baseline for evaluating the effect of the control and experimental miRNA inhibitor on the expression of miRNA and target-genes for all tested times. The miR-294 inhibitor led to a consistent decrease in the miRNA expression at 4 h of infection, which was sustained at 24 h. However, miR-301b did not respond to the inhibition at any tested time (Fig 4A). miR-410 tended to reduce its expression after 4 h of infection, but the inhibition did not decrease the miRNA amount significantly. However, miR-410 had a higher expression than the negative control after 24 h of infection (Fig 4A).

Since we chose miRNAs with the predicted binding site of the 3'UTR of the target genes *Nos2*, *Cat2/Slc7a2*, and *Cat1/Slc7a1*, and because the genes were increased in LPS stimulation but not during infection, it was expected that inhibition would increase the target mRNAs' expression. We observed this phenomenon in two of the tested target genes. Appear the tendency to increase the expression of *Nos2* at 4 h in the inhibition of miR-294 and miR-301b, Its was not significantly, and was reduced significantly at 24 h in miR-294-inhibition compared to the negative control (Fig 4B). miR-294 also targets *Slc7a2*. We monitored whether the infection would promote an increase in the number of transcripts of the transporter in miR-294 inhibition and found a significantly increased at 24 h of infection.

On the other hand, the arginine transporter variant *Slc7a1* is a target of miR-410, and miR410-inhibition increased the expression of *Slc7a1* at 4 h of infection, compared to negative control (Fig 4B).

Regarding the infectivity parameters (Fig 4C), we studied the inhibition of miR-294 compared to the negative control, but the negative control itself promoted a slight increase in the infected macrophage rate and the number of amastigotes per infected macrophage. The infection index was statistically significant when compared to untreated macrophages. On the other hand, treatment with the miR-294 inhibitor promoted a reduction in the number of amastigotes per infected macrophage, reducing the infectivity index at 4 and 24 h compared to the negative control.

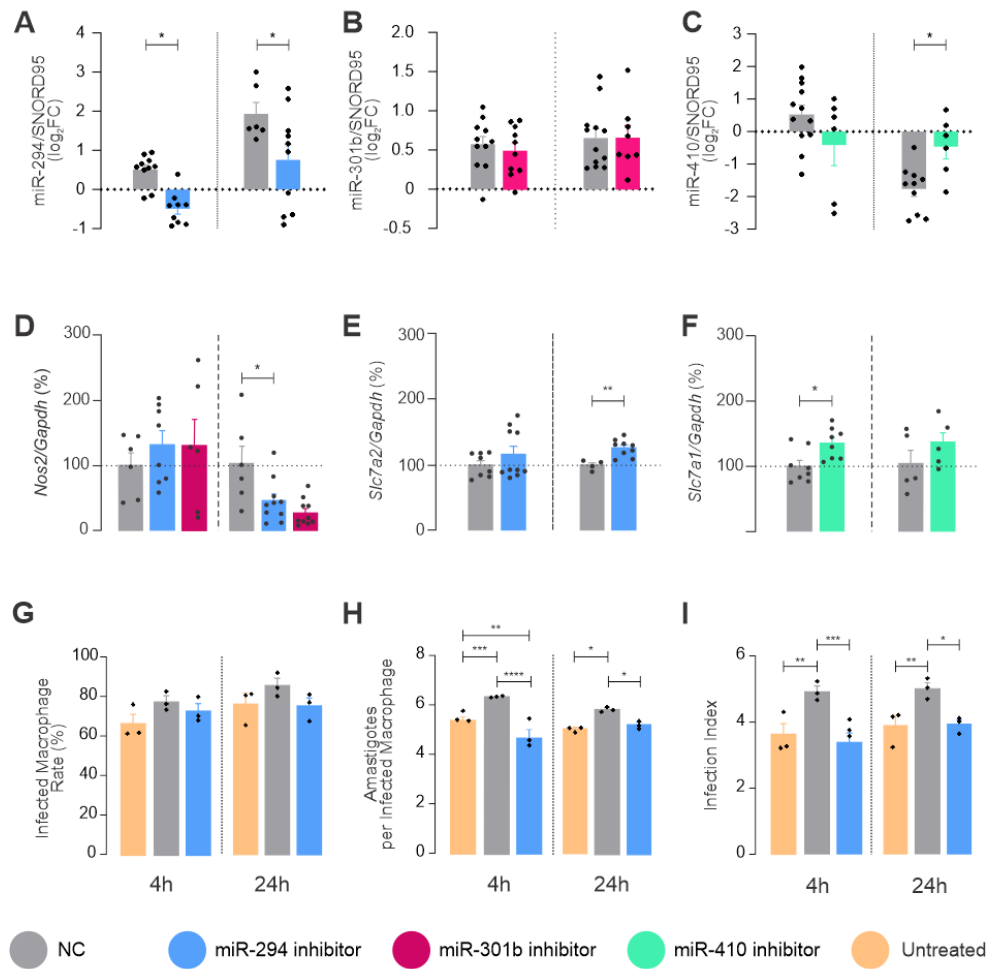


Figure 20. miRNA functional inhibition. Bone marrow derived macrophages were transiently transfected with specific miRNA inhibitors or negative control (NC), and then infected with *L. amazonensis* for 4 or 24 h. Total RNA was extracted to quantify miRNA levels: (a) miR-294, (b) miR-301b, and (c) miR-410. Or to assess the levels of mRNA targets after the inhibition: (d) *Nos2*, (e) *Slc7a2*, and (f) *Slc7a1*. The infected BMDM were fixed and giemsa stained to assess the number of total macrophages (n=300), infected macrophages and amastigotes. (j) infected macrophage rate [(infected macrophage/total macrophage) *100], (k) amastigotes per infected macrophage, and the product of infected macrophages rate with amastigotes per infected macrophage: (l) infection index. Statistics: Each bar represents a total of n = 3-12 from three independent experiments. Mixed-effects analysis, post-hoc test: Sidak's multiple comparisons. *p*-values: *, *p*≤0.05. **, *p*≤0.001, ***, *p*≤0.0005. ****, *p*≤0.0001.

MiR-294 and miR-301b can also interact with other inflammatory factors during macrophage infection with *L. amazonensis*.

Inflammatory stimuli can trigger some signaling cascades, the function of which is to regulate the response, positively and negatively. M1 macrophages produce TNF (tumor necrosis factor), an innate cytokine that promotes inflammatory responses. The prediction analysis showed a putative binding of miR-294 and miR-301 into the 3'UTR of *Tnfa* (Fig 5A).

Leishmania infection promoted *Tnfa* expression compared to uninfected macrophages, but at lower levels than LPS stimulation at 4 h (Fig 5B). However, after 24 h, the pathway seemed to be stopped, since the LPS group remained at the same level as the uninfected control (Fig 4B). We observed that miR-294 functional inhibition decreased the level of *Tnfa* at 4 h and increased it at 24 h of infection compared to the negative control (Fig 5C). However, miR-301b inhibition decreased the *Tnfa* levels only at 24 h compared to miR-294-inhibition.

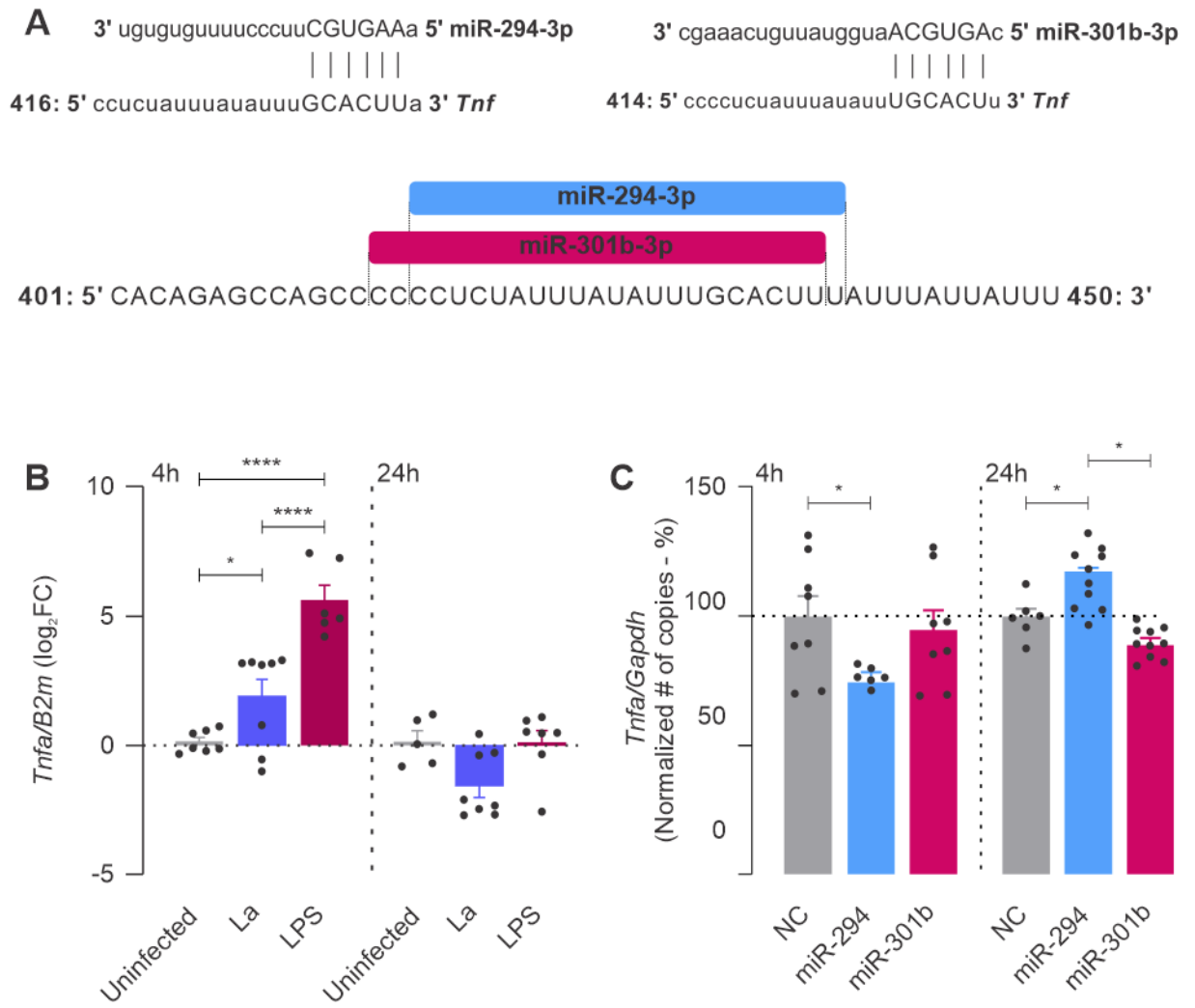


Figure 21. *Tnfa* is an miR-294 and miR-301b target. (a) In silico binding site prediction of miR-294 and miR-301b in the *Tnfa* 3'UTR. (b) Basal levels of *Tnfa* after *L. amazonensis* infection or LPS stimulation. (c) Quantification of the infection's ability to produce *Tnfa* after miRNA inhibition. Statistics: Each bar represents a total of n = 3-9 from three independent experiments. Mixed-effects analysis, post-hoc test: Sidak's multiple comparisons. *p*-values: *, *p*≤0.05. **, *p*≤0.001, ***, *p*≤0.0005. ****, *p*≤0.0001.

Discussion

Macrophages need to control their recognition processes and signaling cascade to promote an adequate immune response against pathogens (GUERFALI *et al.*, 2008). miRNAs can act as powerful tools for this. Some microorganisms can subvert the profile state or the induction of the microbicidal activity of immune cells, as observed in cancers, inflammatory disorders, and infectious diseases caused by viruses, bacteria, fungi, and parasites (ACUÑA; FLOETER-WINTER; MUXEL, 2020a; FU *et al.*, 2011; MANZANO-ROMÁN; SILES-LUCAS, 2012; REYNOSO *et al.*, 2014).

The involvement of *Leishmania* factors impacting miRNAs and subverting macrophage responses, such as glycoprotein GP63 of *Leishmania donovani* targeting the host-Dicer1, results in the downregulation of miR-122 and increasing parasite burden in the mouse liver (GHOSH *et al.*, 2013b), which can globally affect the host-miRNAs and post-transcriptional regulation of gene expression. Indeed, *L. amazonensis*-arginase indirectly interferes with an increase of miR-294 and miR-721, targeting *Nos2* and NO production in BALB/c murine macrophages (MUXEL, SANDRA MARCIA; LARANJEIRA-SILVA; ZAMPIERI; FLOETER-WINTER, 2017b). Infection with *L. amazonensis* induces miR-30e and miR-302d, which regulate *Nos2* and NO levels, and miR-294 and miR-302d, which regulate *Tnf* levels, in BALB/c-BMDM (FERNANDES *et al.*, 2019a). *L. major*-infected human macrophages present with dysregulation of miRNAs and corresponding chemokine targets (LEMAIRE; MKANNEZ; GUERFALI; GUSTIN; ATTIA; SGHAIER; *et al.*, 2013). In *L. major* infection of human macrophages, hypoxia-inducible factor-1 (HIF-1 α) regulates miR-210 levels, linking HIF-1 α to susceptibility in other species, *L. donovani* and *L. amazonensis* (DEGROSSOLI *et al.*, 2007; KUMAR *et al.*, 2018a). miR-146a overexpression downregulates M1 markers such as *Tnf* and *Nos2*, increasing *Arg1* and IL-10 in *L. donovani*-infected BMDM (DAS; MUKHERJEE; ALI, 2021). let-7e interferes in TLR, NF κ B, IRF, and MAPK signalling in B6-BMDM infected with *L. amazonensis* (MUXEL, SANDRA MARCIA; ACUÑA; *et al.*, 2018a). However, the association between miRNAs and *Leishmania* diseases will be fully understood only once the genetic background is complete, along with an undersanding of the parasite species that could interfere in post-transcriptional regulation mediated by miRNAs.

Once the modulation of *Arg1* and *Nos2*, as well as *Tnf*, was implicated in the activation of the macrophage inflammatory response and control of the parasite infection (MARTINEZ, FERNANDO O.; HELMING; GORDON, 2009), we predicted that the interactions of miRNA would be focused on the genes involved or correlated to arginine metabolism, which is implicated in amino acid transport (*Cat1/Slc7a1* and *Cat2/Slc7a2*), polyamine production (*Arg1*, *Arg2*, and *Odc1*), and NO production (*Nos2*) (Fig 1). We found that miR-294-3p interacts with *Nos2* (as previously validated), and predicted the targets of *Cat1/Slc7a1* and *Cat2/Slc7a2*; miR-301b-3p can predict the targets of *Cat1/Slc7a1* and *Arg2*; and miR-410-3p can predict the targets *Cat1/Slc7a1* and *Nos2*. The analysis of the quantities of target genes and miRNAs in B6-macrophages infected with *L. amazonensis* showed lower *Cat1/Slc7a1*, *Cat2/Slc7a2*, *Nos2*, *Arg1*, and *Odc1*, and increased levels of miR-294-3p, miR-301b-3p, and miR-410-3p. miR-301b-3p and miR-410-3p are not modulated in BALB/c-macrophages infected with *L. amazonensis*, but *Cat1/Slc7a1*, *Cat2/Slc7a2*, and *Arg1* are expressed (MUXEL, SANDRA MARCIA; LARANJEIRA-SILVA; ZAMPIERI; FLOETER-WINTER, 2017b). Moreover, miR-294 comprises a miR-290-295 cluster and regulates the cell cycle during embryogenesis (HOUBAVIY; MURRAY, 2003; WANG, Y.; LIANG; LU, 2008). The miR-379/miR-410 gene cluster is a large genomic miRNA cluster involved in various aspects of neurodevelopment and neuronal maturation (WINTER, 2015).

The availability of arginine, a common substrate to ARG1 and NOS2, can regulate the levels of CAT1 and CAT2 transporters in the external plasmatic membrane and the parasitophorous vacuole (DARLYUK *et al.*, 2009; SANS-FONS *et al.*, 2013; WANASEN, NANCHAYA *et al.*, 2007b). This complex regulation in arginine uptake is one of the multiple factors involved in regulating production during *Leishmania* infection, through *Nos2* transcription, NOS2

translation, and the presence of the substrates and co-factors O₂, biopterin, NADPH, and others (NAGARKOTI *et al.*, 2019). As previously shown, the B6-macrophages increased *Nos2*, NOS2, and NO production only when miRNA let-7e was inhibited during *L. amazonensis* infection, reducing the infectivity (MUXEL, SANDRA MARCIA; ACUÑA; *et al.*, 2018a). The IL-1 β and TNF levels also induce NO production (LIMA-JUNIOR *et al.*, 2013b). Our group showed increased levels of arginine, citrulline, and polyamines inside the macrophages infected with *L. amazonensis* (MAMANI-HUANCA *et al.*, 2021a). This data increased the expectation of modulation of genes that can compete for arginine to produce polyamines, such as *Cats*, *Arg1*, *Arg2*, and *Odc1*. Although the levels of *Cat1/Slc7a1*, *Cat2/Slc7a2*, *Arg1*, and *Odc1* did not behave as expected during infection, increased levels of the *Arg2* transcript level were not reflected by the increased competition of cytoplasmic arginine with NOS2, because of its mitochondrial localization. Further, regulation of arginase 2 by miR-155 regulates the arginine availability in DCs, allowing t-cell activation (DUNAND-SAUTHIER *et al.*, 2014). IL-10 and *Arg2* synergy works to reprogrammed the immunometabolic response of macrophages in response to LPS, reducing the levels of succinate, HIF-1 α , and IL-1 β (DOWLING *et al.*, 2021a).

Interestingly, in LPS stimulation, we found an inversion of the phenomenon observed in infected macrophages, evidencing an increased level of the target genes *Cat1/Slc7a1*, *Cat2/Slc7a2*, *Nos2*, *Arg1*, *Arg2*, and *Odc1*, and reduced levels of the miRNAs miR-294-3p, miR-301b-3p, and miR-410-3p, excluding these miRNAs from the inflammatory phenotype of macrophages. LPS induces *Cat2*, *Arg1*, and *Nos2*-NO in macrophages, suppressing T cell proliferation by starvation of arginine and causing glycolysis dependence (DICHTL *et al.*, 2021). This fact guided us to study the functional inhibition of miRNA only in infected macrophages, to understand the miRNA impacts in B6-macrophages.

The reduction in the levels of miR-294, maintenance of miR-301b, and maintenance/reduction of miR-410 in the functional inhibition assay evidenced difficulty and variability in the efficiency in the quantification of miRNA during the inhibition assay, as observed previously in our studies and others (FERNANDES *et al.*, 2019a; MUXEL, SANDRA MARCIA; ACUÑA; *et al.*, 2018a; MUXEL, SANDRA MARCIA; LARANJEIRA-SILVA; ZAMPIERI; FLOETER-WINTER, 2017b; YE *et al.*, 2019). Nevertheless, the modulation of mRNA levels can help us study miRNA interactions during infection, considering the post-transcriptional and translational mechanisms of gene expression regulation which interfere with the mRNA and protein levels, and stability and cellular compartmentalization of proteins (ACUÑA; FLOETER-WINTER; MUXEL, 2020a). The functional inhibition of miR-294 and miR-410 increased the *Cat2/Slc7a2* and *Cat1/Slc7a1* transcripts, respectively, which implies the increase of protein translation and arginine uptake. Kishikawa *et al.* showed that miR-122 represses CAT1 and regulates arginine availability (KISHIKAWA *et al.*, 2015). miR-294 and miR-301b inhibition at 4 h of infection tended to increase *Nos2* levels, and reduce them at 24 h. The amastigote number and infectivity index reduced in inhibition of miR-294. Similarly, *Nos2* transcripts were maintained during inhibition of miR-294 in infected BALB/c-macrophages. Only the NOS2 protein levels increased in this condition (MUXEL, SANDRA MARCIA; LARANJEIRA-SILVA; ZAMPIERI; FLOETER-WINTER, 2017b).

The differential expression of miRNA, previously observed in B6-macrophages in the network regulation of signaling pathways mediated by TLR recognition, supports these ideas (MUXEL, SANDRA MARCIA; ACUÑA; *et al.*, 2018a). In a RAW 264.7 macrophage lineage model, the mimetics of miR-294 using mimics during LPS stimulation reduced the protein levels of TNF- α and IL-6 by miR-294 targeting TREM-1 (LIU *et al.*, 2014). We also showed that miR-294 inhibition increased *Tnfa* levels after 24 h in infected B6-macrophages. Indeed, miR-301b is associated with NF- κ B activity inhibiting p65 nuclear translocation in pancreatic Panc-1 and BxPC-3 cell lines, interfering with LPS signals and corroborating the involvement of these miRNAs in the regulation of inflammation (FUNAMIZU *et al.*, 2014), which is implicated in TNF and NOS2 expression. Intriguingly, miR-130b/miR-301b belongs to the same cluster family, sharing target genes and cell proliferation with prostate cancer (GREGOROVA; VYCHYTILOVA-

FALTEJSKOVA; SEVCIKOVA, 2021). miR-301b inhibition did not interfere in the *Tnfa* transcripts, even though miR-301b shares the same seed as *Tnf* 3'UTR with miR-294, as it probably acts in different way in the absence of miR-294.

Zuo et al. elegantly demonstrated the lower levels of miR-410-3p and increased predicted target TLR2 in LPS-induced sepsis in mice, where miR-410-3p overexpression mediated TLR2 inhibition, relieving mitochondrial dysfunction and chemokine production (ZUO *et al.*, 2020). miR-410 mimics also reduced IL6 and TNF levels in LPS-stimulated chondrocytes (PAN *et al.*, 2020).

Overall, the present study showed that *Leishmania* subverts the macrophage–miRNA profile, altering miR-294, miR-301b, and miR-410 expression and the transcripts of the target genes *Slc7a2*, *Slc7a1*, *Nos2*, and *Tnfa*, building a complex network of miRNAs–mRNAs modulated during recognition and activation of macrophages, leading to an infection outcome.

References

- ACUÑA, Stephanie Maia; FLOETER-WINTER, Lucile Maria; MUXEL, Sandra Marcia. MicroRNAs: Biological Regulators in Pathogen-Host Interactions. *Cells*, [S. l.], v. 9, n. 1, 2020. DOI: 10.3390/cells9010113.
- AKHOUNDI, Mohammad; KUHLS, Katrin; CANNET, Arnaud; VOTÝPKA, Jan; MARTY, Pierre; DELAUNAY, Pascal; SERENO, Denis. A Historical Overview of the Classification, Evolution, and Dispersion of Leishmania Parasites and Sandflies. *PLoS Neglected Tropical Diseases*, 2016. DOI: 10.1371/journal.pntd.0004349.
- AOKI, Juliana Ide; MUXEL, Sandra Marcia; LARANJEIRA-SILVA, Maria Fernanda; ZAMPIERI, Ricardo Andrade; MÜLLER, Karl Erik; NERLAND, Audun Helge; FLOETER-WINTER, Lucile Maria. Dual transcriptome analysis reveals differential gene expression modulation influenced by leishmania arginase and host genetic background. *Microbial Genomics*, [S. l.], v. 6, n. 9, p. 1–13, 2020. DOI: 10.1099/mgen.0.000427.
- ASHFORD, R. W. The leishmaniases as emerging and reemerging zoonoses. *Parasites and Vectors*, [S. l.], v. 3, n. 1, p. 1269–1281, 2000.
- BALTIMORE, David; BOLDIN, Mark P.; O'CONNELL, Ryan M.; RAO, Dinesh S.; TAGANOV, Konstantin D. MicroRNAs: New regulators of immune cell development and function. *Nature Immunology*, [S. l.], v. 9, n. 8, p. 839–845, 2008. DOI: 10.1038/ni.f.209.
- BURZA, Sakib; CROFT, Simon L.; BOELAERT, Marleen. Leishmaniasis. *The Lancet*, [S. l.], v. 392, n. 10151, p. 951–970, 2018. DOI: 10.1016/S0140-6736(18)31204-2.
- DA SILVA, Maria Fernanda Laranjeira; ZAMPIERI, Ricardo Andrade; MUXEL, Sandra M.; BEVERLEY, Stephen M.; FLOETER-WINTER, Lucile M. Leishmania amazonensis arginase compartmentalization in the glycosome is important for parasite infectivity. *PLoS ONE*, [S. l.], v. 7, n. 3, 2012. DOI: 10.1371/journal.pone.0034022.
- DARLYUK, Ilona; GOLDMAN, Adele; ROBERTS, Sigrid C.; ULLMAN, Buddy; RENTSCH, Doris; ZILBERSTEIN, Dan. Arginine Homeostasis and Transport in the Human Pathogen *Leishmania donovani* *. [S. l.], v. 284, n. 30, p. 19800–19807, 2009. DOI: 10.1074/jbc.M901066200.
- DAS, Sonali; MUKHERJEE, Sohritri; ALI, Nahid. Super enhancer-mediated transcription of miR146a-5p drives M2 polarization during *Leishmania donovani* infection. *PLoS Pathogens*, [S. l.], v. 17, n. 2, p. 1–27, 2021. DOI: 10.1371/JOURNAL.PPAT.1009343.
- DEGROSSOLI, Adriana; BOSETTO, Maira Cegatti; LIMA, Camila Bárbara Cantalupo; GIORGIO, Selma. Expression of hypoxia-inducible factor 1 α in mononuclear phagocytes infected with *Leishmania amazonensis*. *Immunology Letters*, [S. l.], v. 114, n. 2, p. 119–125, 2007. DOI: 10.1016/j.imlet.2007.09.009.
- DICHTL, Stefanie; LINDENTHAL, Laura; ZEITLER, Leonie; BEHNKE, Kristina; SCHLÖSSER, Daniela; STROBL, Birgit; SCHELLER, Jürgen; EL KASMI, Karim C.; MURRAY, Peter J. Lactate and IL6 define separable paths of inflammatory metabolic adaptation. *Science Advances*, [S. l.], v. 7, n. 26, p. 1–11, 2021. DOI: 10.1126/sciadv.abg3505.
- DOWLING, Jennifer K. et al. Mitochondrial arginase-2 is essential for IL-10 metabolic reprogramming of inflammatory macrophages. *Nature Communications*, [S. l.], v. 12, n. 1, p. 1–14, 2021. DOI: 10.1038/s41467-021-21617-2.
- DUNAND-SAUTHIER, Isabelle; IRLA, Magali; CARNESECCHI, Stéphanie; SEGUÍN-ESTÉVEZ, Queralt; VEJNAR, Charles E.; ZDOBNOV, Evgeny M.; SANTIAGO-RABER, Marie-Laure; REITH, Walter. Repression of Arginase-2 Expression in Dendritic Cells by MicroRNA-155 Is Critical for Promoting T Cell Proliferation. *The Journal of Immunology*, [S. l.], v. 193, n. 4, p. 1690–1700, 2014. DOI: 10.4049/jimmunol.1301913.

FERNANDES, Juliane Cristina Ribeiro; AOKI, Juliana Ide; MAIA ACUÑA, Stephanie; ZAMPIERI, Ricardo Andrade; MARKUS, Regina P.; FLOETER-WINTER, Lucile Maria; MUXEL, Sandra Marcia. Melatonin and *Leishmania amazonensis* Infection Altered miR-294, miR-30e, and miR-302d Impacting on Tnf, Mcp-1, and Nos2 Expression. *Frontiers in Cellular and Infection Microbiology*, [S. l.], v. 9, n. March, p. 1–15, 2019. DOI: 10.3389/fcimb.2019.00060.

FU, Yurong; YI, Zhengjun; WU, Xiaoyan; LI, Jianhua; XU, Fuliang. Circulating microRNAs in patients with active pulmonary tuberculosis. *Journal of Clinical Microbiology*, [S. l.], v. 49, n. 12, p. 4246–4251, 2011. DOI: 10.1128/JCM.05459-11.

FUNAMIZU, Naotake; LACY, Curtis Ray; PARPART, Sonya T.; TAKAI, Atsushi; HIYOSHI, Yukiharu; YANAGA, Katsuhiko. MicroRNA-301b promotes cell invasiveness through targeting TP63 in pancreatic carcinoma cells. *International Journal of Oncology*, [S. l.], v. 44, n. 3, p. 725–734, 2014. DOI: 10.3892/ijo.2014.2243.

GHOSH, June; BOSE, Mainak; ROY, Syamal; BHATTACHARYYA, Suvendra N. *Leishmania donovani* targets *dicer1* to downregulate miR-122, lower serum cholesterol, and facilitate murine liver infection. *Cell Host and Microbe*, [S. l.], v. 13, n. 3, p. 277–288, 2013. DOI: 10.1016/j.chom.2013.02.005.

GREGOROVA, Jana; VYCHYTILOVA-FALTEJSKOVA, Petra; SEVCIKOVA, Sabina. Epigenetic regulation of microRNA clusters and families during tumor development. *Cancers*, [S. l.], v. 13, n. 6, p. 1–45, 2021. DOI: 10.3390/cancers13061333.

GREGORY, D. J.; OLIVIER, M. Subversion of host cell signalling by the protozoan parasite *Leishmania*. *Parasitology*, [S. l.], v. 130, n. SUPPL. 1, 2005. DOI: 10.1017/S0031182005008139.

GUERFALI, Fatma Z. et al. Simultaneous gene expression profiling in human macrophages infected with *Leishmania major* parasites using SAGE. *BMC Genomics*, [S. l.], v. 9, n. i, p. 1–18, 2008. DOI: 10.1186/1471-2164-9-238.

HOUBAVIY, Hristo B.; MURRAY, Michael F. Embryonic Stem Cell-Specific MicroRNAs the regulation of development. In plants, miRNAs have. *Developmental Cell*, [S. l.], v. 5, p. 351–358, 2003.

KISHIKAWA, Takahiro et al. Decreased miR122 in hepatocellular carcinoma leads to chemoresistance with increased arginine. *Oncotarget*, [S. l.], v. 6, n. 10, p. 8339–8352, 2015. DOI: 10.18632/oncotarget.3234.

KUMAR, Vinod; KUMAR, Ajay; DAS, Sushmita; KUMAR, Ashish; ABHISHEK, Kumar; VERMA, Sudha; MANDAL, Abhishek; SINGH, Rakesh K.; DAS, Pradeep. *Leishmania donovani* activates hypoxia inducible factor-1 α and miR-210 for survival in macrophages by downregulation of NF- κ B mediated pro-inflammatory immune respons. *Frontiers in Microbiology*, [S. l.], v. 9, n. MAR, p. 1–14, 2018. DOI: 10.3389/fmicb.2018.00385.

LEUNG, Anthony K. L. The Whereabouts of microRNA Actions: Cytoplasm and Beyond. *Trends in Cell Biology*, [S. l.], v. 25, n. 10, p. 601–610, 2015. DOI: 10.1016/j.tcb.2015.07.005.

LI, Heng; JIANG, Ting; LI, Meng Qi; ZHENG, Xi Long; ZHAO, Guo Jun. Transcriptional regulation of macrophages polarization by microRNAs. *Frontiers in Immunology*, [S. l.], v. 9, n. MAY, p. 1–12, 2018. DOI: 10.3389/fimmu.2018.01175.

LIMA-JUNIOR, Djalma S. et al. Inflammasome-derived IL-1 β production induces nitric oxide-mediated resistance to *Leishmania*. *Nature Medicine*, [S. l.], v. 19, n. 7, p. 909–915, 2013. DOI: 10.1038/nm.3221.

LIU, Yijun; CAO, Dianqing; MO, Guixi; ZHANG, Liangqing. [Effects of microRNA-294 on inflammatory factor of sepsis by targeting triggering receptor expressed on myeloid cells-1]. *Zhonghua wei zhong bing ji jiu yi xue*, [S. l.], v. 26, n. 9, p. 661–5, 2014. DOI: 10.3760/cma.j.issn.2095-4352.2014.09.011.

MAMANI-HUANCA, Maricruz; MUXEL, Sandra Marcia; ACUÑA, Stephanie Maia; FLOETER-WINTER, Lucile Maria; BARBAS, Coral; LÓPEZ-GONZÁLVEZ, Ángeles. Metabolomic reprogramming of c57bl/6-macrophages during early infection with *L. Amazonensis*. *International Journal of Molecular Sciences*, [S. l.], v. 22, n. 13, 2021. DOI: 10.3390/ijms22136883.

MANZANO-ROMÁN, Raúl; SILES-LUCAS, Mar. MicroRNAs in parasitic diseases: Potential for diagnosis and targeting. *Molecular and Biochemical Parasitology*, [S. l.], v. 186, n. 2, p. 81–86, 2012. DOI: 10.1016/j.molbiopara.2012.10.001.

MARTINEZ, Fernando O.; HELMING, Laura; GORDON, Siamon. Alternative activation of macrophages: An immunologic functional perspective. *Annual Review of Immunology*, [S. l.], v. 27, p. 451–483, 2009. DOI: 10.1146/annurev.immunol.021908.132532.

MATHEW, Rebecca; MATTEI, Valentina; AL HASHMI, Muna; TOMEI, Sara. Updates on the Current Technologies for microRNA Profiling. *MicroRNA*, [S. l.], v. 9, n. 1, p. 17–24, 2019. DOI: 10.2174/2211536608666190628112722.

MUXEL, Sandra M.; AOKI, Juliana I.; FERNANDES, Juliane C. R.; LARANJEIRA-SILVA, Maria F.; ZAMPIERI, Ricardo A.; ACUÑA, Stephanie M.; MÜLLER, Karl E.; VANDERLINDE, Rubia H.; DAMATTA, Renato Augusto. Arginine and Polyamines Fate in *Leishmania* Infection. [S. l.], v. 8, n. January, p. 1–15, 2018. a. DOI: 10.3389/fmicb.2017.02682.

MUXEL, Sandra Marcia; ACUÑA, Stephanie Maia; AOKI, Juliana Ide; ZAMPIERI, Ricardo Andrade; FLOETER-WINTER, Lucile Maria. Toll-Like Receptor and miRNA-let-7e Expression Alter the Inflammatory Response in *Leishmania amazonensis*-Infected Macrophages. *Frontiers in Immunology*, [S. l.], v. 9, n. November, 2018. b. DOI: 10.3389/fimmu.2018.02792.

MUXEL, Sandra Marcia; LARANJEIRA-SILVA, Maria Fernanda; ZAMPIERI, Ricardo Andrade; FLOETER-WINTER, Lucile Maria. *Leishmania* (*Leishmania*) *amazonensis* induces macrophage miR-294 and miR-721 expression and modulates infection by targeting NOS2 and L-arginine metabolism. *Scientific Reports*, [S. l.], v. 7, n. February, p. 1–15, 2017. DOI: 10.1038/srep44141.

NAGARKOTI, Sheela; SADAF, Samreen; AWASTHI, Deepika; CHANDRA, Tulika; JAGAVELU, Kumaravelu; KUMAR, Sachin; DIKSHIT, Madhu. L-Arginine and tetrahydrobiopterin supported nitric oxide production is crucial for the microbicidal activity of neutrophils. *Free Radical Research*, [S. l.], v. 53, n. 3, p. 281–292, 2019. DOI: 10.1080/10715762.2019.1566605.

NATHAN, Carl; SHILOH, Michael U. Reactive oxygen and nitrogen intermediates in the relationship between mammalian hosts and microbial pathogens. *Proceedings of the National Academy of Sciences of the United States of America*, [S. l.], v. 97, n. 16, p. 8841–8848, 2000. DOI: 10.1073/pnas.97.16.8841.

NEILL, Luke a O.; SHEEDY, Frederick J.; MCCOY, Claire E. MicroRNAs: the fine-tuners of Toll-like receptor signalling. *Nature reviews imm*, [S. l.], v. 268, n. February, p. 262–268, 2011. DOI: 10.1038/nri29.

PAN, Hong; DAI, Huming; WANG, Linzhi; LIN, Silong; TAO, Yuefeng; ZHENG, Yi; JIANG, Renyi; FANG, Fan; WU, Yifan. MicroRNA-410-3p modulates chondrocyte apoptosis and inflammation by targeting high mobility group box 1 (HMGB1) in an osteoarthritis mouse model. *BMC Musculoskeletal Disorders*, [S. l.], v. 21, n. 1, p. 1–12, 2020. DOI: 10.1186/s12891-020-03489-7.

PETRINI, E.; CAVIGLIA, G. P.; ABATE, M. L.; FAGOONEEE, S.; SMEDILE, A.; PELLICANO, R. MicroRNAs in HBV-related hepatocellular carcinoma: functions and potential clinical applications. [S. l.], v. 57, n. 4, p. 500–509, 2015.

REYNOSO, Rita et al. MicroRNAs differentially present in the plasma of HIV elite controllers reduce HIV infection in vitro. *Scientific Reports*, [S. l.], v. 4, p. 1–9, 2014. DOI: 10.1038/srep05915.

ROBERTS, Sigrid C.; TANCER, Michael J.; POLINSKY, Michelle R.; GIBSON, K. Michael; HEBY, Olle; ULLMAN, Buddy. Arginase Plays a Pivotal Role in Polyamine Precursor Metabolism in *Leishmania*. [S. l.], v. 279, n. 22, p. 23668–23678, 2004. DOI: 10.1074/jbc.M402042200.

ROSSI, Matteo; FASEL, Nicolas. How to master the host immune system? *Leishmania* parasites have the solutions! *International Immunology*, [S. l.], v. 30, n. 3, p. 103–111, 2018. DOI: 10.1093/intimm/dxx075.

SANS-FONS, M. Gloria; YERAMIAN, Andrée; PEREIRA-LOPES, Selma; SANTAMARÍA-BABI, Luis F.; MODOLELL, Manuel; LLOBERAS, Jorge; CELADA, Antonio. Arginine transport is impaired in C57Bl/6 mouse macrophages as a result of a deletion in the promoter of *Slc7a2* (*CAT2*), and susceptibility to *Leishmania* infection is reduced. *Journal of Infectious Diseases*, [S. l.], v. 207, n. 11, p. 1684–1693, 2013. DOI: 10.1093/infdis/jit084.

WANASEN, Nanchaya; MACLEOD, Carol L.; ELLIES, Lesley G.; SOONG, Lynn. L-arginine and cationic amino acid transporter 2B regulate growth and survival of *Leishmania amazonensis* amastigotes in macrophages. *Infection and Immunity*, [S. l.], v. 75, n. 6, p. 2802–2810, 2007. DOI: 10.1128/IAI.00026-07.

WANASEN, Nanchaya; SOONG, Lynn. L-arginine metabolism and its impact on host immunity against *Leishmania* infection. *Immunologic Research*, [S. l.], v. 41, n. 1, p. 15–25, 2008. DOI: 10.1007/s12026-007-8012-y.

WANG, Y.; LIANG, Y.; LU, Qianjin. MicroRNA epigenetic alterations: Predicting biomarkers and therapeutic targets in human diseases. *Clinical Genetics*, [S. l.], v. 74, n. 4, p. 307–315, 2008. DOI: 10.1111/j.1399-0004.2008.01075.x.

WINTER, Jennifer. MicroRNAs of the mir379–410 cluster: New players in embryonic neurogenesis and regulators of neuronal function. *Neurogenesis*, [S. l.], v. 2, n. 1, 2015. DOI: 10.1080/23262133.2015.1004970.

YE, Jiawei; XU, Mingcheng; TIAN, X.; CAI, S.; ZENG, Su. Research advances in the detection of miRNA. *Journal of Pharmaceutical Analysis*, [S. l.], v. 9, n. 4, p. 217–226, 2019. DOI: 10.1016/j.jpha.2019.05.004.

YERAMIAN, Andrée et al. Macrophages require distinct arginine catabolism and transport systems for proliferation and for activation. *European Journal of Immunology*, [S. l.], v. 36, n. 6, p. 1516–1526, 2006. DOI: 10.1002/eji.200535694.

ZUO, Tongkun; TANG, Qing; ZHANG, Xiangcheng; SHANG, Futai. MicroRNA-410-3p Binds to TLR2 and Alleviates Myocardial Mitochondrial Dysfunction and Chemokine Production in LPS-Induced Sepsis. *Molecular Therapy - Nucleic Acids*, [S. l.], v. 22, n. 1, p. 273–284, 2020. DOI: 10.1016/j.omtn.2020.07.031.

Capítulo 4

Imunometabolismo da resposta de macrófagos infectados com *Leishmania amazonensis*

O texto apresentado a seguir foi publicado no periódico *Frontiers in Immunology*, em 29 de novembro de 2018, como parte da edição especial *Immune Evasion Mechanisms in the Pathogenesis of Trypanosomatid Infection*.

O artigo está no volume 9, artigo 2792 e contém 17 páginas.

O material está disponível *online* por meio do DOI [10.3389/fimmu.2018.02792](https://doi.org/10.3389/fimmu.2018.02792)

Autores: Maricruz Mamani-Huanca, Sandra Marcia Muxel, Stephanie Maia Acuña, Lucile Maria Floeter-Winter, Coral Barbas, Ángeles López-Gonzálvez

Título original:

Immunometabolism of macrophages in response to *Leishmania amazonensis* infection

Resumo

A sobrevivência de parasitas do gênero *Leishmania* no interior de macrófagos depende de fatores que levam aos parasitas à evasão da resposta imune durante a infecção. Neste contexto, a interface entre o parasita e as células do hospedeiro podem ser cruciais na compreensão de como o protozoário pode sobreviver por meio da reprogramação metabólica do hospedeiro. Neste trabalho, nós como objetivo analisar as redes metabólicas de macrófagos, oriundos de camundongos C57BL/6, infectados com *Leishmania amazonensis* selvagem (*La*-WT) ou nocaute para arginase (*La*-arg⁻). Para tal, usamos a Eletroforese Capilar-Espectrometria de Massas (CE-MS) não-direcionada para detecção do perfil metabólico de macrófagos infectados. Estes apresentaram mudanças específicas na quantidade de metabólitos quando infectados com *La*-WT ou *La*-arg⁻. A ausência da arginase do parasita promoveu mudanças no ciclo da ureia, metabolismo de glicina e serina, reciclagem de amônia, e metabolismo de arginina, prolina, aspartato, glutamato, espermidina, espermina, metil-histidina e glutatona em ambos hospedeiro e parasita. Já em macrófagos infectados com *La*-WT houve aumento de arginina, citrulina, glutamina, glutatona oxidada, S-adenosilmetionina, N-acetil-espermidina, tripanotona oxidada; enquanto reduziu os níveis gerais de tripanotona, em comparação com o não infectado. Em comparação entre os dois grupos infectados, a ausência da arginase do parasita provocou um aumento de arginina, ácido arginínico e citrulina; e reduziu os níveis de ornitina, putrescina, S-adenosilmetionina, ácido glutâmico, prolina, N-gama-glutamil-D-alanina, glutamil-arginina, tripanotona oxydade e reduzida. A ausência da arginase também provoca aumento na produção de NO, além de apresentar uma infectividade mais alta após 4h de infecção. Conclui-se que de acordo com os perfis metabólicos, a *L. amazonensis* promove alterações em macrófagos oriundos de C57BL/6, sendo elas: imunometabolismo, interferência da arginase do parasita no ciclo da ureia e nos metabolismos de glicina e glutatona, durante a interação aguda entre hospedeiro e parasita.

Abstract

Leishmania survival inside macrophages depends on factors that lead to the immune response evasion during the infection. In this context, the metabolic interface between parasite and host cells can be crucial to understanding how this parasite can survive inside host cells due to the reprogramming of the host's metabolic pathways. In this work, we aimed to analyze metabolic networks of C57BL/6 macrophages infected with *Leishmania amazonensis* wild type (*La*-WT) or arginase knocked out (*La*-arg⁻), using the untargeted Capillary Electrophoresis-Mass Spectrometry (CE-MS) approach to assess based metabolomic profile. Macrophages showed specific changes in metabolite abundance upon *Leishmania* infection and in the absence of parasite-arginase. The absence of *L. amazonensis*-arginase promoted regulation of both host and parasite urea cycle, glycine and serine metabolism, ammonia recycling, metabolism of arginine, proline, aspartate, glutamate, spermidine, spermine, methylhistidine, and glutathione metabolism. The increased L-arginine, L-citrulline, L-glutamine, oxidized glutathione, S-Adenosylmethionine, *N*-Acetylspermidine, oxidized trypanothione levels, and reduced trypanothione levels were observed in *La*-WT-infected C57BL/6-macrophage compared to uninfected. The absence of parasite arginase increased L-arginine, argininic acid, and citrulline levels and reduced ornithine, putrescine, S-adenosylmethionine, glutamic acid, proline, *N*-gamma-glutamyl-D-alanine, glutamyl-arginine, oxidized trypanothione, and reduced trypanothione when compared to *La*-WT infected macrophage. Also, the absence of parasite arginase leads to increased NO production levels and a higher infectivity rate at 4 hours of infection. In conclusion, metabolome fingerprint given an in-depth profile of the *Leishmania* infected C57BL/6-macrophage immune-metabolism and interference of parasite arginase on the metabolism of the urea cycle, glycine, and glutathione during host-pathogen interactions.

Introduction

Macrophages are a heterogeneous population of cells that can acquire distinct functional phenotypes in response to cytokines or microbial antigens, playing a critical role in innate and adaptive immune response (MARTINEZ, F O *et al.*, 2008; VOGEL *et al.*, 2014). Macrophages have a broad spectrum of functional phenotypes, classically represented by two extreme polarization, pro-inflammatory M1 macrophages presenting microbicidal activity and anti-inflammatory M2 macrophages in tissue repair, wound healing, and in response against parasitic infections (FILARDY *et al.*, 2010b). M1 macrophages are induced by recognition of microbial antigens, such as lipopolysaccharide (LPS) and lipophosphoglycan (LPG), via pattern recognition receptors (PRRs) as Toll-like receptors (TLRs) and by pro-inflammatory cytokines as interferon-gamma (IFN- γ) and tumor necrosis factor-alpha (TNF- α) (BOUCHER; MOALI; TENU, 1999; HRABAK *et al.*, 1996; MANTOVANI *et al.*, 2004). They can also be characterized by the expression of nitric oxide synthase 2 (NOS2) producing microbicidal agent nitric oxide (NO) from L-arginine. The production of this free radical blocks, in many parts, the oxidative phosphorylation (OXPHOS), leading to a glycolytic phenotype upon the ATP production (COVARRUBIAS; AKSOYLAR; HORNG, 2015a; VAN DEN BOSSCHE; BAARDMAN; DE WINTHER, 2015a; VERGADI *et al.*, 2017a). Also, the NOS2 activity is dependent on four co-factors, being the cytosolic NADPH, the very first one (RAFFERTY; MALECH, 1996). To support the NO production, M1 macrophages present a high flux through the pentose phosphate pathway (PPP), generating the NADPH necessary (BLAGIH; JONES, 2012a; JHA *et al.*, 2015a; KOO; GARG, 2019). They also show an increase in particular tricarboxylic cycle (TCA cycle) metabolites such as citrate, succinate, and itaconate (O'NEILL; KISHTON; RATHMELL, 2016b; TANNAHILL *et al.*, 2013b). Moreover, M2 macrophages express arginase-1 (ARG1) that uses arginine to increase ornithine, a substrate to polyamines production (putrescine, spermidine, and spermine). These molecules are used by cells to proliferate, synthesize collagen, and promote tissue remodeling (WANG, N.; LIANG; ZEN, 2014; WHYTE *et al.*, 2010). In a metabolic approach, M2 macrophages have enhanced OXPHOS and fatty acids oxidation (COVARRUBIAS; AKSOYLAR; HORNG, 2015b; VAN DEN BOSSCHE; BAARDMAN; DE WINTHER, 2015b; VERGADI *et al.*, 2017b); sometimes, they can appear foamy, being strongly related to the severity of atherosclerosis due to the accumulation of cholesterol (MILLS, 2012; MOORE; SHEEDY; FISHER, 2013).

A combination of stimuli usually determines macrophages phenotypes. They can recognize many pathogens such as *Leishmania amazonensis*, an intracellular parasite transmitted to mammals via the bite of a sand fly vector. The infection caused by this protozoan leads to tegumental leishmaniasis in humans (BURZA; CROFT; BOELAERT, 2018b; MURRAY, H. W. *et al.*, 2005). On the other hand, during the early phase of mice macrophage infection, the parasite promotes a modulation in host-gene expression, distinctly in BALB/c and C57BL/6, implicating in the metabolism of arginine and consequently implicating in M1/M2 macrophages balance during *in vitro* infection (AOKI, J I *et al.*, 2019; AOKI, J.I. *et al.*, 2019a; MUXEL, SANDRA MARCIA *et al.*, 2019a; MUXEL, S.M.; LARANJEIRA-SILVA; ZAMPIERI; FLOETER-WINTER, 2017c). BALB/c-macrophages are more susceptible to late *in vitro* infection than B6-macrophages, but infectivity in the early phase is similar (AOKI, J I

et al., 2019; AOKI, J.I.; MUXEL; ZAMPIERI; ACUÑA; *et al.*, 2017; MUXEL, S.M.; LARANJEIRA-SILVA; ZAMPIERI; FLOETER-WINTER, 2017b). Also, *in vivo* infections shows that BALB/c mice are susceptible to *L. amazonensis* infection, presenting severe cutaneous lesions, whereas B6 mice present a moderate lesion size(JI; SUN; SOONG, 2003; VELASQUEZ *et al.*, 2016).

The L-arginine metabolism balances the leishmanicidal activity on macrophages and parasite survival(BOITZ *et al.*, 2017; MUXEL, S.M.; AOKI; *et al.*, 2018c; RATH, M *et al.*, 2014; ROBERTS, S C *et al.*, 2004). *Leishmania* arginase enzyme is essential for parasite survival and infectivity(DA SILVA, M.F.L. *et al.*, 2012a). Promastigote forms of *L. amazonensis* knockout for arginase (*La-arg*⁻) regulates the gene expression and metabolites content to surpass the absence of the enzyme, increasing the proline and glutamate levels to supply ornithine and putrescine to parasite survival(AOKI, J.I.; MUXEL; ZAMPIERI; LARANJEIRA-SILVA; *et al.*, 2017b; CASTILHO-MARTINS *et al.*, 2015; DA SILVA, M.F.L. *et al.*, 2012b). Lower levels of ornithine and putrescine contrasting with higher arginine and citrulline levels are present promastigotes of *La-arg*⁻ compared to *L. amazonensis* wild-type (*La-WT*). The arginase from parasite competes to arginine inside the macrophage, interfering in gene expression and metabolism of host cells(MCCONVILLE, M J *et al.*, 2007; MCCONVILLE, MALCOLM J., 2016a). The modulation of arginine transporters can control the arginine availability on parasite and host cells (AOKI, J.I.; MUXEL; ZAMPIERI; ACUÑA; *et al.*, 2017; INIESTA, V; GOMEZ-NIETO; CORRALIZA, 2001; LARANJEIRA-SILVA *et al.*, 2015; THOMPSON *et al.*, 2008; WANASEN, N; SOONG, 2008).

The metabolome profile of BALB/c-macrophages indicates the L-arginine metabolism favoring the polyamines production(MUXEL, SANDRA MARCIA *et al.*, 2019a). Here, we explore the metabolome fingerprint of B6-macrophages infection during early infection with *L. amazonensis*, using untargeted Capillary Electrophoresis-Mass Spectrometry (CE-MS) approach. The *L. amazonensis* infection alters the mix of host and parasite metabolites from the urea cycle, glycine and serine metabolism, ammonia recycling, metabolism of arginine, proline, aspartate, glutamate, spermidine, histidine, and glutathione metabolism. The absence of parasite arginase implicates in the increased levels of arginine, NO, and polyamines production and reduced oxidization and reduction of glutathione and trypanothione, and the function of parasite arginase on macrophage metabolism.

Materials and Methods

Macrophage culture

C57BL/6 mice 6–8-week old female was obtained from the Animal Center of the Faculty of Medicine of the University of São Paulo and maintained in the Animal Center of the Department of Physiology at the Institute of Bioscience of the University of São Paulo.

Mice bones were harvested, cut at each end, and flushed with a 23-gauge needle (BD, USA), removing the bone marrow with cold PBS to generate bone marrow-derived macrophages (BMDMs). Then, the cells were collected by centrifugation at 500 x g for 10 min at 4 °C, and resuspended in RPMI 1640 medium (LCBiotecnologia, São LGC, SP, Brazil), supplemented with penicillin (100 U/ml) (Invitrogen), streptomycin (100 µg/ml) (Invitrogen), 5% heat-inactivated FBS (Invitrogen), and 10% FBS9 cell supernatant into Vented-cap Culture Flask 75 cm² (SPL Lifescience, Pocheon, Ko). The cells were submitted to differentiation for 7–8 days at 34 °C in an atmosphere of 5% CO₂. The macrophage differentiation was confirmed by phenotypic analysis using flow cytometry (FACScalibur-Becton Dickinson, San Jose, CA, USA, considering 95% F4/80⁺/CD11b⁺ cells, as previously described (MUXEL, SANDRA MARCIA *et al.*, 2019a).

Parasite culture

L. amazonensis (MHOM/BR/1973/M2269) wild type promastigotes (La-WT) were maintained in culture at 25 °C in M199 medium (Invitrogen, Grand Island, NY, USA supplemented with 10% heat-inactivated fetal bovine serum (Invitrogen), 5 mg/L hemin, 100 µM adenine, 100 U penicillin, 100 µg/mL streptomycin, 40 mM Hepes-NaOH, and 12 mM NaHCO₃, at pH 6.85, for a week-long culture at low passage (P1-5). *L. amazonensis* arginase knockout (La-arg⁻) promastigotes were maintained in the same conditions as previously described, with medium supplemented with 30 µg/mL hygromycin B, 30 µg/mL puromycin (Sigma, St. Louis, MO, USA and 50 µM putrescine (Sigma) (DA SILVA, M.F.L. *et al.*, 2012b).

In Vitro Macrophage Infections

The BMDMs were seeded into 24-well plates (SPL Lifescience, Pocheon, Korea) (5x10⁵/SPL) for infectivity and NO production analysis, or into 6-well plates (SSPL Lifescience, Pocheon, Korea) (5x10⁶/wel) for metabolite analysis. After 18 h of incubation at 34 °C in an atmosphere of 5% CO₂, BMDMs were infected with La-WT or La-arg⁻ promastigotes in the stationary growth phase (MOI 5:1). After 4 h of infection, non-phagocyte promastigotes were washed with fresh medium, and samples were collected for metabolite extraction or fixed for infectivity index determination. The uninfected macrophages were maintained in the same conditions.

Infectivity quantification

For infectivity analysis, before infection La-WT or La-arg⁻ promastigotes were labeled with 5 µM CFSE (Invitrogen) for 30 min and washed in RPMI supplemented as previously described. The infectivity was analyzed by Image Flow Cytometry (Amnis) after cell-fixation with 1 % paraformaldehyde (Merck, Darmstadt, Germany) for 20 min at 4 °C, followed by

PBS washing. Infectivity was analyzed in Spot Count wizard (ideas Software, Amnis), single gating cells, and CFSE⁺ population (infected macrophages) to count the number of amastigotes per infected/macrophage in at least 80000 macrophages in three independent experiments. The infection index was calculated by multiplying the macrophage infection rate by the mean number of amastigotes per macrophage.

NO quantification

For NO quantification, after 4 h of infection, macrophages were ungripped by incubation with 1mM EDTA in PBS 1X for 10 min at 34 °C and cell scraping on ice after add RPMI plus 10% FBS Cells were centrifuged (500 g, 10 min, 4 °C) FBS resuspended in 50 uL of 5 uM of DAF-FM. After 30 min of incubation, cells were washed and resuspended in cold PBS 1X. NO was quantified by image flow cytometry, gating the frequency of DAF-FM⁺ cell and the media MFI of DAF-FM

Metabolite Extraction

Pellets with 5xMFI uninfected or infected macrophages were resuspended in 350 µL of cold methanol/water (3:1, v:v) and 25 mg of glass beads (710–1180 µM, G1152, SigmaAldrich, Germany), followed by four cycles of frost/defrosting in a liquid N₂/37 °C bath. The cells were disrupted at 50 mHz for 10 min in TissueLyser LT (Qiagen, Germany). The samples were clarified by 15,700 x g for 10 min at 4 °C centrifugation, and the supernatant was collected and evaporated to dryness by SpeedVac SPD121P (Thermo Fisher Scientific, Waltham, MA.) at 35 °C for 2 h. After this, the solid residue was resuspended in 100 µL 0.1 M formic acid with 0.2 mM of methionine sulfone, homogenized for 15 min in a vortex, and centrifuged at 15,700 x g for 15 min at 4 °C. The 35 µL of supernatant was transferred to polypropylene vials (Agilent Techno Vials, Waldbronn, Germany) for analysis(MUXEL, SANDRA MARCIA *et al.*, 2019a). Quality-control (QQC samples were prepared by pooling equal volumes of QC samples and were analyzed along the analytical sequence to evaluate the instruments stability and performance during measurements.

CE-MS Metabolic Fingerprinting

The samples were analyzed by a capillary electrophoresis system (7100 Agilent Technologies) coupled to a time-of-flight mass spectrometer (6224 Agilent Technologies), equipped with an ESI sprayer G1607 from Agilent Technologies. The compound ESI was separated in a fused silica capillary (Agilent Technologies) with a total length of 100 cm and an internal diameter of 50 µm in normal polarity with a background electrolyte (BGE containing 1.0 mol.L⁻¹ formic acid solution in 10% methanol (v/v). New capillaries were pre-conditioned with a flush (950 mbars) of NaOH 1.0 mol.L⁻¹ for 30 min, followed by MilliQ water for 30 min and BGE for 30 min. Before each analysis, the capillaries were conditioned with BGE for 5 min. Samples were hydro-dynamically injected at 50 mbar for 50 s, and stacking was carried out, applying BGE at 100 mbar for 10 s. Metabolite separation occurred when a voltage of 30 kV with 25 mbar of internal pressure was applied. The observed current during the experiment under these conditions was 23 µA.

The sheath liquid flow composition was methanol/water 50:50 (v/v) with two reference standards, 121.0509 purine (C₅H₄N₄) and 922.0098 HP-0921 (C₁₈H₁₈O₆N₃P₃F₂₄), for mass

accuracy monitoring was supplied by ISO Pump 1200 from Agilent Technologies Santa Clara, CA, USA. After the separated sample compounds leave the capillary, a positively charged spray is formed by a flow of the sheath liquid (6 μ L min⁻¹), a nitrogen spraying pressure of 10 psi, and a capillary voltage of 3500 V. The spray is dried with a hot nitrogen flow of 10 mL min⁻¹ at 200 °C. All ions formed in the gaseous state are directed to the TOF-MS following the parameter voltages: fragmentor 125 V, skimmer 65V, octopole 750V. Data was collected in the positive ionization (+) mode of ESI, and ions between 70 and 1000 Da were acquired at a scan rate of 1.41 scans per second. All systems were controlled by Agilent MassHunter TOF data acquisition software version B.06.01 (Agilent Technologies Inc.).

CE-MS Data treatment

Data acquired after CE-MS analysis was processed using MassHunter Profinder (B.10.00, Agilent Technologies Santa Clara, CA, USA) to obtain a data matrix. The software first performed an alignment and correlation of all electropherograms migration time using a specific algorithm for CE. Then the software applies two consecutive algorithms to perform the deconvolution. First, it performs the extraction of the critical variables (compounds) and reduces the data by removing the unspecified information. A second algorithm improves the reliability of the search for data features. Find by Ion (FbI) algorithm performs a targeted extraction of specific features. The abundance of the molecule, mass accuracy, and migration time of each feature in all samples was finally obtained as matrix data. Data quality was ensured by excluding background noise and non-related ions, the characteristics present in the QC were maintained at 50 %. For missing values, the k-nearest neighbors (kNN) algorithm was applied. Data was re-filtered on relative standard deviation (RSD in the QC features were removed from all samples with an RSD 30%).

Statistical RSDlysis

We analyzed the data using multivariate analysis (MVA) and univariate statistics (UVA). A centroid scaling was used for MVA using SIMCA P+14.0.1MVAmetrics (Umea, Sweden). Unsupervised principal component analysis (PCA) was used to verify quality, detect outliers, and check sample patterns. A partial least squares discriminant analysis (PLS-DA) model and orthogonal OPLS-DA were carried out to discriminate variation between groups. Model aptitude and predictive ability were evaluated using the explained variance (R^2) and predicted variance (Q^2), respectively, provided by the software. For UVA, we used MATLAB R2015a software (Mathworks, Inc., Natick, USA), non-parametric 1-way ANOVA test (Kruskal-Wallis) was used to obtain the significant signals, followed by Benjamini-Hochberg post hoc correction (FDR false discovery rate) ($q=0.05$). Also, pairwise comparisons were obtained using the Mann-Whitney U-test. The level of statistical significance was established with a 95% confidence interval ($p<0.05$). Finally, the percentage change was calculated (%). For infectivity and NO production analysis, the differences were evaluated by Student T-test (GraphPad software).

Ethics Statement

The experimental protocol was approved by the Comissão de Ética no Uso de Animais (CEUA - approval number CEUA-IB: 314/2018)) from the Institute of Bioscience of the University of São Paulo. This study was carried out according to the recommendations in the guide and policies for the care and use of laboratory animals of the Brazilian government (Lei Federal 11.794, de 08/10/2008).

Results

The absence of parasite arginase modulates NO production in *Leishmania*-infected macrophages.

To compare the infectivity of La-WT or La-arg⁻ in C57BL/6 macrophages were infected for 4, 24, 48, and 72 h and the analysis of the frequency of infected macrophages, the number of amastigotes per infected macrophages, and index of infection (rate of infected macrophages multiplied by the number of amastigotes per infected macrophages) was performed in image flow cytometry. The frequency of infected macrophages was reduced in C57BL/6-La-arg⁻ (95.20%±0.19) compared to C57BL/6-La-WT (90.46%±0.60) at 4 h of infection, but the number of amastigotes per infected macrophages was increased in C57BL/6-La-arg⁻ (2.07±0.01) compared to C57Bl/6-La-WT (2.79±0.06) at 4 h of infection. Also, after 24 and 48 h of infection, the number of amastigotes per infected macrophages was higher in C57Bl/6-La-arg⁻ than C57BL/6-La-WT. Consequently, the index of infection was higher in C57BL/6-La-arg⁻ than to C57BL/6-La-WT at 4, 24, and 48 h of infection.

To evaluate the ability of C57BL/6 macrophages infected with *L. amazonensis* to produce NO and the impact of parasite arginase, macrophages uninfected and infected for 4 hours with *L. amazonensis* La-WT or La-arg⁻ were labeled with DAF-FM and analyzed the frequency of DAF-FM⁺ cells and (MFI in flow cytometry (Fig 1B). After 4 h, the frequency of cells producing NO and MFI in C57BL/6-La-WT was MFIreased 1.98-times and 1.35-times in relation to uninfected, respectively. Also, the MFIection with La-arg⁻ the frequency increased to 2.68-times and MFI 1.69-times in relation to uninfected. The frequency of cells producing NO was 1.35-times, and MFI was 1.25 high in C57BL/6-La-arg⁻ compared with C57BL/6-La-WT. These data indicated a differential regulation of NO-production during infection with *L. amazonensis*; parasite arginase influences NO production.

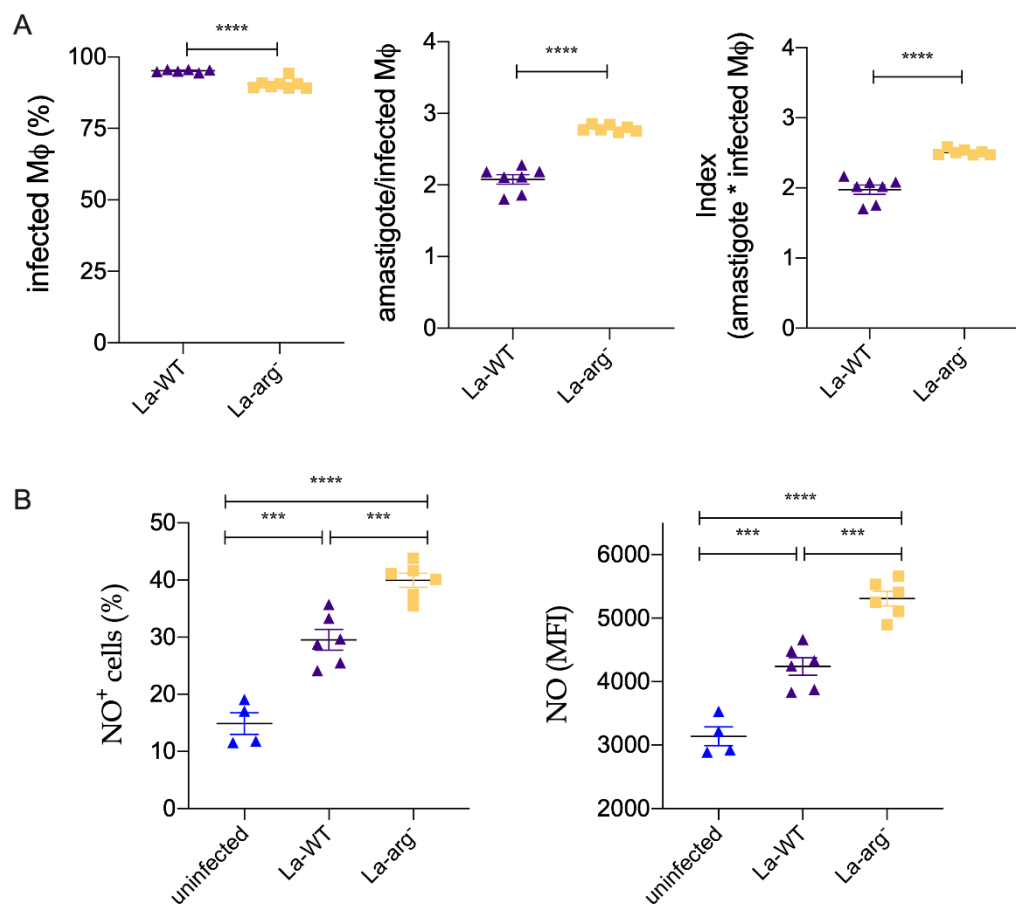


Figure 22. Infection index and NO production in C57BL/6 macrophages infected with *L. amazonensis* La-WT or La-arg. (A) C57BL/6-macrophages (5×10^5) were infected with CFSE-labelled *L. amazonensis* (MOI5:1) and collected after 4 h for analysis of infectivity by image flow cytometer, gating in the CFSE-internalized cells to count the frequency of infected macrophages (infected MØ), and spot count tool to determine the number of infected MØ; index of infection was calculated by multiplying the rate of infected MØ by the number of amastigotes per infected MØ. (B) C57BL/6-macrophages (5×10^5) were infected with *L. amazonensis* (MOI5:1), and after 4 h was labeled with 5 uM of DAF-FM for NO quantification in image flow cytometry, gating in DAF-FM+ cell quantify the frequency of NO producing cells (NO⁺ cells) and media of fluorescence intensity (MFI). Each point represents the individual values (n=6). (*) *p*-value < 0.05; (**) *p*-value < 0.01; (***) *p*-value < 0.001.

Statistical analyses of the metabolic profile of *Leishmania* infected C57BL/6-macrophages.

Three groups of samples from C57BL/6 macrophages infected with *L. amazonensis* (La-WT (n=9), C57BL/6 macrophages infected with *L. amazonensis* knockout for arginase (La-arg⁻) (n=10), and uninfected C57BL/6 macrophages (n=10) were used for the untargeted metabolomics CE-MS approach.

As a result of sample analysis and data processing, a total of 269 characteristics were obtained. The quality of the analysis was evaluated along with the experiment by observing the quality control (QC) clustering in the unsupervised PCA-X plot model (figure S2), where the data are entered without the previous information the group designation. PCA-X plot model showed $R^2 = 0.991$ indicating good sample quality. The model was also built to analyze PLS-DA discrimination. The clustering of the three different groups is observed, indicating that the metabolites' levels have changed due to the macrophages' infection. These differences were

evaluated by an OPLS-DA model, concerning the quality of the multivariate models obtained in all the models presented good quality presenting $R^2 \geq 0.957$ and $Q^2 \geq 0.947$ values (figure 2). Confidence intervals of Jack-Knife (not including 0), correlation p ($\text{pcorr} > |0.5|$), and variables important in projection ($\text{VVIP} > 1$) were calculated to identify the features that are statistically significant in the MVA statistics.

Also, the UVA statistics results using non-parametric one-way ANOVA showed a greater number of significant variables. Consequently, pairs of groups were compared, and those with a $p < 0.05$ were considered significant metabolites. These features were annotated using relative migration time (RMT) and exact mass using an in-house library available at CEUMassMediator (CE-MS search), an online open-source tool developed in our laboratory (http://ceumass.eps.uspceu.es/index_cesearch.xhtml). Fifty-eight metabolites were found to be statistically significant, revealing the modulation of infection. These 57 metabolites appeared to be modulated in La-WT-infected compared to non-infected macrophages, indicating that infection with *L. amazonensis* results in an increased abundance of metabolites mediated by its metabolism within macrophages and/or manipulate the metabolism of the host. Fifty-one metabolites appeared modified in those infected by La-arg⁻ as compared to non-infected macrophages, as a result of the metabolism of the parasite in the host cell and the activation of microbicides mechanisms in macrophages (Table S1). To observe parasite arginase activity inside the host cell, the La-arg⁻ and La-WT-infected C57BL/6-macrophages were compared (Table 1), revealing 37 modulated metabolites.

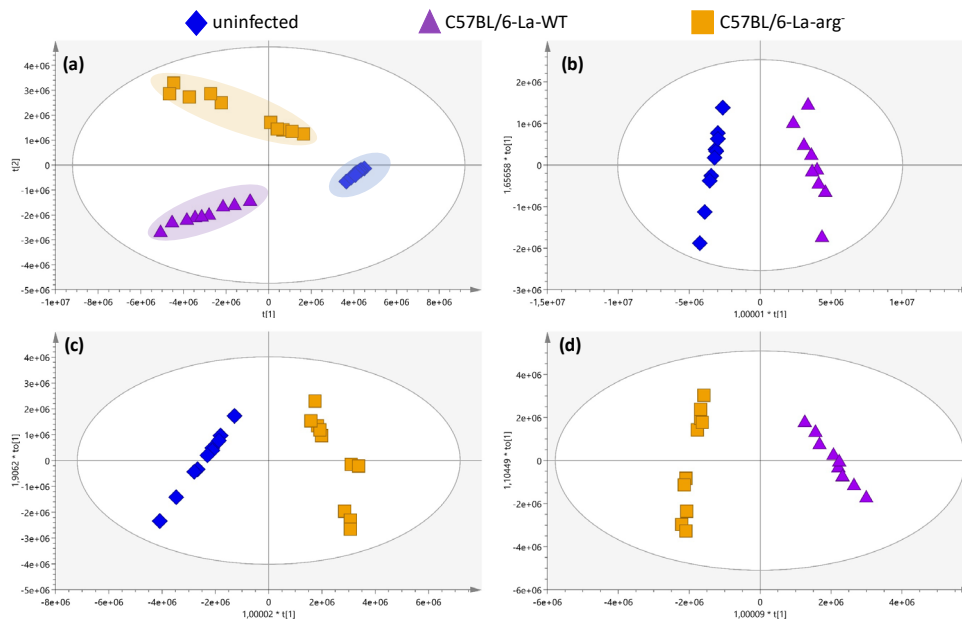


Figure 23. Partial least squares discriminant analysis (PLS-DA) and Orthogonal partial least-squares-discriminant analysis (OPLS-DA) analysis of variation between the two groups of *L. amazonensis* infected C57BL/6-macrophages. (a) Score plots for the PLS-DA and model were built to compare 3 conditions: C57BL/6-La-arg⁻ infected macrophage, C57BL/6-La-WT infected macrophage, and uninfected macrophage ($R^2=0.957$ and $Q^2=0.934$). OPLS-DA model was built for the comparison: (b) C57BL/6-La-WT infected macrophage vs. uninfected macrophage ($R^2 = 0.975$ and $Q^2 = 0.965$), (c) C57BL/6-La-arg⁻-infected macrophage vs. uninfected macrophage ($R^2 = 0.914$ and $Q^2 = 0.901$), and (d) C57BL/6-La-arg⁻ infected macrophage vs. C57BL/6-La-WT infected macrophage ($R^2 = 0.957$ and $Q^2 = 0.947$).

Differential metabolites during B6-macrophages infection with *L. amazonensis*

The overview of the untargeted metabolome of La-WT-infected macrophages or La-arg⁻-infected macrophages compared to uninfected macrophages showed an increased level of arginine, argininic acid, citrulline, argininic succinate acid, ornithine, putrescine, N-acetylspermidine, S-adenosylmethionine, oxidized glutathione, trypanothione disulfide, proline, glutamine, and glutamic acid, as observed by % change in Table S1 and intensity of peak area of each metabolite in Figure 3. The variations of the predictors correlated and orthogonal to the response of each group were evaluated in Figure 2b-c.

Focusing on the investigation of the parasite arginase impacts on the metabolism of infected macrophages, we compared the levels of metabolites from La-arg⁻-infected macrophages versus La-WT-infected macrophages (Table 1, Figure 3-4). Based on metabolites from L-arginine metabolism, the absence of parasite arginase upregulated arginine, citrulline, and argininic acid levels. On the other hand, it downregulated the levels of putrescine, proline, ornithine, glutamic acid, S-adenosylmethionine, cystathionine, carbamyl-L-arginine, oxidized trypanothione and reduced trypanothione.

Table 1. Metabolite content from the comparison of macrophages infected with *La-arg-* compared to *La-WT* infection.

Name	Mass (Da)	RRMT	%RSD of QQC	p	p FFDR	p-value	%change	p(corr)	VVIP
Glycine	75.0330	0.72	8.24	4.5E-06	2.2E-05	4.3E-05	-41.30	-0.84	<1
Putrescine	88.1000	0.RMT	5.81	3.9E-06	2.1E-05	2.2E-05	-58.46	-0.80	<1
Alanine	89.0483	0.77	7.31	1.8E-05	4.7E-05	1.0E-02	-24.82	-0.62	2.81
4-aminobutanoic acid	103.0647	0.67	7.41	1.8E-05	4.7E-05	1.0E-02	57.39	0.57	<1
Serine	105.0429	0.85	6.1	7.5E-06	2.8E-05	2.6E-04	-37.88	-0.79	<1
Proline	115.0634	0.92	7.42	5.1E-06	2.3E-05	2.2E-05	-73.83	-0.96	1.73
Valine	117.0792	0.85	6.73	1.3E-05	3.7E-05	3.0E-03	-30.00	-0.69	2.06
Pipecolic acid	129.0789	0.87	6.71	5.0E-06	2.3E-05	6.5E-04	117.06	0.67	4.05
Isoleucine leucine	131.0945	0.87	6.51	3.9E-06	2.1E-05	2.2E-05	-56.42	-0.91	4.16
Asparagine	132.0528	0.89	6.82	5.7E-06	2.5E-05	1.5E-04	-41.67	-0.78	<1
Ornithine	132.0896	0.60	6.67	1.0E-04	1.8E-04	2.2E-05	-92.47	-0.99	2.00
Aspartic acid	133.0374	0.97	6.46	2.1E-02	2.9E-02	1.7E-02	-19.58	-0.56	<1
Hypoxanthine	136.0385	1.01	5.95	1.7E-05	4.6E-05	7.6E-03	-26.98	-0.61	<1
Glutamic acid	147.0532	0.92	5.46	6.3E-05	1.2E-04	4.1E-03	-26.26	-0.66	3.45

Methionine	149.0512	0.91	3.94	1.1E-05	3.5E-05	2.1E-03	-34.19	-0.75	<1
Xanthine	152.0271	1.72	12.19	1.5E-02	2.1E-02	2.8E-02	19.21	0.50	<1
Histidine	155.0696	0.64	6.61	3.9E-06	2.1E-05	2.2E-05	-59.90	-0.93	1.96
Imidazolelactic acid	156.0554	0.76	8.51	1.1E-05	3.4E-05	7.6E-03	-27.91	-0.61	<1
Phenylalanine	165.0808	0.93	6.5	8.2E-06	2.9E-05	6.5E-04	-36.86	-0.75	1.05
1-Methylhistidine	169.0856	0.66	10.42	2.3E-06	1.8E-05	2.2E-05	-81.52	-0.98	<1
Arginine	174.1117	0.63	6.37	9.1E-06	3.0E-05	9.7E-04	100.48	0.66	3.77
Citrulline	175.0972	0.94	6.14	2.3E-06	1.8E-05	2.2E-05	220.70	0.82	<1
Argininic acid ^a	175.0975	0.79	5.67	2.3E-06	1.8E-05	2.2E-05	1919.49	0.86	<1
Glucose ^a	180.0608	1.72	10.82	3.92E-06	1.98E-05	2.17E-05	-49.42	NS	<1
Tyrosine	181.0739	0.96	5.81	7.3E-06	2.8E-05	4.1E-04	-37.73	-0.78	<1
Tryptophan	204.0894	0.93	5.11	1.3E-05	3.7E-05	3.0E-03	-27.53	-0.70	<1
<i>N</i> -alpha-Carbamyl-L-arginine ^a	217.1191	0.84	22.26	1.5E-06	1.8E-05	2.2E-05	↓	NS	NS
<i>N</i> -gamma-L-Glutamyl-D-alanine ^a	218.0906	1.03	7.04	2.7E-06	1.8E-05	4.3E-05	-51.06	-0.86	<1
Cystathionine	222.0679	0.85	4.06	2.3E-06	1.8E-05	2.2E-05	-57.72	-0.93	<1
Neuraminic acid ^a	267.0961	1.13	7.88	6.6E-06	2.6E-05	1.5E-04	-40.89	-0.79	<1
Ser Gly Asn ^a	276.1061	0.98	6.27	1.5E-06	1.8E-05	2.2E-05	↓	NS	NS
<i>N</i> -(1-Deoxy-1-fructosyl)threonine ^a	281.1118	1.13	7.78	2.7E-06	1.8E-05	4.3E-05	-44.93	-0.86	<1
Glutamylarginine ^a	303.1550	0.76	9.35	1.5E-06	1.8E-05	2.2E-05	↓	NS	NS
S-Adenosylmethionine ^a	398.1385	0.63	4.84	9.1E-06	3.0E-05	9.7E-04	-33.16	-0.74	<1
Ala His Thr Trp Ala His Trp Thr ^a	513.2329	1.03	13.27	1.8E-06	1.8E-05	2.2E-05	0.00	NS	NS
Oxidized trypanothione	721.2896	0.82	25.13	6.3E-06	2.6E-05	1.5E-03	-35.56	-0.71	<1
Reduced trypanothione	723.3057	0.84	25.12	2.65E-06	1.71E-05	4.33E-05	-52.10	-0.80	<1

^a tentative identification using only monoisotopic mass

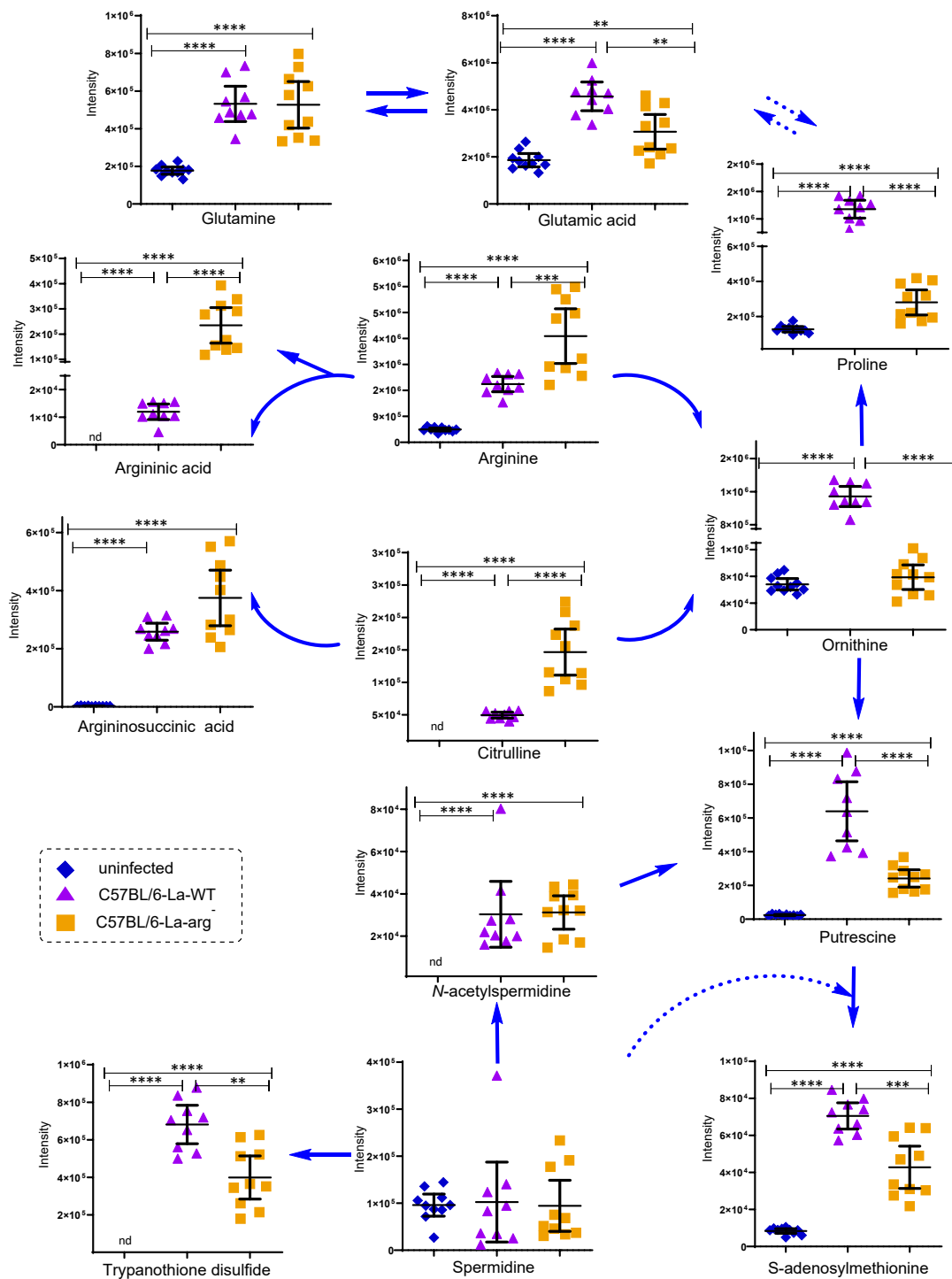


Figure 24. Metabolic profile of infected macrophages with *L. amazonensis*. Using an untargeted CE-MS, the intensity peak area of metabolites from the metabolic profile of macrophages infected with *La*-WT or *La*-arg- and uninfected were compared, focusing on the L-arginine metabolism pathways. The graphs are representing the average metabolite amount in each group. (*) p-value < 0.05; (**) p-value < 0.01; (***) p-value < 0.001, was used non-parametric 1-way ANOVA test (Kruskal-Wallis).

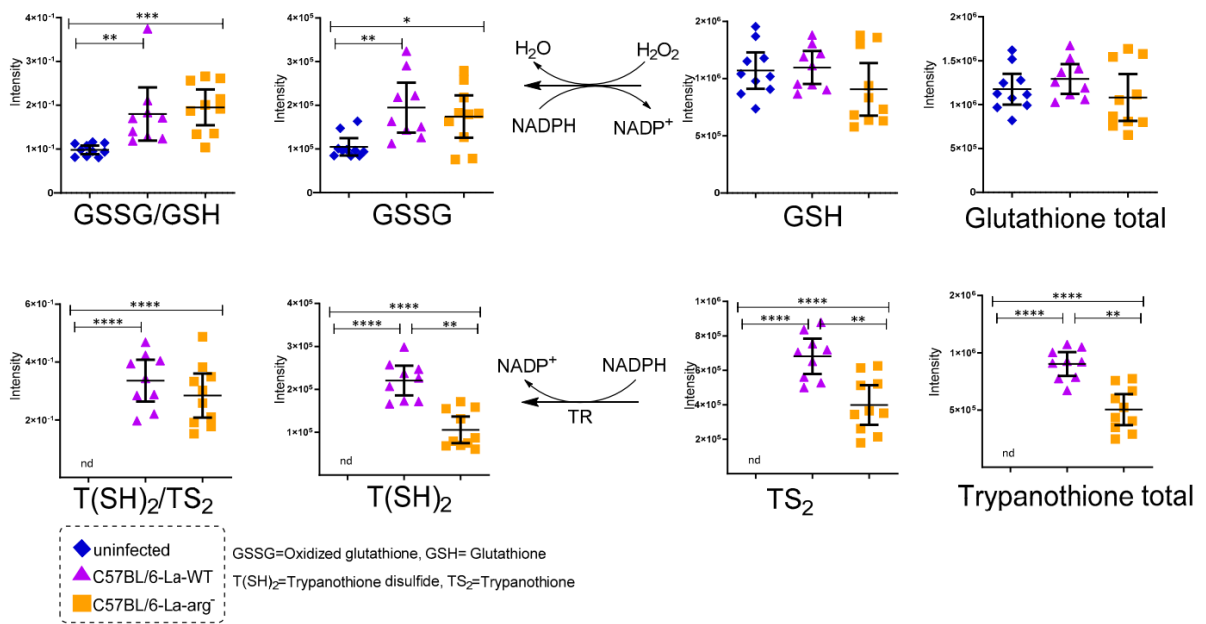


Figure 25. Antioxidant systems glutathione and trypanothione. Total glutathione (GSH + GSSG), oxidative stress (GSSG/GSH ratio), total trypanothione (T(SH)₂+TS₂) and T(SH)₂/TS₂ ratio were compared in macrophages infected with *La*-WT or *La*-arg⁻ and uninfected. (*) p-value < 0.05; (**) p-value < 0.01; (***) p-value < 0.001, was used non-parametric 1-way ANOVA test (Kruskal-Wallis).

Furthermore, heatmap analysis of the magnitude, directionality, and significance for the association of 58 differentially modulated metabolites showed the clustering of La-arg⁻-infected macrophages and La-WT-infected macrophages in a distinct way of uninfected macrophages (Figure 5).

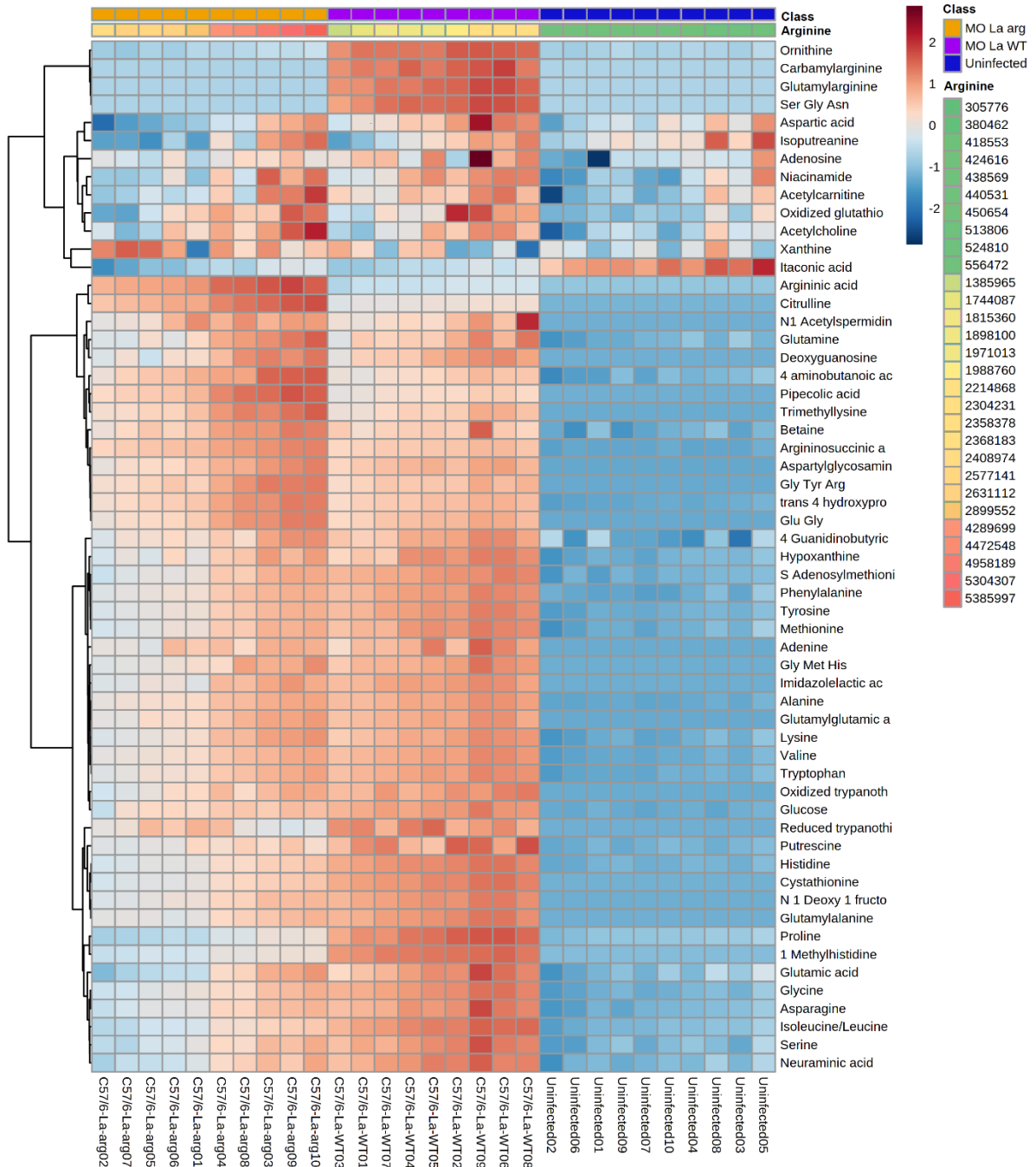


Figure 26. Heatmap of 58 metabolites differentially modulated in the metabolomic analysis of macrophages infected with La-WT or La-arg⁻ versus uninfected macrophages. Each column represents a sample, and each row represents a metabolite. Two factors order the samples: the first one arranged in three main groups (Phenotype: uninfected, La-arg⁻ and La-WT), and inside each one, samples are ordered by the abundance of arginine, that has a pseudo-color ranging from the lowest amount – green; to the highest – red. The color code inside the heatmap depicts each metabolite relative fold change between groups. The parameters used for the analysis were the Euclidean distance measure and the Ward cluster algorithm.

Pathway enrichment analysis

Aiming to understand which pathways were modulated during the macrophage infection with *L. amazonensis* and evaluate how the parasite arginase can impact them even more. The biological pathways involved in the metabolism of the 58 metabolites from La-WT and La-arg⁻ infected C57BL/6 -macrophages differentially modulated in comparison with uninfected and the biological function were analyzed by enrichment analysis using MetaboAnalyst (Fig. 6). The corresponding pathways were showed based on *p* values from the enrichment analysis (y-axis) and fold enrichment (x-axis). The Top10 most impacted pathway was colored in red, measured as closely related to *Leishmania*-infection of C57BL/6-macrophage, including urea cycle, glycine and serine metabolism, ammonia recycling, methionine metabolism, aspartate metabolism, glutamate metabolism, spermidine and spermine biosynthesis, methylhistidine metabolism and glutathione metabolism, supporting the involvement of arginine metabolism during infection. As expected, we observed that the amino acid L-arginine pathways were the most impacted during the infection.

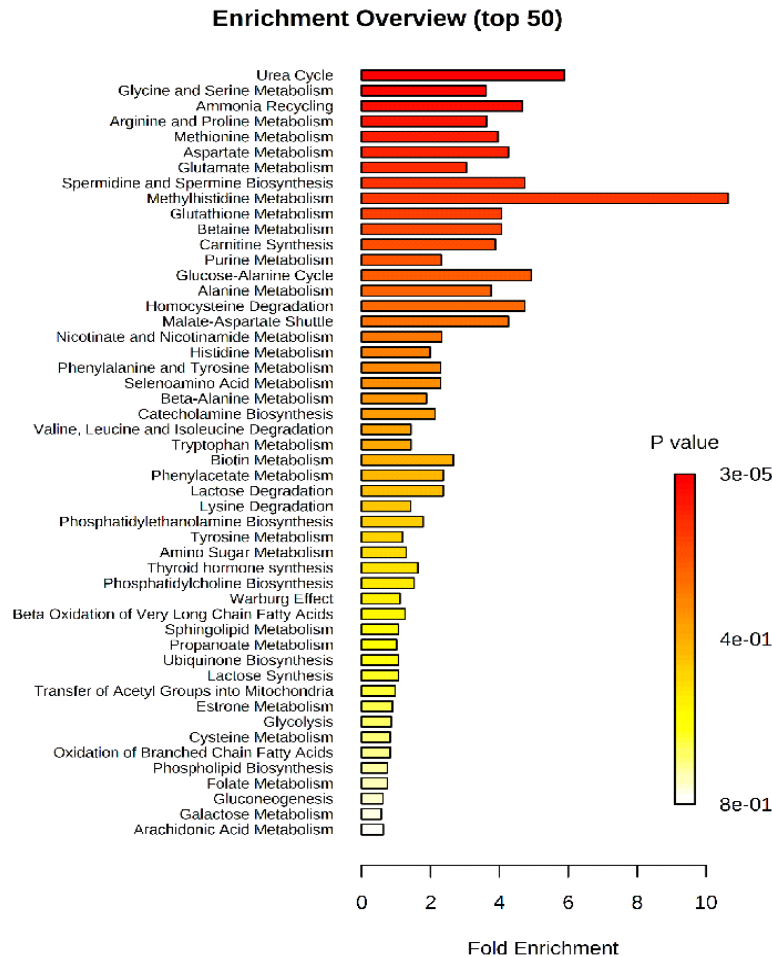


Figure 27. Metabolic pathways associated with metabolite enrichment in *L. amazonensis* infected macrophages. Analysis of dysregulated pathways based in metabolite peak areas from macrophages infected with La-WT or La-arg⁻, comparing to the uninfected one. We used the hypergeometric test to evaluate a particular metabolite set. The red color represents the maximum *p*-value, and the white color the minimum *p*-value.

This information guides us to integrate the differential regulated metabolites from arginine metabolism with other pathways in La-WT infected macrophages versus uninfected macrophages, as shown in figure 7. The higher levels of arginine correlate with increased production of citrulline and ornithine. Ornithine support increased levels of trypanothione via polyamines production. Putrescine and spermidine were converted into glutathionylspermidine, and subsequent in trypanothione disulfide increased in La-WT infected macrophages. Also, ornithine can be interconverted in proline, and glutamate, raising the glutathione disulfide, both in higher infected macrophages. The alteration in pipecolate and xanthine levels showed the influences of *Leishmania* infection in the lysine degradation and purine metabolism.

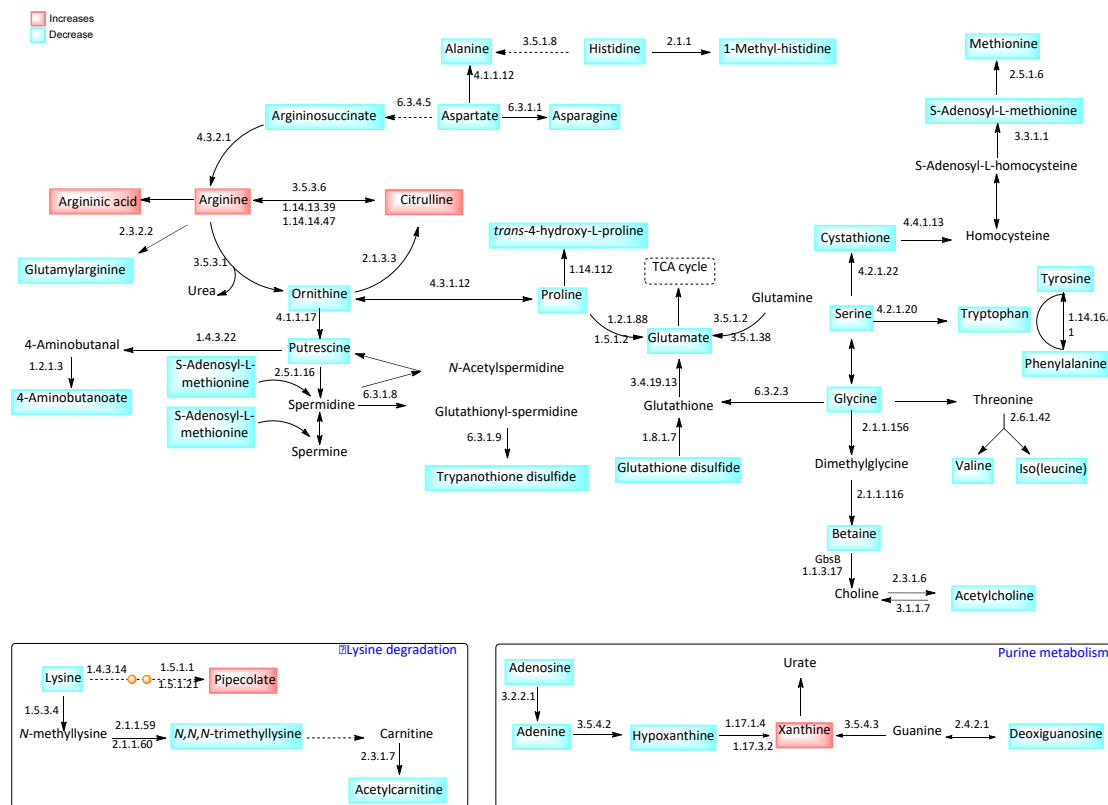


Figure 28. Modulation of metabolite content in the L-arginine metabolic pathways in macrophages infected with *La-arg-* compared to *La-WT*. Representation of modulated metabolic pathways during the infection of macrophages with *L. amazonensis*. The blue boxes represent unchanged metabolites, while the red boxes represent the increased metabolites in the comparison of *La-arg-* to *La-WT*. The KEGG EC entry of enzymes involved in the pathway is shown as a number close to the arrows, indicating the catalyzed reactions.

Discussion

Macrophage activation and functional plasticity are strictly connected to metabolic reprogramming, supplying energy and metabolites participation in anabolic and catabolic pathways, modifying cell response to infections. Macrophages alter the demands for glucose, fatty acids, amino acids, purines, ATP, and NADPH to allow an appropriate response against pathogens, avoiding excessive inflammation or tissue injury(LOCATI; CURTALE; MANTOVANI, 2020a; QUINN *et al.*, 2016; RYAN; O'NEILL, 2020a).

Also, *Leishmania* can regulate its metabolites content during the differentiation from promastigote to amastigote inside macrophages. They can also evade microbicidal mechanisms(MUXEL, S.M.; AOKI; *et al.*, 2018c; ROSENZWEIG *et al.*, 2008). *Leishmania* is auxotrophic for many nutrients, and the amastigote can uptake from phagolysosomes, such as amino acids, lipids, purines, pyrimidines, heme, and vitamins(MCCONVILLE, MALCOLM J., 2016b; MCCONVILLE, MALCOLM J. *et al.*, 2015; SAUNDERS *et al.*, 2018). The metabolite uptake and de novo synthesis correlate with virulence maintenance and parasite survival and can be favored by phagolysosome niche(MCCONVILLE, MALCOLM J., 2016b; MCCONVILLE, MALCOLM J. *et al.*, 2015; SAUNDERS *et al.*, 2018). Many studies have shown that the metabolism from parasite interferes in macrophages metabolism but is still poorly understood. However, to fill this gap, our group has previously demonstrated the influence of *L. amazonensis* arginase in their metabolism in promastigotes forms, changing arginine, glutamine and proline metabolism, and polyamines biosynthesis, as revealed by CE-MS ESI+ strategy(CASTILHO-MARTINS *et al.*, 2015). Also, the changes on arginine levels and arginine metabolism are showed in *L. braziliensis* resistant to antimony treatment using CE-MS ESI+ strategy(CASTILHO-MARTINS *et al.*, 2015), evidencing alterations in the amino acids content and metabolism, and thiol-dependent redox (CANUTO *et al.*, 2012).

Clinical data of diffused cutaneous leishmaniasis (DCL) showed that patients present higher ornithine, spermidine, and citrulline in plasma samples than mucocutaneous leishmaniasis (MCL), using HPLC tool(MALTA-SANTOS *et al.*, 2020). Indeed, DCL skin biopsies upregulated arginase 1 (ARG1) and spermine synthase mRNAs involved in polyamines biosynthesis concerning localized cutaneous leishmaniasis (LC) and MCL lesions, highlighting the significance of host ARG1 and arginine transporter (cationic amino acid transporter, CAT2) in MCL(MALTA-SANTOS *et al.*, 2020). However, the ARG1 and arginase 2 (ARG2) transcripts are lower in DCL than healthy controls(MALTA-SANTOS *et al.*, 2020). *L. amazonensis* infection of BALB/c-macrophages increases host *Cat2* and *Arg1* transcripts and parasite arginine transporter (amino acid permease 3, AAP3) and parasite arginase(MUXEL, SANDRA MARCIA; LARANJEIRA-SILVA; ZAMPIERI; FLOETER-WINTER, 2017c). Despite that, C57BL/6-macrophages infected with *L. amazonensis* did not modulate those genes(AOKI, JULIANA IDE *et al.*, 2020b; MUXEL, S.M.; ACUÑA; *et al.*, 2018).

Additionally, we evaluated the metabolome fingerprint of infected-macrophages by CE-MS ESI+ and early steps of *L. amazonensis* infection in BALB/c macrophages to modify the blend of metabolites content, changing the amino acids, polyamines, and purine pathways(MUXEL, SANDRA MARCIA *et al.*, 2019a). In a similar way to BALB/c macrophages infected with *L. amazonensis*(MUXEL, SANDRA MARCIA *et al.*, 2019a),

C57BL/6-macrophages also showed increased levels of L-arginine, ornithine, and putrescine, supporting the metabolization of L-arginine in polyamines, which supply the production of trypanothione in detriment of glutathione.

However, L-arginine is used to produce polyamines and is necessary to access the main M1 character: NO production. This production is dependent on the availability of the amino acid, O₂ plus the co-factors: reduced nicotinamide-adenine-dinucleotide phosphate (NADPH), flavin adenine dinucleotide (FAD, flavin mononucleotide (FMN), and tetrahydrobiopterin (BH₄). Unlike the constitutive forms, NOS2 depends on calmodulin and heme to form a functional hFADDimer(BLAGIH; JONES, 2012a; JHA *et al.*, 2015a; ZHENG *et al.*, 2020). Contrasting with *L. amazonensis* infection of BALB/c macrophages that presents lower levels of *Nos2*, NO, and citrulline(AOKI, J I *et al.*, 2019; AOKI, JULIANA IDE *et al.*, 2019; MUXEL, SANDRA MARCIA *et al.*, 2019a; MUXEL, S.M.; LARANJEIRA-SILVA; ZAMPIERI; FLOETER-WINTER, 2017c), the increased levels of citrulline in C57BL/6-macrophages infected with *L. amazonensis* compared to uninfected ones support the high levels of NO production by NOS2 and reduction in infectivity in the time-course of infection. These can allow the maintenance of parasite in lower levels inside C57BL/6-macrophages, as observed in the time-course of in vitro infection (Fig. S1) in comparison with susceptible BALB/c macrophage(MUXEL, S.M.; LARANJEIRA-SILVA; ZAMPIERI; FLOETER-WINTER, 2017c). The absence of parasite arginase increased the number of amastigotes per macrophages at 4-48 hours, suggesting growth in parasite phagocytoses. The higher levels of frequency of NO producing cells increased MFI of DAF-FM labeling per cell, and citrulline in C57BL/6 macrophages infected with La-arg⁻ indicate a microbicidal macrophages phenotype in this condition. Interesting note that the correlation of ARG1/NOS2 ratio and increase in susceptibility to *Leishmania* infection is extensively studied(BOGDAN, CHRISTIAN, 2020), but more information can be explored in the relation of polyamines/NO production. However, polyamines production can reduce NO production since they are mutually excluded pathways. Polyamines are polycationic metabolites crucial for cell proliferation, gene transcription, protein translation, oxidative stress regulation, and immunosuppression signals(MUXEL, S.M.; AOKI; *et al.*, 2018c; PEGG, A. E.; MCCANN, 1982; THOMAS; THOMAS, 2001)(PULESTON *et al.*, 2019). Their biosynthesis also depends on arginine content competing with NO production(GOGOI *et al.*, 2016; PEREZ-LEAL *et al.*, 2012; RATH, MEERA *et al.*, 2014). The intricate cascade of enzymes that use L-arginine and their substrates or products and transporters allows the integration of polyamines biosynthesis with other metabolites, modulating the immune response(HESTERBERG; CLEVELAND; EPLING-BURNETTE, 2018; PULESTON; VILLA; PEARCE, 2017). Furthermore, increased ornithine levels, a product of ARG1, in C57BL/6 macrophages infected with *L. amazonensis* can be converted in proline, as indicated by the ornithine cyclodeaminase (OCD) in higher levels(GOODMAN *et al.*, 2004; WU *et al.*, 2008). Ornithine and proline can supply the increased levels of glutamate and glutamine in a complex enzyme network(DICKINSON; FORMAN, 2002; PULESTON; VILLA; PEARCE, 2017) involving the production of metabolites: L-1-pyrroline 5-carboxylate, L-glutamate 5-semialdehyde, and L-glutamyl-P(MUXEL, S.M.; AOKI; *et al.*, 2018c), which are characterized in macrophages metabolism but did not identify by our method of analysis.

Further, we found the same spermidine levels between La-WT infected and uninfected macrophages but higher S-adenosylmethionine and *N*-acetylspermidine levels in infected macrophages. S-adenosylmethionine donates an aminopropyl group to spermidine and spermine guided by aminopropyl transferases called spermidine synthase and spermine synthase, respectively(DICKINSON; FORMAN, 2002; PULESTON; VILLA; PEARCE, 2017). The S-acetylspermidine is a polyamine with an acetyl group at the spermidine *N*₁-position received by spermidine/spermine *N*₁-acetyltransferase (SSAT)(PEGG, ANTHONY E., 2008). The mammalian cell polyamine content is maintained by enzymes that have a crucial role to this(JELL *et al.*, 2007; NIIRANEN *et al.*, 2006; POLITICELLI *et al.*, 2012), we can exemplify: a) ARG1; b) ODC c) SSAT d) APAO (acetyl polyamine oxidase - that converts *N*₁-acetylspermidine into putrescine plus *N*-acetyl-3-aminopropanaldehyde(TAKAO *et al.*, 2009)); and e) SMO (spermine oxidase - that converts spermine to spermidine plus 3-aminopropanaldehyde)(CERVELLI *et al.*, 2012; IKEGUCHI; BEWLEY; PEGG, 2006). Although mammalian, the presence of an APO and SMO(LÜERSEN, 2005) in *Leishmania* still not to be fully understood and must be confirmed.

Another role of polyamines in the control of translation, mediated by spermidine that happens essential activity in the activation of eukaryotic initiation factor 5A (eIF5A), adding a hypusine through a process that cleaves the spermidine and transfer of 4-aminobutyl moiety to an internal lysine to form an intermediate deoxyhypusine and subsequently hypusine residue and mature eIF5A, being a post-translational modification. This protein modification is required to synthesize proteins in host cells (LI, C. H. *et al.*, 2010; PULESTON *et al.*, 2019; SAINI *et al.*, 2009) and *Leishmania*(CHAWLA *et al.*, 2010).

Regarding the redox state control, the L-arginine also has a function: serve as a glutathione source, which has particular relevance when detoxifies the cell from mitochondrial oxidants, regulating the redox environment(DICKINSON; FORMAN, 2002). The relative increase in oxidized glutathione (glutathione disulfide, GSSG)/reduced glutathione (GSH ratio observed in La-WT and La-arg⁻ infected macrophages versus uninfected macrophages may indicate that response led to the oxidative stress condition. Peroxides oxidize GSH glutathione in a reaction catalyzed by glutathione peroxidase (GPx), ligating two reduced glutathione (GSH with a disulfide bond, forming the GSSG. This reaction diminishes peroxide levels, removing these oxidants(DIOTALLEVI, M. *et al.*, 2017; RIBAS; GARCÍA-RUIZ; FERNÁNDEZ-CHECA, 2014a). The turnover is mediated by the reduction of GSSG to GSH using NADPH as an electron donor. Glutathione reductase (GR) mediates this reaction. Also, glutathione biosynthesis is involved in resistance to anti-leishmanicidal agent pentavalent antimonial (Sb v)(CARTER *et al.*, 2003). The fine-tuning integration of oxidative stress and polyamines biosynthesis may balance the parasite killing in macrophages.

Trypanosomatids do not show glutathione but an analogous: trypanothione, formed by conjugation of spermidine and glutathione by enzyme trypanothione synthetase amidase (TRYS) unique in *T. brucei*, *T. cruzi*, and *Leishmania* spp.(COMINI; MENGE; FLOHÉ, 2003; FONSECA *et al.*, 2017; KOCH *et al.*, 2013; OZA; WYLLIE; FAIRLAMB, 2006; SAUDAGAR,; DUBEY, 2011; TRAN *et al.*, 2003), presenting a crucial function in combat oxidative stress(COLOTTI; ILARI, 2011; KARRETH *et al.*, 2011) and resistance to anti-trypanosome drugs(MESÍAS *et al.*, 2019; SAUDAGAR *et al.*, 2013; SAUDAGAR,; DUBEY,

2011). This molecule is also related to L-arginine metabolism. We also found higher oxidized trypanothione (T(SH₂)/reduced trypanothione (TS₂) ratio in macrophages infected with La-WT compared to La-arg⁻ or uninfected macrophages., probably impacting on redox state. We suggest that this can also influence in the macrophage killing activity(DICKINSON; FORMAN, 2002; IRIGOÍN *et al.*, 2009; MESÍAS; GARG; ZAGO, 2019). Similarly to glutathione, trypanothione needs to be recycled, depending on the NADPH availability produced by the pentose phosphate pathway (PPP) and by the balance of competition between NADPH electron donor for NOS2 to produce NO, NADPH oxidase to produce ROS and trypanothione reductase(IRIGOÍN *et al.*, 2009; MESÍAS; GARG; ZAGO, 2019; RICHARDSON *et al.*, 2009; VIOLA *et al.*, 2019a). Noteworthy, the higher levels of NO in La-arg⁻-infected compared to La-WT-infected macrophages appeared in accord with higher levels of xanthine, once NO can help to inactive xanthine dehydrogenase and xanthine oxidase (interconvertible forms of xanthine oxidoreductase), increasing xanthine and decreasing ROS production and assisting in balancing in damaging and helpful outcome(BATTELLI *et al.*, 2016; GIULIA BATTELLI *et al.*, 2016). Another antioxidant molecule involved in protecting host and parasite against oxidative stress is pipecolate, related to proline-ornithine metabolism, found in higher levels in La-arg⁻-infected compared to La-WT-infected macrophages(OZA; WYLLIE; FAIRLAMB, 2006).

In accordance, the arginase absence, glutamate, and proline metabolism. It increases polyamines production and arginine, citrulline, and argininic acid levels. It also decreases putrescine, proline, ornithine, glutamic acid, S-Adenosylmethionine, cystathionine, and carbamyl-L-arginine levels. Despite that, in a previous study, we did not find a modulation of the transcripts levels involved in these metabolic pathways in the *L. amazonensis* infection context, comparing macrophages infected with La-WT and La-arg⁻(AOKI, JULIANA IDE *et al.*, 2020b). Indeed, axenic promastigotes and amastigote, arginase lack impacts in transcriptional levels of arginine and proline metabolism, and oxidative stress-related genes(AOKI, J.I. *et al.*, 2019b; AOKI, J.I.; MUXEL; ZAMPIERI; LARANJEIRA-SILVA; *et al.*, 2017b).

In conclusion, we showed the role of parasite arginase in the immunometabolism of C57BL/6 macrophages infected with *Leishmania*, involving the metabolism of arginine, proline and glutamate, and polyamines biosynthesis. It can implicate in the redox balance of host and parasite cells by oxidization and reduction of glutathione and trypanothione, NO production, the microbicidal activity of macrophages, and parasite survival. It is complicated to extrapolate in vitro infections to in vivo models and natural infection by *Leishmania*. Our data can contribute to metabolomic area and macrophages response to infection(ROSENZWEIG *et al.*, 2008).

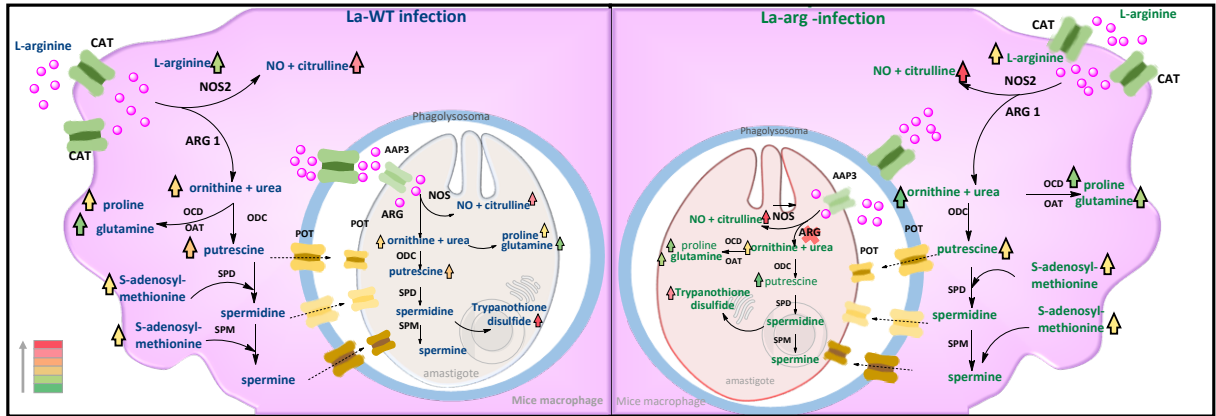
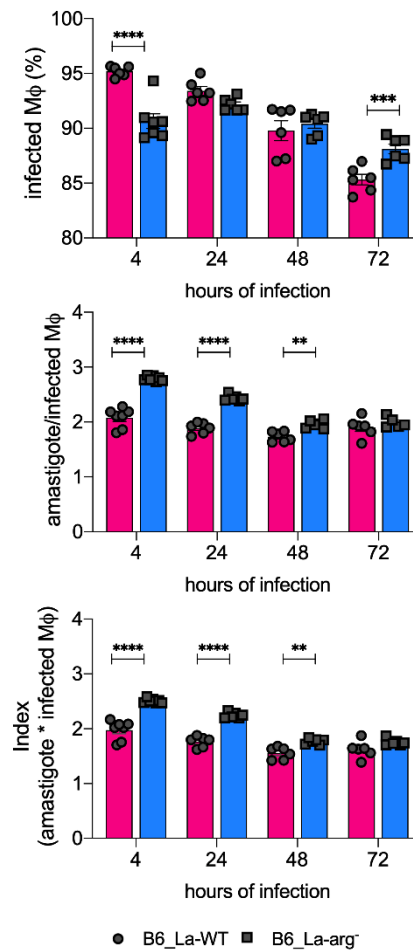
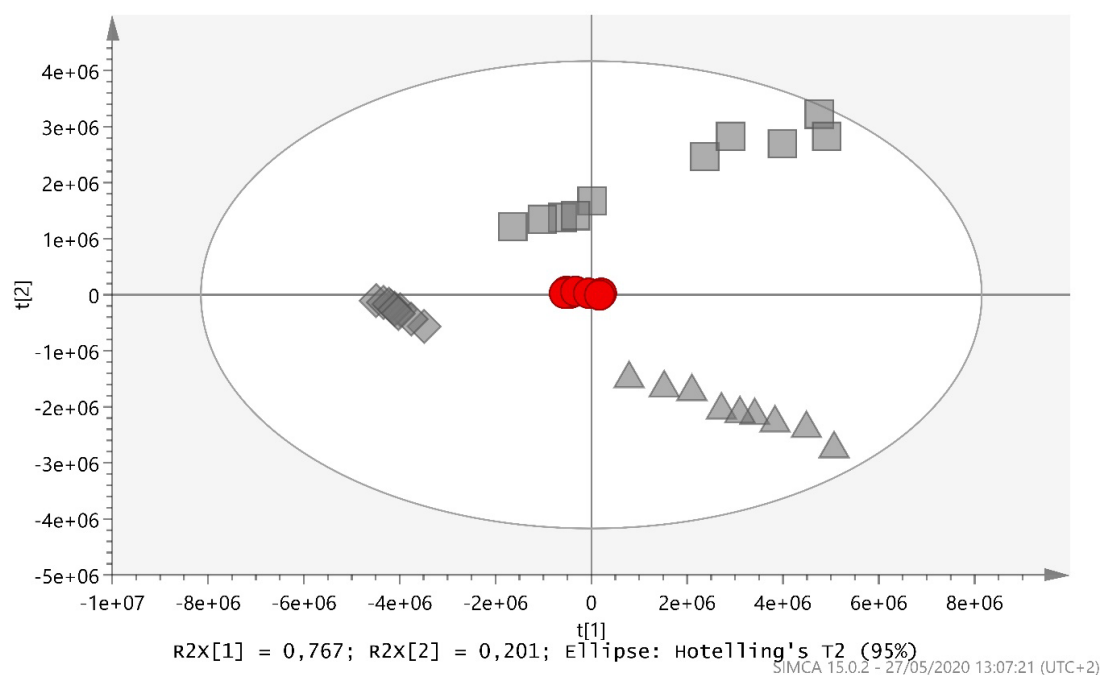


Figure 29. Schematic representation of L-arginine metabolism in Leishmania-infected macrophages. *L. amazonensis* WT infection can increase the levels of L-arginine via uptake by cationic amino acid transporter (CAT) in macrophage, and via amino acid permease 3 (AAP3) in amastigote form of *Leishmania*. L-arginine can be converted by host nitric oxide synthase 2 in nitric oxide and citrulline, as seen at its increased levels, leading a leishmanicidal activity or parasite-NOS, regulating amastigote survival and replication. On the other hand, host arginase 1 (ARG1) and parasite arginase (ARG) competes by arginine to produce ornithine and subsequent in polyamines: putrescine via ornithine decarboxylase (ODC), which is used to produce spermidine via spermidine synthase (SPD) and subsequently used by spermine synthase (SPM) to produce spermine, using S-adenosylmethionine as substrate. Ornithine can be used by ornithine decarboxylase (OCD) to produce proline or by ornithine aminotransferase (OAT) to produce glutamine. The absence of parasite arginase in La-arg-infected macrophages increased arginine availability, production of higher levels of citrulline, and a slight increase in ornithine levels production altering the levels of polyamines and trypanothione disulfide. Red color indicates increased levels of metabolites, and green indicates reduced levels of metabolites.

Supplementary Material



Supplementary Figure 5. Infectivity of La-WT and La-arg⁻ in C57BL/6-BMDMs macrophages. C57BL/6-macrophages (5×10^5) were infected with CFSE-labelled *L. amazonensis* (MOI5:1) and collected after 4, 24, 48, and 72 h for analysis of infectivity by image flow cytometer, gating in the CFSE-internalized cells to count the frequency of infected macrophages (infected M ϕ) and spot count tool to determine the number of infected M ϕ ; index of infection was calculated by multiplying the rate of infected M ϕ by the number of amastigotes per infected M ϕ . Each bar represents the average and SEM of values (n=6). (**) *p*-value < 0.01; (***) *p*-value < 0.001; (****) *p*-value < 0.0001;



Supplementary Figure 6. PCA-X score map of *L. amazonensis* infected C57BL-6 macrophages and quality control samples (QC, red circle) using pareto scaling in non-normalized setting C57BL/6-La-WT-infected macrophages (green squares), C57BL/6-La-arg-infected macrophages (gray triangle), uninfected macrophages (gray diamond).

Table 1. Metabolite content differentially identification in the comparison of C57BL/6-La-arg-infected or C57BL/6-La-WT-infected macrophages and uninfected macrophages

						C57BL/6-La-arg vs. uninfected				C57BL/6-La-WT vs. uninfected			
Name	Mass (Da)	RRM T	%RS D (QQ C)	<i>p</i>	<i>p</i> FF DR	<i>p</i> value	%Change	<i>p</i> (corr)	VV IP	<i>p</i> value	%Change	<i>p</i> (corr)	VV IP
Glycine	75.0330	0.72	8.24	4.47E-06	2.23E-05	1.08E-05	281.5	0.87	<1	2.17E-05	549.9	0.98	<1
Putrescine	88.1000	0.42	5.81	3.92E-06	2.07E-05	1.08E-05	891.8	0.94	<1	2.17E-05	2287.5	0.91	<1
Alanine	89.0483	0.77	7.31	1.85E-05	4.74E-05	1.08E-05	1885.6	0.92	3.81	2.17E-05	2541.2	0.99	4.75

4-aminobutanoic acid	103.0647	0.67	7.41	1.85E-05	4.74E-05	1.08E-05	404.0	0.90	<1	2.17E-05	220.2	0.96	<1
Serine	105.0429	0.85	6.1	7.46E-06	2.76E-05	2.17E-05	143.4	0.82	<1	2.17E-05	291.8	0.97	<1
Proline	115.0634	0.92	7.42	5.14E-06	2.34E-05	4.33E-05	120.2	0.79	<1	2.17E-05	741.6	0.98	<1
Valine	117.0792	0.85	6.73	1.26E-05	3.70E-05	1.08E-05	1274.8	0.92	2.33	2.17E-05	1863.9	0.99	3.17
Betaine	117.0794	0.96	8.49	5.63E-05	1.06E-04	1.08E-05	421.5	0.93	<1	2.17E-05	321.1	0.89	<1
Niacinamide	122.049	0.65	4.94	1.95E-02	2.71E-02	1.23E-01	24.7	0.30	<1	5.67E-03	33.4	0.64	<1
Pipecolic acid	129.0789	0.87	6.71	4.98E-06	2.34E-05	1.08E-05	↑	0.93	5.60	2.17E-05	↑	0.99	2.36
Itaconic acid ^a	130.0266	1.79179	5.24524	5.39E-05	9.81E-05	1.08E-05	-55.76	-0.91	<1	2.17E-05	51.1442	-0.92	<1
<i>trans</i> -4-hydroxyproline	131.0586	1.01	6.18	6.82E-05	1.24E-04	1.08E-05	1660.1	0.92	1.06	2.17E-05	1200.2	0.99	<1
Isoleucine/Leucine	131.0945	0.87	6.51	3.92E-06	2.07E-05	1.08E-05	224.5	0.85	1.57	2.17E-05	644.5	0.98	4.03
Asparagine	132.0528	0.89	6.82	5.74E-06	2.50E-05	1.08E-05	287.8	0.88	<1	2.17E-05	564.9	0.96	<1
Ornithine	132.0896	0.60	6.67	1.04E-04	1.80E-04	0.435872	15.5	0.32	<1	2.17E-05	1433.8	0.99	1.38
Aspartic acid	133.0374	0.97	6.46	2.10E-02	2.88E-02	3.53E-01	-6.2	-0.14	<1	2.20E-02	16.6	0.55	<1
Adenine	135.0558	0.67	25.43	2.40E-05	5.58E-05	1.08E-05	↑	0.92	<1	2.17E-05	↑	0.94	<1

Hypoxanthine	136.0385	1.01	5.95	1.69E-05	4.56E-05	1.08E-05	426.3	0.87	<1	2.17E-05	620.7	0.96	1.22
4-Guanidinobutyric acid	145.0875	0.72	8.99	3.19E-05	7.17E-05	1.08E-05	457.5	0.85	<1	2.17E-05	614.7	0.96	<1
Acetylcholine	145.1118	0.70	19.85	1.23E-02	1.81E-02	9.45E-03	52.2	0.58	<1	1.01E-02	37.3	0.61	<1
Glutamine	146.069	0.91	2.68	7.31E-05	1.28E-04	1.08E-05	197.5	0.88	<1	2.17E-05	172.9	0.93	<1
Lysine	146.1055	0.61	6.66	3.47E-05	7.53E-05	1.08E-05	390.5	0.90	1.06	2.17E-05	481.3	0.98	1.22
Glutamic acid	147.0532	0.92	5.46	6.34E-05	1.17E-04	2.09E-03	64.9	0.66	2.26	2.17E-05	123.7	0.93	3.63
Methionine	149.0512	0.91	3.94	1.13E-05	3.54E-05	1.08E-05	431.3	0.89	<1	2.17E-05	707.3	0.98	<1
Xanthine	152.0271	1.72	12.19	1.53E-02	2.15E-02	5.20E-03	24.51	0.50	<1	9.68E-01	0.17	0.50	<1
Histidine	155.0696	0.64	6.61	3.92E-06	2.07E-05	1.08E-05	905.0	0.92	<1	2.17E-05	2406.4	0.99	1.99
Imidazolelactic acid	156.0554	0.76	8.51	1.06E-05	3.41E-05	1.08E-05	↑	0.91	<1	2.17E-05	↑	0.99	<1
Phenylalanine	165.0808	0.93	6.5	8.17E-06	2.92E-05	1.08E-05	1000.5	0.91	<1	2.17E-05	1643.0	0.98	1.43
1-Methylhistidine	169.0856	0.66	10.42	2.32E-06	1.77E-05	1.08E-05	↑	0.94	<1	2.17E-05	↑	0.99	<1
Arginine	174.1117	0.63	6.37	9.14E-06	3.05E-05	1.08E-05	726.4	0.92	5.05	2.17E-05	312.2	0.98	2.06
Citrulline	175.0972	0.94	6.14	2.32E-06	1.77E-05	1.08E-05	↑	0.94	<1	2.17E-05	↑	0.99	<1

Argininic acid ^a	175.0 975	0.79	5.67	2.32 E- 06	1.77 E- 05	1.08E -05	↑	0.92	<1	2.17E -05	↑	0.96	<1
Glucose ^a	180.0 608	1.72	10.82	3.92 E- 06	1.98 E- 05	1.08E -05	↑	0.93	<1	2.17E -05	↑	0.98	<1
Tyrosine	181.0 739	0.96	5.81	7.29 E- 06	2.76 E- 05	1.08E -05	638.3	0.91	<1	2.17E -05	1085. 6	0.99	<1
<i>N</i> -Acetylspermi dine ^a	187.1 661	0.56	14.7	4.43 E- 05	9.42 E- 05	1.08E -05	↑	0.92	<1	2.17E -05	↑	0.79	<1
<i>N</i> ₆ , <i>N</i> ₆ , <i>N</i> ₆ - Trimethyl-L- lysine	188.1 507	0.63	5.21	3.23 E- 05	7.17 E- 05	1.08E -05	↑	0.93	<1	2.17E -05	↑	0.98	<1
Acetyl-L- carnitine	203.1 174	0.77	2.35	1.51 E- 02	2.15 E- 02	8.92E -02	30.3	0.37	<1	4.14E -03	31.9	0.66	<1
Glu Gly ^a	204.0 745	1.01	4.69	4.97 E- 05	9.57 E- 05	1.08E -05	↑	0.94	<1	2.17E -05	↑	0.99	<1
Tryptophan	204.0 894	0.93	5.11	1.26 E- 05	3.7 E- 05	1.08E -05	607.4	0.92	<1	2.17E -05	876.2	0.99	<1
<i>N</i> -alpha- Carbamyl-L- arginine ^a	217.1 191	0.84	22.26	1.54 E- 06	1.77 E- 05	1.00E +00	↑	NS	NS	2.17E -05	↑	NS	NS
<i>N</i> -gamma-L- Glutamyl-D- alanine ^a	218.0 906	1.03	7.04	2.65 E- 06	1.77 E- 05	1.08E -05	↑	0.93	<1	2.17E -05	↑	0.99	<1
Cystathionine	222.0 679	0.85	4.06	2.32 E- 06	1.77 E- 05	1.08E -05	↑	0.94	<1	2.17E -05	↑	0.99	1
Neuraminic acid ^a	267.0 961	1.13	7.88	6.61 E- 06	2.64 E- 05	2.17E -05	124.3	0.80	<1	2.17E -05	279.5	0.97	<1
Deoxyguanos ine	267.0 968	1.03	23.03	4.74 E- 05	9.57 E- 05	1.08E -05	↑	0.85	<1	2.17E -05	↑	0.95	<1
Adenosine	267.0 98	0.86	4.84	8.83 E- 03	1.38 E- 02	4.33E -02	41.6	0.22	<1	7.62E -03	149.4	0.53	<1

Argininosuccinic acid ^b	272.1132	0.74	5.24	7.10E-05	1.27E-04	1.08E-05	8015.5	0.89	<1	2.17E-05	6790.0	0.98	<1
Gamma Glutamylglutamic acid ^a	276.0944	1.09	7.87	2.24E-05	5.34E-05	1.08E-05	↑	0.94	<1	2.17E-05	↑	0.99	<1
Ser Gly Asn ^a	276.1061	0.98	6.27	1.54E-06	1.77E-05	1.00E+00	↑	NS	NS	2.17E-05	↑	NS	NS
<i>N</i> -(1-Deoxy-1-fructosyl)threonine ^a	281.1118	1.13	7.78	2.65E-06	1.77E-05	1.08E-05	↑	0.94	<1	2.17E-05	↑	0.99	<1
Glutamylarginine ^a	303.155	0.76	9.35	1.54E-06	1.77E-05	1.00E+00	↑	NS	NS	2.17E-05	↑	NS	NS
Aspartylglycosamine ^a	335.1332	1.08	6.63	4.89E-05	9.57E-05	1.08E-05	↑	0.94	<1	2.17E-05	↑	0.99	<1
Gly Met His ^a	343.1299	0.85	13.16	2.09E-05	5.22E-05	1.08E-05	↑	0.90	<1	2.17E-05	↑	0.98	<1
Gly Tyr Arg ^a	394.1946	0.99	10.72	4.54E-05	9.46E-05	1.08E-05	↑	0.94	<1	2.17E-05	↑	0.99	<1
S-Adenosylmethionine ^a	398.1385	0.63	4.84	9.14E-06	3.05E-05	1.08E-05	411.4	0.89	<1	2.17E-05	665.2	0.99	<1
Ala His Thr Trp Ala His Trp Thr ^a	513.2329	1.03	13.27	1.83E-06	1.77E-05	1.08E-05	↑	0.92	<1	1.00E+00	↑	NS	NS
Oxidized glutathione	612.1536	1.02	28.87	1.14E-02	1.70E-02	4.33E-02	66.1	0.61	<1	1.45E-03	71.5	0.68	<1
Oxidized trypanothione	721.2896	0.82	25.13	6.27E-06	2.61E-05	1.08E-05	↑	0.91	<1	2.17E-05	↑	0.98	<1
Reduced trypanothione	723.3057	0.84	25.12	2.65E-06	1.71E-05	1.08E-05	↑	0.91	<1	2.17E-05	↑	0.97	<1

^a tentative identification using only monoisotopic mass.

References

- AOKI, J.I.; MUXEL, S. M.; ZAMPIERI, R. A.; ACUÑA, S. M.; et al. L-arginine availability and arginase activity: Characterization of amino acid permease 3 in *Leishmania amazonensis*. *PLoS Neglected Tropical Diseases*, v. 11, n. 10, 2017.
- AOKI, J.I.; MUXEL, S. M.; ZAMPIERI, R. A.; LARANJEIRA-SILVA, M. F.; et al. RNA-seq transcriptional profiling of *Leishmania amazonensis* reveals an arginase-dependent gene expression regulation. *PLoS Neglected Tropical Diseases*, v. 11, n. 10, 2017.
- AOKI, JULIANA IDE et al. Differential immune response modulation in early *Leishmania amazonensis* infection of BALB/c and C57BL/6 macrophages based on transcriptome profiles. *Scientific Reports*, 2019.
- AOKI, JULIANA IDE et al. Dual transcriptome analysis reveals differential gene expression modulation influenced by *Leishmania* arginase and host genetic background. *Microbial Genomics*, 2020a.
- AOKI, JULIANA IDE et al. Dual transcriptome analysis reveals differential gene expression modulation influenced by *Leishmania* arginase and host genetic background. *Microbial Genomics*, 2020b.
- BATTELLI, M. G. et al. Xanthine oxidoreductase-derived reactive species: Physiological and pathological effects. *Oxidative Medicine and Cellular Longevity*. [S.l: s.n.], 2016
- BLAGIH, J.; JONES, R. G. Polarizing macrophages through reprogramming of glucose metabolism. *Cell Metabolism*. [S.l: s.n.], 2012a
- BLAGIH, J.; JONES, R. G. Polarizing macrophages through reprogramming of glucose metabolism. *Cell Metabolism*. [S.l: s.n.], 2012b
- BOGDAN, C. Macrophages as host, effector and immunoregulatory cells in leishmaniasis: impact of tissue micro-environment and metabolism. *Cytokine: X*, 2020.
- BOITZ, J. M. et al. Arginase Is Essential for Survival of *Leishmania donovani* Promastigotes but Not Intracellular Amastigotes. *Infect Immun*, v. 85, n. 1, 2017.
- BOUCHER, J. L.; MOALI, C.; TENU, J. P. Nitric oxide biosynthesis, nitric oxide synthase inhibitors and arginase competition for L-arginine utilization. *Cell Mol Life Sci*, v. 55, n. 8–9, p. 1015–1028, 1999.
- BURZA, S.; CROFT, S. L. L.; BOELAERT, M. Leishmaniasis. *Lancet*, From Duplicate 3 (Leishmaniasis - Burza, Sakib; Croft, Simon L. L; Boelaert, Marleen) From Duplicate 2 (Leishmaniasis - Burza, S; Croft, S L; Boelaert, M) Burza, Sakib Croft, Simon L Boelaert, Marleen eng England London, England *Lancet*. 2018 Sep 15;392(10151):951-970. doi: 10.1016/S0140-6736(18)31204-2. Epub 2018 Aug 17., v. 392, n. 10151, p. 951–970, 2018.
- CANUTO, G. A. B. A. et al. CE-ESI-MS metabolic fingerprinting of *Leishmania* resistance to antimony treatment. *Electrophoresis*, From Duplicate 2 (CE-ESI-MS metabolic fingerprinting of *Leishmania* resistance to antimony treatment - Canuto, G A; Castilho-Martins, E A; Tavares, M; Lopez-Gonzalvez, A; Rivas, L; Barbas, C) And Duplicate 3 (CE-ESI-MS metabolic fingerprinting of *Leishmania* resistance to antimony treatment - Canuto, G A; Castilho-Martins, E A; Tavares, M; Lopez-Gonzalvez, A; Rivas, L; Barbas, C) Canuto, Gisele A B Castilho-Martins, Emerson A Tavares, Marina Lopez-Gonzalvez, Angeles Rivas, Luis Barbas, Coral eng Germany *Electrophoresis*. 2012 Jul;33(12):1901-10. doi: 10.1002/elps.201200007., v. 33, n. 12, p. 1901–1910, 2012.
- CARTER, K. C. et al. The in vivo susceptibility of *Leishmania donovani* to sodium stibogluconate is drug specific and can be reversed by inhibiting glutathione biosynthesis. *Antimicrobial Agents and Chemotherapy*, 2003.

- CASTILHO-MARTINS, E. A. et al. Capillary electrophoresis reveals polyamine metabolism modulation in *Leishmania (Leishmania) amazonensis* wild-type and arginase-knockout mutants under arginine starvation. *Electrophoresis*, v. 36, n. 18, 2015.
- CERVELLI, M. et al. Spermine oxidase: Ten years after. *Amino Acids*. [S.l: s.n.], 2012
- CHAWLA, B. et al. Identification and characterization of a novel deoxyhypusine synthase in *Leishmania donovani*. *J Biol Chem*, From Duplicate 2 (Identification and characterization of a novel deoxyhypusine synthase in *Leishmania donovani* - Chawla, B; Jhingran, A; Singh, S; Tyagi, N; Park, M H; Srinivasan, N; Roberts, S C; Madhubala, R) Chawla, Bhavna Jhingran, Anupam Singh, Sushma Tyagi, Nidhi Park, Myung Hee Srinivasan, N Roberts, Sigrid C Madhubala, Rentala eng *J Biol Chem*. 2010 Jan 1;285(1):453-63. doi: 10.1074/jbc.M109.048850. Epub 2009 Oct 30., v. 285, n. 1, p. 453–463, 2010.
- COLOTTI, G.; ILARI, A. Polyamine metabolism in *Leishmania*: From arginine to trypanothione. *Amino Acids*. [S.l: s.n.], 2011
- COMINI, M.; MENGE, U.; FLOHÉ, L. Biosynthesis of trypanothione in *Trypanosoma brucei brucei*. *Biological Chemistry*, 2003.
- COVARRUBIAS, A. J.; AKSOYLAR, H. I.; HORNG, T. Control of macrophage metabolism and activation by mTOR and Akt signaling. *Seminars in Immunology*. [S.l: s.n.], 2015a
- COVARRUBIAS, A. J.; AKSOYLAR, H. I.; HORNG, T. Control of macrophage metabolism and activation by mTOR and Akt signaling. *Seminars in Immunology*. [S.l: s.n.], 2015b
- DA SILVA, M. F. L. et al. *Leishmania amazonensis* arginase compartmentalization in the glycosome is important for parasite infectivity. *PLoS ONE*, v. 7, n. 3, 2012.
- DICKINSON, D. A.; FORMAN, H. J. Cellular glutathione and thiols metabolism. *Biochemical Pharmacology*, 2002a.
- DICKINSON, D. A.; FORMAN, H. J. Cellular glutathione and thiols metabolism. *Biochemical Pharmacology*, 2002b.
- DIOTALLEVI, M. et al. Glutathione Fine-Tunes the Innate Immune Response toward Antiviral Pathways in a Macrophage Cell Line Independently of Its Antioxidant Properties. *Front Immunol*, From Duplicate 2 (Glutathione Fine-Tunes the Innate Immune Response toward Antiviral Pathways in a Macrophage Cell Line Independently of Its Antioxidant Properties - Diotallevi, M; Checconi, P; Palamara, A T; Celestino, I; Coppo, L; Holmgren, A; Abbas, K; Peyrot, F; Mengozzi, M; Ghezzi, P) Diotallevi, Marina Checconi, Paola Palamara, Anna Teresa Celestino, Ignacio Coppo, Lucia Holmgren, Arne Abbas, Kahina Peyrot, Fabienne Mengozzi, Manuela Ghezzi, Pietro eng Switzerland *Front Immunol*. 2017 Sep 29;8:1239. doi: 10.3389/fimmu.2017.01239. eCollection 2017., v. 8, p. 1239, 2017.
- FILARDY, A. A. et al. Proinflammatory Clearance of Apoptotic Neutrophils Induces an IL-12 low IL-10 high Regulatory Phenotype in Macrophages . *The Journal of Immunology*, 2010.
- FONSECA, M. S. et al. Ornithine decarboxylase or gamma-glutamylcysteine synthetase overexpression protects *Leishmania (Vianna) guyanensis* against antimony. *Experimental Parasitology*, 2017.
- GIULIA BATTELLI, M. et al. Xanthine Oxidoreductase in Drug Metabolism: Beyond a Role as a Detoxifying Enzyme. *Current Medicinal Chemistry*, 2016.
- GOGOI, M. et al. Dual role of arginine metabolism in establishing pathogenesis. *Current Opinion in Microbiology*. [S.l: s.n.], 2016
- GOODMAN, J. L. et al. Ornithine cyclodeaminase: Structure, mechanism of action, and implications for the μ -crystallin family. *Biochemistry*, 2004.
- HESTERBERG, R.; CLEVELAND, J.; EPLING-BURNETTE, P. Role of Polyamines in Immune Cell Functions. *Medical Sciences*, 2018.

HRABAK, A. et al. The inhibitory effect of nitrite, a stable product of nitric oxide (NO) formation, on arginase. *FEBS Lett*, v. 390, n. 2, p. 203–206, 1996.

IKEGUCHI, Y.; BEWLEY, M. C.; PEGG, A. E. Aminopropyltransferases: Function, structure and genetics. *Journal of Biochemistry*. [S.l: s.n.], 2006

INIESTA, V.; GOMEZ-NIETO, L. C.; CORRALIZA, I. The inhibition of arginase by N(omega)-hydroxy-l-arginine controls the growth of *Leishmania* inside macrophages. *J Exp Med*, Iniesta, V Gomez-Nieto, L C Corraliza, I eng *J Exp Med*. 2001 Mar 19;193(6):777-84., v. 193, n. 6, p. 777–784, 2001.

IRIGOÍN, F. et al. Mitochondrial calcium overload triggers complement-dependent superoxide-mediated programmed cell death in *Trypanosoma cruzi*. *Biochemical Journal*, 2009a.

IRIGOÍN, F. et al. Mitochondrial calcium overload triggers complement-dependent superoxide-mediated programmed cell death in *Trypanosoma cruzi*. *Biochemical Journal*, 2009b.

JELL, J. et al. Genetically altered expression of spermidine/spermine N1- acetyltransferase affects fat metabolism in mice via acetyl-CoA. *Journal of Biological Chemistry*, 2007.

JHA, A. K. et al. Network integration of parallel metabolic and transcriptional data reveals metabolic modules that regulate macrophage polarization. *Immunity*, 2015a.

JHA, A. K. et al. Network integration of parallel metabolic and transcriptional data reveals metabolic modules that regulate macrophage polarization. *Immunity*, 2015b.

JI, J.; SUN, J.; SOONG, L. Impaired expression of inflammatory cytokines and chemokines at early stages of infection with *Leishmania amazonensis*. *Infect Immun*, v. 71, n. 8, p. 4278–4288, 2003.

KARRETH, F. A. A. et al. In vivo identification of tumor- suppressive PTEN ceRNAs in an oncogenic BRAF-induced mouse model of melanoma. *Cell*, From Duplicate 1 (In vivo identification of tumor- suppressive PTEN ceRNAs in an oncogenic BRAF-induced mouse model of melanoma - *Cell*. 2011 Oct 14;147(2):382-95. doi: 10.1016/j.cell.2011.09.032., v. 147, n. 2, p. 382–395, 2011.

KOCH, O. et al. Molecular Dynamics Reveal Binding Mode of Glutathionylspermidine by Trypanothione Synthetase. *PLoS ONE*, 2013.

KOO, S. JIE; GARG, N. J. Metabolic programming of macrophage functions and pathogens control. *Redox Biology*. [S.l: s.n.], 2019

LARANJEIRA-SILVA, M. F. et al. Melatonin attenuates *Leishmania (L.) amazonensis* infection by modulating arginine metabolism. *Journal of Pineal Research*, v. 59, n. 4, 2015.

LI, C. H. et al. eIF5A promotes translation elongation, polysome disassembly and stress granule assembly. *PLoS ONE*, 2010.

LOCATI, M.; CURTALE, G.; MANTOVANI, A. Diversity, Mechanisms, and Significance of Macrophage Plasticity. *Annual Review of Pathology: Mechanisms of Disease*, 2020.

LÜERSEN, K. *Leishmania major* thialysine Nε-acetyltransferase: Identification of amino acid residues crucial for substrate binding. *FEBS Letters*, 2005.

MALTA-SANTOS, H. et al. Differential expression of polyamine biosynthetic pathways in skin lesions and in plasma reveals distinct profiles in diffuse cutaneous leishmaniasis. *Scientific Reports*, 2020a.

MALTA-SANTOS, H. et al. Differential expression of polyamine biosynthetic pathways in skin lesions and in plasma reveals distinct profiles in diffuse cutaneous leishmaniasis. *Scientific Reports*, 2020b.

MAMANI-HUANCA, M. et al. Enhancing confidence of metabolite annotation in Capillary Electrophoresis-Mass Spectrometry untargeted metabolomics with relative migration time and in-source fragmentation. *Journal of Chromatography A*, 2021.

- MANTOVANI, A. et al. The chemokine system in diverse forms of macrophage activation and polarization. *Trends Immunol*, v. 25, n. 12, p. 677–686, 2004.
- MARTINEZ, F. O. et al. Macrophage activation and polarization. *Front Biosci*, v. 13, p. 453–461, 2008.
- MCCONVILLE, M J et al. Living in a phagolysosome; metabolism of *Leishmania* amastigotes. *Trends Parasitol*, v. 23, n. 8, p. 368–375, 2007.
- MCCONVILLE, MALCOLM J. et al. *Leishmania* carbon metabolism in the macrophage phagolysosome- feast or famine? *F1000Research*. [S.l: s.n.], 2015a
- MCCONVILLE, MALCOLM J. et al. *Leishmania* carbon metabolism in the macrophage phagolysosome- feast or famine? *F1000Research*. [S.l: s.n.], 2015b
- MCCONVILLE, MALCOLM J. Metabolic Crosstalk between *Leishmania* and the Macrophage Host. *Trends in Parasitology*. [S.l: s.n.], 2016
- MESÍAS, A. C. et al. Trypanothione synthetase confers growth, survival advantage and resistance to anti-protozoal drugs in *Trypanosoma cruzi*. *Free Radical Biology and Medicine*, 2019.
- MESÍAS, A. C.; GARG, N. J.; ZAGO, M. P. Redox Balance Keepers and Possible Cell Functions Managed by Redox Homeostasis in *Trypanosoma cruzi*. *Frontiers in Cellular and Infection Microbiology*. [S.l: s.n.], 2019a
- MESÍAS, A. C.; GARG, N. J.; ZAGO, M. P. Redox Balance Keepers and Possible Cell Functions Managed by Redox Homeostasis in *Trypanosoma cruzi*. *Frontiers in Cellular and Infection Microbiology*. [S.l: s.n.], 2019b
- MILLS, C. D. M1 and M2 Macrophages: Oracles of Health and Disease. *Critical Reviews TM in Immunology*. [S.l: s.n.], 2012.
- MOORE, K. J.; SHEEDY, F. J.; FISHER, E. A. Macrophages in atherosclerosis: A dynamic balance. *Nature Reviews Immunology*. [S.l: s.n.], 2013
- MURRAY, H. W. W. et al. Advances in leishmaniasis. *Lancet*, v. 366, n. 9496, p. 1561–1577, 2005.
- MUXEL, SANDRA MARCIA et al. *Leishmania* (*Leishmania*) *amazonensis* induces macrophage miR-294 and miR-721 expression and modulates infection by targeting NOS2 and L-arginine metabolism. *Scientific Reports*, v. 7, p. 44141, 2017.
- MUXEL, SANDRA MARCIA et al. Metabolomic Profile of BALB/c Macrophages Infected with *Leishmania amazonensis*: Deciphering L-Arginine Metabolism. *Int J Mol Sci*, From Duplicate 1 (Metabolomic Profile of BALB/c Macrophages Infected with *Leishmania amazonensis*: Deciphering L-Arginine Metabolism - Muxel, S M; Mamani-Huanca, M; Aoki, J I; Zampieri, R A; Floeter-Winter, L M; Lopez-Gonzalvez, A; Barbas, C) Muxel, Sandra Marcia Mamani-Huanca, Maricruz Aoki, Juliana Ide Zampieri, Ricardo Andrade Floeter-Winter, Lucile Maria Lopez-Gonzalvez, Angeles Barbas, Coral eng 2018/24693-9/Fundacao de Amparo a Pesquisa do Estado de Sao Paulo 2018/23512-0/Fundacao de Amparo a Pesquisa do Estado de Sao Paulo 406351/2018-0/Conselho Nacional de Desenvolvimento Cientifico e Tecnologico Switzerland *Int J Mol Sci*. 2019 Dec 11;20(24). pii: ijms20246248. doi: 10.3390/ijms20246248. From Duplicate 2 (Metabolomic Profile of BALB/c Macrophages Infected with *Leishmania amazonensis*: Deciphering L-Arginine Metabolism - Muxel, Sandra Marcia S.M.; Mamani-Huanca, Maricruz; Aoki, Juliana Ide J.I.; Zampieri, R.A. Ricardo Andrade; Floeter-Winter, Lucile Maria L.M.; López-González, Ángeles; Barbas, Coral; Lopez-Gonzalvez, A; Barbas, Coral; López-González, Ángeles; Barbas, Coral) From Duplicate 1 (Metabolomic Profile of BALB/c Macrophages Infected with *Leishmania amazonensis*: Deciphering L-Arginine Metabolism - Muxel, Sandra Marcia; Mamani-Huanca, Maricruz; Aoki, Juliana Ide; Zampieri, Ricardo Andrade; Floeter-Winter, Lucile Maria; López-González, Ángeles; Barbas, Coral; Lopez-Gonzalvez, A; Barbas, Coral; López-González, Ángeles; Barbas, Coral) From Duplicate 2 (Metabolomic Profile of

BALB/c Macrophages Infected with *Leishmania amazonensis*: Deciphering L-Arginine Metabolism - Muxel, S M; Mamani-Huanca, M; Aoki, J I; Zampieri, R A; Floeter-Winter, L M; Lopez-Gonzalvez, A; Barbas, C) Muxel, Sandra Marcia Mamani-Huanca, Maricruz Aoki, Juliana Ide Zampieri, Ricardo Andrade Floeter-Winter, Lucile Maria Lopez-Gonzalvez, Angeles Barbas, Coral eng 2018/24693-9/Fundacao de Amparo a Pesquisa do Estado de Sao Paulo 2018/23512-0/Fundacao de Amparo a Pesquisa do Estado de Sao Paulo 406351/2018-0/Conselho Nacional de Desenvolvimento Cientifico e Tecnologico Switzerland Int J Mol Sci. 2019 Dec 11;20(24). pii: ijms20246248. doi: 10.3390/ijms20246248., v. 20, n. 24, p. 6248, 11 dez. 2019.

MUXEL, S.M.; AOKI, J. I.; et al. Arginine and polyamines fate in leishmania infection. *Frontiers in Microbiology*, v. 8, n. JAN, 2018.

MUXEL, S.M.; ACUÑA, S. M.; et al. Toll-like receptor and miRNA-let-7e expression alter the inflammatory response in leishmania amazonensis-infected macrophages. *Frontiers in Immunology*, v. 9, n. NOV, 2018.

NIIRANEN, K. et al. Mice with targeted disruption of spermidine/spermine N 1 - acetyltransferase gene maintain nearly normal tissue polyamine homeostasis but show signs of insulin resistance upon aging . *Journal of Cellular and Molecular Medicine*, 2006.

O'NEILL, L. A.; KISHTON, R. J.; RATHMELL, J. A guide to immunometabolism for immunologists. *Nat Rev Immunol*, v. 16, n. 9, p. 553–565, 2016.

OZA, S. L.; WYLLIE, S.; FAIRLAMB, A. H. Mapping the functional synthetase domain of trypanothione synthetase from *Leishmania major*. *Molecular and Biochemical Parasitology*, 2006a.

OZA, S. L.; WYLLIE, S.; FAIRLAMB, A. H. Mapping the functional synthetase domain of trypanothione synthetase from *Leishmania major*. *Molecular and Biochemical Parasitology*, 2006b.

PEGG, A. E.; MCCANN, P. P. Polyamine metabolism and function. *American Journal of Physiology - Cell Physiology*, 1982.

PEGG, ANTHONY E. Spermidine/spermine-N1-acetyltransferase: A key metabolic regulator. *American Journal of Physiology - Endocrinology and Metabolism*. [S.l: s.n.], 2008

PEREZ-LEAL, O. et al. Polyamine-Regulated Translation of Spermidine/Spermine-N1-Acetyltransferase. *Molecular and Cellular Biology*, 2012.

POLTICELLI, F. et al. Molecular evolution of the polyamine oxidase gene family in Metazoa. *BMC Evolutionary Biology*, 2012.

PULESTON, D. J. et al. Polyamines and eIF5A Hypusination Modulate Mitochondrial Respiration and Macrophage Activation. *Cell Metabolism*, 2019a.

PULESTON, D. J. et al. Polyamines and eIF5A Hypusination Modulate Mitochondrial Respiration and Macrophage Activation. *Cell Metabolism*, 2019b.

PULESTON, D. J.; VILLA, M.; PEARCE, E. L. Ancillary Activity: Beyond Core Metabolism in Immune Cells. *Cell Metabolism*. [S.l: s.n.], 2017a

PULESTON, D. J.; VILLA, M.; PEARCE, E. L. Ancillary Activity: Beyond Core Metabolism in Immune Cells. *Cell Metabolism*. [S.l: s.n.], 2017b

RAFFERTY, S.; MALECH, H. L. High reductase activity of recombinant NOS2 flavoprotein domain lacking the calmodulin binding regulatory sequence. *Biochemical and Biophysical Research Communications*, v. 220, n. 3, p. 1002–1007, mar. 1996.

RATH, M. et al. Metabolism via arginase or nitric oxide synthase: Two competing arginine pathways in macrophages. *Frontiers in Immunology*. [S.l: s.n.], 2014

RIBAS, V.; GARCÍA-RUIZ, C.; FERNÁNDEZ-CHECA, J. C. Glutathione and mitochondria. *Frontiers in Pharmacology*. [S.l: s.n.], 2014

RICHARDSON, J. L. et al. Improved tricyclic inhibitors of trypanothione reductase by screening and chemical synthesis. *ChemMedChem*, 2009.

- ROBERTS, S. C. et al. Arginase plays a pivotal role in polyamine precursor metabolism in *Leishmania*. Characterization of gene deletion mutants. *J Biol Chem*, v. 279, n. 22, p. 23668–23678, 2004.
- ROSENZWEIG, D. et al. Retooling *Leishmania* metabolism: from sand fly gut to human macrophage . *The FASEB Journal*, 2008a.
- ROSENZWEIG, D. et al. Retooling *Leishmania* metabolism: from sand fly gut to human macrophage . *The FASEB Journal*, 2008b.
- RYAN, D. G.; O'NEILL, L. A. J. Krebs Cycle Reborn in Macrophage Immunometabolism. *Annual Review of Immunology*. [S.l: s.n.]. , 2020
- SAINI, P. et al. Hypusine-containing protein eIF5A promotes translation elongation. *Nature*, 2009.
- SAUDAGAR, P. et al. Molecular mechanism underlying antileishmanial effect of oxabicyclo[3.3.1]nonanones: Inhibition of key redox enzymes of the pathogen. *European Journal of Pharmaceutics and Biopharmaceutics*, 2013.
- SAUDAGAR, P.; DUBEY, V. K. Cloning, expression, characterization, and inhibition studies on Trypanothione Synthetase, a drug target enzyme, from *Leishmania donovani* . *Biological Chemistry*, 2011a.
- SAUDAGAR, P.; DUBEY, V. K. Cloning, expression, characterization, and inhibition studies on Trypanothione Synthetase, a drug target enzyme, from *Leishmania donovani* . *Biological Chemistry*, 2011b.
- SAUNDERS, E. C. et al. *Leishmania mexicana* can utilize amino acids as major carbon sources in macrophages but not in animal models. *Molecular Microbiology*, 2018a.
- SAUNDERS, E. C. et al. *Leishmania mexicana* can utilize amino acids as major carbon sources in macrophages but not in animal models. *Molecular Microbiology*, 2018b.
- TAKAO, K. et al. A conceptual model of the polyamine binding site of N 1-acetylpolyamine oxidase developed from a study of polyamine derivatives. *Amino Acids*, 2009.
- TANNAHILL, G. M. et al. Succinate is an inflammatory signal that induces IL-1beta through HIF-1alpha. *Nature*, v. 496, n. 7444, p. 238–242, 2013.
- THOMAS, T.; THOMAS, T. J. Polyamines in cell growth and cell death: Molecular mechanisms and therapeutic applications. *Cellular and Molecular Life Sciences*. [S.l: s.n.]. , 2001
- THOMPSON, R. W. et al. Cationic amino acid transporter-2 regulates immunity by modulating arginase activity. *PLoS Pathog*, v. 4, n. 3, p. e1000023, 2008.
- TRAN, A. N. et al. Trypanothione synthetase locus in *Trypanosoma cruzi* CL Brener strain shows an extensive allelic divergence. *Acta Tropica*, 2003.
- VAN DEN BOSSCHE, J.; BAARDMAN, J.; DE WINTHER, M. P. J. Metabolic characterization of polarized M1 and M2 bone marrow-derived macrophages using real-time extracellular flux analysis. *Journal of Visualized Experiments*, 2015a.
- VAN DEN BOSSCHE, J.; BAARDMAN, J.; DE WINTHER, M. P. J. Metabolic characterization of polarized M1 and M2 bone marrow-derived macrophages using real-time extracellular flux analysis. *Journal of Visualized Experiments*, 2015b.
- VELASQUEZ, L. G. et al. Distinct courses of infection with *Leishmania (L.) amazonensis* are observed in BALB/c, BALB/c nude and C57BL/6 mice. *Parasitology*, v. 143, n. 6, p. 692–703, 2016.
- VERGADI, E. et al. Akt Signaling Pathway in Macrophage Activation and M1/M2 Polarization. *The Journal of Immunology*, 2017a.
- VERGADI, E. et al. Akt Signaling Pathway in Macrophage Activation and M1/M2 Polarization. *The Journal of Immunology*, 2017b.

- VIOLA, A. et al. The metabolic signature of macrophage responses. *Frontiers in Immunology*. [S.l: s.n.], 2019
- VOGEL, D. Y. S. et al. Human macrophage polarization in vitro: Maturation and activation methods compared. *Immunobiology*, 2014.
- WANASEN, N.; SOONG, L. L-arginine metabolism and its impact on host immunity against *Leishmania* infection. *Immunol Res*, v. 41, n. 1, p. 15–25, 2008.
- WANG, N.; LIANG, H.; ZEN, K. Molecular mechanisms that influence the macrophage m1-m2 polarization balance. *Front Immunol*, v. 5, p. 614, 2014.
- WHYTE, C. S. et al. Regulation of alternative (M2) macrophage activation by Suppressor of Cytokine Signalling (SOCS) 1. *Immunology*, 2010.
- WU, G. et al. Proline metabolism in the conceptus: implications for fetal growth and development. *Amino Acids*, Wu, G Bazer, F W Datta, S Johnson, G A Li, P Satterfield, M C Spencer, T E eng 1R21 HD049449/HD/NICHD NIH HHS/ 5P30ES09106/ES/NIEHS NIH HHS/ R25 CA90301/CA/NCI NIH HHS/ Austria *Amino Acids*. 2008 Nov;35(4):691-702. doi: 10.1007/s00726-008-0052-7. Epub 2008 Mar 11., v. 35, n. 4, p. 691–702, 2008.
- ZHENG, X. et al. Correction of arginine metabolism with sepiapterin—the precursor of nitric oxide synthase cofactor BH4—induces immunostimulatory-shift of breast cancer. *Biochemical Pharmacology*, 2020.

Capítulo 5

A ausência de NNT mitocondrial piora a capacidade de camundongos resolverem a infecção com *Leishmania amazonensis*

O texto apresentado a seguir é um manuscrito original a ser publicado em periódico. E não está disponível online.

Autores: Stephanie Maia Acuña, Jonathan Miguel Zanatta, Alicia Juliana Kowaltowski e Sandra Marcia Muxel

Título original:

Mitochondrial NNT ablation worsens mice's ability to clear *Leishmania amazonensis* infection.

Resumo

Macrófagos necessitam de energia para lidar com estímulos que os ativam ou estressam, assim como a infecção com *Leishmania amazonensis*. Este protozoário parasita induz a modulação de fenótipos macrofágicos intermediários ao pró-inflamatório e anti-inflamatório. Quando ativados, a produção de espécies reativas de oxigênio ou nitrogênio podem promover um desbalanço redox se os sistemas antioxidantes não estiverem suficientemente ativos. Mitocôndrias expressam a Trans-hidrogenase de Nucleotídeos de Nicotinamida (NNT), enzima produtora de NADPH a partir de NADH, usando a força iônica o transporte de H⁺ do espaço intermembrana para a matriz mitocondrial para produzir tal molécula. O NADPH pode ser usado pela célula na reciclagem de glutatona e das tioredoxinas na matriz da organela. A ausência da enzima não é letal, porém reduz a capacidade de remoção de antioxidantes mitocondriais. De fato, camundongos mutante no locus de *Nnt* são mais propensos a desenvolverem síndromes metabólicas. Como a infecção com *L. amazonensis* induz a produção de espécies reativas, nós hipotetizamos que a ausência da enzima impactaria negativamente na resistência/susceptibilidade, promovendo a sobrevivência do parasita. Nós usamos as linhagens de camundongo C57BL/6Tac (*Nnt*^{WT}), C57BL/6J (*Nnt*^{-/-}) e B6.129P2-*Nos2*^{tm/Lau/J} (*Nos2*^{-/-} - controle suscetível) para o estudo. Macrófagos derivados de medula óssea de ambas as linhagens foram infectados com *L. amazonensis* e tiveram o curso da infecção observado por 4, 24, 48 e 72 h. Nós observamos que macrófagos *Nnt*^{-/-} e *Nos2*^{-/-} apresentaram taxas de infectividade similares. nós também acompanhamos a infecção in vivo nas patas traseiras desses animais durante 8 semanas. Ambas a linhagens mutantes apresentaram lesões de espessuras similares em todos os tempos testados. Nossos dados sugerem que o ambiente redox desregulado causado pela mutação no locus de *Nnt* produz um fenótipo de susceptibilidade comparável à ausência de *Nos2*, piorando o prognóstico da infecção. Os dados apresentados dão luz a um novo aspecto na relação entre parasita e hospedeiro, na qual o balanço redox mitocondrial é um fator essencial.

Abstract

Macrophages need to be fuelled to cope with activating and stress stimuli, like *Leishmania amazonensis* infection. This protozoan parasite induces macrophage expression of a blended phenotype, between pro and anti-inflammatory (M1 and M2, respectively). Cytosolic reactive oxygen/nitrogen species production associated with activation can promote redox imbalance if antioxidant systems are not sufficiently active. Mitochondria express Nicotinamide Nucleotide Transhydrogenase (NNT), which produces NADPH from NADH using H⁺ transmembrane transport from intermembrane space to the matrix as a driving force. This NADPH can be used to recycle glutathione or thioredoxin systems in the organellar matrix. The absence of this enzyme does not make mice unviable but reduces their mitochondrial antioxidant capacity. Indeed, mice with mutant *Nnt* are prone to develop metabolic syndromes. Since infection with *L. amazonensis* induces the production of reactive species, we hypothesized that the *Nnt* absence would negatively impact on parasite clearance, promoting its survival. Using C57BL/6Tac (*Nnt*^{WT}), C57BL/6J (*Nnt*^{-/-}) and B6.129P2-*Nos2*^{tm/Lau}/J (*Nos2*^{-/-} - a susceptible control) mouse strains; we infected macrophages with *L. amazonensis* and monitored the infection after 4, 24, 48 and 72 h. We observed that *Nnt*^{-/-} and *Nos2*^{-/-} macrophages showed a similar rate of infected macrophages, differing after 24 h when *Nnt*^{-/-} reduced this rate, although the number of amastigotes per infected macrophage was higher than *Nnt*^{WT}, and lower than *Nos2*^{-/-}. We also accompanied the *in vivo* infection of these mice strains for 8 weeks. Both mutant mice presented similar footpad thickness during all tested times. Our data suggest that the imbalanced redox environment promoted by NNT absence is comparable to nitric oxide synthase 2 (NOS2) absence, worsening parasite clearance ability. The data presented bring forward a new aspect regarding the relationship between host and parasite, by indicating that mitochondrial redox balance is an essential player in this process.

Introduction

Leishmaniasis is a disease complex caused by the genus *Leishmania* spp. protozoan parasites. They infect phagocytic cells such as macrophages. *Leishmania* PAMPs promote metabolic reprogramming upon macrophage activation (MAMANI-HUANCA *et al.*, 2021b; MUXEL, SANDRA MARCIA *et al.*, 2019b; TY *et al.*, 2019). The macrophage starts producing ATP in a glycolysis-dependent way, repressing oxidative phosphorylation (OXPHOS), and producing reactive species of oxygen (ROS) and nitrogen (RNS), as a response against the parasite's harmful signals (OSPINA; GUAY-VINCENT; DESCOTEAUX, 2022). The ROS and RNS production help the macrophage to kill the parasite.

However, the disbalance in the redox system causes harm to both host and pathogen biochemical structures, such as proteins, lipids, or polymers as the DNA molecule. As a way to prevent harm, the host immune cells have a system to clear the reactive species and prevent damage, in which some mechanisms rely on nicotinamide adenine dinucleotide phosphate (NADPH) oxidization. The main source of the mitochondrial NADPH pool is the enzyme Nicotinamide Nucleotide Transhydrogenase (NNT), which is coupled with the mitochondrial inner membrane potential to reduce NADP⁺ into NADPH (RONCHI, JULIANA APARECIDA *et al.*, 2016). Although, the C57BL/6J mice strain has a spontaneous mutation on the *Nnt* locus, being a natural knockout (HUANG *et al.*, 2006).

It has been shown that immune cells highly express NNT (RIPOLL *et al.*, 2012). Also, the classical LPS and IFN γ /LPS macrophage activation reduce NNT expression at transcriptional and protein levels time-dependently (RIPOLL *et al.*, 2012). Although, the mechanism in which the inflammation modulates the NNT function is still completely non-understood (REGAN; CONWAY; BHARATH, 2022).

This work aims to evaluate the impact of the NNT absence in the *Leishmania amazonensis* infection context. Comparing the C57BL/6J (*Nnt*^{-/-}) *in vitro* and *in vivo* infections with the susceptible *Nos2*^{-/-} and the resistant C57BL/6.Tac (WT) mice, we observed that the *Nnt* mutation worsens the infection outcome, turning a resistant strain into a susceptible one.

Materials and Methods

Animals

Female C57BL/6Tac mice (6–8 weeks old) were obtained from the Animal Center of the Medical School of the University of São Paulo. Female C57BL/6J (*Nnt*^{-/-}) and B6;129P2-Nos2tm1Lau/J (*Nos2*^{-/-}) were purchased from the *Biotério de Matrizes* – Immunology department of Institute of Biomedical Sciences of the University of São Paulo. All animals were maintained at the Animal Center of the Department of Physiology of the Institute of Bioscience of the University of São Paulo with access to food and water *ad libitum*.

Leishmania culture

L. amazonensis (MHOM/BR/1973/M2269) was grown at 25 °C in M199 medium (Gibco, Grand Island NY, USA), pH 7.0, supplemented with L-glutamine, 10% heat-inactivated fetal bovine serum, 0.25% hemin, 40 mM NaHCO₃, 100 μ M adenine, 40 mM HEPES, 100 U/mL penicillin and 100 μ g/mL streptomycin. The parasites' numbers were assessed with a Neubauer chamber.

BMDM harvesting and culture

The mice were euthanized inside a CO₂ chamber. Afterward, bone marrow was extracted from the femurs, tibias, and humeri by flushing with ice-cold PBS 1 x with a 24 G x 3/4 needle. The

cell suspension was separated with a 21 G x ½ needle, followed by centrifugation at 4 °C, 500 x g, for 10 minutes. The cells were resuspended in complete RPMI 1640 (LGC Biotechnologies, São Paulo, Brazil) supplemented with 10% heat-inactivated FBS (Gibco, South America), 0.5% Pen/Strep (1 U/mL), 2-mercaptoethanol (50 µM), L-glutamine (2 mM), sodium pyruvate (1 mM), and 10% L9-29 supernatant as a source of Macrophage Colony-Stimulating Factor (M-CSF). The cells were cultivated for 7 days at 34 °C, in 5% CO₂.

Macrophage infection

After the macrophage differentiation, cells were seeded into 24-well plates (1x10⁶ cells/well; SPL, Lifescience, Pocheon, Korea) or 8-well chamber slides (5x10⁴ cells/well; Millipore, Merck, Darmstadt, Germany). Then, stationary phase promastigotes were added into the wells at MOI 5:1. After 4 h, the cells were washed two times with PBS 1x at room temperature to clean the unphagocytosed parasites. The culture was maintained for 4 and 24 h. The cells were stimulated with LPS (100 ng/mL; Escherichia coli LPS serotype 0127:B8, Sigma-Aldrich, St Louis, MO) to induce M1-inflammatory macrophages.

Infection assessment

After 4 and 24 h of infection, the chamber slides were washed two times with PBS 1x and then fixed with acetone/methanol (1:1 v/v; Sigma-Aldrich, St Louis, MO) and incubated at -20 °C for 24 h, followed by Giemsa staining (Fast Panotic Kit, Laborclin, São Paulo). At least 600 macrophages were counted per well to achieve the parameters of Macrophage Infection Rate (infected macrophage/total macrophage), Amastigotes per infected macrophage, and the infection index.

RNA extraction and cDNA preparation

For RNA extraction, macrophages (3 x 10⁶) were mixed with 750 µL of Trizol (Ambion, Thermo Scientific) and 250 µL PBS 1x. Then, chloroform was added to separate the aqueous and organic phases. Following the manufacturer's instructions, the aqueous phase was added into miRNeasy (Qiagen, Hilden, Germany) columns. The extracted RNA was measured using Nanodrop (ND-100, Thermo Scientific) to reach a 200 ng/µL RNA solution. The total RNA was used to produce complementary DNA (cDNA) of mature mRNA, starting from 2 µg of RNA, we used random hexamer primer (1.5 µg/mL; Thermo Scientific), dNTP (10 µM; Fermentas, Thermo Scientific), RevertAid Reverse Transcriptase (200U; Thermo Scientific), and RiboLock (Thermo Scientific), to a final volume of 40 µL. The cycling protocol was used following the manufacturer's recommendations. All cycles were undertaken using Mastercycler Nexus Gradient (Eppendorf, Hamburg, Germany).

In vivo infection

Results

The NNT absence negatively impacts *Leishmania amazonensis* clearance in a resistant model *in vitro* and *in vivo*.

To understand how the absence of a functional NNT would impact the ability to control *in vitro* BMDM (bone marrow-derived macrophages) *L. amazonensis* infection, we infected macrophages with late stationary promastigotes and measured three infection parameters after 4-, 24-, 48-, and 72 hours. We observed that *Nnt*^{-/-} macrophages had similar infection rates to *Nos2*^{-/-} in all tested time points. The resistant strain presented around 40% of infected macrophages, while both susceptible strains presented an 80% population of infected

macrophages (fig.1 a). Also, the number of amastigotes inside the infected macrophages was higher in both susceptible strains, with an average of 5.78 amastigotes per macrophage, while the resistant strain presented 3.7 amastigotes per macrophage (fig.1 b). The product of both parameters gives us the infection index (fig.1 c), which shows the macrophage's ability to clear the infection. The infection index of the resistant strain is around 1.8 while the susceptible strains had an average index of 4. This information suggests that the NNT ablation negatively impacts these macrophages' parasite clearance and resistance.

We also infected mouse hind footpads with 10^6 late stationary promastigotes and measured the footpad thickness weekly for 8 weeks. We observed that both *Nnt*^{-/-} and *Nos2*^{-/-} showed the same behavior, during the observed period.

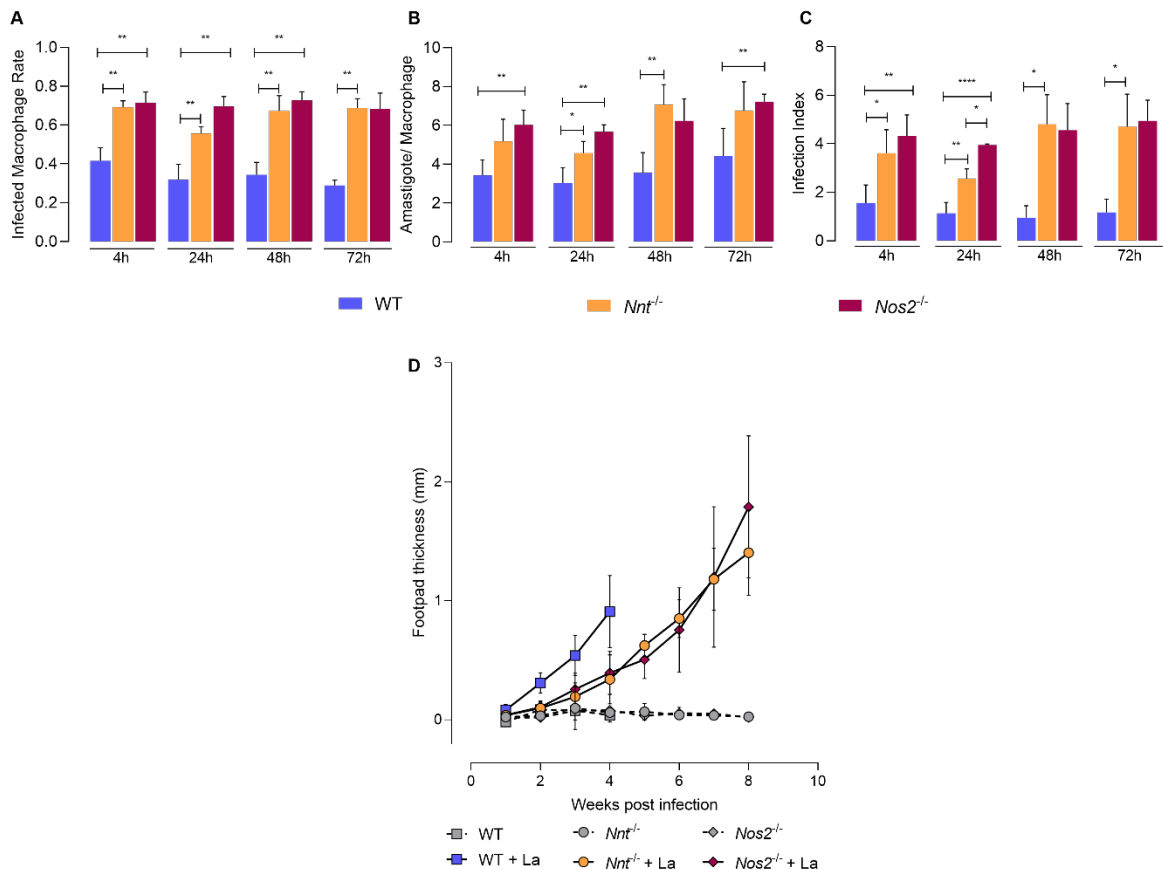


Figure 30. *In vitro*, and *in vivo*, infection with *L. amazonensis*. 2×10^5 BMDM were infected with late-stationary *L. amazonensis* promastigotes (MOI 1:5), then washed unphagocytosed parasites after 4h. Infected macrophages were fixed, and Giemsa stained to access infection parameters with a light microscope. (A) Infected macrophage rate. (B) The number of amastigotes per infected macrophage. (C) Infection Index. A-C statistics: 2-way ANOVA with Tukey's Comparison post hoc. *, $p \leq 0.05$. **, $p \leq 0.005$. ***, $p \leq 0.0005$. ****, $p \leq 0.0001$. $n = 600$ macrophages per well, 4 wells per condition. (D) 6–8-week-old females were infected with 1×10^6 stationary phase promastigotes in the left footpad and had weekly thickness measured with a pachymeter. Values in the y-axis represent Δ thickness (left footpad – right footpad). PBS 1x was used as the negative control.

Leishmania amazonensis infection reduces the *Nnt* transcripts amount.

To understand how the *Nnt*/NNT would impact *L. amazonensis* infection, we retrieved data from the BioProject numbers PRJNA481041 and PRJNA481042 where we identified the FPKM of *Nnt* in *L. amazonensis* infected BMDM after 4 h of infection (AOKI et al., 2019) We observed the basal levels of C57BL/6Tac is slightly lower than BALB/c basal *Nnt* levels (fig. 2-A). Besides, the parasite presence reduced the number of *Nnt* transcripts in both strains, suggesting that the inflammatory signalization impacts the number of *Nnt*. We also measured *Nnt* amounts through RT-qPCR to validate the transcriptomic data (fig. 2-B). C57BL/6Tac

BMDM was also stimulated with TLR agonists (LPS – TLR4; Poly-IC – TLR3 and Guardiquimod – TLR7/8) to identify possible inflammatory pathways in which the *Nnt* expression is regulated.

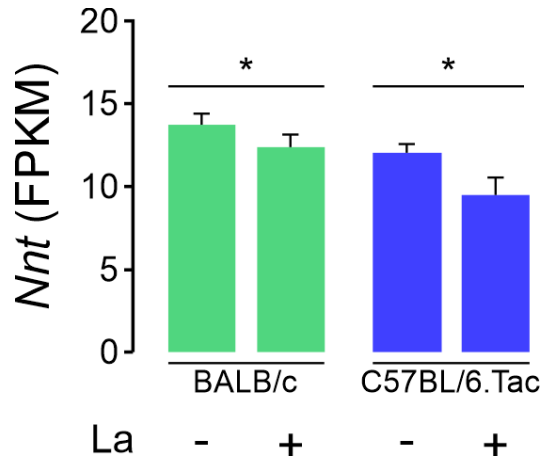


Figure 31. Expression of *Nnt* transcripts during BMDM *L. amazonensis* infection. (A) Transcriptomic BALB/c and C57BL/6Tac *Nnt* profile in FPKM...

Nnt^{-/-} macrophages present lower *Tnfa* amounts.

To understand if the *Nnt* mutation impacts the inflammatory signals, we measured the Tumor Necrosis Factor (*Tnfa*) number of transcripts of *L. amazonensis* infected macrophages (fig. 3). Both susceptible strains presented lower levels of *Tnfa* in all tested conditions compared to the resistant. However, *Nnt*^{-/-} macrophages presented lower *Tnfa* levels in relation to *Nos2*^{-/-} at basal levels and after 4 h of infection.

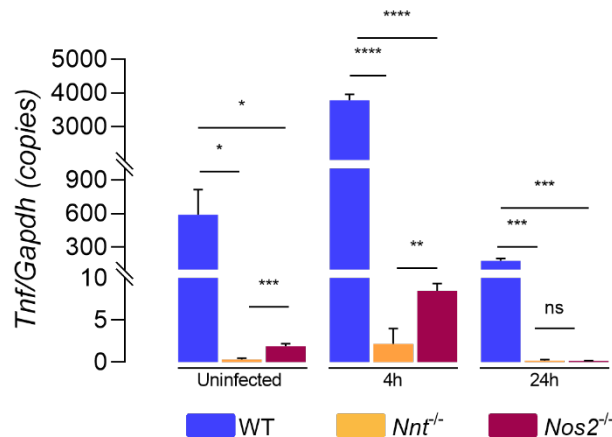


Figure 32. *Tnfa* transcripts behavior in *L. amazonensis* BMDM infection. 3x10⁶ BMDM were infected with late-stationary *L. amazonensis* promastigotes (MOI 1:5), then washed unphagocytosed parasites after 4h. After 4 or 24 h of infection, total RNA was extracted, converted to cDNA, and quantified to access the number of *Tnfa* copies with absolute quantification. Statistics: 2-way ANOVA with Tukey's Comparison post hoc. *, $p \leq 0.05$. **, $p \leq 0.005$. ***, $p \leq 0.0005$. ****, $p \leq 0.0001$.

Discussion

Cellular and mitochondrial redox homeostasis is guaranteed by reactive species detoxification. As the inflammatory response produces ROS and RNS, the *Leishmania-infected* macrophages need to prevent damage yet clear the parasite. The NADPH oxidase enzymes and Nitric Oxide Synthase 2 are the main reactive species source (JHA et al., 2015; VAN ASSCHE et al., 2011). In addition, mitochondrial production also helps the cell to control the infection by producing ROS at the Electron Transfer Chain Complex I (DUBOUCHAUD et al., 2018) or delivering Mitochondria-derived vesicles (MDV) to the phagolysosome, sustaining the H₂O₂ internal phagosome concentration (ABUAITA; SCHULTZ; O'RIORDAN, 2018; REGAN; CONWAY; BHARATH, 2022; WANG et al., 2021). However, excessive reactive species production can lead to cellular and tissue damage.

As the inflammatory response needs to be regulated, the reactive species production also needs to be controlled. The e⁻ donation to molecular oxygen generates the superoxide anion (O₂⁻), which is disabled into H₂O₂, but the mitochondria do not express catalase (BAI et al., 1999; BAI; CEDERBAUM, 2001; RADI et al., 1991; WANG et al., 2021). The hydrogen peroxide needs to be cleared by other systems, such as glutathione and thioredoxin oxidization and reduction reactions. The reduced glutathione (GSH) exists in a higher concentration, being available to be oxidized by enzymes that pick an electron (e⁻) and form a disulfide ligation between 2 GSH while donors the e⁻ to the H₂O₂, resulting in H₂O and the oxidized glutathione (GSSG) (DICKINSON; FORMAN, 2002). The same is observed in thioredoxins, oxidized and reduced proteins during the H₂O₂ dismutation (NORDBERG; ARNÉR, 2001). Additionally, glutathione and thioredoxins turnover depend on the NADPH concentration. On the cytoplasm, the pentose-phosphate pathway provides the NADPH pool, while the mitochondrial pool relies on a system of three redundant pathways formed by Malate Dehydrogenase 3 (ME3), Isocitrate Dehydrogenase 2 (IDH2) and Nicotinamide Nucleotide Transhydrogenase (NNT). NNT is responsible for around 50% of mitochondrial NADPH production (RONCHI et al., 2016). Cells extracted from C57BL/6J mice do not express NNT (HUANG et al., 2006). Our group demonstrated before the C57BL/6Tac *L. amazonensis* infected BMDM have an altered redox state, as shown by the GSSG/GSH ratio, and the elevation of the GSSG amount, however, the concentration of GSH did not change (MAMANI-HUANCA et al., 2021).

It is well-established that infection with *Leishmania* impacts mitochondrial metabolism (ARANGO DUQUE; DESCOTEAUX, 2015; FERREIRA; ESTAQUIER; SILVESTRE, 2021; MOREIRA et al., 2015). But how the clearance of reactive species impacts the infection, or the parasite clearance remains unknown. Here we show the first evidence that the absence of NNT worsens the macrophagic ability to clear *L. amazonensis*. We observed that *L. amazonensis* infection reduces the *Nnt* transcripts amount, likewise, the results found by Ripoll *et al.* (RIPOLL et al., 2012) with the treatment with LPS and IFN γ /LPS, classical macrophage activation molecules.

Also, the *Nnt* ablation seems to be a worsening factor to control *in vivo* *L. amazonensis* infection (fig. 1). We observed that the natural *Nnt*^{-/-} mice have a similar infection course as the *Nos2*^{-/-} infected mice, suggesting that the NNT expression plays a protective role. Ripoll also demonstrated that NNT overexpression on RAW 264.7 macrophages reduced the expression of TNF α , IL-1 β , and IL-6 after 8 h of LPS treatment (RIPOLL et al., 2012). These cytokines are important to control leishmaniasis (ACUÑA et al., 2022; FERNANDES et al., 2019; LIMA-JUNIOR et al., 2013; WILHELM et al., 2001). Nevertheless, we observed the opposite in *L. amazonensis* expression since the *Nnt*^{-/-} BMDM presented a dramatically reduced *Tnfa* expression, in the same way, *Nos2*^{-/-} presented reduced *Tnfa*.

In cutaneous leishmaniasis caused by *L. mexicana* lesions, the more inflammatory signalization, the greater the lesion size (MELBY, ' et al., 1994). The same behavior is seen in mucocutaneous

leishmaniasis – caused majorly by *L. braziliensis*, where the lesion severity, palate, and nasal septum loss are related to the inflammatory response. There is a necessity to have a balance between pro-inflammatory and regulatory macrophages to control human skin lesions(SCORZA; CARVALHO; WILSON, 2017).

Taken together, our data suggest that the control of redox metabolism is necessary to control the immune response against *L. amazonensis*.

References

- ABUAITA, Basel H.; SCHULTZ, Tracey L.; O'RIORDAN, Mary X. Mitochondria-Derived Vesicles Deliver Antimicrobial Reactive Oxygen Species to Control Phagosome-Localized *Staphylococcus aureus*. **Cell Host & Microbe**, [S. l.], v. 24, n. 5, p. 625- 636.e5, 2018. DOI: 10.1016/J.CHOM.2018.10.005. Acesso em: 20 abr. 2023.
- ACUÑA, Stephanie Maia; ZANATTA, Jonathan Miguel; BENTO, Camilla de Almeida; FLOETER-WINTER, Lucile Maria; MUXEL, Sandra Marcia. miR-294 and miR-410 Negatively Regulate *Tnfa*, Arginine Transporter *Cat1/2*, and *Nos2* mRNAs in Murine Macrophages Infected with *Leishmania amazonensis*. **Non-Coding RNA** 2022, Vol. 8, Page 17, [S. l.], v. 8, n. 1, p. 17, 2022. DOI: 10.3390/NCRNA8010017. Disponível em: <https://www.mdpi.com/2311-553X/8/1/17/htm>. Acesso em: 25 abr. 2023.
- AOKI, J. I.; MUXEL, S. M.; ZAMPIERI, R. A.; MULLER, K. E.; NERLAND, A. H.; FLOETER-WINTER, L. M. Differential immune response modulation in early *Leishmania amazonensis* infection of BALB/c and C57BL/6 macrophages based on transcriptome profiles. **Sci Rep**, [S. l.], v. 9, n. 1, p. 19841, 2019. DOI: 10.1038/s41598-019-56305-1.
- ARANGO DUQUE, Guillermo; DESCOTEAUX, Albert. *Leishmania* survival in the macrophage: where the ends justify the means. **Current Opinion in Microbiology**, [S. l.], v. 26, p. 32–40, 2015. DOI: 10.1016/J.MIB.2015.04.007. Acesso em: 20 abr. 2023.
- BAI, Jingxiang; CEDERBAUM, Arthur I. Mitochondrial Catalase, and Oxidative Injury. **Biological Signals and Receptors**, [S. l.], v. 10, n. 3–4, p. 189–199, 2001. DOI: 10.1159/000046887. Disponível em: <https://karger.com/nsg/article/10/3-4/189/334938/Mitochondrial-Catalase-and-Oxidative-Injury>. Acesso em: 23 maio. 2023.
- BAI, Jingxiang; RODRIGUEZ, Ana M.; MELENDEZ, J. Andres; CEDERBAUM, Arthur I. Overexpression of catalase in cytosolic or mitochondrial compartment protects HepG2 cells against oxidative injury. **Journal of Biological Chemistry**, [S. l.], v. 274, n. 37, p. 26217–26224, 1999. DOI: 10.1074/jbc.274.37.26217. Disponível em: <http://www.jbc.org/article/S002192581955205X/fulltext>. Acesso em: 23 maio. 2023.
- DICKINSON, Dale A.; FORMAN, Henry Jay. Cellular glutathione and thiols metabolism. **Biochemical Pharmacology**, [S. l.], v. 64, n. 5–6, p. 1019–1026, 2002. DOI: 10.1016/S0006-2952(02)01172-3. Disponível em: <https://pubmed.ncbi.nlm.nih.gov/12213601/>. Acesso em: 17 jan. 2023.
- DUBOUCHAUD, Hervé; WALTER, Ludivine; RIGOLET, Michel; BATANDIER, Cécile. Mitochondrial NADH redox potential impacts the reactive oxygen species production of reverse Electron transfer through complex I. **Journal of Bioenergetics and Biomembranes**, [S. l.], v. 50, n. 5, p. 367–377, 2018. DOI: 10.1007/S10863-018-9767-7/FIGURES/5. Disponível em: <https://link.springer.com/article/10.1007/s10863-018-9767-7>. Acesso em: 20 abr. 2023.
- FERNANDES, Juliane Cristina Ribeiro; AOKI, Juliana Ide; MAIA ACUÑA, Stephanie; ZAMPIERI, Ricardo Andrade; MARKUS, Regina P.; FLOETER-WINTER, Lucile Maria; MUXEL, Sandra Marcia. Melatonin and *Leishmania amazonensis* Infection Altered miR-294, miR-30e, and miR-302d Impacting on *Tnf*, *Mcp-1*, and *Nos2* Expression. **Frontiers in Cellular and Infection Microbiology**, [S. l.], v. 9, 2019. DOI: 10.3389/fcimb.2019.00060. Disponível em: <https://www.frontiersin.org/article/10.3389/fcimb.2019.00060/full>.
- FERREIRA, Carolina; ESTAQUIER, Jérôme; SILVESTRE, Ricardo. Immune-metabolic interactions between *Leishmania* and macrophage host. **Current Opinion in Microbiology**, [S. l.], v. 63, p. 231–237, 2021. DOI: 10.1016/J.MIB.2021.07.012. Acesso em: 20 abr. 2023.
- HUANG, Ting-Ting; NAEEMUDDIN, Mohammed; ELCHURI, Sailaja; YAMAGUCHI, Mutsuo; KOZY, Heather M.; CARLSON, Elaine J.; EPSTEIN, Charles J. Genetic modifiers of the phenotype of mice deficient in mitochondrial superoxide dismutase. **Human**

Molecular Genetics, [S. l.], v. 15, n. 7, p. 1187–1194, 2006. DOI: 10.1093/hmg/ddl034. Disponível em: <http://academic.oup.com/hmg/article/15/7/1187/715422/Genetic-modifiers-of-the-phenotype-of-mice>. Acesso em: 16 jan. 2020.

JHA, Abhishek K. et al. Network integration of parallel metabolic and transcriptional data reveals metabolic modules that regulate macrophage polarization. **Immunity**, [S. l.], v. 42, n. 3, p. 419–430, 2015. DOI: 10.1016/J.IMMUNI.2015.02.005. Acesso em: 20 abr. 2023.

LIMA-JUNIOR, Djalma S. et al. Inflammasome-derived IL-1 β production induces nitric oxide-mediated resistance to Leishmania. **Nature medicine**, [S. l.], v. 19, n. 7, p. 909–15, 2013. DOI: 10.1038/nm.3221. Disponível em: <http://www.ncbi.nlm.nih.gov/pubmed/23749230>.

MAMANI-HUANCA, Maricruz; MUXEL, Sandra Marcia; ACUÑA, Stephanie Maia; FLOETER-WINTER, Lucile Maria; BARBAS, Coral; LÓPEZ-GONZÁLVEZ, Ángeles. Metabolomic reprogramming of c57bl/6-macrophages during early infection with *L. amazonensis*. **International Journal of Molecular Sciences**, [S. l.], v. 22, n. 13, 2021. DOI: 10.3390/ijms22136883.

MELBY, Peter C. et al. **Increased Expression of Proinflammatory Cytokines in Chronic Lesions of Human Cutaneous Leishmaniasis**. **INFECTION AND IMMUNITY**. [s.l.: s.n.]. Disponível em: <https://journals.asm.org/journal/iai>.

MOREIRA, Diana et al. Leishmania infantum Modulates Host Macrophage Mitochondrial Metabolism by Hijacking the SIRT1-AMPK Axis. **PLOS Pathogens**, [S. l.], v. 11, n. 3, p. e1004684, 2015. DOI: 10.1371/JOURNAL.PPAT.1004684. Disponível em: <https://journals.plos.org/plospathogens/article?id=10.1371/journal.ppat.1004684>. Acesso em: 20 abr. 2023.

MUXEL, Sandra Marcia; MAMANI-HUANCA, Maricruz; AOKI, Juliana Ide; ZAMPIERI, Ricardo Andrade; FLOETER-WINTER, Lucile Maria; LÓPEZ-GONZÁLVEZ, Ángeles; BARBAS, Coral. Metabolomic Profile of BALB/c Macrophages Infected with Leishmania amazonensis: Deciphering L-Arginine Metabolism. **International Journal of Molecular Sciences**, [S. l.], v. 20, n. 24, p. 6248, 2019. DOI: 10.3390/ijms20246248. Disponível em: <https://www.mdpi.com/1422-0067/20/24/6248>. Acesso em: 20 jan. 2020.

NORDBERG, Jonas; ARNER, Elias S. J. Reactive oxygen species, antioxidants, and the mammalian thioredoxin system. **Free Radical Biology and Medicine**, [S. l.], v. 31, n. 11, p. 1287–1312, 2001. DOI: 10.1016/S0891-5849(01)00724-9. Acesso em: 23 maio. 2023.

OSPINA, Hamlet Acevedo; GUAY-VINCENT, Marie Michèle; DESCOTEAUX, Albert. Macrophage Mitochondrial Biogenesis and Metabolic Reprogramming Induced by Leishmania donovani Require Lipophosphoglycan and Type I Interferon Signaling. **mBio**, [S. l.], v. 13, n. 6, 2022. DOI: 10.1128/MBIO.02578-22/SUPPL_FILE/MBIO.02578-22-S0009.TIF. Disponível em: <https://journals.asm.org/doi/10.1128/mbio.02578-22>. Acesso em: 20 abr. 2023.

RADI, R.; TURRENS, J. F.; CHANG, L. Y.; BUSH, K. M.; CRAPO, J. D.; FREEMAN, B. A. Detection of catalase in rat heart mitochondria. **Journal of Biological Chemistry**, [S. l.], v. 266, n. 32, p. 22028–22034, 1991. DOI: 10.1016/S0021-9258(18)54740-2. Acesso em: 23 maio. 2023.

REGAN, Thomas; CONWAY, Rachel; BHARATH, Leena P. Regulation of immune cell function by nicotinamide nucleotide transhydrogenase. **American Journal of Physiology - Cell Physiology**, [S. l.], v. 322, n. 4, p. C666–C673, 2022. DOI: 10.1152/AJPCELL.00607.2020. Disponível em: www.ajpcell.org. Acesso em: 20 abr. 2023.

RIPOLL, Vera M.; MEADOWS, Nicholas A.; BANGERT, Mathieu; LEE, Angela W.; KADIOGLU, Aras; COX, Roger D. Nicotinamide nucleotide transhydrogenase (NNT) acts as a novel modulator of macrophage inflammatory responses. **The FASEB Journal**, [S. l.], v.

26, n. 8, p. 3550–3562, 2012. DOI: 10.1096/FJ.11-199935. Disponível em: <https://onlinelibrary.wiley.com/doi/full/10.1096/fj.11-199935>. Acesso em: 20 abr. 2023.

RONCHI, Juliana Aparecida; FRANCISCO, Annelise; PASSOS, Luiz Augusto Correa; FIGUEIRA, Tiago Rezende; CASTILHO, Roger Frigério. The Contribution of Nicotinamide Nucleotide Transhydrogenase to Peroxide Detoxification Is Dependent on the Respiratory State and Counterbalanced by Other Sources of NADPH in Liver Mitochondria. **Journal of Biological Chemistry**, [S. l.], v. 291, n. 38, p. 20173–20187, 2016. DOI: 10.1074/JBC.M116.730473. Acesso em: 20 abr. 2023.

SCORZA, Breanna M.; CARVALHO, Edgar M.; WILSON, Mary E. Cutaneous Manifestations of Human and Murine Leishmaniasis. **International Journal of Molecular Sciences** 2017, Vol. 18, Page 1296, [S. l.], v. 18, n. 6, p. 1296, 2017. DOI: 10.3390/IJMS18061296. Disponível em: <https://www.mdpi.com/1422-0067/18/6/1296/htm>. Acesso em: 20 abr. 2023.

TY, Maureen C.; LOKE, Ping; ALBEROLA, Jordi; RODRIGUEZ-CORTES, Alheli; RODRIGUEZ-CORTES, Alheli. Immuno-metabolic profile of human macrophages after Leishmania and Trypanosoma cruzi infection. **PLoS ONE**, [S. l.], v. 14, n. 12, 2019. DOI: 10.1371/JOURNAL.PONE.0225588. Disponível em: [/pmc/articles/PMC6913957/](https://pubmed.ncbi.nlm.nih.gov/33913957/). Acesso em: 20 abr. 2023.

VAN ASSCHE, Tim; DESCHACHT, Maartje; DA LUZ, Raquel A. Inoc??ncio; MAES, Louis; COS, Paul. Leishmania-macrophage interactions: Insights into the redox biology. **Free Radical Biology and Medicine**, [S. l.], v. 51, n. 2, p. 337–351, 2011. DOI: 10.1016/j.freeradbiomed.2011.05.011. Disponível em: <http://dx.doi.org/10.1016/j.freeradbiomed.2011.05.011>.

WANG, Yafang; LI, Na; ZHANG, Xin; HORNG, Tiffany. Mitochondrial metabolism regulates macrophage biology. **Journal of Biological Chemistry**, [S. l.], v. 297, n. 1, p. 297–298, 2021. DOI: 10.1016/J.JBC.2021.100904. Disponível em: <http://www.jbc.org/article/S0021925821007043/fulltext>. Acesso em: 20 abr. 2023.

WILHELM, Patricia; RITTER, Uwe; LABBOW, Stefanie; DONHAUSER, Norbert; RÖLLINGHOFF, Martin; BOGDAN, Christian; KÖRNER, Heinrich. Rapidly Fatal Leishmaniasis in Resistant C57BL/6 Mice Lacking TNF. **The Journal of Immunology**, [S. l.], v. 166, n. 6, p. 4012–4019, 2001. DOI: 10.4049/JIMMUNOL.166.6.4012. Disponível em: <https://journals.aai.org/jimmunol/article/166/6/4012/70389/Rapidly-Fatal-Leishmaniasis-in-Resistant-C57BL-6>. Acesso em: 17 jan. 2023.

Capítulo 6

Imunometabolismo de Células Dendríticas iCD103⁺ infectadas com *Leishmania infantum*

O texto apresentado a seguir é um manuscrito original a ser publicado em periódico. E não está disponível online.

Autores: Stephanie Maia Acuña, Sandra Marcia Muxel e Ricardo Silvestre

Título original:

Immunometabolic Networks during dendritic cell-*Leishmania* interactions

Resumo

A relação estabelecida entre *Leishmania* e seus hospedeiros é complexa e resultante de um longo processo co-evolutivo. Tal processo dá-se pelas constantes alterações repentinas impostas pelo hospedeiro ao microambiente, como a interação metabólica entre ambos que deve ser ajustada constantemente. A espécie *Leishmania infantum* é conhecida por ser uma causadora de leishmaniose visceral, pois infecta fagócitos de órgãos como baço, fígado e medula óssea, subvertendo a resposta inflamatória. Neste trabalho nós focamos em Células Dendríticas (DCs), que são as principais responsáveis pela conversão da resposta imune inata para a adaptativa. Além disso, o perfil metabólico de DCs durante infecções é um campo aberto para estudos. Ainda que as DCs formem uma classe heterogênea de células, a maior parte das DCs esplênicas convencionais expressam CD8a; e, CD103 dependentemente de Batf3 (Fator de Transcrição Básico 3), sendo um subgrupo profissional em apresentação antigênica cruzada. Neste trabalho, nós produzimos DCs que expressam CD103 de maneira induzida (iCD103⁺-DCs) a partir da medula óssea de camundongos C57BL/6J. Então as iCD103⁺-DCs foram infectadas com *Leishmania infantum* a fim de avaliarmos as variações no fluxo metabólico destas células. Nós identificamos uma alta expressão de MHC-II e CD86, ambos marcadores de maturidade em iCD103⁺-DCs incubadas com antígenos de *L. infantum*. Essas células também apresentaram um aumento no consumo de glicose e produção de lactato nas células co-cultivadas com parasitas viáveis ou mortos por calor, um comportamento similar ao apresentado por células estimuladas com LPS nas primeiras 8 h de estimulação. O perfil transcriptômico de iCD103⁺-DCs infectadas apresentou uma regulação positiva de genes associados com o metabolismo energético, em especial no consumo de glicose após 24 h de infecção. Nós também observamos um aumento na carga parasitária quando essas células foram tratadas com 2-desoxiglicose (2-DG). Nossos dados sugerem que iCD103⁺-DCs usam a glicose como a maior fonte de energia após a ativação causada pela infecção com *L. infantum*.

Abstract

The dynamic and complex metabolic coupling established between *Leishmania* and its host results from a long co-evolutionary process. Due to the constant and sudden alterations imposed by the host microenvironment, such metabolic coupling continues to be dynamically regulated. *Leishmania infantum* is known to cause visceral leishmaniasis, infecting the spleen, liver, and bone-marrow phagocytic cells, subverting their response against the parasite. In this work, we focus on Dendritic Cells (DCs), which are important players in the conversion of innate to adaptive immune response, and whose metabolic profile during general infections are an open field of study. Although DCs are a heterogeneous cell class, the splenic conventional DCs can express CD8a and CD103 in a *Batf3* (Basic transcription factor 3) dependent manner, being professional cross-antigen presenters. Here, we induced CD103 DCs (iCD103-DCs) from C57BL/6J mice bone marrow infected with *L. infantum* to evaluate DCs metabolic shifts related to infection. We identified a high expression of maturity markers MHC-II/CD86 on iCD103-DCs incubated with *L. infantum* antigens. Also, we showed increased consumption of glucose and lactate production in the iCD103-DCs co-cultured with viable or heat-killed *L. infantum*, in a similar way with LPS stimulation at the first 8 h of analysis. The transcriptomic analysis of *L. infantum*-infected iCD103-DCs revealed an upregulation of genes associated with glucose and energetic metabolic pathways after 24h of infection. We also observed an increase in parasite burden when treated iCD103-DCs with 2-DG (2-deoxyglucose). Our data suggest that iCD103-DCs can use glucose as their main energy source when infected with *L. infantum*.

Introduction

Leishmaniasis is a complex group of diseases caused by the protozoan parasite of the *Leishmania* sp. genus. In humans, there are 20 species that cause leishmaniasis, divided into three types: cutaneous, mucocutaneous, and visceral; the latter being the most aggressive form of the disease. In Brazil, cases of visceral leishmaniasis are caused by the species *Leishmania infantum*. The parasite has a simple life cycle, dependent on two hosts. Sandflies, invertebrate hosts, hold the promastigote form – elongated and flagellated. These transmit the parasite to vertebrate hosts through the blood meal, in which the infecting forms are rapidly phagocytosed by phagocytic cells and inside them, the parasite differentiates into amastigotes – rounded forms with no apparent flagellum. These are obligate intracellular parasites, infecting phagocytic cells such as neutrophils, macrophages, and dendritic cells.

Macrophages and Dendritic Cells (DC) are classified as professional antigen-presenting cells, with dendritic cells being even more specialized in this process. DCs are responsible for the presentation of antigens to T cells, being an important mediator of the activation of the adaptive immune response. Like macrophages, they may have a myeloid origin, being possible to cultivate them through the stimulation of cells extracted from the bone marrow of mice.

The metabolic activities of immune cells have been demonstrated, over the last few years, as a determining factor in the ability to respond to various stimuli, whether associated with pathogens, damage, tissue repair or maintenance of homeostasis. Thus, studying the relationships between pathogens and hosts gains a new light

Therefore, the objective of this study period is to analyze the parasite-host relationship under the metabolic aspect, in order to identify how these cells react to infection.

Objectives and tasks

As the causality in the immunometabolic connections during infection remains poorly tested, we propose employing an integrative approach to map the *Leishmania*-induced shifts in metabolic networks in dendritic cells, deciphering the molecular mechanisms of this phenomenon and establishing its causal relationship with the anti-leishmanial immune response mediated by both cells. Using *L. infantum* infection as a model, we test the novel postulate that manipulating metabolic programs or the signals that regulate them holds the key to redirect the course of pathogenesis or recovery decisively.

Specific objectives:

- To elucidate the immunometabolic network in *L. infantum*-infected dendritic cells relating the metabolic influences on resistance or susceptibility.
- To discover the metabolic causality of host-protective immune response and infection outcome.

By combining ground-breaking technologies, a scarcely explored perspective on host-pathogen interactions and a multidisciplinary and integrated approach, by the end of this project, we will:

1. generate the first comprehensive view on how *L. infantum* differentially modulate dendritic cell metabolic network to influence anti-leishmanial immune response.
2. identify the central metabolic nodes that can be future targets for innovative prognostic, diagnostic, immunometabolic and therapeutic approaches.

Task 1 – Analysis of *L. infantum*-infected dendritic cells metabolism

As other obligate intracellular pathogens, *Leishmania* spp. must intimately rewire host cellular pathways to their own ends to maintain infectivity. We anticipate that the outcome of leishmaniasis can be decisively influenced by the host immunometabolic profile upon and during infection. We aim to prepare an interactive map with completed host metabolic profile by analysing perturbations of its structure induced by *Leishmania* parasites, achieved by integrating metabolic pathway analysis on results obtained from combined metabolic, flow cytometry immunophenotyping and transcriptomic profiling.

Task 2 – Immunometabolic crosstalk upon infection

After identifying transcript/metabolic central nodes in Task 1, we aim to target some of them to assess their role in the infection control or create a permissive intracellular environment for parasite survival. Choosing two or three nodes, we will evaluate their importance through pharmacological modulation or genetic modification, which will be chosen at the proper time.

Materials and methods

Mice

Wild-type C57BL/6 purchased from Charles River Laboratories; were bred and maintained in accredited animal facilities at the Life and Health Sciences Research Institute (ICVS). They will be housed in groups of 3-6, in HEPA filter-bearing cages, under 12-h light/dark cycles. Autoclaved chow and water were provided *ad libitum* and enriched cages with nesting materials (paper towels). Males and females with 8-12 weeks are used. Experimental animal procedures agreed with the European Council Directive (2010/63/EU) guidelines that were transposed into Portuguese law (Decree-Law n.º113/2013, August 7th). Experiments are conducted with the UMinho Ethical Committee (process no. SECVS 074/2016) and complied with the guidelines of the Committee and National Council of Ethics for the Life Sciences (CNECV). RS has accreditation for animal research given from Portuguese Veterinary Direction (Ministerial Directive 1005/92).

Parasite culture and staining

Leishmania infantum (ITMAP 263) promastigotes were maintained with weekly sub passages at 26°C in complete RPMI 1640 medium, supplemented with 10% heat-inactivated fetal bovine serum, 2 mM L-glutamine, 100 U/ml penicillin plus 100 mg/ml streptomycin and 20 mM HEPES buffer, until they reach ten passages. *L. infantum* promastigotes were stained with carboxyfluorescein succinimidyl ester (CFSE), or Tag-it Violet Proliferation Cell Tracking Dye (Biolegend). The parasites were centrifuged and washed twice with warm phosphate-buffered saline (PBS) twice, centrifuged, and resuspended in a solution of PBS with 5 mM CFSE or 20 µM Tag-it Violet (10×10^6 parasites/ml of PBS) and proceeded to incubation at 37°C for 10 minutes if CFSE labelling, or for 20 minutes if Tag-it violet labelling. Afterwards, parasites were washed with PBS to quench fluorescence excess and suspended in complete RPMI. Parasite numbers are assessed by counting on Neubauer's chamber. Uninfected DCs were used as negative control. Heat-killed parasites (56°C for 40 minutes) were used as positive control.

Dendritic cell culture and infection

The generation of induced CD103-Dendritic Cells was performed by murine bone marrow (BM) differentiation. The BM was harvested through needle washing and cultured in complete RPMI 1640 medium, supplemented with 10% heat-inactivated FBS, 50 µM 2-mercaptoethanol, and 100 U/ml penicillin plus 100 mg/ml streptomycin. At day zero, 15×10^6 BM cells were plated in a 10 cm² Petri dish to be cultured in the presence of the growth factor GM-CSF (5 ng/mL – PeproTech) and FLT3L (200 ng/mL – PeproTech) to induce Dendritic Cells proliferation and differentiation. After 5/6 days complete RPMI, with no growth factor, was added to avoid cell death. On day 9, the cells had the medium renewed by replating 3×10^6 cells in a new Petri dish, containing complete RPMI plus growth factors. The cells were, then, left in culture until it reached day 15, when DCs were counted and divided into 96-well U-bottom plate, without washing or changing the medium; and left overnight to rest. On day 16, cells were labelled with surface markers – CD103, CD11c, MHC-II, and CD86 – to confirm the iDC-CD103⁺ population. Then, the cells were infected with stationary phase promastigotes of *L. infantum* using the multiplicity of infection (MOI) equal 1:2, 1:5 or 1:10. As DCs are a semi-adherent population, after 4 hours of infection, the non-phagocytosed parasites were washed out 2 times through 1500 x g centrifugation for 5 minutes at room temperature, resuspended in PBS. After the last centrifugation, DCs were resuspended in complete RPMI and left for 24h, when essays will be performed.

Flow cytometry

Bodipy 493/503 (3 mg/ml) and Bodipy FL C16 (1 mM) were diluted in complete media and added to adherent cells for 30 minutes at 37°C. DAF-FM (2 mg/ml) was diluted in PBS and incubated for 30 minutes at 37°C. The cells were then washed with PBS, detached and analysed. Before analysis, cells stained with DAF-FM were left to rest for 20 minutes, to complete de-esterification of intracellular diacetates. Surface staining was performed with the following antibodies: BV605 anti-mouse CD11c, clone N418; APC anti-mouse I-A/I-E, clone M5/114.15.2; BV785 anti-mouse NK1.1, clone PK136; PE/Cy7 anti-mouse CD11b, clone M1/70; BV711 anti-mouse Ly6G, clone 1A8; PerCP/Cy5.5 anti-mouse Ly6C, clone HK14. Samples were acquired on an LSR II flow cytometer (BD Biosciences), and data analysed using FlowJo software.

High-performance liquid chromatography

Glucose and lactate were quantified in the cell culture supernatant using HPLC technology (Gilson bomb system); HyperREZ XP Carbohydrate H+ 8 μ M. Samples were filtered with a 0.2 mm filter and the mobile phase (0.0025M H₂SO₄) is similarly filtered and degasified for 40 minutes. Each sample is analyzed using the following running protocols (sensitivity 8): 15 min at a constant flux of 0.7 mL/min at 54 °C for glucose and lactate detection. The peaks are detected in a refractive index detector (IOTA 2, Reagents), and integration will be performed using Gilson Uniprot Software, version 5.11.

RNA sequencing

Reads are trimmed using Trimmomatic v0.36 with the following options: TRAILING:30, SLIDINGWINDOW:4:20 and MINLEN:30. All other options used the default values. Quality check was performed on raw and trimmed data to ensure the quality of the reads using FastQC v0.11.5 and MultiQC v1.5. The quantification is performed with Kallisto v0.44. Differential expression analysis is performed in R v3.5.0 using the DESeq2 v1.20.0 and volcano plots are produced with the ggplot2 package.

Quantification and statistical analysis

Statistical analyses were performed with the GraphPad Prism 8 software. A one-way analysis of variance (ANOVA) followed by a Bonferroni's post hoc test was employed for multiple group comparisons. A Mann-Whitney test of variance and Kruskal-Wallis non-parametric test were performed accordingly with the correspondent experimental design. The statistical details of each experiment can be found in figure legends, and the data is presented as mean \pm SD. Statistically significant values are as follows: * $p < 0.05$, ** $p < 0.01$, *** $p < 0.001$.

Results and Discussion

In vitro iCD103-DC differentiation

The Dendritic Cell class is a complex group of immune cells, which functions, and activities are still under study. They are tissue-resident and commonly referred to as sentinel leukocytes, playing a key role in the shifting between innate to adaptive immune response since they are well a known professional antigen presenter, priming T lymphocytes into their effector activities (CABEZA-CABRERIZO *et al.*, 2021). However, many cells are put under the DC umbrella, causing confusion, and misunderstanding regarding their characteristics.

In 1992, a protocol to differentiate DCs from murine bone marrow was published. It was the simple addition of GM-CSF into the bone marrow cells culture (INBA *et al.*, 1992) and in some cases the culture with more cytokines to improve the quality of DCs yield. However, it was found that these cultures were not pure DCs cultures as it was expected, but a mixture of DC-like cells and other myeloid cells that were not fully differentiated into DCs or macrophages (HELFT *et al.*, 2015). It shed light on many works that were published with DCs that were not DCs. However, in parallel, it was found that fully differentiated plasmacytoid cells and DCs was achieved using FMS-like Tyrosine Kinase 3 Ligand (FLT3L) (NAIK *et al.*, 2005). For this reason, Mayer (et al. 2014) (MAYER *et al.*, 2014) has proposed a protocol that increases the number and the quality of splenic-like DCs cultured *in vitro*, which consists of the addition of GM-CSF combined with FLT3L to generate iCD103⁺-DCs, which are CD8a⁺CD103⁺MHC-II⁺CD24⁺. In the leishmaniasis context, these cells are important to confer resistance against the parasite (ASHOK *et al.*, 2014; MARTÍNEZ-LÓPEZ *et al.*, 2015; SOTO *et al.*, 2020). Here, we differentiated induced CD103⁺ Dendritic Cells from C57BL/6J murine bone marrow cells following the protocol proposed by Mayer.

We observed that these cells presented a fastidious differentiation process, with several critical points when they can be lost. The first step of differentiation is akin to the traditional GM-CSF BMDC differentiation, with complete conventional RPMI plus the addition of 2-mercaptoethanol and both growth factors: GM-CSF and FLT3L. We chose to not perform red blood cell lysis to avoid cell loss. We took care to not put them into the BM cells count since we start with 15×10^6 cells per 10 mL in a 10 cm² Petri dish. The Petri dish itself is a risk factor for the culture medium evaporation or culture contamination. It is more sensitive when the cell culture is made in a shared cell culture facility as we did in our lab. We needed to synchronize our cell culture with the lab cleaning schedule because just removing the cells from the incubator can lead to contamination, and massive cell death. This is especially true after day 9 when we need to renew the growth factors and reduce the cell number to the next differentiation step. The more the cells differentiate into DCs. Time that DCs become sensitive, and the handling must be executed with extra care. External perturbations must be avoided at all costs during this period between days 9 and 16.

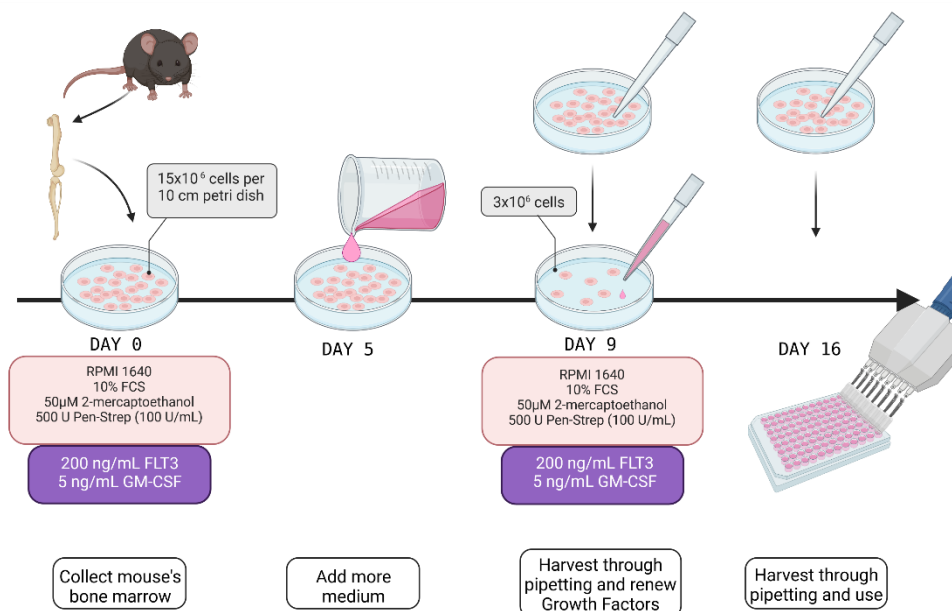


Figure 33. Schematic view of the iCD103⁺ DC differentiation protocol. Starting from the right to the left. Mice femurs and tibias were collected to harvest bone marrow (BM), and culture 15×10^6 cells to every 10 cm² Petri dish, with complete RPMI plus the growth factors FLT3L and GM-CSF. They were left at 37 °C under a CO₂ atmosphere for five days. On the fifth day the cells received more complete RPMI, but with no growth factor. After 4 days more, on the ninth day, 3×10^6 cells were harvested and replaced in a new Petri dish with complete RPMI plus growth factors. Then the cells were cultured until they reached 16 days of culture when they are fully differentiated and ready to use. As they are semi-adherent, just the pipetting is enough to harvest cells.

As cited before, the number of cells decreases along the protocol execution, this means that the expected number of cells on day 16 is lower than the harvested cells on day 0 (fig.2-A). Starting with 15×10^6 cells at day zero, at day 9 (fig.2-B) it is expected around 10×10^6 cells that are reduced to 3×10^6 cells in the replacement. Between days 9 and 16 the cells do not proliferate much, then the number of expected cells on day 16 is approximately between $3-5 \times 10^6$ cells per Petri dish. Also, there is a recommendation to not re-plate the cells to perform the stimulation after the 16 days of differentiation,

because harvesting itself can activate these cells due to the mechanical stress and reduction of growth factors. As our experimentation procedure is based on multiple comparisons, we needed to replace the cells. To reduce the problems with the activation and data misinterpretations we hypothesized that once the differentiation is fully complete at day 16, we could plate cells at day 15 without changing their culture media, to maintain all the conditions, and let the cells sit to decrease activation, like what is normally done to macrophages. As expected, on day 16 the cells were clustered with a few single cells. Also, they presented the typical DC shape, being a round cell surrounded by dendrons (fig.2-C).

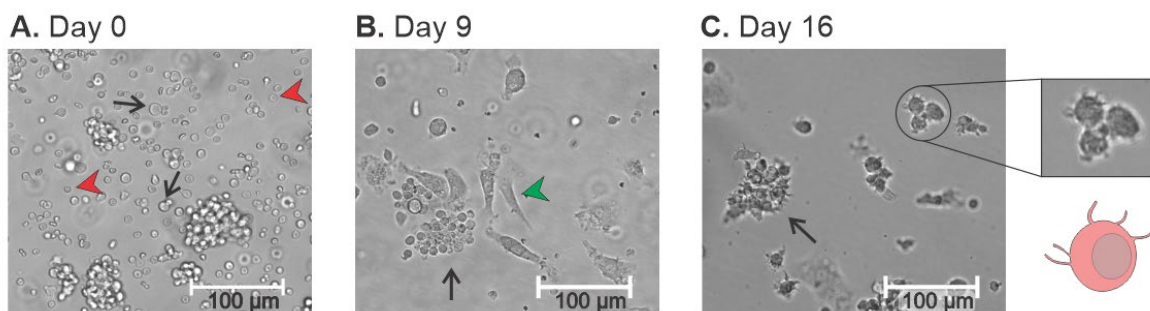


Figure 34. iCD103⁺-DCs number and morphology along the differentiation protocol. Bright-field inverted microscopy of cells along the differentiation. (a) Bone marrow cells in culture on day 0. The black arrows indicate the cells that will continue in the culture, and be differentiated into other cell types, and the red arrows represent the red blood cells that will be excluded by death. (b) DC-like cells on day 9, when they are replated. There are semi-adherent/suspended cells (black arrow) that will be replaced in another Petri dish, with a new culture medium; and some adherent cells (green arrows) that will be discarded. (c) iCD103⁺-DCs after 16 days of differentiation. They grow grouped in clusters (arrow) and present a round shape, being surrounded by dendrons, as shown in the highlight, and the proposed representation below the highlight.

iCD103⁺-DCs phenotypic characterization and infection with *L. infantum*

We aimed to understand how the infection with *L. infantum* affects the DCs phenotypical markers, and how these cells behave when challenged with the parasite. For this reason, we infected iCD103⁺-DCs with Tag-it Violet Cell Tracker labeled *L. infantum* promastigotes. We used different MOI (1:2, 1:5, and 1:10); heat-killed parasites, and LPS as immunological controls; and uninfected iCD103⁻ DCs as the negative control. After 24h of infection, we labeled these cells with surface markers to uncover their infectivity and maturity level. As a gating strategy, we started selecting the double positive population CD11c⁺CD103⁺ (fig.3-A). After we used the co-expression of MHC-II and CD86 as maturity markers (fig.3-B). We set the MHC-II⁺ population to detect the fluorescence of the labeled parasite (fig.3-C-D) and compare different MOI (fig.3-E). We observed a lower frequency of infection on iCD103⁺-DCs, varying from 5% in MOI 1:2 to 20% in MOI 1:10. The data present a lower infection compared to the literature for *L. infantum* infection of DCs differentiated only with GM-CSF (RESENDE *et al.*, 2013), which are a mixed population, with not only DCs but also

macrophages (HELFT *et al.*, 2015). Also, the increase in the infectivity is parasite-dose dependent, presenting 20% of infection when the used MOI was 1:10 (fig.3-D-E).

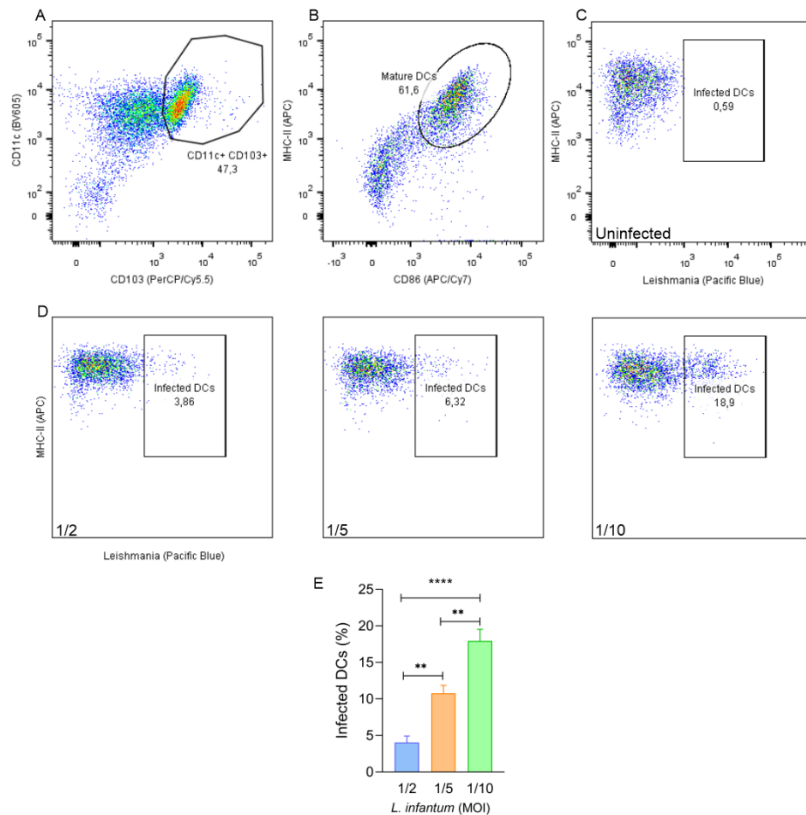


Figure 35. Infectivity of *L. infantum* into iCD103⁺-DCs. The generated iCD103⁺-DCs were labeled with DCs surface markers and separated into populations. (a) CD11c⁺CD103⁺, from which it was selected the (b) population MHC-II⁺CD86⁺. The last one was divided into (d) infected and uninfected populations due to the presence of *L. infantum* fluorescence in different MOI. (e) Represents the calculation of infected DCs percentage. Statistics: One-way ANOVA. Post-hoc test: Tukey's Comparison. **, $p \leq 0.0021$. ***, $p \leq 0.0002$.

Next, using the same gate strategy, we analyzed the impact of *L. infantum* on the maturity markers expression in iCD103⁺-DCs. In figure 4, we observed a distinct modulation of the maturity markers expression in iCD103⁺-DCs. In figure 4, we observed a distinct modulation of the maturity markers expression in iCD103⁺-DCs. In figure 4, we observed a distinct modulation of the maturity markers expression in iCD103⁺-DCs. Without any stimulation, the cells presented a maturity of 69% (fig.4 – upper left panel). Although, the LPS stimulation promoted the maturation of 90.9% of these cells (fig.4 – upper central panel). Besides that, all the groups that entered into contact with *Leishmania* antigens had all cells gated as mature DCs (fig. 4 – upper right panel and lower panels). It is independent of the parasite viability since the heat-killed group presented a similar behavior to the groups that entered into contact with viable parasites. Also, considering a lower frequency in the infected DCs (Fig 3), the presence of *Leishmania* antigens promoted the maturation of the entire population. It may suggest that these cells have a strong response to the parasite in vitro condition and early time of co-culture with the parasite.

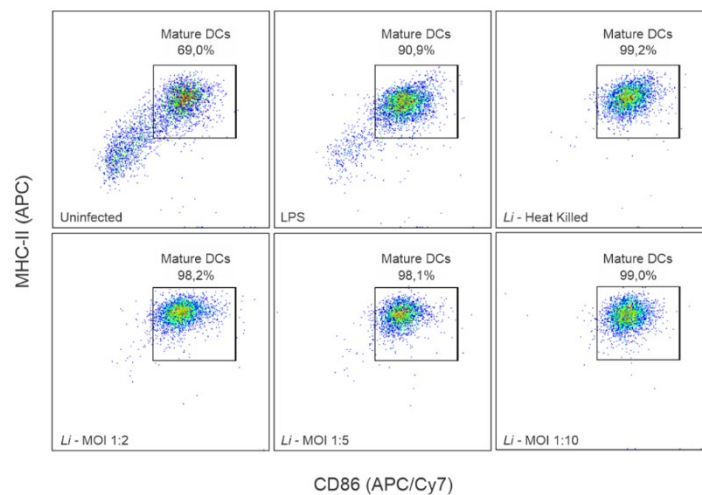


Figure 36. *L. infantum* infected iCD103⁺-DCs maturity. CD11c⁺CD103⁺ cells were selected to observe the maturity level through MHC-II and CD86 expression levels upon infection and inflammatory signals. The percentage of the infected population is shown in each panel.

Interestingly this behavior is contrary to what we were expected. Our previous work demonstrated diverse states of maturation of DCs differentiated using GM-CSF (200 U/mL – 10 days of culture) after infection with *L. infantum* (RESENDE *et al.*, 2013). We observed in this previous study that GM-CSF differentiated DCs present four populations of MHC-II vs CFSE labeled *L. infantum*. The GM-CSF-induced DCs present different states of maturation when infected with *L. infantum*, especially the bystanders, cells that were not infected but had contact with *L. infantum* antigens. These cells were more prone to induce a Th1 response than the infected DCs, which were prone to prime T cells into Th2 and Th17 (RESENDE *et al.*, 2013).

Also, iCD103⁺-DCs are less phagocytic than GM-CSF-DCs. However, as discussed before, distinct protocols lead to the generation of distinct cell subsets, but the results we obtained with this new protocol opened a new path to understanding the function of each subset of DCs during infection.

Transcriptomic profile of iCD103⁺-DC infected with *L. infantum*

We infected iCD103-DCs with *L. infantum* using MOI 1:5 to perform Illumina RNA deep sequencing of non-coding and coding RNAs. The material was processed and analyzed by Novogene incorporation, which made the DNA digestion, library construction, sequencing, and data analysis. It obtained an average of 60 million reads in the *L. infantum*-infected DCs and half in the uninfected DCs. These reads were aligned to the murine genome dataset GRCm38 (Ensembl GCA_000001635.9). After the total sequenced RNA was organized in a PCA graph based on FPKM (fragments per kilobase of exon per million mapped fragments – fig.5), which measures intragroup variations. It is possible to observe that samples from uninfected cells are uniformly grouped in the PCA graph, and samples from infected cells

presented a dispersed cluster separated from uninfected samples (fig.5). This phenomenon can eventually occur due to fluctuation in the number of parasites inside the cells, or other possible events.

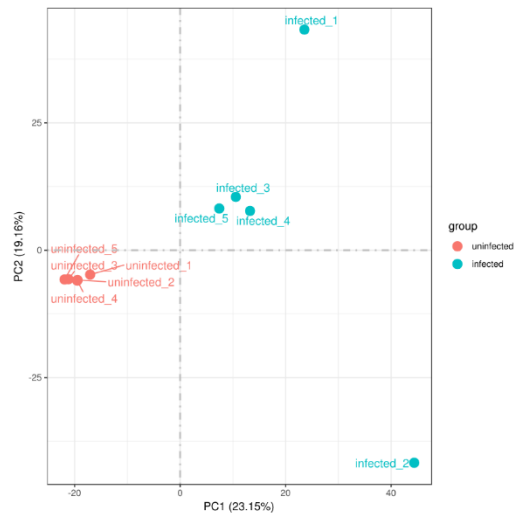


Figure 37. PCA samples group. The PCA grouping was calculated based on FPKM values.

After, the differentially expressed genes were calculated between biological replicates using the software DESeq2(ANDERS; HUBER, 2010), and between groups using the software EdgeR(ROBINSON; MCCARTHY; SMYTH, 2010). The uninfected group was set as the basal control, and the infected was the tested group.

The following analysis was the pathways enrichment, in which KEGG and GO terms were used to uncover the most modulated pathways in these cells. In the KEGG enrichment (fig.6), we observed a modulation of genes related to the inflammatory response, such as toll-like receptor signaling pathways, cytokine-cytokine receptor interaction, phagosome, and genes related to viral and parasite response.

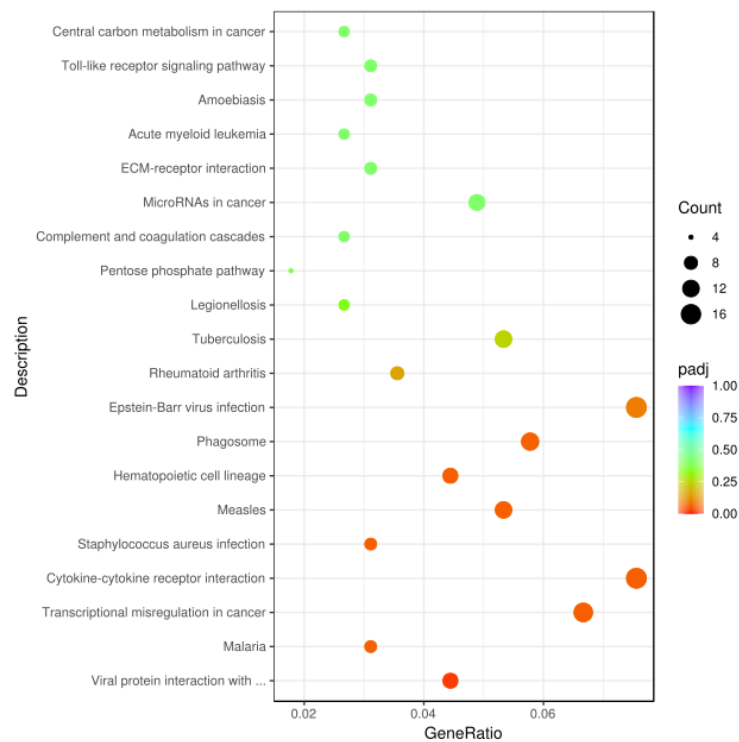


Figure 38. Top 20 enriched KEGG pathways. The top 20 modulated pathways on KEGG enrichment are disposed of on the right. Each pathway name represents a line in the chart, where the dots represent the genes presence. The dots size represents the number of genes modulated on the pathway represented on the line where it sits. The dots colors represent the value of the *p*-adjusted value for each enriched pathway, where purple is the higher *padj*, decreasing the number when green is the medium value, and orange is the lowest value. KEGG pathways with *padj*<0.05 are significant enrichment.

The infected iCD103⁺-DCs presented a molecular signature of energetic metabolism-related genes modulated on GO enrichment (fig.7). We highlight genes from pathways related to glucose and pyruvate metabolism, ADP/ATP formation, and generation of precursor metabolites and energy. These genes are listed on table 1, comparing the infected group with the uninfected. Also, these genes had their FPKM compared on figure 8, where we can observe in which condition genes are up or down-regulated, based on the color of the heat-map (red is for the up-regulated genes, while blue is for the down-regulated).

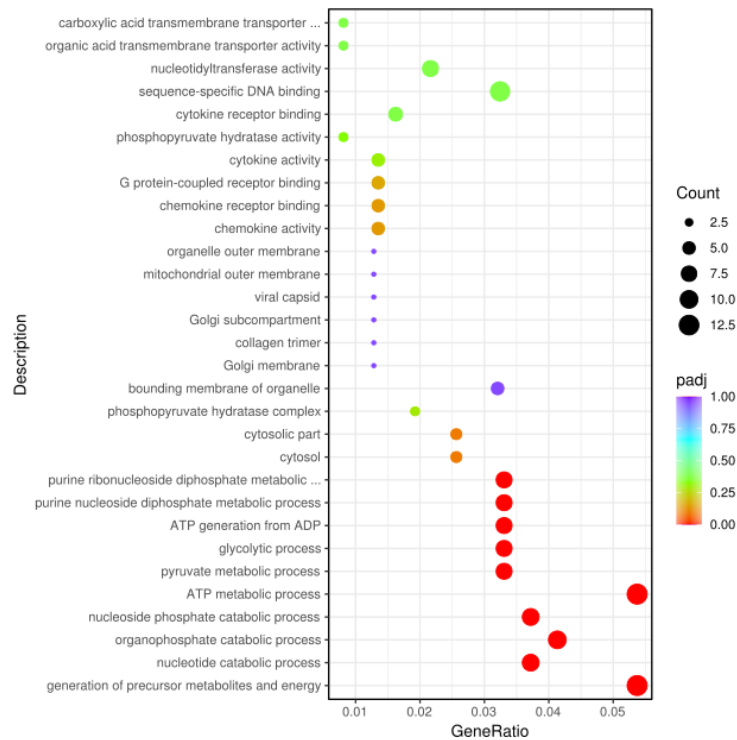


Figure 39. Top 20 enriched GO terms. The top 20 modulated pathways on GO enrichment are disposed of on the right. Each pathway name represents a line in the chart, where the dots represent the genes presence. The dots size represents the number of genes modulated on the pathway represented on the line where it sits. The dots colors represent the value of the *p*-adjusted value for each enriched pathway, where purple is the higher *padj*, decreasing the number when green is the medium value, and orange is the lowest value. GO terms with *padj*<0.05 are significant enrichment.

Table 1. Modulated genes between infected versus uninfected. The table shows the modulated genes found in the GO enrichment – energetic metabolism signature. It also shows the difference between both groups (\log_2FC), *p*-value, and adjusted *p*-value.

Gene Name	Log ₂ FC	<i>p</i> -value	<i>p</i> -adj
<i>Pfkl</i>	2,07E+14	2,14E-50	1,49E-46
<i>Eno1</i>	1,24E+16	1,43E-36	5,73E-36
<i>Aldoa</i>	1,05E+16	2,98E-35	8,52E-34
<i>Pgk1</i>	1,29E+16	4,86E-16	4,05E-15
<i>mt-Nd5</i>	1,49E+16	3,49E+00	5,58E+02
<i>mt-Nd2</i>	1,84E+14	4,08E+00	6,37E+02
<i>Gys1</i>	1,00E+14	4,07E+04	4,55E+06
<i>mt-Nd4</i>	1,45E+14	2,05E+06	1,69E+06
<i>Eno1b</i>	1,64E+13	2,06E+11	4,55E-04
<i>Ndufb3</i>	-2,00E+16	3,81E-04	5,03E-03
<i>Aldoc</i>	1,35E+14	2,88E-03	2,40E-02
<i>Cnp</i>	-1,20E+14	5,23E-03	3,70E-02
<i>Pla2g4f</i>	1,72E+16	3,66E-09	2,09E-08
<i>mt-Atp6</i>	1,76E+16	6,37E+10	1,18E-03

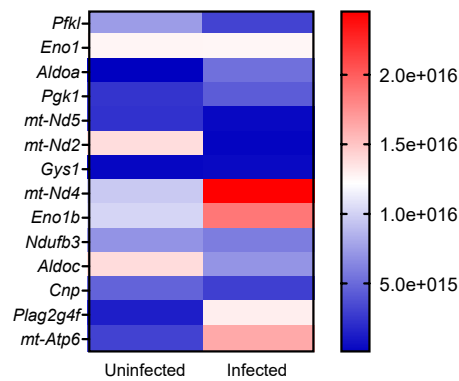


Figure 40. Modulated genes FPKM comparison. Modulated genes found in the GO enrichment – energetic metabolism signature – FPKM comparison between uninfected and infected groups. The blue-red heat map shows the absolute values of FPKM. Red represents the higher values, and blue the lower values.

Based on the data, we highlight the modulated genes on the glycolytic pathway (fig.9). It is possible to observe some key points with more than one isoform modulated.

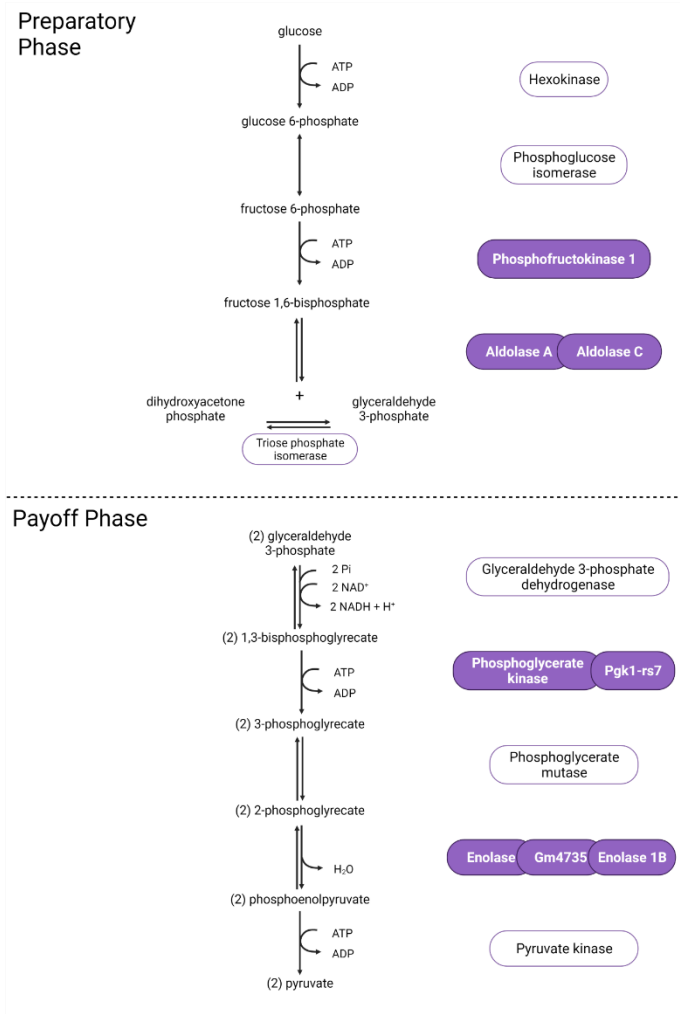


Figure 41. Modulated genes on the glycolytic pathway. The glycolytic pathway is shown with the metabolites and participant enzymes. Purple squares represent the modulated genes on each node pathway.

Metabolic shift screening of iCD103⁺-DC infected with *L. infantum*

To study how iCD103⁺-DCs shift their glucose metabolism in contact with *L. infantum*, we tracked the kinetics of glucose consumption and lactate production through HPLC analysis every 2 hours post-infection until it reached 8 hours (fig.10-a). The uninfected cells were used as the negative control, and LPS and heat-killed parasites as inflammatory controls. We could not retrieve the data from LPS and heat-killed parasite samples after 2h of infection.

All studied groups presented changes in glucose consumption and lactate production. However, the distinct *L. infantum* MOI – 1:2, light blue dots; 1:5, medium dots; and 1:10, dark blue dots – presented different levels of glucose consumption in all tested time points (fig.10-b). Interestingly, inflammatory stimuli presented distinct behaviors of glucose consumption. The LPS stimulation promoted consumption rates like uninfected and MOI 1:2 after 4, 6, and 8h of infection (fig.10-b). In addition, heat-killed parasites promoted an intermediary glucose consumption between MOI 1:5 and 1:10. It may suggest that *L. infantum* antigens alone can promote glucose consumption by iCD103-DCs. Nevertheless, glucose consumption alone cannot answer what respiration type these cells are using to produce energy – via anaerobic respiration or OXPHOS. For this reason, we also measured lactate production (fig.10-c). It is possible to observe a regular and steady lactate production of uninfected DCs while the other stimuli disturb this behavior (fig.10-c). The infection in all MOI presented the same variation along the time course: a conspicuous increase in lactate production between 2 and 4h of infection, followed by a plateau, then followed by another ascent ramp in the lactate production, while both inflammatory controls presented slight modifications (fig.10-c). However, contrary to our expectations, the MOI 1:10 presented the lowest lactate production after 2h of infection and did not increase it to higher levels than the other MOI or even the uninfected control (fig.10-c). These preliminary data indicate that the infection of iCD103-DCs with *L. infantum* leads to a shift in the glucose metabolism along the early course of infection, corroborating with the transcriptomic profile.

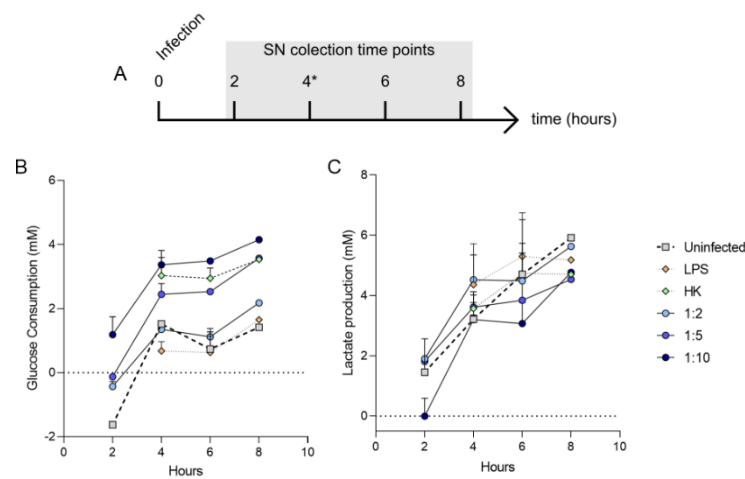


Figure 42. Glucose/Lactate Kinetics behavior during the early infection. (A) iCD103-Dcs were stimulated with *L. infantum* antigens - via infection with viable or heat-killed parasites, or LPS stimulated at time 0. The culture supernatant was collected every 2h, up to 8h, to measure (B) glucose consumption, and (C) lactate production. The gray squares plus dashed lines represent uninfected cells. The orange diamonds represent LPS stimulation. The dots represent *L. infantum* antigens - green dots are for heat-killed parasites, and blue dots are for viable parasites, varying in lightness - light blue dots are for MOI 1:2, medium blue is for MOI 1:5, and the dark blue it is for MOI 1:10. Statistics: (n = 1) *Usually there is a washing step after 4h of infection, which removes unphagocytosed parasites, but we did not perform this washing step.

If glycolysis is important to iCD103⁺-DCs response against the parasite, its inhibition would lead to an increase in the parasite burden. We treated these cells with two different doses of 2-deoxyglucose (2-DG) and infected them with different MOI of *L. infantum* (fig.41). As expected, the treatment with 2-DG increased the parasite burden on both tested doses, doubling the infectivity.

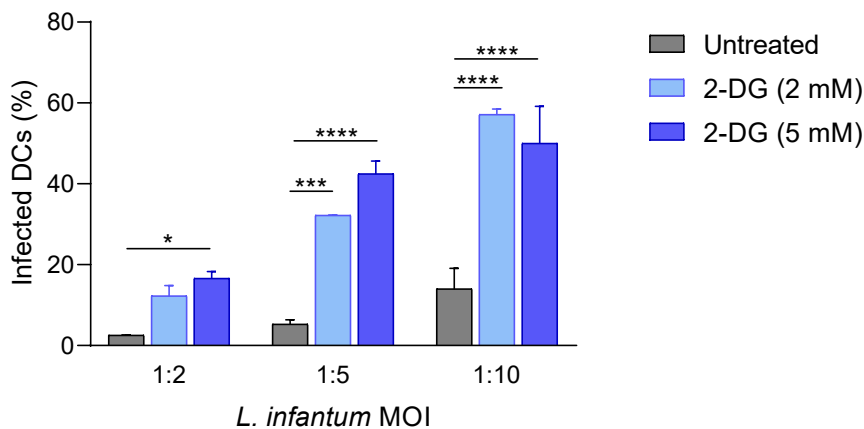


Figure 43. Glycolysis pathway inhibition. DCs were treated with 2-deoxy-D-glucose (2-DG) when they were infected. After 24h, the number of infected cells was determined by flow cytometry. Statistics: Two-way ANOVA. Tukey's multiple comparisons as a post hoc test. *, p<0.05. ***, p<0.005. ****, p<0.0001.

Our data suggests that iCD103⁺-DCs activation leads to a dependence on glucose metabolism, in similar way of the literature.

Krawczyk (et al., 2010) demonstrated that the stimulation of murine GM-CSF DCs with Toll-like receptors (TLRs) agonists provoked a behavior analogous to the Warburg effect – a dependence on the glycolytic respiration even in the presence of oxygen observed in tumoral cells (LIBERTI; LOCASALE, 2016). They showed that the stimulation led to a switch from OXPHOS to aerobic glycolysis, but unlike cancer cells, glycolysis does not fuel cellular division but is indispensable to DCs maturation – the expression of co-stimulatory molecules, such as CD40 and CD86, and the production of IL-12p40. It also is important to their survival upon TLR stimulation since this activation dramatically reduces DCs life span (KRAWCZYK *et al.*, 2010).

Although, this mechanism needs to be regulated, and it was observed that the activation of PI3K/AKT in DCs – by TLRs stimulation – leads to the observed switch from OXPHOS to aerobic glycolysis (Krawczyk). The activities of AKT in the glycolysis promotion rely on the increased glucose transporter 1 (GLUT1) and mTOR activation, and down-regulation of palmitate consumption (KRAWCZYK *et al.*, 2010). However, the mTOR inhibition by rapamycin did not alter the production of the proinflammatory cytokines IL-12p70 or TNF α in GM-CSF DCs, also increasing their life span and the stability of co-stimulatory molecules (AMIÉL *et al.*, 2012). Another regulator of DCs energetical metabolism shift is the production of Nitric Oxide (NO), which inhibits mitochondrial respiration, promoting the switch to glycolysis. Everts (*et al.* 2012) demonstrated that OXPHOS blockage by NO promotes the switch to glycolysis to maintain the ATP levels compatible with their survival. Also, when NO production is inhibited, glycolysis is abrogated and β -oxidation and OXPHOS return in TLR-stimulated DCs (EVERTS *et al.*, 2012).

It is important to point out that these mechanisms are well demonstrated in DCs differentiated with only GM-CSF, and they present distinct immunobiology to iCD103⁺-DCs. However, this data can support our preliminary findings.

Leishmania antigens such as lipophosphoglycan (LPG), can activate the TLR downstream signaling (FARIA; REIS; LIMA, 2012b; LIESE; SCHLEICHER; BOGDAN, 2007; MUXEL, SANDRA MARCIA; ACUÑA; *et al.*, 2018b; SCHLEICHER *et al.*, 2007; SHWEASH *et al.*, 2011; TUON *et al.*, 2008). We observed that the infection with *L. infantum* led iCD103⁺-DCs to maturation by the expression of CD86 (fig.3). Also, the transcriptomic profile showed that these cells increased the number of glycolysis pathway genes (fig.4). This is consistent with the reports presented.

However, our findings are the first step to understanding the function of this specific DC subset within the *Leishmania* infection context. More experiments need to be done to fully comprehend their activities and how the parasite interferes with the host metabolism.

References

- AMIEL, Eyal; EVERTS, Bart; FREITAS, Tori C.; KING, Irah L.; CURTIS, Jonathan D.; PEARCE, Erika L.; PEARCE, Edward J. Inhibition of Mechanistic Target of Rapamycin Promotes Dendritic Cell Activation and Enhances Therapeutic Autologous Vaccination in Mice. *The Journal of Immunology*, [S. l.], v. 189, n. 5, p. 2151–2158, 2012. DOI: 10.4049/JIMMUNOL.1103741. Disponível em: <https://journals.aai.org/jimmunol/article/189/5/2151/39952/Inhibition-of-Mechanistic-Target-of-Rapamycin>. Acesso em: 29 nov. 2022.
- ANDERS, Simon; HUBER, Wolfgang. Differential expression analysis for sequence count data. *Genome biology*, [S. l.], v. 11, n. 10, 2010. DOI: 10.1186/GB-2010-11-10-R106. Disponível em: <https://pubmed.ncbi.nlm.nih.gov/20979621/>. Acesso em: 29 nov. 2022.
- ASHOK, Devika et al. Cross-presenting dendritic cells are required for control of *Leishmania major* infection. *European Journal of Immunology*, [S. l.], v. 44, n. 5, p. 1422–1432, 2014. DOI: 10.1002/EJI.201344242. Disponível em: <https://onlinelibrary.wiley.com/doi/full/10.1002/eji.201344242>. Acesso em: 29 nov. 2022.
- CABEZA-CABRERIZO, Mar; CARDOSO, Ana; MINUTTI, Carlos M.; PEREIRA DA COSTA, Mariana; REIS E SOUSA, Caetano. Dendritic Cells Revisited. *Annual Review of Immunology*, 2021. DOI: 10.1146/annurev-immunol-061020-053707.
- EVERTS, Bart; AMIEL, Eyal; VAN DER WINDT, Gerritje J. W.; FREITAS, Tori C.; CHOTT, Robert; YARASHESKI, Kevin E.; PEARCE, Erika L.; PEARCE, Edward J. Commitment to glycolysis sustains survival of NO-producing inflammatory dendritic cells. *Blood*, [S. l.], v. 120, n. 7, p. 1422–1431, 2012. DOI: 10.1182/blood-2012-03-419747. Disponível em: <http://ashpublications.org/blood/article-pdf/120/7/1422/1499188/zh803312001422.pdf>. Acesso em: 29 nov. 2022.
- FARIA, Marília S.; REIS, Flavia C. G.; LIMA, Ana Paula C. A. Toll-Like Receptors in *Leishmania* Infections: Guardians or Promoters? *Journal of Parasitology Research*, [S. l.], v. 2012, p. 12, 2012. DOI: 10.1155/2012/930257. Disponível em: </pmc/articles/PMC3317170/>. Acesso em: 29 nov. 2022.
- HELFT, Julie; BÖTTCHER, Jan; CHAKRAVARTY, Probir; ZELENAY, Santiago; HUOTARI, Jatta; SCHRAML, Barbara U.; GOUBAU, Delphine; REIS E SOUSA, Caetano. GM-CSF Mouse Bone Marrow Cultures Comprise a Heterogeneous Population of CD11c+MHCII+ Macrophages and Dendritic Cells. *Immunity*, [S. l.], v. 42, n. 6, p. 1197–1211, 2015. DOI: 10.1016/j.immuni.2015.05.018. Disponível em: <http://www.cell.com/article/S1074761315002162/fulltext>. Acesso em: 29 nov. 2022.
- INBA, Kayo; INABA, Muneo; ROMANI, Nikolaus; AYA, Hideki; DEGUCHI, Masashi; IKEHARA, Susumu; MURAMATSU, Shigeru; STEINMAN, Ralph M. Generation of large numbers of dendritic cells from mouse bone marrow cultures supplemented with granulocyte/macrophage colony-stimulating factor. *The Journal of experimental medicine*, [S. l.], v. 176, n. 6, p. 1693–1702, 1992. DOI: 10.1084/JEM.176.6.1693. Disponível em: <https://pubmed.ncbi.nlm.nih.gov/1460426/>. Acesso em: 29 nov. 2022.
- KRAWCZYK, Connie M. et al. Toll-like receptor-induced changes in glycolytic metabolism regulate dendritic cell activation. *Blood*, [S. l.], v. 115, n. 23, p. 4742–4749, 2010. DOI: 10.1182/BLOOD-2009-10-249540. Disponível em: <https://ashpublications.org/blood/article/115/23/4742/27736/Toll-like-receptor-induced-changes-in-glycolytic>. Acesso em: 29 nov. 2022.
- LIBERTI, Maria V.; LOCASALE, Jason W. The Warburg Effect: How Does it Benefit Cancer Cells? *Trends in biochemical sciences*, [S. l.], v. 41, n. 3, p. 211, 2016. DOI: 10.1016/J.TIBS.2015.12.001. Disponível em: </pmc/articles/PMC4783224/>. Acesso em: 29 nov. 2022.

LIESE, Jan; SCHLEICHER, Ulrike; BOGDAN, Christian. TLR9 signaling is essential for the innate NK cell response in murine cutaneous leishmaniasis. *European Journal of Immunology*, [S. l.], v. 37, n. 12, p. 3424–3434, 2007. DOI: 10.1002/eji.200737182.

MARTÍNEZ-LÓPEZ, María; IBORRA, Salvador; CONDE-GARROSA, Ruth; SANCHO, David. Batf3-dependent CD103⁺ dendritic cells are major producers of IL-12 that drive local Th1 immunity against *Leishmania major* infection in mice. *European Journal of Immunology*, [S. l.], v. 45, n. 1, p. 119–129, 2015. DOI: 10.1002/EJI.201444651. Disponível em: <https://onlinelibrary.wiley.com/doi/full/10.1002/eji.201444651>. Acesso em: 29 nov. 2022.

MAYER, Christian Thomas et al. Selective and efficient generation of functional Batf3-dependent CD103⁺ dendritic cells from mouse bone marrow. *Blood*, [S. l.], v. 124, n. 20, 2014. DOI: 10.1182/blood-2013-12-545772.

MUXEL, Sandra Marcia; ACUÑA, Stephanie Maia; AOKI, Juliana Ide; ZAMPIERI, Ricardo Andrade; FLOETER-WINTER, Lucile Maria. Toll-Like Receptor and miRNA-let-7e Expression Alter the Inflammatory Response in *Leishmania amazonensis*-Infected Macrophages. *Frontiers in Immunology*, [S. l.], v. 9, 2018. DOI: 10.3389/fimmu.2018.02792. Disponível em: <https://www.frontiersin.org/article/10.3389/fimmu.2018.02792/full>.

NAIK, Shalin H. et al. Cutting Edge: Generation of Splenic CD8⁺ and CD8⁻ Dendritic Cell Equivalents in Fms-Like Tyrosine Kinase 3 Ligand Bone Marrow Cultures. *The Journal of Immunology*, [S. l.], v. 174, n. 11, p. 6592–6597, 2005. DOI: 10.4049/JIMMUNOL.174.11.6592. Disponível em: <https://journals.aai.org/jimmunol/article/174/11/6592/101633/Cutting-Edge-Generation-of-Splenic-CD8-and-CD8>. Acesso em: 29 nov. 2022.

RESENDE, Mariana; MOREIRA, Diana; AUGUSTO, Jorge; CUNHA, Joana; NEVES, Bruno; CRUZ, Maria Teresa; ESTAQUIER, Jérôme; CORDEIRO-DA-SILVA, Anabela; SILVESTRE, Ricardo. *Leishmania* -Infected MHC Class II high Dendritic Cells Polarize CD4⁺ T Cells toward a Nonprotective T-bet⁺ IFN- γ + IL-10 + Phenotype . *The Journal of Immunology*, [S. l.], v. 191, n. 1, 2013. DOI: 10.4049/jimmunol.1203518.

ROBINSON, Mark D.; MCCARTHY, Davis J.; SMYTH, Gordon K. edgeR: a Bioconductor package for differential expression analysis of digital gene expression data. *Bioinformatics (Oxford, England)*, [S. l.], v. 26, n. 1, p. 139–140, 2010. DOI: 10.1093/BIOINFORMATICS/BTP616. Disponível em: <https://pubmed.ncbi.nlm.nih.gov/19910308/>. Acesso em: 29 nov. 2022.

SCHLEICHER, Ulrike et al. NK cell activation in visceral leishmaniasis requires TLR9, myeloid DCs, and IL-12, but is independent of plasmacytoid DCs. *The Journal of Experimental Medicine*, [S. l.], v. 204, n. 4, p. 893, 2007. DOI: 10.1084/JEM.20061293. Disponível em: </pmc/articles/PMC2118560/>. Acesso em: 29 nov. 2022.

SHWEASH, Muhannad; ADRIENNE MCGACHY, H.; SCHROEDER, Juliane; NEAMATALLAH, Thikryat; BRYANT, Clare E.; MILLINGTON, Owain; MOTTRAM, Jeremy C.; ALEXANDER, James; PLEVIN, Robin. *Leishmania mexicana* promastigotes inhibit macrophage IL-12 production via TLR-4 dependent COX-2, iNOS and arginase-1 expression. *Molecular Immunology*, [S. l.], v. 48, n. 15–16, p. 1800–1808, 2011. DOI: 10.1016/j.molimm.2011.05.013. Disponível em: <http://dx.doi.org/10.1016/j.molimm.2011.05.013>.

SOTO, Manuel et al. Resistance to Experimental Visceral Leishmaniasis in Mice Infected With *Leishmania infantum* Requires Batf3. *Frontiers in Immunology*, [S. l.], v. 11, p. 3216, 2020. DOI: 10.3389/FIMMU.2020.590934/BIBTEX. Acesso em: 29 nov. 2022.

TUON, Felipe F.; AMATO, Valdir S.; BACHA, Hélio A.; ALMUSAWI, Tariq; DUARTE, Maria I.; NETO, Vicente Amato. Toll-Like Receptors and Leishmaniasis. *Infection and Immunity*, [S. l.], v. 76, n. 3, p. 866, 2008. DOI: 10.1128/IAI.01090-07. Disponível em: </pmc/articles/PMC2258802/>. Acesso em: 29 nov. 2022.

Discussão Geral e Conclusões

As diversas células do sistema imune estão conectadas por uma rede de sinalização complexa, baseada no reconhecimento de sinais nocivos ou inócuos, além de uma resposta adequada a esses sinais. Cada célula possui uma maneira de responder a esses sinais. Por exemplo, macrófagos são células diversas cuja ativação, função e plasticidade estão conectadas com a reprogramação metabólica e a regulação da expressão de fatores efetivos. Quando ativados, eles alteram a demanda de glicose, ácidos graxos, amino ácidos, purinas, ATP e NADPH, além de induzirem a produção de citocinas e quimiocinas, de modo que possam responder adequadamente contra patógenos. A resposta precisa ser equilibrada para que não haja danos teciduais ligados à uma inflamação excessiva (LOCATI; CURTALE; MANTOVANI, 2020a; QUINN *et al.*, 2016; RYAN; O'NEILL, 2020a).

Neste trabalho, nós apresentamos dados referente a modulação de expressão gênica e metabólica em macrófagos murinos infectados com *Leishmania amazonensis* e de Células Dendríticas infectadas com *Leishmania infantum*. Aqui apresentamos regulação metabólica, bem como a regulação da expressão de fatores inflamatórios por meio de miRNAs.

Dentre os pontos de regulação da resposta dos macrófagos, a regulação no perfil de expressão de miRNAs se destaca como um ponto-chave no controle da regulação dos níveis de RNA de genes relacionados a resposta imune e metabolismo nos macrófagos infectados com *L. amazonensis*. Nosso grupo já havia demonstrado que tratamento de macrófagos RAW 264.7 com melatonina (hormônio regulador do ciclo claro-escuro) aumenta a atividade fagocítica dos macrófagos, com produção NO, mesmo com baixa produção de citocinas pró-inflamatórias como TNF α , RANTES e MCP-1, levando a redução na infecção de *L. amazonensis* (MUXEL, SANDRA MARCIA *et al.*, 2012). A modulação dos genes pró-inflamatórios tem correlação com perfil de expressão de miRNAs em macrófagos derivados de medula óssea de camundongos BALB/c infectados com *L. amazonensis*, nos quais o tratamento com melatonina reduziu a expressão global de miRNAs (FERNANDES *et al.*, 2019b). No entanto, o miR-294 permaneceu positivamente regulado nos macrófagos infectados não tratados e tratados com melatonina. Nós já havíamos demonstrado a relação de miR-294 com a expressão de *Nos2/NOS2* e produção de NO (MUXEL, SANDRA MARCIA; LARANJEIRA-SILVA; ZAMPIERI; FLOETER-WINTER, 2017a). Neste caso, ao realizarmos a inibição funcional, observamos o aumento da expressão de *Tnfa*, citocina pró-inflamatória importante na resposta contra *Leishmania* (FERNANDES *et al.*, 2019b). Esses dados sugerem que os miRNAs

modulados pela infecção e que não se alteram com o tratamento com melatonina, podem ser fazer parte do mecanismo de controle da resposta imune.

Também verificamos que miR-294 é um fator importante de regulação da resposta imune frente à infecção com *L. amazonensis*, mesmo em modelo de resistência. Nossa hipótese era de que miR-294 tivesse expressão exclusiva em linhagem susceptível – BALB/c e que não fosse expresso em linhagem resistente a infecção com *L. amazonensis* – C57BL/6 (B6). Surpreendentemente, neste trabalho observamos que macrófagos derivados de medula óssea de B6 (B6-BMDM) também aumentam a expressão de miR-294 e miR-721 e estes participam do controle da infecção com *L. amazonensis* (ACUÑA *et al.*, 2022; MUXEL, SANDRA MARCIA; ACUÑA; *et al.*, 2018c).

Em seguida buscamos identificar quais vias promoviam a expressão de miR-294 e miR-721. Ao estudarmos a via de reconhecimento e ativação mediada por TLR2, TLR4 e MyD88, observamos que a expressão desses miRNAs é independente dessas vias de sinalização, pois não houve mudanças no padrão de expressão em macrófagos oriundos dos nocautes de *Tlr2*^{-/-}, *Tlr4*^{-/-} e *Myd88*^{-/-} infectados com *L. amazonensis*. Mesmo não encontrando uma correlação entre as vias de TLR e indução de miR-294 e miR-721, continuamos a explorar estes dados. Neste caso, observamos que os miRNAs pertencentes à família let-7 foram os mais modulados na ausência dos TLR e Myd88. Destaco o miRNA regulado positivamente let-7e de modo dependente da via de sinalização mediada por TLR-MyD88 e possui os transcritos de *Tlr4* como seu alvo. A inibição de let-7e impactou o número de transcritos de moléculas da via de sinalização de TLR, impactando também na expressão dos fatores de transcrição pró-inflamatórios NF-κB (*Nuclear factor kappa B*) e IRF1 (*Interferon responsive factor 1*). Também observamos que a inibição de let-7e aumentou a expressão de *Nos2/NOS2* e a produção de NO, além de afetar indiretamente a expressão de moléculas pro-inflamatórias (MUXEL, SANDRA MARCIA; ACUÑA; *et al.*, 2018b). Com isso, observamos que há uma complexa rede de sinais que levam a modulação dos miRNAs nos macrófagos infectados, incluindo TLR-Myd88, mas ainda há outros sinais que podem alterar os níveis dos miRNAs e a resposta dos macrófagos à infecção.

Como a expressão de miR-294 é independente da via de sinalização de TLRs, nós também realizamos o ensaio de inibição em C57BL/6-BMDM, em que observamos o aumento da expressão de *Tnfa*, alvo direto do miRNA. Já havíamos demonstrado anteriormente que miR-294 é importante para a regulação do metabolismo de L-arginina, pois possui *Nos2* como seu alvo direto, e sua inibição modula a expressão de NOS2 e ARG1 (MUXEL, S.M.;

LARANJEIRA-SILVA; ZAMPIERI; FLOETER-WINTER, 2017b), enzimas que competem pelo mesmo substrato. Verificamos que miR-294 também é capaz de modular a expressão da isoforma 2B do transportador de L-arginina (*Slc7a2*). Então verificamos se a isoforma 1 do transportador (*Slc7a1*) também era passível de regulação por miRNAs e identificamos o miR-410, que também é modulado pela infecção com *L. amazonensis*. A inibição de ambos os miRNAs levou ao aumento do número de transcritos de ambas as isoformas do transportador, sugerindo que tais miRNAs possuem função de regular respostas pró-inflamatórias baseadas no metabolismo de L-arginina, levando à diminuição da infectividade dos macrófagos (ACUÑA *et al.*, 2022).

A dualidade do metabolismo de L-arginina na produção de NO ou de poliaminas não reside apenas na regulação da expressão das enzimas que competem pelo mesmo substrato, mas também na regulação metabólica das vias. Sabe-se, por exemplo, que a produção de NO possui a N- ω -hidroxil-L-arginina como intermediário, cuja presença na célula inibe potentemente a atividade de ARG1 (BOUCHER *et al.*, 1994). Assim, compreender o estado metabólico dos macrófagos infectados com *Leishmania* também pode elucidar pontos-chaves na resposta. Dessa forma, optamos por avaliar o perfil metabólico de C57BL/B6-BMDM. Mesmo sendo um modelo de resistência, observamos que existe a produção de poliaminas, ainda que a produção de NO seja maior que em macrófagos BALB/c-BMDM, como observamos anteriormente. No entanto, o dado mais relevante que obtivemos foi a modulação de glutatona e tripanotona, que tiveram as razões entre a forma reduzida e oxidada moduladas pela infecção, além de serem dependentes da arginase do parasita (MAMANI-HUANCA *et al.*, 2021b).

A glutatona é uma molécula importante para o balanceamento do estado redox das células. Em conjunto com as tripanotonas, realizam a detoxificação das células de espécies reativas de oxigênio, com atenção especial a H₂O₂, pois o reduzem à água. Essas moléculas antioxidantes dependem de NADPH para sua reciclagem. Descobrimos, ao longo do caminho, que camundongos da linhagem C57BL/6J (*Nnt*^{-/-}) são naturalmente deficientes da enzima mitocondrial NNT, responsável por cerca de 50% da produção de NADPH mitocondrial, levando a um desbalanço do metabolismo redox (HUANG *et al.*, 2006; RONCHI, JULIANA A. *et al.*, 2013; RONCHI, JULIANA APARECIDA *et al.*, 2016). A redução da produção de NADPH mitocondrial nesses camundongos mostrou-se como um fator debilitador da resposta contra *L. amazonensis*, pois elevou a infectividade de macrófagos C57BL/6J (*Nnt*^{-/-}) derivados de medula óssea a patamares similares aos observados em macrófagos oriundos de camundongos deficientes de NOS2 (*Nos2*^{-/-}). O mesmo comportamento foi observado em

infecção *in vivo*, em que o tamanho da lesão observado foi o mesmo entre camundongos C57BL/6J e *Nos2*^{-/-}. Além disso, a mutação altera a capacidade de expressão de *Tnfa* desses macrófagos, sendo um dos possíveis pontos de regulação da resposta inflamatória e, por conseguinte, a susceptibilidade adquirida por essa linhagem.

Apesar dessa mutação, os camundongos C57BL/6J são amplamente utilizados em diversos estudos, mesmo na avaliação da capacidade de resposta contra *Leishmania*. Observamos que iCD103⁺-DCs infectadas com *L. infantum* apresentaram uma dependência metabólica de glicose para a montagem de uma resposta contra o parasita (ACUÑA *et al*, *in prep.*).

Os dados adquiridos ao longo do andamento desta tese indicam que a combinação da regulação da resposta inflamatória por meio de miRNAs e por meio da reprogramação metabólica é uma ferramenta de estudo poderosa que permite compreender como células hospedeiras se comportam frente a um estímulo danoso causado pelo parasita. Assim, compreendermos essa relação entre patógeno e hospedeiro dá-nos a possibilidade de buscar novos alvos terapêuticos com maiores taxas de sucesso, além de compreender como cada paciente responde ao tratamento. Os dados gerados nesta tese abrem novos caminhos e suportam a necessidade de mais estudos na área do imunometabolismo e a integração com outros tipos de regulação da resposta imune, como o caso dos miRNAs.

Resumo Geral

As leishmanioses são um conjunto de doenças que ainda hoje possuem vítimas fatais ou com severas sequelas, em todo Brasil e no mundo. São causadas por parasitas protozoários do gênero *Leishmania* spp. que infectam células fagocíticas do sistema imune de vertebrados, tais como macrófagos e células dendríticas. Essas células podem ter respostas que promovem a inflamação e eliminam o parasita ou respostas que permitem a sobrevivência do protozoário. O principal objetivo desta tese é compreender como a infecção com *Leishmania* afeta as respostas imunes de fagócitos murinos por meio da modulação do perfil de miRNAs de macrófagos ou do perfil metabólico de macrófagos e células dendríticas. Os macrófagos murinos infectados com *L. amazonensis* apresentam modulação na expressão de pequenos RNAs não codificantes, denominados microRNAs, dentre os quais destaca-se o miR-294. Este possui expressão inerente à infecção com *L. amazonensis* e é independente de fatores como a linhagem de camundongo hospedeira, modulação hormonal com melatonina ou da via de sinalização de receptores de padrão do tipo Toll. MiR-294 possui papel importante na regulação do metabolismo de L-arginina por modular a produção de óxido nítrico pela Óxido Nítrico Sintase 2 (NOS2) e o transportador de arginina CAT2B (transportador de aminoácidos catiônicos), além de regular a expressão da citocina pró-inflamatória TNF α (fator de necrose tumoral). Semelhantemente, observa-se a expressão de miR-410, que regula a isoforma CAT1B do transportador de L-arginina. O metabolismo deste aminoácido destacou-se como um dos mais modulados durante a infecção de macrófagos com *L. amazonensis* em perfil metabólico. A partir dele há a produção de moléculas antioxidantes como glutatona e tripanotona, que apresentaram mudanças em suas concentrações e na razão entre oxidada e reduzida, indicando mudanças no estado redox. Este sofre interferências do estado mitocondrial como a presença de uma mutação espontânea no gene da Trans-hidrogenase de Nucleotídeos de Nicotinamida (NNT), responsável pela maior produção do pool mitocondrial de NADPH, co-fator importante na reciclagem de glutatona. Sem uma NNT funcional, macrófagos de uma linhagem resistente tornam-se tão suscetíveis quanto os nocautes de NOS2. Já em relação às células dendríticas, foi observado que a infecção com *L. infantum* leva a um aumento da produção de ATP dependente da oxidação de glicose a lactato, indicando que a respiração mitocondrial é inibida. Juntos, os dados sugerem uma forte relação da função imune das células hospedeiras com o estado metabólico e a regulação da expressão gênica mediada por miRNAs.

General abstract

Leishmaniasis are a group of diseases that still today claim fatal victims or leave severe sequelae throughout Brazil and the world. They are caused by protozoan parasites of the genus *Leishmania* spp., which infect phagocytic cells of the vertebrate immune system, such as macrophages and dendritic cells. These cells can have responses that promote inflammation and eliminate the parasite or responses that allow the survival of the protozoan. The main objective of this thesis is to understand how infection with *Leishmania* affects the immune responses of murine phagocytes through the modulation of the miRNA profile of macrophages or the metabolic profile of macrophages and dendritic cells. Murine macrophages infected with *L. amazonensis* show modulation in the expression of non-coding small RNAs, called microRNAs, among which miR-294 stands out. It has inherent expression in *L. amazonensis* infection and is independent of factors such as the host mouse strain, hormonal modulation with melatonin, or the Toll-like receptor signaling pathway. MiR-294 plays an important role in regulating L-arginine metabolism by modulating the production of nitric oxide by Nitric Oxide Synthase 2 (NOS2) and the arginine transporter CAT2B (cationic amino acid transporter), as well as regulating the expression of the pro-inflammatory cytokine TNF α (tumor necrosis factor). Similarly, the expression of miR-410, which regulates the CAT1B isoform of the L-arginine transporter, is observed. The metabolism of this amino acid has emerged as one of the most modulated during macrophage infection with *L. amazonensis* in the metabolomic profile. From it, the production of antioxidant molecules such as glutathione and trypanothione is carried out, which showed changes in their concentrations and in the ratio between oxidized and reduced forms, indicating changes in the redox state. This is influenced by the mitochondrial state, such as the presence of a spontaneous mutation in the Nicotinamide Nucleotide Transhydrogenase (NNT) gene, responsible for the greater production of the mitochondrial NADPH pool, an important co-factor in glutathione recycling. Without functional NNT, macrophages from a resistant lineage become as susceptible as NOS2 knockouts. Regarding dendritic cells, it was observed that infection with *L. infantum* leads to an increase in ATP production dependent on the oxidation of glucose to lactate, indicating inhibited mitochondrial respiration. Together, the data suggest a strong relationship between the immune function of host cells, the metabolic state, and the regulation of gene expression mediated by miRNAs.

Referências Bibliográficas

- ABUAITA, B. H.; SCHULTZ, T. L.; O'RIORDAN, M. X. Mitochondria-Derived Vesicles Deliver Antimicrobial Reactive Oxygen Species to Control Phagosome-Localized *Staphylococcus aureus*. *Cell Host & Microbe*, v. 24, n. 5, p. 625- 636.e5, 14 nov. 2018. Acesso em: 20 abr. 2023.
- ACUÑA, S. M. *et al.* miR-294 and miR-410 Negatively Regulate *Tnfa*, Arginine Transporter *Cat1/2*, and *Nos2* mRNAs in Murine Macrophages Infected with *Leishmania amazonensis*. *Non-Coding RNA* 2022, Vol. 8, Page 17, v. 8, n. 1, p. 17, 6 fev. 2022. Disponível em: <<https://www.mdpi.com/2311-553X/8/1/17/htm>>. Acesso em: 25 abr. 2023.
- ACUÑA, S. M.; FLOETER-WINTER, L. M.; MUXEL, S. M. MicroRNAs: Biological Regulators in Pathogen-Host Interactions. *Cells*, v. 9, n. 1, 2020a.
- AKHOUNDI, M. *et al.* A Historical Overview of the Classification, Evolution, and Dispersion of *Leishmania* Parasites and Sandflies. *PLoS Neglected Tropical Diseases*. [S.l: s.n.], 2016
- AKIRA, S.; SATO, S. Toll-like Receptors and Their Signaling Mechanisms. *Scandinavian Journal of Infectious Diseases*, v. 35, n. 9, p. 555–562, 8 jan. 2003.
- ALVAR, J. *et al.* *Leishmaniasis worldwide and global estimates of its incidence*. *PLoS ONE*. [S.l: s.n.], 2012
- AMIEL, E. *et al.* Inhibition of Mechanistic Target of Rapamycin Promotes Dendritic Cell Activation and Enhances Therapeutic Autologous Vaccination in Mice. *The Journal of Immunology*, v. 189, n. 5, p. 2151–2158, 1 set. 2012. Disponível em: <<https://journals.aai.org/jimmunol/article/189/5/2151/39952/Inhibition-of-Mechanistic-Target-of-Rapamycin>>. Acesso em: 29 nov. 2022.
- ANDERS, S.; HUBER, W. Differential expression analysis for sequence count data. *Genome biology*, v. 11, n. 10, 27 out. 2010. Disponível em: <<https://pubmed.ncbi.nlm.nih.gov/20979621/>>. Acesso em: 29 nov. 2022.
- AOKI, J.I.; MUXEL, S. M.; ZAMPIERI, R. A.; ACUÑA, S. M.; *et al.* L-arginine availability and arginase activity: Characterization of amino acid permease 3 in *Leishmania amazonensis*. *PLoS Neglected Tropical Diseases*, v. 11, n. 10, 2017.
- AOKI, J.I.; MUXEL, S. M.; ZAMPIERI, R. A.; LARANJEIRA-SILVA, M. F.; *et al.* RNA-seq transcriptional profiling of *Leishmania amazonensis* reveals an arginase-dependent gene expression regulation. *PLoS Neglected Tropical Diseases*, v. 11, n. 10, 2017a.
- AOKI, J.I. *et al.* The impact of arginase activity on virulence factors of *Leishmania amazonensis*. *Current Opinion in Microbiology*, v. 52, 2019a.
- AOKI, JULIANA IDE *et al.* Differential immune response modulation in early *Leishmania amazonensis* infection of BALB/c and C57BL/6 macrophages based on transcriptome profiles. *Scientific Reports*, 2019.
- AOKI, JULIANA IDE *et al.* Dual transcriptome analysis reveals differential gene expression modulation influenced by leishmania arginase and host genetic background. *Microbial Genomics*, v. 6, n. 9, p. 1–13, 2020a.
- AOKI, JULIANA IDE *et al.* Dual transcriptome analysis reveals differential gene expression modulation influenced by *Leishmania* arginase and host genetic background. *Microbial Genomics*, 2020b.
- ARANGO DUQUE, G.; DESCOTEAUX, A. *Leishmania* survival in the macrophage: where the ends justify the means. *Current Opinion in Microbiology*, v. 26, p. 32–40, 1 ago. 2015. Acesso em: 20 abr. 2023.
- ASHFORD, R. W. The leishmaniasis as emerging and reemerging zoonoses. *Parasites and Vectors*, v. 3, n. 1, p. 1269–1281, 2000.

ASHOK, D. *et al.* Cross-presenting dendritic cells are required for control of *Leishmania* major infection. *European Journal of Immunology*, v. 44, n. 5, p. 1422–1432, 1 maio 2014. Disponível em: <<https://onlinelibrary.wiley.com/doi/full/10.1002/eji.201344242>>. Acesso em: 29 nov. 2022.

BACELLAR, O. *et al.* IL-10 AND IL-12 ARE THE MAIN REGULATORY CYTOKINES IN VISCERAL LEISHMANIASIS. *Cytokine*, v. 12, n. 8, p. 1228–1231, ago. 2000.

BALTIMORE, D. *et al.* MicroRNAs: New regulators of immune cell development and function. *Nature Immunology*, v. 9, n. 8, p. 839–845, 2008.

BARTEL, D. P. MicroRNAs: Genomics, Biogenesis, Mechanism, and Function. *Cell*, v. 116, n. 2, p. 281–297, 2004.

BARTONS, R.; CARO, J. Hypoxia, glucose metabolism and the Warburg's effect Metabolic reprogramming of tumor cells View project. *Article in Journal of Bioenergetics and Biomembranes*, 2007. Disponível em: <<https://www.researchgate.net/publication/6178212>>. Acesso em: 11 maio 2023.

BATTELLI, M. G. *et al.* Xanthine oxidoreductase-derived reactive species: Physiological and pathological effects. *Oxidative Medicine and Cellular Longevity*. [S.l: s.n.], 2016

BECKER, I. *et al.* *Leishmania* lipophosphoglycan (LPG) activates NK cells through toll-like receptor-2. *Molecular and Biochemical Parasitology*, v. 130, n. 2, p. 65–74, 2003.

BLAGIH, J.; JONES, R. G. Polarizing macrophages through reprogramming of glucose metabolism. *Cell Metabolism*. [S.l: s.n.], 2012a

BLAGIH, J.; JONES, R. G. Polarizing macrophages through reprogramming of glucose metabolism. *Cell metabolism*, v. 15, n. 6, p. 793–795, 6 jun. 2012b. Disponível em: <<https://pubmed.ncbi.nlm.nih.gov/22682218/>>. Acesso em: 17 jan. 2023.

BOGDAN, C. Nitric oxide and the immune response. *Nature Immunology*. [S.l: s.n.], 2001

BOGDAN, C. Nitric oxide and the regulation of gene expression. *Trends in Cell Biology*, v. 11, n. 2, p. 66–75, 2001. Disponível em: <http://www.sciencedirect.com/science?_ob=MIimg&_imagekey=B6TCX-428DK90-N-7&_cdi=5182&_user=687336&_pii=S0962892400019000&_origin=search&_coverDate=02%2F01%2F2001&_sk=999889997&view=c&wchp=dGLbVIW-zSkzS&md5=92aeb0346da9b44b241b265a4388aa9f&ie=/sdarticle.pdf>.

BOGDAN, CHRISTIAN. Macrophages as host, effector and immunoregulatory cells in leishmaniasis: impact of tissue micro-environment and metabolism. *Cytokine: X*, 2020.

BOGDAN, CHRISTIAN. Mechanisms and consequences of persistence of intracellular pathogens: Leishmaniasis as an example. *Cellular Microbiology*, v. 10, n. 6, p. 1221–1234, 2008.

BOITZ, J. M. *et al.* Arginase Is Essential for Survival of *Leishmania donovani* Promastigotes but Not Intracellular Amastigotes. *Infect Immun*, v. 85, n. 1, 2017.

BOUCHER, J. L. *et al.* N ω -Hydroxy-L-Arginine, an Intermediate in the L-Arginine to Nitric Oxide Pathway, Is a Strong Inhibitor of Liver and Macrophage Arginase. *Biochemical and Biophysical Research Communications*, v. 203, n. 3, p. 1614–1621, 30 set. 1994. Acesso em: 14 maio 2023.

BOUCHER, J. L.; MOALI, C.; TENU, J. P. Nitric oxide biosynthesis, nitric oxide synthase inhibitors and arginase competition for L-arginine utilization. *Cell Mol Life Sci*, v. 55, n. 8–9, p. 1015–1028, 1999.

BRAGATO, J. P. *et al.* miRNA-21 regulates CD69 and IL-10 expression in canine leishmaniasis. *PLOS ONE*, v. 17, n. 3, p. e0265192, 1 mar. 2022. Disponível em: <<https://journals.plos.org/plosone/article?id=10.1371/journal.pone.0265192>>. Acesso em: 14 maio 2023.

BRONTE, V.; ZANOVELLO, P. Regulation of immune responses by L-arginine metabolism. *Nature Reviews Immunology*, v. 5, n. 8, p. 641–654, 2005. Disponível em: <<http://www.nature.com/doi/10.1038/nri1668>>.

BRYAN, N. S.; GRISHAM, M. B. Methods to detect nitric oxide and its metabolites in biological samples. *Free radical biology & medicine*, v. 43, n. 5, p. 645–57, 2007. Disponível em: <<http://www.ncbi.nlm.nih.gov/pubmed/17664129>> <<http://www.pubmedcentral.nih.gov/articlerender.fcgi?artid=PMC2041919>>.

BUFFI, G. *et al.* The host micro-RNA cfa-miR-346 is induced in canine leishmaniasis. *BMC Veterinary Research*, v. 18, n. 1, p. 1–11, 1 dez. 2022. Disponível em: <<https://bmcvetres.biomedcentral.com/articles/10.1186/s12917-022-03359-5>>. Acesso em: 14 maio 2023.

BURZA, S.; CROFT, S. L.; BOELAERT, M. Leishmaniasis. *The Lancet*, v. 392, n. 10151, p. 951–970, 2018a.

CABEZA-CABRERIZO, M. *et al.* *Dendritic Cells Revisited. Annual Review of Immunology*. [S.l: s.n.], 2021

CANUTO, G. A. B. *et al.* CE-ESI-MS metabolic fingerprinting of *Leishmania* resistance to antimony treatment. *Electrophoresis*, 2012.

CARTER, K. C. *et al.* The in vivo susceptibility of *Leishmania donovani* to sodium stibogluconate is drug specific and can be reversed by inhibiting glutathione biosynthesis. *Antimicrobial Agents and Chemotherapy*, 2003.

CASTILHO-MARTINS, E. A. *et al.* Capillary electrophoresis reveals polyamine metabolism modulation in *Leishmania (Leishmania) amazonensis* wild-type and arginase-knockout mutants under arginine starvation. *Electrophoresis*, v. 36, n. 18, 2015.

CERVELLI, M. *et al.* *Spermine oxidase: Ten years after. Amino Acids*. [S.l: s.n.], 2012

CHAWLA, B. *et al.* Identification and characterization of a novel deoxyhypusine synthase in *Leishmania donovani*. *Journal of Biological Chemistry*, 2010.

COLOTTI, G.; ILARI, A. *Polyamine metabolism in Leishmania: From arginine to trypanothione. Amino Acids*. [S.l: s.n.], 2011

COMINI, M.; MENGE, U.; FLOHÉ, L. Biosynthesis of trypanothione in *Trypanosoma brucei*. *Biological Chemistry*, 2003.

COVARRUBIAS, A. J.; AKSOYLAR, H. I.; HORNG, T. *Control of macrophage metabolism and activation by mTOR and Akt signaling. Seminars in Immunology*. [S.l: s.n.], 2015a

DA SILVA, M.F.L. *et al.* *Leishmania amazonensis* arginase compartmentalization in the glycosome is important for parasite infectivity. *PLoS ONE*, v. 7, n. 3, 2012b.

DARLYUK, I. *et al.* Arginine Homeostasis and Transport in the Human Pathogen *Leishmania donovani* *. v. 284, n. 30, p. 19800–19807, 2009.

DAS, S.; MUKHERJEE, S.; ALI, N. Super enhancer-mediated transcription of miR146a-5p drives M2 polarization during *Leishmania donovani* infection. *PLoS Pathogens*, v. 17, n. 2, p. 1–27, 2021.

DAVIS-DUSENBERY, B. N.; HATA, A. *Mechanisms of control of microRNA biogenesis. Journal of Biochemistry*. [S.l: s.n.], 2010

DE VEER, M. J. *et al.* MyD88 is essential for clearance of *Leishmania major*: possible role for lipophosphoglycan and Toll-like receptor 2 signaling. *European journal of immunology*, v. 33, n. 10, p. 2822–2831, out. 2003. Disponível em: <<https://pubmed.ncbi.nlm.nih.gov/14515266/>>. Acesso em: 16 jan. 2023.

DEGROSSOLI, A. *et al.* Expression of hypoxia-inducible factor 1 α in mononuclear phagocytes infected with *Leishmania amazonensis*. *Immunology Letters*, v. 114, n. 2, p. 119–125, 2007.

DEMIRKOL, O.; ERCAL, N. Glutathione! *Integrative Medicine: A Clinician's Journal*, v. 13, n. 1, p. 8, 1 jan. 2014. Disponível em: <[pmc/articles/PMC4684116/](https://pubmed.ncbi.nlm.nih.gov/24684116/)>. Acesso em: 18 abr. 2023.

DENGLER, F. Activation of AMPK under Hypoxia: Many Roads Leading to Rome. *International Journal of Molecular Sciences* 2020, Vol. 21, Page 2428, v. 21, n. 7, p. 2428, 31 mar. 2020. Disponível em: <<https://www.mdpi.com/1422-0067/21/7/2428/htm>>. Acesso em: 11 maio 2023.

DI LORIA, A. *et al.* Expression of serum exosomal miRNA 122 and lipoprotein levels in dogs naturally infected by *Leishmania infantum*: A preliminary study. *Animals*, v. 10, n. 1, 1 jan. 2020.

DICHTL, S. *et al.* Lactate and IL6 define separable paths of inflammatory metabolic adaptation. *Science Advances*, v. 7, n. 26, p. 1–11, 2021.

DICKINSON, D. A.; FORMAN, H. J. Cellular glutathione and thiols metabolism. *Biochemical Pharmacology*, 2002.

DIEFENBACH, A. Requirement for Type 2 NO Synthase for IL-12 Signaling in Innate Immunity. *Science*, v. 284, n. 5416, p. 951–955, 1999. Disponível em: <<http://www.sciencemag.org/cgi/doi/10.1126/science.284.5416.951>>.

DIOTALLEVI, A. *et al.* *Leishmania* infection induces MicroRNA hsa-miR-346 in human cell line-derived macrophages. *Frontiers in Microbiology*, v. 9, n. MAY, p. 1019, 17 maio 2018. Acesso em: 14 maio 2023.

DIOTALLEVI, M. *et al.* Glutathione Fine-Tunes the innate immune response toward antiviral pathways in a macrophage cell line independently of its antioxidant properties. *Frontiers in Immunology*, 2017.

DONNELLY, R. P. *et al.* Inhibition of IL-10 expression by IFN-gamma up-regulates transcription of TNF-alpha in human monocytes. *Journal of immunology (Baltimore, Md. : 1950)*, v. 155, n. 3, p. 1420–7, 1 ago. 1995. Disponível em: <<http://www.ncbi.nlm.nih.gov/pubmed/7636207>>. Acesso em: 27 mar. 2019.

DOWLING, J. K. *et al.* Mitochondrial arginase-2 is essential for IL-10 metabolic reprogramming of inflammatory macrophages. *Nature Communications*, v. 12, n. 1, p. 1–14, 2021a.

DUBOUCHAUD, H. *et al.* Mitochondrial NADH redox potential impacts the reactive oxygen species production of reverse Electron transfer through complex I. *Journal of Bioenergetics and Biomembranes*, v. 50, n. 5, p. 367–377, 1 out. 2018. Disponível em: <<https://link.springer.com/article/10.1007/s10863-018-9767-7>>. Acesso em: 20 abr. 2023.

DUNAND-SAUTHIER, I. *et al.* Repression of Arginase-2 Expression in Dendritic Cells by MicroRNA-155 Is Critical for Promoting T Cell Proliferation. *The Journal of Immunology*, v. 193, n. 4, p. 1690–1700, 2014.

DUQUE-CORREA, M. A. *et al.* Macrophage arginase-1 controls bacterial growth and pathology in hypoxic tuberculosis granulomas. *Proceedings of the National Academy of Sciences*, v. 111, n. 38, p. E4024–E4032, 2014. Disponível em: <<http://www.pnas.org/cgi/doi/10.1073/pnas.1408839111>>.

ESSER-VON BIEREN, J. *et al.* Antibodies Trap Tissue Migrating Helminth Larvae and Prevent Tissue Damage by Driving IL-4R α -Independent Alternative Differentiation of Macrophages. *PLoS Pathogens*, v. 9, n. 11, 2013.

EVERTS, B. *et al.* Commitment to glycolysis sustains survival of NO-producing inflammatory dendritic cells. *Blood*, v. 120, n. 7, p. 1422–1431, 2012. Disponível em: <<http://ashpublications.org/blood/article-pdf/120/7/1422/1499188/zh803312001422.pdf>>. Acesso em: 29 nov. 2022.

FARIA, M. S.; REIS, F. C. G.; LIMA, A. P. C. A. Toll-Like Receptors in Leishmania Infections: Guardians or Promoters? *Journal of Parasitology Research*, v. 2012, p. 12, 2012b. Disponível em: </pmc/articles/PMC3317170/>. Acesso em: 29 nov. 2022.

FERNANDES, J. C. R. *et al.* Melatonin and Leishmania amazonensis Infection Altered miR-294, miR-30e, and miR-302d Impacting on Tnf, Mcp-1, and Nos2 Expression. *Frontiers in Cellular and Infection Microbiology*, v. 9, n. March, p. 1–15, 2019a.

FERREIRA, C.; ESTAQUIER, J.; SILVESTRE, R. Immune-metabolic interactions between Leishmania and macrophage host. *Current Opinion in Microbiology*, v. 63, p. 231–237, 1 out. 2021. Acesso em: 20 abr. 2023.

FILARDY, A. A. *et al.* Proinflammatory Clearance of Apoptotic Neutrophils Induces an IL-12 low IL-10 high Regulatory Phenotype in Macrophages. *The Journal of Immunology*, 2010a.

FONSECA, M. S. *et al.* Ornithine decarboxylase or gamma-glutamylcysteine synthetase overexpression protects Leishmania (Vianna) guyanensis against antimony. *Experimental Parasitology*, 2017.

FONTAINE, D. A.; DAVIS, D. B. Attention to Background Strain Is Essential for Metabolic Research: C57BL/6 and the International Knockout Mouse Consortium. *Diabetes*, v. 65, n. 1, p. 25, 1 jan. 2016. Disponível em: </pmc/articles/PMC4686949/>. Acesso em: 11 maio 2023.

FRANK, B. *et al.* Autophagic digestion of Leishmania major by host macrophages is associated with differential expression of BNIP3, CTSE, and the miRNAs miR-101c, miR-129, and miR-210. *Parasites & Vectors*, v. 8, n. 1, 31 jul. 2015. Disponível em: </pmc/articles/PMC4521392/>. Acesso em: 16 jan. 2023.

FU, Y. *et al.* Circulating microRNAs in patients with active pulmonary tuberculosis. *Journal of Clinical Microbiology*, v. 49, n. 12, p. 4246–4251, 2011.

FUNAMIZU, N. *et al.* MicroRNA-301b promotes cell invasiveness through targeting TP63 in pancreatic carcinoma cells. *International Journal of Oncology*, v. 44, n. 3, p. 725–734, 2014.

GERACI, N. S.; TAN, J. C.; MCDOWELL, M. A. Characterization of microRNA Expression Profiles in Leishmania Infected Human Phagocytes. *Parasite immunology*, v. 37, n. 1, p. 43, 1 jan. 2015. Disponível em: </pmc/articles/PMC4287219/>. Acesso em: 14 maio 2023.

GHALIB, H. W. *et al.* IL-12 enhances Th1-type responses in human Leishmania donovani infections. *The Journal of Immunology*, v. 154, n. 9, p. 4623–4629, 1 maio 1995. Disponível em: <https://journals.aai.org/jimmunol/article/154/9/4623/29123/IL-12-enhances-Th1-type-responses-in-human>. Acesso em: 16 jan. 2023.

GHOSH, J. *et al.* Leishmania donovani targets dicer1 to downregulate miR-122, lower serum cholesterol, and facilitate murine liver infection. *Cell Host and Microbe*, v. 13, n. 3, p. 277–288, 2013a.

GIULIA BATTELLI, M. *et al.* Xanthine Oxidoreductase in Drug Metabolism: Beyond a Role as a Detoxifying Enzyme. *Current Medicinal Chemistry*, 2016.

GOGOI, M. *et al.* Dual role of arginine metabolism in establishing pathogenesis. *Current Opinion in Microbiology*. [S.l.: s.n.], 2016

GOLDMAN-PINKOVICH, A. *et al.* An Arginine Deprivation Response Pathway Is Induced in Leishmania during Macrophage Invasion. *PLoS Pathogens*, v. 12, n. 4, 2016.

GOODMAN, J. L. *et al.* Ornithine cyclodeaminase: Structure, mechanism of action, and implications for the μ -crystallin family. *Biochemistry*, 2004.

GREEN, S. J. *et al.* Activated macrophages destroy intracellular Leishmania major amastigotes by an L-arginine-dependent killing mechanism. *Journal of immunology (Baltimore, Md. : 1950)*, v. 144, n. 1, p. 278–83, 1990. Disponível em: <http://www.ncbi.nlm.nih.gov/pubmed/2104889>.

GREGOROVA, J.; VYCHYTILOVA-FALTEJSKOVA, P.; SEVCIKOVA, S. Epigenetic regulation of microRNA clusters and families during tumor development. *Cancers*, v. 13, n. 6, p. 1–45, 2021.

GREGORY, D. J.; OLIVIER, M. Subversion of host cell signalling by the protozoan parasite *Leishmania*. *Parasitology*, v. 130, n. SUPPL. 1, 2005.

GUERFALI, F. Z. *et al.* Simultaneous gene expression profiling in human macrophages infected with *Leishmania major* parasites using SAGE. *BMC Genomics*, v. 9, n. i, p. 1–18, 2008.

HALLIWELL, B. Phagocyte-derived reactive species: salvation or suicide? *Trends in Biochemical Sciences*, v. 31, n. 9, p. 509–515, 1 set. 2006. Acesso em: 11 maio 2023.

HASHEMI, N. *et al.* Expression of hsa Let-7a MicroRNA of Macrophages Infected by *Leishmania Major*. *International Journal of Medical Research & Health Sciences*, v. 5, p. 27–32, 2016. Disponível em: <www.ijmrhs.com>. Acesso em: 14 maio 2023.

HELFT, J. *et al.* GM-CSF Mouse Bone Marrow Cultures Comprise a Heterogeneous Population of CD11c+MHCII+ Macrophages and Dendritic Cells. *Immunity*, v. 42, n. 6, p. 1197–1211, 16 jun. 2015. Disponível em: <<http://www.cell.com/article/S1074761315002162/fulltext>>. Acesso em: 29 nov. 2022.

HESTERBERG, R.; CLEVELAND, J.; EPLING-BURNETTE, P. Role of Polyamines in Immune Cell Functions. *Medical Sciences*, 2018.

HOUBAVIY, H. B.; MURRAY, M. F. Embryonic Stem Cell-Specific MicroRNAs the regulation of development. In plants, miRNAs have. *Developmental Cell*, v. 5, p. 351–358, 2003.

HRABAK, A. *et al.* The inhibitory effect of nitrite, a stable product of nitric oxide (NO) formation, on arginase. *FEBS Lett*, v. 390, n. 2, p. 203–206, 1996.

HSIEH, C. S. *et al.* Development of TH1 CD4+ T cells through IL-12 produced by Listeria-induced macrophages. *Science*, v. 260, n. 5107, p. 547 LP – 549, 23 abr. 1993. Disponível em: <<http://science.sciencemag.org/content/260/5107/547.abstract>>.

HUANG, T.-T. *et al.* Genetic modifiers of the phenotype of mice deficient in mitochondrial superoxide dismutase. *Human Molecular Genetics*, v. 15, n. 7, p. 1187–1194, 1 abr. 2006. Disponível em: <<http://academic.oup.com/hmg/article/15/7/1187/715422/Genetic-modifiers-of-the-phenotype-of-mice>>. Acesso em: 16 jan. 2020.

IKEGUCHI, Y.; BEWLEY, M. C.; PEGG, A. E. *Aminopropyltransferases: Function, structure and genetics*. *Journal of Biochemistry*. [S.l.: s.n.], 2006

INBA, K. *et al.* Generation of large numbers of dendritic cells from mouse bone marrow cultures supplemented with granulocyte/macrophage colony-stimulating factor. *The Journal of experimental medicine*, v. 176, n. 6, p. 1693–1702, 1 dez. 1992. Disponível em: <<https://pubmed.ncbi.nlm.nih.gov/1460426/>>. Acesso em: 29 nov. 2022.

INIESTA, V.; GOMEZ-NIETO, L. C.; CORRALIZA, I. The inhibition of arginase by N(omega)-hydroxy-L-arginine controls the growth of *Leishmania* inside macrophages. *J Exp Med*, v. 193, n. 6, p. 777–784, 2001.

INIESTA, VIRGINIA *et al.* Arginase I induction in macrophages, triggered by Th2-type cytokines, supports the growth of intracellular *Leishmania* parasites. *Parasite Immunology*, v. 24, n. 3, p. 113–118, 2002.

IRIGOÍN, F. *et al.* Mitochondrial calcium overload triggers complement-dependent superoxide-mediated programmed cell death in *Trypanosoma cruzi*. *Biochemical Journal*, 2009.

JELL, J. *et al.* Genetically altered expression of spermidine/spermine N1-acetyltransferase affects fat metabolism in mice via acetyl-CoA. *Journal of Biological Chemistry*, 2007.

JHA, A. K. *et al.* Network integration of parallel metabolic and transcriptional data reveals metabolic modules that regulate macrophage polarization. *Immunity*, 2015a.

JI, J.; SUN, J.; SOONG, L. Impaired expression of inflammatory cytokines and chemokines at early stages of infection with *Leishmania amazonensis*. *Infect Immun*, v. 71, n. 8, p. 4278–4288, 2003.

KANE, M. M.; MOSSER, D. M. The role of IL-10 in promoting disease progression in leishmaniasis. *Journal of immunology (Baltimore, Md. : 1950)*, v. 166, n. 2, p. 1141–1147, 15 jan. 2001. Disponível em: <<https://pubmed.ncbi.nlm.nih.gov/11145695/>>. Acesso em: 16 jan. 2023.

KARRETH, F. A. *et al.* In vivo identification of tumor-suppressive PTEN ceRNAs in an oncogenic BRAF-induced mouse model of melanoma. *Cell*, 2011.

KIM, V. N.; HAN, J.; SIOMI, M. C. Biogenesis of small RNAs in animals. *Nat Rev Mol Cell Biol*, v. 10, n. 2, p. 126–139, 2009. Disponível em: <<http://www.nature.com/doi/10.1038/nrm2632>>.

KISHIKAWA, T. *et al.* Decreased miR122 in hepatocellular carcinoma leads to chemoresistance with increased arginine. *Oncotarget*, v. 6, n. 10, p. 8339–8352, 2015.

KOCH, O. *et al.* Molecular Dynamics Reveal Binding Mode of Glutathionylspermidine by Trypanothione Synthetase. *PLoS ONE*, 2013.

KOO, S. JIE; GARG, N. J. *Metabolic programming of macrophage functions and pathogens control*. *Redox Biology*. [S.l: s.n.], , 2019

KRAWCZYK, C. M. *et al.* Toll-like receptor-induced changes in glycolytic metabolism regulate dendritic cell activation. *Blood*, v. 115, n. 23, p. 4742–4749, 10 jun. 2010. Disponível em: <<https://ashpublications.org/blood/article/115/23/4742/27736/Toll-like-receptor-induced-changes-in-glycolytic>>. Acesso em: 29 nov. 2022.

KROPF, P. *et al.* Toll-like receptor 4 contributes to efficient control of infection with the protozoan parasite *Leishmania major*. *Infection and immunity*, v. 72, n. 4, p. 1920–1928, abr. 2004. Disponível em: <<https://pubmed.ncbi.nlm.nih.gov/15039311/>>. Acesso em: 16 jan. 2023.

KUMAR, V. *et al.* *Leishmania donovani* activates hypoxia inducible factor-1 α and miR-210 for survival in macrophages by downregulation of NF- κ B mediated pro-inflammatory immune respons. *Frontiers in Microbiology*, v. 9, n. MAR, p. 1–14, 2018a.

KUSAKABE, H.; KUNINAKA, A.; YOSHINO, H. Purification and Properties of a New Enzyme, Glutathione Oxidase from *Penicillium* sp. K-6-5. *Agricultural and Biological Chemistry*, v. 46, n. 8, p. 2057–2067, 1982. Acesso em: 11 maio 2023.

LAGO, T. S. *et al.* The miRNA 361-3p, a Regulator of GZMB and TNF Is Associated With Therapeutic Failure and Longer Time Healing of Cutaneous Leishmaniasis Caused by *L. (viannia) braziliensis*. *Frontiers in Immunology*, v. 9, p. 2621, 14 nov. 2018. Acesso em: 14 maio 2023.

LARANJEIRA-SILVA, M. F. *et al.* Melatonin attenuates *Leishmania (L.) amazonensis* infection by modulating arginine metabolism. *Journal of Pineal Research*, v. 59, n. 4, 2015.

LEMAIRE, J.; MKANNEZ, G.; GUERFALI, F. Z.; GUSTIN, C.; ATTIA, H. H.; RENARD, P.; *et al.* MicroRNA Expression Profile in Human Macrophages in Response to *Leishmania major* Infection. *PLoS Neglected Tropical Diseases*, v. 7, n. 10, 2013.

LEUNG, A. K. L. The Whereabouts of microRNA Actions: Cytoplasm and Beyond. *Trends in Cell Biology*, v. 25, n. 10, p. 601–610, 2015.

LI, C. H. *et al.* eIF5A promotes translation elongation, polysome disassembly and stress granule assembly. *PLoS ONE*, 2010.

LI, H. *et al.* Transcriptional regulation of macrophages polarization by microRNAs. *Frontiers in Immunology*, v. 9, n. MAY, p. 1–12, 2018a.

LI, H. *et al.* Transcriptional Regulation of Macrophages Polarization by MicroRNAs. *Frontiers in Immunology*, v. 9, n. MAY, p. 1, 28 maio 2018b. Disponível em: <<https://pubmed.ncbi.nlm.nih.gov/31555539/>>. Acesso em: 17 jan. 2023.

LIBERTI, M. V.; LOCASALE, J. W. The Warburg Effect: How Does it Benefit Cancer Cells? *Trends in biochemical sciences*, v. 41, n. 3, p. 211, 1 mar. 2016. Disponível em: </pmc/articles/PMC4783224/>. Acesso em: 29 nov. 2022.

LIESE, J.; SCHLEICHER, U.; BOGDAN, C. TLR9 signaling is essential for the innate NK cell response in murine cutaneous leishmaniasis. *European Journal of Immunology*, v. 37, n. 12, p. 3424–3434, 2007.

LIMA-JUNIOR, D. S. *et al.* Inflammasome-derived IL-1 β production induces nitric oxide-mediated resistance to Leishmania. *Nature medicine*, v. 19, n. 7, p. 909–15, 2013a. Disponível em: <http://www.ncbi.nlm.nih.gov/pubmed/23749230>.

LIU, Y. *et al.* [Effects of microRNA-294 on inflammatory factor of sepsis by targeting triggering receptor expressed on myeloid cells-1]. *Zhonghua wei zhong bing ji jiu yi xue*, v. 26, n. 9, p. 661–5, set. 2014.

LOCATI, M.; CURTALE, G.; MANTOVANI, A. Diversity, Mechanisms, and Significance of Macrophage Plasticity. *Annual Review of Pathology: Mechanisms of Disease*, 2020a.

LÜERSEN, K. Leishmania major thialysine N ϵ -acetyltransferase: Identification of amino acid residues crucial for substrate binding. *FEBS Letters*, 2005.

MALTA-SANTOS, H. *et al.* Differential expression of polyamine biosynthetic pathways in skin lesions and in plasma reveals distinct profiles in diffuse cutaneous leishmaniasis. *Scientific Reports*, 2020.

MAMANI-HUANCA, M. *et al.* Metabolomic reprogramming of c57bl/6-macrophages during early infection with *L. Amazonensis*. *International Journal of Molecular Sciences*, v. 22, n. 13, 2021a.

MANTOVANI, A. *et al.* The chemokine system in diverse forms of macrophage activation and polarization. *Trends Immunol*, v. 25, n. 12, p. 677–686, 2004.

MANZANO-ROMÁN, R.; SILES-LUCAS, M. MicroRNAs in parasitic diseases: Potential for diagnosis and targeting. *Molecular and Biochemical Parasitology*, v. 186, n. 2, p. 81–86, 2012.

MARÍ, M. *et al.* Mitochondrial Glutathione, a Key Survival Antioxidant. *https://home.liebertpub.com/ars*, v. 11, n. 11, p. 2685–2700, 15 out. 2009. Disponível em: <https://www.liebertpub.com/doi/10.1089/ars.2009.2695>. Acesso em: 20 abr. 2023.

MARTINEZ, F O *et al.* Macrophage activation and polarization. *Front Biosci*, v. 13, p. 453–461, 2008.

MARTINEZ, FERNANDO O.; HELMING, L.; GORDON, S. Alternative activation of macrophages: An immunologic functional perspective. *Annual Review of Immunology*, v. 27, p. 451–483, 2009.

MARTÍNEZ-LÓPEZ, M. *et al.* Batf3-dependent CD103⁺ dendritic cells are major producers of IL-12 that drive local Th1 immunity against Leishmania major infection in mice. *European Journal of Immunology*, v. 45, n. 1, p. 119–129, 1 jan. 2015. Disponível em: <https://onlinelibrary.wiley.com/doi/full/10.1002/eji.201444651>. Acesso em: 29 nov. 2022.

MATHEW, R. *et al.* Updates on the Current Technologies for microRNA Profiling. *MicroRNA*, v. 9, n. 1, p. 17–24, 2019.

MAYER, C. T. *et al.* Selective and efficient generation of functional Batf3-dependent CD103⁺ dendritic cells from mouse bone marrow. *Blood*, v. 124, n. 20, 2014.

MCCONVILLE, M J *et al.* Living in a phagolysosome; metabolism of Leishmania amastigotes. *Trends Parasitol*, v. 23, n. 8, p. 368–375, 2007.

MCCONVILLE, MALCOLM J. *et al.* Leishmania carbon metabolism in the macrophage phagolysosome- feast or famine? *F1000Research*. [S.l: s.n.], 2015

MCCONVILLE, MALCOLM J. *Metabolic Crosstalk between Leishmania and the Macrophage Host. Trends in Parasitology*. [S.l: s.n.], 2016a

MELBY, P. C. *et al.* Increased Expression of Proinflammatory Cytokines in Chronic Lesions of Human Cutaneous Leishmaniasis. *INFECrION AND IMMUNITY*. [S.l: s.n.], 1994. Disponível em: <<https://journals.asm.org/journal/iai>>.

MESÍAS, A. C. *et al.* Trypanothione synthetase confers growth, survival advantage and resistance to anti-protozoal drugs in *Trypanosoma cruzi*. *Free Radical Biology and Medicine*, 2019.

MESÍAS, A. C.; GARG, N. J.; ZAGO, M. P. Redox Balance Keepers and Possible Cell Functions Managed by Redox Homeostasis in *Trypanosoma cruzi*. *Frontiers in Cellular and Infection Microbiology*. [S.l: s.n.], 2019

MILLS, C. D. *M1 and M2 Macrophages: Oracles of Health and Disease. Critical Reviews™ in Immunology*. [S.l: s.n.], 2012.

MOORE, K. J.; SHEEDY, F. J.; FISHER, E. A. *Macrophages in atherosclerosis: A dynamic balance. Nature Reviews Immunology*. [S.l: s.n.], 2013

MOREIRA, D. *et al.* Leishmania infantum Modulates Host Macrophage Mitochondrial Metabolism by Hijacking the SIRT1-AMPK Axis. *PLOS Pathogens*, v. 11, n. 3, p. e1004684, 1 mar. 2015. Disponível em: <<https://journals.plos.org/plospathogens/article?id=10.1371/journal.ppat.1004684>>. Acesso em: 20 abr. 2023.

MURRAY, H. W. *et al.* Advances in leishmaniasis. 2005, [S.l: s.n.], 2005.

MURRAY, P. J.; WYNN, T. A. Obstacles and opportunities for understanding macrophage polarization. *Journal of Leukocyte Biology*, v. 89, n. 4, p. 557–563, 2011. Disponível em: <<http://www.jleukbio.org/cgi/doi/10.1189/jlb.0710409>>.

MURRAY, PETER J.; WYNN, T. A. Protective and pathogenic functions of macrophage subsets. *Nature Reviews Immunology*, v. 11, n. 11, p. 723–737, 2011. Disponível em: <<http://www.nature.com/doi/10.1038/nri3073>>.

MUXEL, SANDRA MARCIA; FERNANDA, M.; SILVA, L.; ZAMPIERI, R. A.; *et al.* Functional validation of miRNA mRNA interactions in macrophages by inhibition / competition assays based in transient transfection. *Protocol Exchange - NPG*, p. 1–13, 2017a.

MUXEL, SANDRA MARCIA; LARANJEIRA-SILVA, M. F.; ZAMPIERI, R. A.; FLOETER-WINTER, L. M. Leishmania (*Leishmania*) amazonensis induces macrophage miR-294 and miR-721 expression and modulates infection by targeting NOS2 and L-arginine metabolism. *Scientific Reports*, v. 7, n. February, p. 1–15, 2017b.

MUXEL, SANDRA MARCIA *et al.* Metabolomic profile of BALB/c macrophages infected with *Leishmania amazonensis*: Deciphering L-arginine metabolism. *International Journal of Molecular Sciences*, 2019a.

MUXEL, SANDRA MARCIA *et al.* NF- κ B Drives the Synthesis of Melatonin in RAW 264.7 Macrophages by Inducing the Transcription of the Arylalkylamine-N-Acetyltransferase (AA-NAT) Gene. *PLoS ONE*, v. 7, n. 12, 2012.

MUXEL, SANDRA MARCIA; ACUÑA, S. M.; *et al.* Toll-Like Receptor and miRNA-let-7e Expression Alter the Inflammatory Response in *Leishmania amazonensis*-Infected Macrophages. *Frontiers in Immunology*, v. 9, n. November, 2018a.

MUXEL, SANDRA MARCIA; ACUÑA, S. M.; *et al.* Toll-Like Receptor and miRNA-let-7e Expression Alter the Inflammatory Response in *Leishmania amazonensis*-Infected Macrophages. *Frontiers in Immunology*, v. 9, 29 nov. 2018b. Disponível em: <<https://www.frontiersin.org/article/10.3389/fimmu.2018.02792/full>>.

MUXEL, S.M.; AOKI, J. I.; *et al.* Arginine and polyamines fate in leishmania infection. *Frontiers in Microbiology*, v. 8, n. JAN, 2018b.

MUXEL, S.M.; AOKI, J. I.; *et al.* Arginine and polyamines fate in leishmania infection. *Frontiers in Microbiology*, v. 8, n. JAN, 2018c.

NAGARKOTI, S. *et al.* L-Arginine and tetrahydrobiopterin supported nitric oxide production is crucial for the microbicidal activity of neutrophils. *Free Radical Research*, v. 53, n. 3, p. 281–292, 2019.

NAIK, S. H. *et al.* Cutting Edge: Generation of Splenic CD8⁺ and CD8⁻ Dendritic Cell Equivalents in Fms-Like Tyrosine Kinase 3 Ligand Bone Marrow Cultures. *The Journal of Immunology*, v. 174, n. 11, p. 6592–6597, 1 jun. 2005. Disponível em: <<https://journals.aai.org/jimmunol/article/174/11/6592/101633/Cutting-Edge-Generation-of-Splenic-CD8-and-CD8>>. Acesso em: 29 nov. 2022.

NAKAI, K. *et al.* IL-17A induces heterogeneous macrophages, and it does not alter the effects of lipopolysaccharides on macrophage activation in the skin of mice. *Scientific Reports* 2017 7:1, v. 7, n. 1, p. 1–14, 29 set. 2017. Disponível em: <<https://www.nature.com/articles/s41598-017-12756-y>>. Acesso em: 11 maio 2023.

NATHAN, C.; CUNNINGHAM-BUSSEL, A. Beyond oxidative stress: an immunologist's guide to reactive oxygen species. *Nature reviews. Immunology*, v. 13, n. 5, p. 349–61, 2013. Disponível em: <<http://www.nature.com/doi/10.1038/nri3423>>.

NATHAN, C.; SHILOH, M. U. Reactive oxygen and nitrogen intermediates in the relationship between mammalian hosts and microbial pathogens. *Proceedings of the National Academy of Sciences of the United States of America*, v. 97, n. 16, p. 8841–8848, 2000.

NATHAN, C.; XIE, Q. WEN. Nitric oxide synthases: Roles, tolls, and controls. *Cell*, v. 78, n. 6, p. 915–918, 1994.

NEILL, L. A O.; SHEEDY, F. J.; MCCOY, C. E. MicroRNAs: the fine-tuners of Toll-like receptor signalling. *Nature reviews imm*, v. 268, n. February, p. 262–268, 2011.

NIIRANEN, K. *et al.* Mice with targeted disruption of spermidine/spermine N 1 - acetyltransferase gene maintain nearly normal tissue polyamine homeostasis but show signs of insulin resistance upon aging . *Journal of Cellular and Molecular Medicine*, 2006.

NISOLI, E. *et al.* Mitochondrial biogenesis by NO yields functionally active mitochondria in mammals. *Proceedings of the National Academy of Sciences of the United States of America*, v. 101, n. 47, p. 16507–16512, 2004. Disponível em: <<http://www.pnas.org/cgi/doi/10.1073/pnas.0405432101>>.

O'FARRELL, A. *et al.* Il-10 inhibits macrophage activation and proliferation by distinct signaling mechanisms: evidence for Stat3-dependent and -independent pathways. *EMBO Journal*, v. 17, n. 4 SRC-GoogleScholar FG-0, p. 1006–1018, 1998.

O'NEILL, L. A.; KISHTON, R. J.; RATHMELL, J. A guide to immunometabolism for immunologists. *Nat Rev Immunol*, v. 16, n. 9, p. 553–565, 2016.

OSPINA, H. A.; GUAY-VINCENT, M. M.; DESCOTEAUX, A. Macrophage Mitochondrial Biogenesis and Metabolic Reprogramming Induced by *Leishmania donovani* Require Lipophosphoglycan and Type I Interferon Signaling. *mBio*, v. 13, n. 6, 1 dez. 2022. Disponível em: <<https://journals.asm.org/doi/10.1128/mbio.02578-22>>. Acesso em: 20 abr. 2023.

OZA, S. L.; WYLLIE, S.; FAIRLAMB, A. H. Mapping the functional synthetase domain of trypanothione synthetase from *Leishmania major*. *Molecular and Biochemical Parasitology*, 2006.

PACHER, P.; BECKMAN, J. S.; LIAUDET, L. Nitric Oxide and Peroxynitrite in Health and Disease. *Physiological Reviews*, v. 87, n. 1, p. 315–424, 2007. Disponível em: <<http://physrev.physiology.org/cgi/doi/10.1152/physrev.00029.2006>>.

PAN AMERICAN HEALTH ORGANIZATION. *Interactive Atlas of Leishmaniasis in the Americas: Clinical Aspects and Differential Diagnosis*. Washington DC: [s.n.], 2020. Disponível em: <<http://apps.who.int/iris/>>.

PAN, H. *et al.* MicroRNA-410-3p modulates chondrocyte apoptosis and inflammation by targeting high mobility group box 1 (HMGB1) in an osteoarthritis mouse model. *BMC Musculoskeletal Disorders*, v. 21, n. 1, p. 1–12, 2020.

PEGG, A. E.; MCCANN, P. P. Polyamine metabolism and function. *American Journal of Physiology - Cell Physiology*, 1982.

PEGG, ANTHONY E. *Spermidine/spermine-N1-acetyltransferase: A key metabolic regulator. American Journal of Physiology - Endocrinology and Metabolism.* [S.l: s.n.], 2008

PEREZ-LEAL, O. *et al.* Polyamine-Regulated Translation of Spermidine/Spermine-N1-Acetyltransferase. *Molecular and Cellular Biology*, 2012.

PETRINI, E. *et al.* MicroRNAs in HBV-related hepatocellular carcinoma: functions and potential clinical applications. v. 57, n. 4, p. 500–509, 2015.

POLTICELLI, F. *et al.* Molecular evolution of the polyamine oxidase gene family in Metazoa. *BMC Evolutionary Biology*, 2012.

PULESTON, D. J. *et al.* Polyamines and eIF5A Hypusination Modulate Mitochondrial Respiration and Macrophage Activation. *Cell Metabolism*, 2019.

PULESTON, D. J.; VILLA, M.; PEARCE, E. L. *Ancillary Activity: Beyond Core Metabolism in Immune Cells. Cell Metabolism.* [S.l: s.n.], 2017

QUINN, J. J. *et al.* Local regulation of gene expression by lncRNA promoters, transcription and splicing. *Nature*, 2016.

RAFFERTY, S.; MALECH, H. L. High reductase activity of recombinant NOS2 flavoprotein domain lacking the calmodulin binding regulatory sequence. *Biochemical and Biophysical Research Communications*, v. 220, n. 3, p. 1002–1007, mar. 1996.

RATH, M *et al.* Metabolism via arginase or nitric oxide synthase: two competing arginine pathways in macrophages. *Front Immunol*, v. 5, 2014.

RATH, MEERA *et al.* *Metabolism via arginase or nitric oxide synthase: Two competing arginine pathways in macrophages. Frontiers in Immunology.* [S.l: s.n.], 2014

REGAN, T.; CONWAY, R.; BHARATH, L. P. Regulation of immune cell function by nicotinamide nucleotide transhydrogenase. *American Journal of Physiology - Cell Physiology*, v. 322, n. 4, p. C666–C673, 1 abr. 2022. Disponível em: <www.ajpcell.org>. Acesso em: 20 abr. 2023.

RESENDE, M. *et al.* Leishmania -Infected MHC Class II high Dendritic Cells Polarize CD4 + T Cells toward a Nonprotective T-bet + IFN- γ + IL-10 + Phenotype . *The Journal of Immunology*, v. 191, n. 1, 2013.

REYNOSO, R. *et al.* MicroRNAs differentially present in the plasma of HIV elite controllers reduce HIV infection in vitro. *Scientific Reports*, v. 4, p. 1–9, 2014.

RIBAS, V.; GARCÍA-RUIZ, C.; FERNÁNDEZ-CHECA, J. C. *Glutathione and mitochondria. Frontiers in Pharmacology.* [S.l: s.n.], 2014.

RICHARDSON, J. L. *et al.* Improved tricyclic inhibitors of trypanothione reductase by screening and chemical synthesis. *ChemMedChem*, 2009.

RIPOLL, V. M. *et al.* Nicotinamide nucleotide transhydrogenase (NNT) acts as a novel modulator of macrophage inflammatory responses. *The FASEB Journal*, v. 26, n. 8, p. 3550–3562, 1 ago. 2012. Disponível em: <https://onlinelibrary.wiley.com/doi/full/10.1096/fj.11-199935>. Acesso em: 20 abr. 2023.

ROBERTS, S C *et al.* Arginase plays a pivotal role in polyamine precursor metabolism in Leishmania. Characterization of gene deletion mutants. *J Biol Chem*, v. 279, n. 22, p. 23668–23678, 2004.

ROBINSON, M. D.; MCCARTHY, D. J.; SMYTH, G. K. edgeR: a Bioconductor package for differential expression analysis of digital gene expression data. *Bioinformatics (Oxford,*

England), v. 26, n. 1, p. 139–140, 11 nov. 2010. Disponível em: <<https://pubmed.ncbi.nlm.nih.gov/19910308/>>. Acesso em: 29 nov. 2022.

RONCHI, JULIANA A. *et al.* A spontaneous mutation in the nicotinamide nucleotide transhydrogenase gene of C57BL/6J mice results in mitochondrial redox abnormalities. *Free Radical Biology and Medicine*, 2013.

RONCHI, JULIANA APARECIDA *et al.* The Contribution of Nicotinamide Nucleotide Transhydrogenase to Peroxide Detoxification Is Dependent on the Respiratory State and Counterbalanced by Other Sources of NADPH in Liver Mitochondria. *Journal of Biological Chemistry*, v. 291, n. 38, p. 20173–20187, 16 set. 2016. Acesso em: 20 abr. 2023.

ROSENZWEIG, D. *et al.* Retooling Leishmania metabolism: from sand fly gut to human macrophage. *The FASEB Journal*, 2008.

ROSSI, M.; FASEL, N. How to master the host immune system? Leishmania parasites have the solutions! *International Immunology*, v. 30, n. 3, p. 103–111, 2018.

RYAN, D. G.; O'NEILL, L. A. J. *Krebs Cycle Reborn in Macrophage Immunometabolism. Annual Review of Immunology*. [S.l: s.n.], 2020a

SAINI, P. *et al.* Hypusine-containing protein eIF5A promotes translation elongation. *Nature*, 2009.

SANS-FONS, M. G. *et al.* Arginine transport is impaired in C57Bl/6 mouse macrophages as a result of a deletion in the promoter of Slc7a2 (CAT2), and susceptibility to Leishmania infection is reduced. *Journal of Infectious Diseases*, v. 207, n. 11, p. 1684–1693, 2013.

SAUDAGAR, P. *et al.* Molecular mechanism underlying antileishmanial effect of oxabicyclo[3.3.1]nonanones: Inhibition of key redox enzymes of the pathogen. *European Journal of Pharmaceutics and Biopharmaceutics*, 2013.

SAUDAGAR, P.; DUBEY, V. K. Cloning, expression, characterization, and inhibition studies on Trypanothione Synthetase, a drug target enzyme, from Leishmania donovani. *Biological Chemistry*, 2011.

SAUNDERS, E. C. *et al.* Leishmania mexicana can utilize amino acids as major carbon sources in macrophages but not in animal models. *Molecular Microbiology*, 2018.

SCHINDLER, H.; BOGDAN, C. NO as a signaling molecule: effects on kinases. *International Immunopharmacology*, v. 1, n. 8, p. 1443–1455, 2001. Disponível em: <<http://www.sciencedirect.com/science/article/pii/S1567576901000893>>. Acesso em: 11 jun. 2017.

SCHLEICHER, U. *et al.* NK cell activation in visceral leishmaniasis requires TLR9, myeloid DCs, and IL-12, but is independent of plasmacytoid DCs. *The Journal of Experimental Medicine*, v. 204, n. 4, p. 893, 4 abr. 2007. Disponível em: <[pmc/articles/PMC2118560/](https://pubmed.ncbi.nlm.nih.gov/16841693/)>. Acesso em: 29 nov. 2022.

SCORZA, B. M.; CARVALHO, E. M.; WILSON, M. E. Cutaneous Manifestations of Human and Murine Leishmaniasis. *International Journal of Molecular Sciences 2017, Vol. 18, Page 1296*, v. 18, n. 6, p. 1296, 18 jun. 2017. Disponível em: <<https://www.mdpi.com/1422-0067/18/6/1296/htm>>. Acesso em: 20 abr. 2023.

SÉGUIN, O.; DESCOTEAUX, A. Leishmania, the phagosome, and host responses: The journey of a parasite. *Cellular Immunology*, v. 309, p. 1–6, 2016.

SHEN, J. *et al.* IL-17 induces macrophages to M2-like phenotype via NF- κ B. *Cancer Management and Research*, v. 10, p. 4217–4228, 4 out. 2018. Disponível em: <<https://www.dovepress.com/il-17-induces-macrophages-to-m2-like-phenotype-via-nf-kappab-peer-reviewed-fulltext-article-CMAR>>. Acesso em: 11 maio 2023.

SHWEASH, M. *et al.* Leishmania mexicana promastigotes inhibit macrophage IL-12 production via TLR-4 dependent COX-2, iNOS and arginase-1 expression. *Molecular Immunology*, v. 48, n. 15–16, p. 1800–1808, 2011. Disponível em: <<http://dx.doi.org/10.1016/j.molimm.2011.05.013>>.

Situação epidemiológica da Leishmaniose Visceral — Ministério da Saúde. Disponível em: <<https://www.gov.br/saude/pt-br/assuntos/saude-de-a-a-z/l/leishmaniose-visceral/situacao-epidemiologica-da-leishmaniose-visceral>>. Acesso em: 29 jan. 2023.

Situação Epidemiológica da LT — Ministério da Saúde. Disponível em: <<https://www.gov.br/saude/pt-br/assuntos/saude-de-a-a-z/l/lt/situacao-epidemiologica>>. Acesso em: 29 jan. 2023.

SOARES, M. F. *et al.* Differential expression of miRNAs in canine peripheral blood mononuclear cells (PBMC) exposed to *Leishmania infantum* in vitro. *Research in Veterinary Science*, v. 134, p. 58–63, 1 jan. 2021. Acesso em: 14 maio 2023.

SOTO, M. *et al.* Resistance to Experimental Visceral Leishmaniasis in Mice Infected With *Leishmania infantum* Requires Batf3. *Frontiers in Immunology*, v. 11, p. 3216, 10 dez. 2020. Acesso em: 29 nov. 2022.

SOUZA, M. DE A. *et al.* miR-548d-3p Alters Parasite Growth and Inflammation in *Leishmania (Viannia) braziliensis* Infection. *Frontiers in Cellular and Infection Microbiology*, v. 11, p. 511, 10 jun. 2021. Acesso em: 14 maio 2023.

STÄGER, S. *et al.* Distinct roles for IL-6 and IL-12p40 in mediating protection against *Leishmania donovani* and the expansion of IL-10+ CD4+ T cells. *European Journal of Immunology*, v. 36, n. 7, p. 1764–1771, 1 jul. 2006. Disponível em: <<https://onlinelibrary.wiley.com/doi/full/10.1002/eji.200635937>>. Acesso em: 25 abr. 2023.

STEIN, S. C. *et al.* The regulation of AMP-activated protein kinase by phosphorylation. *Biochemical Journal*, v. 345, n. 3, p. 437–443, 1 fev. 2000. Acesso em: 11 maio 2023.

TAKAO, K. *et al.* A conceptual model of the polyamine binding site of N 1- acetyl polyamine oxidase developed from a study of polyamine derivatives. *Amino Acids*, 2009.

TAKEDA, K.; KAISHO, T.; AKIRA, S. Toll-like receptors. *Annual review of immunology*, v. 21, p. 335–376, 2003. Disponível em: <<https://pubmed.ncbi.nlm.nih.gov/12524386/>>. Acesso em: 17 jan. 2023.

TANNAHILL, G. M. *et al.* Succinate is an inflammatory signal that induces IL-1 β through HIF-1 α . *Nature*, v. 496, n. 7444, p. 238–242, 2013a.

The Induction of IL-1 β Secretion Through the NLRP3 Inflammasome During Ebola Virus Infection. *Journal of Infectious Diseases*, [S.d.]. Disponível em: <<http://doi.org/10.1093/infdis/jiy433>>.

THOMAS, T.; THOMAS, T. J. *Polyamines in cell growth and cell death: Molecular mechanisms and therapeutic applications. Cellular and Molecular Life Sciences*. [S.l.: s.n.], 2001

THOMPSON, R. W. *et al.* Cationic amino acid transporter-2 regulates immunity by modulating arginase activity. *PLoS Pathog*, v. 4, n. 3, p. e1000023, 2008.

TRAN, A. N. *et al.* Trypanothione synthetase locus in *Trypanosoma cruzi* CL Brener strain shows an extensive allelic divergence. *Acta Tropica*, 2003.

TUON, F. F. *et al.* Toll-Like Receptors and Leishmaniasis. *Infection and Immunity*, v. 76, n. 3, p. 866, 2008. Disponível em: </pmc/articles/PMC2258802/>. Acesso em: 29 nov. 2022.

TY, M. C. *et al.* Immuno-metabolic profile of human macrophages after *Leishmania* and *Trypanosoma cruzi* infection. *PLoS ONE*, v. 14, n. 12, 1 dez. 2019. Disponível em: </pmc/articles/PMC6913957/>. Acesso em: 20 abr. 2023.

UEMATSU, S.; AKIRA, S. Toll-like receptors and innate immunity. *Journal of molecular medicine (Berlin, Germany)*, v. 84, n. 9, p. 712–725, set. 2006. Disponível em: <<https://pubmed.ncbi.nlm.nih.gov/16924467/>>. Acesso em: 17 jan. 2023.

VAN ASSCHE, T. *et al.* *Leishmania*-macrophage interactions: Insights into the redox biology. *Free Radical Biology and Medicine*, v. 51, n. 2, p. 337–351, 2011. Disponível em: <<http://dx.doi.org/10.1016/j.freeradbiomed.2011.05.011>>.

VAN DEN BOSSCHE, J.; BAARDMAN, J.; DE WINTHER, M. P. J. Metabolic characterization of polarized M1 and M2 bone marrow-derived macrophages using real-time extracellular flux analysis. *Journal of Visualized Experiments*, 2015.

VARIKUTI, S. *et al.* MicroRNA-21 Deficiency Promotes the Early Th1 Immune Response and Resistance toward Visceral Leishmaniasis. *The Journal of Immunology*, v. 207, n. 5, p. 1322–1332, 1 set. 2021. Disponível em: <<https://journals.aai.org/jimmunol/article/207/5/1322/234638/MicroRNA-21-Deficiency-Promotes-the-Early-Th1>>. Acesso em: 11 maio 2023.

VELASQUEZ, L. G. *et al.* Distinct courses of infection with *Leishmania (L.) amazonensis* are observed in BALB/c, BALB/c nude and C57BL/6 mice. *Parasitology*, v. 143, n. 6, p. 692–703, 2016.

VERGADI, E. *et al.* Akt Signaling Pathway in Macrophage Activation and M1/M2 Polarization. *The Journal of Immunology*, 2017.

VERRECK, F. A. W. *et al.* Human IL-23-producing type 1 macrophages promote but IL-10-producing type 2 macrophages subvert immunity to (myco)bacteria. *Proceedings of the National Academy of Sciences of the United States of America*, v. 101, n. 13, p. 4560–4565, 30 mar. 2004. Disponível em: <<https://www.pnas.org/doi/abs/10.1073/pnas.0400983101>>. Acesso em: 17 jan. 2023.

VIOLA, A. *et al.* *The metabolic signature of macrophage responses*. *Frontiers in Immunology*. [S.l.: s.n.], 2019a

VOGEL, D. Y. S. *et al.* Human macrophage polarization in vitro: Maturation and activation methods compared. *Immunobiology*, 2014.

WALKER, P. S. *et al.* Immunostimulatory oligodeoxynucleotides promote protective immunity and provide systemic therapy for leishmaniasis via IL-12- and IFN-gamma-dependent mechanisms. *Proceedings of the National Academy of Sciences of the United States of America*, v. 96, n. 12, p. 6970–6975, 1999.

WANASEN, N; SOONG, L. L-arginine metabolism and its impact on host immunity against *Leishmania* infection. *Immunol Res*, v. 41, n. 1, p. 15–25, 2008.

WANASEN, NANCHAYA *et al.* L-arginine and cationic amino acid transporter 2B regulate growth and survival of *Leishmania amazonensis* amastigotes in macrophages. *Infection and Immunity*, v. 75, n. 6, p. 2802–2810, 2007.

WANG, N.; LIANG, H.; ZEN, K. Molecular mechanisms that influence the macrophage m1-m2 polarization balance. *Front Immunol*, v. 5, p. 614, 2014.

WANG, Y.; LIANG, Y.; LU, Q. MicroRNA epigenetic alterations: Predicting biomarkers and therapeutic targets in human diseases. *Clinical Genetics*, v. 74, n. 4, p. 307–315, 2008.

WANG, YAFANG *et al.* Mitochondrial metabolism regulates macrophage biology. *Journal of Biological Chemistry*, v. 297, n. 1, p. 297–298, 1 jul. 2021. Disponível em: <<http://www.jbc.org/article/S0021925821007043/fulltext>>. Acesso em: 20 abr. 2023.

WEINKOPFF, T. *et al.* Role of Toll-Like Receptor 9 Signaling in Experimental *Leishmania braziliensis* Infection. 2013. Disponível em: <<http://dx.doi.org/10.1128>>. Acesso em: 11 maio 2023.

WHO | World Health Organization. Disponível em: <https://apps.who.int/neglected_diseases/ntddata/leishmaniasis/leishmaniasis.html>. Acesso em: 22 jan. 2023.

WHYTE, C. S. *et al.* Regulation of alternative (M2) macrophage activation by Suppressor of Cytokine Signalling (SOCS) 1. *Immunology*, 2010.

WILHELM, P. *et al.* Rapidly Fatal Leishmaniasis in Resistant C57BL/6 Mice Lacking TNF. *The Journal of Immunology*, v. 166, n. 6, p. 4012–4019, 15 mar. 2001. Disponível em: <<https://journals.aai.org/jimmunol/article/166/6/4012/70389/Rapidly-Fatal-Leishmaniasis-in-Resistant-C57BL-6>>. Acesso em: 17 jan. 2023.

WINTER, J. Micromas of the mir379–410 cluster: New players in embryonic neurogenesis and regulators of neuronal function. *Neurogenesis*, v. 2, n. 1, 2015.

WINTERBOURN, C. C. Reconciling the chemistry and biology of reactive oxygen species. *Nature Chemical Biology* 2008 4:5, v. 4, n. 5, p. 278–286, 17 abr. 2008. Disponível em: <<https://www.nature.com/articles/nchembio.85>>. Acesso em: 16 fev. 2023.

WU, G. *et al.* Proline metabolism in the conceptus: Implications for fetal growth and development. *Amino Acids*. [S.l: s.n.], 2008

YE, J. *et al.* Research advances in the detection of miRNA. *Journal of Pharmaceutical Analysis*, v. 9, n. 4, p. 217–226, 2019.

YERAMIAN, ANDRÉE *et al.* Macrophages require distinct arginine catabolism and transport systems for proliferation and for activation. *European Journal of Immunology*, v. 36, n. 6, p. 1516–1526, 2006.

YERAMIAN, ANDRÉE; MARTIN-JAULAR, L.; SOLER, C. Arginine Transport via Cationic Amino Acid Transporter 2 Plays a Critical Regulatory Role in Classical or Alternative Activation of Macrophages Plasmodium vivax View project MRes Thesis: Synthetic Carriers View project. *Article in The Journal of Immunology*, 2006. Disponível em: <<https://www.researchgate.net/publication/7110890>>. Acesso em: 11 maio 2023.

ZHENG, X. *et al.* Correction of arginine metabolism with sepiapterin—the precursor of nitric oxide synthase cofactor BH4—induces immunostimulatory-shift of breast cancer. *Biochemical Pharmacology*, 2020.

ZUO, T. *et al.* MicroRNA-410-3p Binds to TLR2 and Alleviates Myocardial Mitochondrial Dysfunction and Chemokine Production in LPS-Induced Sepsis. *Molecular Therapy - Nucleic Acids*, v. 22, n. 1, p. 273–284, 2020.

Anexos e Apêndices

DECLARAÇÃO

Declaramos para os devidos fins que Stephanie Maia Acuna, CPF 428.157.698-32, recebe/recebeu auxílio da FUNDAÇÃO DE AMPARO À PESQUISA DO ESTADO DE SÃO PAULO, CNPJ 43.828.151/0001-45, na(s) modalidade(s):

Programas Regulares / Bolsas / No País / Doutorado Direto

Processo: 2017/23519-2

Título: Análise do papel de fatores de transcrição e miRNAs na regulação da expressão gênica em macrófagos murinos infectados por *Leishmania amazonensis*

Instituição: Instituto de Biociências/IB/USP

Período: 01/03/2018 a 31/01/2023

Orientador Prof(a). Dr(a).: Sandra Marcia Muxel

Programas Regulares / Bolsas / No Exterior / Bolsa Estágio de Pesquisa no Exterior / BEPE - Doutorado Direto

Processo: 2021/07144-4

Título: Redes imunometabólicas durante interação entre Células Dendríticas e *Leishmania*

Instituição: Instituto de Biociências/IB/USP

Período: 05/10/2021 a 04/10/2022

Orientador Prof(a). Dr(a).: Sandra Marcia Muxel

São Paulo, 25 de maio de 2023.


Flávio Cardoso da Silva
Assessor

FLÁVIO CARDOSO DA SILVA
Assessor



Documento emitido em: 25 de maio de 2023 15:35:38 Horário Padrão de Brasília.

Código para verificação: 138E-0D99-6781-A750

Documento válido até: 24/06/2023

Consulta à autenticidade em: <http://edoc.fapesp.br?docId=138E-0D99-6781-A750>

CERTIFICADO

Certificamos que a proposta intitulada “Análise do perfil de transcriptômica e metabolômica de macrófagos murinos infectados com *Leishmania amazonensis*: análise de transcritos e metabólitos do parasita e do hospedeiro”, registrada com o nº 314/2018, sob a responsabilidade da Profa. Dra. Lucile Maria Floeter Winter e com a participação dos colaboradores Juliana Ide Aoki (IB/USP), Sandra Marcia Muxel (IB/USP), Ricardo Andrade Zampieri (IB/USP), Stephanie Maia Acuna (IB/USP), Juliane Cristina Ribeiro Fernandes (IB/USP), Felipe Cortez (IB/USP), (*)Jonatham Miguel Zanatta (IB/USP), (*)Leonardo Cortazzo (IB/USP) e (*)Camilla de Almeida Bento (IB/USP), que envolve a utilização de animais pertencentes ao filo Chordata, subfilo Vertebrata (exceto humanos), para fins de pesquisa científica encontra-se de acordo com os preceitos da Lei nº 11.794, de 08 de outubro de 2008, do Decreto nº 6.899, de 15 de julho de 2009 e com as normas editadas pelo Conselho Nacional de Controle da Experimentação Animal (CONCEA), e foi aprovada pela Comissão de Ética no Uso de Animais – CEUA do Instituto de Biociências da Universidade de São Paulo, em reunião de 17 de abril de 2018.

Vigência da autorização: 17/04/2018 a 05/04/2020

Finalidade: Pesquisa Científica

Espécie/linhagem: camundongo isogênico/BALB/c e C57BL/6


Nº de animais: 150 (F) de cada linhagem **Peso:** 20-30g **Idade:** 4-8sem. **Total:** 300 animais

Origem: Centro de Bioterismo da Faculdade de Medicina da USP – São Paulo, SP

Adendo

A Comissão de Ética no Uso de Animais – CEUA do Instituto de Biociências da Universidade de São Paulo, em 10/10/2019 aprovou a prorrogação do prazo de vigência do projeto, de 06/04/2020 a 05/04/2022 e a inclusão de (*)novos pesquisadores colaboradores.

OBS.: Qualquer intercorrência ou alteração do projeto em andamento deverá ser previamente autorizada pela Comissão de Ética no Uso de Animais – CEUA-IB.


Prof. Dr. Pedro Augusto Carlos Magno Fernandes
Coordenador da Comissão de Ética no Uso de Animais

Biografia Stephanie Maia Acuña

Títulos

Bacharela em Ciências Fundamentais Para a Saúde.
Instituto de Ciências Biomédicas – Universidade de São Paulo
2017

Trajectoria científica

Iniciação Científica com bolsa nos projetos:

- Papel da arginase na composição de microRNA em macrófagos infectados por *Leishmania amazonensis*. CNPq. Duração: 1 ano (2014-2015).
- Estabelecimento de perfil de miRNA de macrófagos murinos infectados por *Leishmania amazonensis*. (FAPESP) Duração: 2 anos (2015-2017).

Doutorado Direto com bolsa no projeto:

- Análise do papel de fatores de transcrição e miRNAs na regulação da expressão gênica em macrófagos murinos infectados por *Leishmania amazonensis*. FAPESP. Duração prevista: 48 meses. Início em fevereiro de 2018.

Bolsa de Estágio de Pesquisa no Exterior

- Redes imunometabólicas durante interação entre Células Dendríticas e *Leishmania*. FAPESP. Vigência de 05/10/2021 a 04/10/2022. Execução em Life and Health Sciences Research Institute - University of Minho - Braga, Portugal.

Participação em Congressos e Simpósios:

- III Semana de Inovações Biológicas e Biotecnológicas Aplicadas à Saúde (SIBBAS). Instituto de Ciências Biomédicas – USP. 2014 (Organização)
- 23º Simpósio Internacional de Iniciação Científica e Tecnológica da USP (SIICUSP). Instituto de Biociências – USP. 2015.
- IV Semana de Inovações Biológicas e Biotecnológicas Aplicadas à Saúde (SIBBAS). Instituto de Ciências Biomédicas – USP. 2015 (Organização)
- V Semana de Inovações Biológicas e Biotecnológicas Aplicadas à Saúde (SIBBAS). Instituto de Ciências Biomédicas – USP. 2017 (Ouvinte)
- XXXI Reunião Anual da Sociedade Brasileira de Protozoologia. Novembro de 2015. Caxambu – MG.
- XXXII Reunião Anual da Sociedade Brasileira de Protozoologia. Novembro de 2016. Caxambu – MG.
- XXXIII Reunião Anual da Sociedade Brasileira de Protozoologia. Novembro de 2017. Caxambu – MG.
- VI Simpósio de Inovações Biológicas e Biotecnológicas Aplicadas à Saúde (SIBBAS). Instituto de Ciências Biomédicas – USP. Junho de 2018 (Palestrante).
- XLIII Congresso da Sociedade Brasileira de Imunologia. Outubro de 2018. Ouro Preto – MG.
- XXXIV Reunião Anual da Sociedade Brasileira de Protozoologia. Novembro de 2018. Caxambu – MG.

Apresentação de Trabalhos:

Autoria

- 23º Simpósio Internacional de Iniciação Científica e Tecnológica da USP (SIICUSP). Produção de Óxido Nítrico por *Leishmania amazonensis*. 2015. (Pôster).
- XXXI Reunião Anual da Sociedade Brasileira de Protozoologia. Production of Nitric Oxide by *Leishmania amazonensis*. 2015. (Pôster)
- XXXII Reunião Anual da Sociedade Brasileira de Protozoologia. Correlation of NOS2 and arginase from parasite in regulate miRNA profile and mRNA expression of murine macrophages infected with *Leishmania amazonensis*. 2016. (Pôster)
- XXXIII Reunião da Sociedade Brasileira de Protozoologia. Nitric Oxide production by *Leishmania amazonensis* depends on arginase activity. Novembro de 2017 (Pôster).
- XXXIII Reunião da Sociedade Brasileira de Protozoologia. *Leishmania amazonensis* modulates murine macrophage miRNA profile by the cross-regulation between host NOS2 and parasite-arginase during infection. Novembro de 2017 (Pôster).
- XLIII Congresso da Sociedade Brasileira de Imunologia. Host NOS2 and *Leishmania amazonensis* arginase modulate microRNAs involved in macrophage inflammatory response. Outubro de 2018 (Pôster).
- XXXIV Congresso da Sociedade Brasileira de Protozoologia. Role of Toll-like receptors and miRNA-let-7e to macrophage inflammatory response during *Leishmania amazonensis* infection. Novembro de 2018 (Comunicação Oral).

Colaborações

- XXXI Reunião Anual da Sociedade Brasileira de Protozoologia. *Leishmania amazonensis* arginase altered miRNA profile of infected macrophages to modulate NO/polyamines. Muxel S.M.; Da Silva, M.F.L; Zampieri, R.A.; **Acuña, S.M.**; Floeter-Winter, L.M. 2015. (Pôster)
- 6th World Congress on Leishmaniasis. Genetic background shifts miRNA profile of *Leishmania amazonensis* infected macrophages and adjusts NO/polyamines production. Muxel S.M.; **Acuña, S.M.**; Zampieri, R.A.; Floeter-Winter, L.M. 2017. (Comunicação oral)
- XXXIII Reunião Anual da Sociedade Brasileira de Protozoologia. Toll-like receptors operate in miRNA and mRNA targets involved in NO/polyamines production of *Leishmania amazonensis* infected macrophages. Muxel S.M.; **Acuña, S.M.**; Aoki, J.I.; Zampieri, R.A.; Floeter-Winter, L.M. 2017. (Pôster)
- XXXIII Reunião Anual da Sociedade Brasileira de Protozoologia. Expression of amino acid permease 3 in *Leishmania amazonensis* depends of L-arginine availability and arginase activity. Muxel S.M.; **Acuña, S.M.**; Aoki, J.I.; Zampieri, R.A.; Floeter-Winter, L.M. 2017. (Pôster)

Publicações

- Arginase expression modulates Nitric Oxide production in *Leishmania (Leishmania) amazonensis*. **Acuña SM**, Aoki JI, Laranjeira-Silva MF, Zampieri RA, Fernandes JCR,

Muxel SM, Floeter-Winter, LM. PLOS ONE. 2017. doi: 10.1371/journal.pone.0187186.

- L-arginine availability and arginase activity: characterization of amino acid permease 3 in *Leishmania amazonensis*. Aoki JI, Muxel SM, Zampieri RA, **Acuña SM**, Fernandes JCR, Vanderlinde RH, Sales MCOP, Floeter-Winter LM. PLOS Neglected Tropical Diseases. 2017. doi: 10.1371/journal.pntd.0006025.
- Functional Validation of miRNA-mRNA interactions in macrophages by inhibition/competition assays based in transient transfection. Muxel, SM; Laranjeira-Silva, MF; Zampieri, RA; Aoki, JI; **Acuña, SM**; Floeter-Winter, LM. Protocol Exchange. 2017. Doi; 10.1038/protex.2017.034.
- Arginine and polyamines fate in *Leishmania* infection. Muxel SM, Laranjeira-Silva MF, Aoki, JI, Zampieri RA, **Acuña SM**, Fernandes JCR, Vanderlinde RH and Floeter-Winter LM. Frontiers in Microbiology. 2018. Doi: [10.3389/fmicb.2017.02682](https://doi.org/10.3389/fmicb.2017.02682).
- Toll-like receptor and miRNA-let-7e expression alter the inflammatory response in *Leishmania amazonensis*-infected macrophages. Muxel SM, **Acuña SM**, Aoki JI, Zampieri RA, Floeter-Winter, LM. Frontiers in Immunology. 2018. Doi: 10.3389/fimmu.2018.02792.
- **Metabolomic Reprogramming of C57BL/6-Macrophages during Early Infection with *L. amazonensis***
Maricruz Hamani-Huanca, Sandra Marcia Muxel, Stephanie Maia Acuña, Lucile Maria Floeter-Winter, Coral Barbas e Ángeles López-González.
International Journal of Molecular Sciences – MDPI
Doi: <https://doi.org/10.3390/ijms22136883>
Publicado em 26 de junho de 2021.
- **Atypical Prolonged Viral Shedding With Intra-Host SARS-CoV-2 Evolution in a Mildly Affected Symptomatic Patient**
Marielton dos Passos Cunha, Ana Paula Pessoa Vilela, Camila vieira Molina, Stephanie Maia Acuña, Sandra Marcia Muxel, Vinícius de Moraes Barroso, Sabrina Baroni, Lilian Gomes de Oliveira, Yan de Souza Angelo, Jean Pierre Schatzmann Peron, Luiz Gustavo Bentim Góes, Angélica Cristine de Almeida Campos e Paola Minóprio.
Frontiers in medicine
Doi: <https://doi.org/10.3389/fmed.2021.760170>
Publicado em 26 de novembro de 2021.
- **miR-294 and miR-410 Negatively Regulate Tnfa, Arginine Transporter Cat1/2, and Nos2 mRNAs in Murine Macrophages Infected with *Leishmania amazonensis***
Stephanie Maia Acuña, Jonathan Miguel Zanatta, Camilla de Almeida Bento, Lucile Maria Floeter-Winter e Sandra Marcia Muxel.
Non-Coding RNA – MDPI
Doi: <https://doi.org/10.3390/ncrna8010017>
Publicado em 06 de fevereiro de 2022

Trajetória acadêmica

Disciplinas Pós-Graduação

- Seminários em Parasitologia I. Instituto de Ciências Biomédicas – USP. 60 horas. 2018.

- Tópicos Avançados em Fisiologia. Instituto de Biociências – USP. 30 horas. 2018
- Ciências Ômicas em Doenças Infecciosas. Instituto de Ciências Biomédicas – USP. 90 horas. 2018.
- Regulação da Expressão Gênica em Processos Fisiológicos. Instituto de Biociências – USP. 120 horas. 2018.
- Regulação da Resposta Imune. Instituto de Ciências Biomédicas – USP. 120 horas. 2019
- Didática em Bioquímica. Instituto de Química – USP. 30 horas. 2019
- Divulgação Científica. Instituto de Ciências Biomédicas – USP. 60 horas. 2019
- Seminário Didático-Científico em Imunologia. Instituto de Ciências Biomédicas – USP. 60 horas. 2019.
- Seminários em Parasitologia II. Instituto de Ciências Biomédicas – USP. 2019.
- Bioenergética Mitochondrial: Abordagens *in situ* e *in vivo*. Instituto de Química – USP. 60 horas. 2020.
- Processos Redox em Bioquímica. Instituto de Química – USP. 60 horas 2020.

Disciplinas Optativas na Graduação

- Processo Saúde-Doença na Amazônia Brasileira. Instituto de Ciências Biomédicas – USP. Carga Horária: 180 horas. 2016.
- Introdução à Análise Computacional de Macromoléculas. Instituto de Ciências Biomédicas – USP. Carga Horária: 120 horas. 2016.

Projetos de Cultura e Extensão Universitária

- Vice-Presidente na gestão do Centro Acadêmico Rosalind Franklin dos estudantes de Ciências Biomédicas e Ciências Fundamentais para a Saúde do ICB-USP. Duração: 1 ano (2015-2016).